Design and Analysis of Novel Fractional Controllers for Integer and Non-integer Order System

Thesis submitted in partial fulfilment of the requirements for the award of the degree of

DOCTOR OF PHILOSOPHY

in

CHEMICAL ENGINEERING

by

RAYALLA RANGANAYAKULU

Roll No: 714149

Under the Supervision of

Dr. G. UDAY BHASKAR BABU

Assistant Professor

DEPARTMENT OF CHEMICAL ENGINEERING

NATIONAL INSTITUTE OF TECHNOLOGY WARANGAL

TELANGANA – 506004, INDIA.

MAY 2019

NATIONAL INSTITUTE OF TECHNOLOGY
Warangal – 506004, Telangana, INDIA.

CERTIFICATE

This is to certify that the thesis entitled **"Design and Analysis of Novel Fractional Controllers for Integer and Non-integer Order System"** being submitted by **Mr. R. Ranganayakulu** for the award of the degree of Doctor of Philosophy (Ph.D.) in Chemical Engineering to the **National Institute of Technology, Warangal, India** is a record of the bonafide research work carried out by him under my supervision. The thesis has fulfilled the requirements according to the regulations of this Institute and in my opinion has reached the standards for submission. The results embodied in the thesis have not been submitted to any other University or Institute for the award of any degree or diploma.

Date:

Dr. G. Uday Bhaskar Babu

Assistant Professor
Department of Chemical Engineering
National Institute of Technology, Warangal
Warangal - 506004

DECLARATION

This is to certify that the work presented in the thesis entitled "Design and Analysis of Novel Fractional Controllers for Integer and Non-integer Order System" is a bonafide work done by me under the supervision of Dr. G. Uday Bhaskar Babu and is not submitted elsewhere for award of any degree.

I declare that this written submission represents my ideas in my own words and where others' ideas or words have been included, I have adequately cited and referenced the original source. I also declare that I have adhered to all principles of academic honesty and integrity and have not misrepresented or fabricated or falsified any idea/data/fact/source in my submission.

I understand that any violation of the above will be a cause for disciplinary action by the Institute and can also evoke penal action from the sources which have thus not been properly cited or from whom proper permission has not been taken when needed.

RAYALLA RANGANAYAKULU

Roll No.714149

ACKNOWLEDGEMENTS

It gives me great pleasure to thank all the people who have contributed in making this thesis a success. I wish to tender my unbound gratitude and sincere thanks to my supervisor and mentor Dr. G. Uday Bhaskar Babu, Assistant professor, Department of Chemical Engineering, whose esteemed moral support, immense involvement, innovative ideas and incessant encouragement enabled me to accomplish this thesis. His guidance is a great learning experience to me throughout my stay at NITW by strengthening me all the time. I owe a lot to him for his positive encouragement and guidance.

It is an honor to thank Prof. N.V. Ramana Rao, Director, NIT Warangal for providing me institute fellowship for completing the Ph.D. I extend my sincere thanks Prof. Sonawane Shirish Hari, Head, Department of Chemical Engineering for providing necessary facilities in the department and his valuable suggestions. I am very thankful to Dr. A. Seshagiri Rao for his valuable suggestions. I would like to express my sincere thanks to Dr. T. Sunil Kumar and Dr. V. Ramsagar for their helpful comments regarding the numerical aspects of my study. I am thankful to Dr. P. Chandrasekhar, Department of Electrical Engineering and Dr. D. Jaya Krishna, Department of Mechanical Engineering for their valuable suggestions.

I am very thankful to all the faculty members and staff of the department for their cooperation throughout my research work.

I would like to thank my colleagues D. Purushottama Rao, U. Vinay kumar, Sudeep Surendran, Basant Kumar Pillai and Dr. Devender Rao Kodati for the useful discussions we experienced in all steps of my study.

This thesis would not have been possible without the support of my family. I would like to thank my beloved parents (R. Venkateswarlu, R. Vijaya Lakshmi), sister (R. Lakshmi Prasanna), wife (G. Susmitha) and all my family members for their patience, courageous and consistent motivation and affection throughout my career.

Rayalla Ranganayakulu

CONTENTS

ABSTRACT

Controller design for level, flow, temperature and pressure processes in chemical industries, power plants, oil industries and aerospace systems is challenging as they are often associated with problems such as structural complexity, uncertainties, large transportation lags, nonlinearities and external perturbations. Desired response of these control loops cannot be achieved with the conventional PID controller. The performance of these control loops can be enhanced using fractional controllers.

The Internal model control (IMC) scheme based design of PID controller has advantage of a single tuning parameter which is usually selected for a tradeoff between closed loop performance and robustness to model inaccuracies. The performance of IMC based PID controller is determined by the IMC filter structure used for designing the controller. In majority of the previous works, an integer order IMC filter structure of first order and higher orders have been used for designing the controller. These controllers doesn't always result in an improved closed loop performance. Along with these controllers, one may need to use set point filter or set point weighting to minimize the overshoot in the response. The advantage of using fractional IMC filter structure is that it eliminates the need to use set point filter or set point weighting. The fractional term in the controller serves the purpose of minimizing the overshoot. Though, it has the additional tuning parameter it offers the tuning flexibility for achieving the desired performance.

In this research work, a systematic design procedure is proposed for designing the fractional controllers for integer and non-integer order systems based on maximum sensitivity (M_s). An optimum higher order fractional IMC filter structure is identified from the systematic procedure. In addition, Pade's procedure is incorporated for higher order approximation of time delay. The resulting controller has an interesting structure composed of fractional term and controller (PI/PID for integer order systems and fractional order PI/PID for non-integer order systems) term. The fractional term has additional degree of freedom which offers flexibility in tuning there by enhance the performance based on M_s.

Several examples representing integer order time delay systems (second order plus time delay systems, integrating plus time delay systems and first order plus time delay systems in cascade loops) and noninteger order plus time delay systems have been considered for simulation study. Robustness analysis is carried out to determine the robust stability of closed loop system. Fragility

analysis is carried out on all the proposed controllers to investigate the performance deterioration for uncertainties in the controller parameters.

The performance of closed loop system with the proposed fractional controllers is compared with the recent methods proposed in the literature. The proposed method shows improved closed loop performance in terms of disturbance rejection and set point tracking with low values of errors such as IAE and ITAE for all the time delay systems. The work shows that the controller design with higher order fractional IMC filter structure and higher order pade's approximation for time delay gives enhanced performance than the controller designed with lower order fractional IMC filter structure and first order Pade's approximation for time delay. Simulation results show that the error values are decreasing with increase in the order fractional IMC filter structure but the control effort is increasing. The proposed method is also proved to be effective for perturbations in the process parameters and noise in the output.

Keywords: PID controller, Fractional filter IMC-PID controller, Internal Model Control, Fractional IMC filter, Pade's approximation, Robustness, Maximum sensitivity, Fragility

LIST OF FIGURES

LIST OF TABLES

ABBREVIATIONS

DIPTD	Double integrating plus time delay
DS	Direct synthesis
FFPID	Fractional filter proportional integral derivative
FFFOPID	Fractional filter fractional order proportional integral derivative
FI	Fragility index
FOPD	Fractional order proportional derivative
FOPI	Fractional order proportional integral
FOPID	Fractional order proportional integral derivative
FOPTD	First order plus time delay
F-MIGO	Fractional M_s constrained integral gain optimization
IAE	Integral absolute error
IFPTD	Integrating first order plus time delay
IMC	Internal model control
IMC-PID	Internal model control - proportional integral derivative
IPTD	Integrating plus time delay
ISE	Integral squared error
ITAE	Integral time absolute error
LQR	Linear quadratic regulator
MIGO	M_s constrained integral gain optimization
NIOPTD	Noninteger order plus time delay
OS	Overshoot
PD	Proportional derivative
PFI	Performance fragility index
PI	Proportional integral
PID	Proportional integral derivative
RFI	Robustness fragility index
SOPTD	Second order plus time delay
ST	Settling time
TV	Total variation

NOMENCLATURE

C	Controller
C_{IMC}	IMC controller
d	Disturbance
e	Error
F/f	IMC filter/ fractional IMC filter
$FI_{\Delta 20}$	Delta 20 fragility index
G	Process
G_c	Controller
G_{IMC}	IMC controller
G_m	Process model
G_p	Process
$\widetilde{G}$	Process model
J_E	Integral absolute error
K	System gain
K_d	Derivative gain
ΔK	Change in system gain
L	Time delay
ΔL	Change in time delay
M_s	Maximum sensitivity
PI^{λ}	Fractional order proportional integral
$PI^{\lambda}D^{\mu}$	Fractional order proportional integral derivative
p	Fractional order of IMC filter
r	Set point
S	Sensitivity function
T	Time constant
T_d	Derivative time
T_i	Integral time
T_1, T_2	Time constants
$T(s)$	Complementary sensitivity function
u	Controller output

W	Multiplicative uncertainty bound on S
y	Controlled variable
λ	Fractional order of the integrator
μ	Fractional order of the differentiator
γ	Fractional filter time constant
l/δ	Multiplicative uncertainty bound on T
β	Additional degree of freedom of IMC filter
ε	Variation in controller parameters
α,β	Fractional orders of the NIOPTD system
η	Additional degree of freedom

Chapter 1

Introduction and Objectives

1. Introduction and Objectives

1.1 Introduction

In modern control engineering, the design gap exists between the complex physical system under investigation and the process model used in the control system synthesis. Controller design for many industrial systems such as level, flow, temperature and pressure control loops in chemical industries, power plants, oil industries and aerospace systems is challenging as they are often burdened with problems such as structural complexity, uncertainties, large transportation lags, nonlinearities and external perturbations. The main difficulty is associated with the design of controller for processes modeled as second order systems, integrating systems and non-integer order systems with time delay. For these systems, desired closed loop response cannot be achieved with conventional PID (Proportional Integral Derivative) controller because of the practical problems (lags, nonlinearities and perturbations) (Feliu-Batlle et al., 2009; Barbosa et al., 2007) associated with the industrial processes. The situation worsens if disturbance rejection is the major requirement along with set point tracking to meet the specification of desired output.

1.1.1 General

Mathematical models of a process take various forms, such as differential equations, state-space equations and transfer functions. Most of the real processes are modeled by constructing mathematical equations based on physical laws. The success of controller design can be attributed to reasonably accurate modeling of the real process. A process model has to be used in practice before their application in industries. Real processes modeled using integer order differential equations results in integer order models. There has been tremendous work on the design of controller for classical integer order models. However, delay is present in all the industrial processes due to the transport delays associated with sensors and delays involved in the communication of signals. The transfer functions models of the majorly used the integer order time delay systems in this research work are:

Second order plus time delay (SOPTD) system, $G_m(s)=\frac{Ke^{-Ls}}{(T_1s+1)(T_2s+1)}$ (1.1)

Integrating plus time delay (IPTD) system, $G_m(s)=\frac{K}{s}e^{-Ls}$ (1.2)

Now a days, processes are even modeled as time delay systems of non-integer order as they represent the process dynamics in a better way than integer order systems. Any physical system represented by a differential equation whose derivative order is a real fractional number can be called a non-integer order system (Atherton et al., 2014). The significance of non-integer order representation is that fractional-order differential equations are more adequate to describe some real world systems than integer-order models. The NIOPTD process models are:

NIOPTD-I, $G_m(s)=\frac{K}{Ts^{\alpha}+1}e^{-Ls}$ (1.3)

NIOPTD-II, $G_m(s)=\frac{K}{s^{\alpha}+2\zeta\omega_n s^{\beta}+\omega_n^2}e^{-Ls}$ (1.4)

The closed loop performance of any time delay system can be assessed with the measures listed in Table 1.1.

Table 1.1 Performance measures

Integral square error, ISE	$\int_0^{\infty} e^2(t)dt$
Integral absolute error, IAE	$\int_0^{\infty} \|e(t)\|dt$
Integral time absolute error, ITAE	$\int_0^{\infty} t\|e(t)\|dt$
Percentage overshoot, %OS	$\frac{y_{peak}-y_{ss}}{y_{ss}}\times 100$
Settling time	time taken for the response to settle within 2% to 5% of its final value
Sensitivity, S(jω)	$\frac{1}{1+G_c(j\omega)G_p(j\omega)}$
Maximum sensitivity, M_s	$\max_{0<\omega<\infty} \|S(j\omega)\|$
Total variation, TV	$\sum_{i=0}^{\infty} \|u_{i+1}-u_i\|$

The closed loop stability of system should be verified in presence of model uncertainties for robustness of the designed controller which is derived under nominal process conditions. The designed controller should be able to provide better closed loop performance (good servo response and regulatory response) irrespective of the perturbations in process parameters which are common in practice. The controller that ensures good response characteristics for perturbations in system

gain, time delay and time constant is said to be robust. This robust stability of closed loop system can be verified with small gain theorem (Morari and Zafiriou, 1989; Maciejowski, 1989).

The performance of any controller need to be estimated not only for perturbations in process parameters but also for perturbations in controller parameters. This is done with the help of controller fragility analysis (Alfaro and Vilanova, 2012). The fragile nature of the controller can be investigated both in terms of robustness and performance.

1.2 Motivation

A closed loop control system encounters different combinations of plant and controllers while handling real world problems. They include the integer or fractional order of either plant or controller or both. In practice, the plant models have been obtained as integer order models and it is natural to consider the fractional nature of the controller. PID controllers are still widely used in the industry because they are easy to implement and perform well for wide class of processes. PID controllers in general are not very well suited for control of processes with long dead time, nonlinearities and perturbations since they can cause stability issues for these closed loop systems. The controller design of these processes is a challenging problem.

The efforts of control engineers and scientists lead to the development of fractional order controller ($PI^{\lambda}/PI^{\lambda}D^{\mu}$) tuning rules. Podlubny (1999) demonstrated a better response for integrator and differentiator of the PID controller rise to the fractional powers λ and μ. This is achieved with the help of fractional calculus (Miller and Ross, 1993). Fractional order PID (FOPID) controllers with additional tuning parameters can provide better closed loop performance and robustness features compared to classical PID controllers. Although there are many rule based methods and analytical tuning methods, it is difficult to adjust PID parameters properly to meet the requirements. The closed loop performance of such systems can be enhanced using fractional controller. The fractional controller means any controller consisting of fractional term in their structure. The fractional controller structure considered in this thesis comprises of PID/FOPID term cascaded with fractional term rather FOPID controller. Though, there are many works on the design of FOPID controller there is limited work on the design of considered fractional controller structure. The standard internal model control (IMC) design procedure has been used to design the proposed fractional controller.

The well-known internal model control based tuning rules have the advantage of using only a single tuning parameter to achieve a clear tradeoff between closed-loop performance and robustness to model inaccuracies. It is clear that, in the IMC-PID approach, the performance of the PID controller is mainly determined by the IMC filter structure. In majority of the previous works on IMC based controller design, the integer IMC filter structure has been used. Integer order IMC filter structures of higher order have also been used for controller design. Clearly, the controller designed using IMC procedure and integer order IMC filter structure results in integer order controller. Therefore, in the present thesis fractional IMC filter structure has been chosen for designing the fractional controller. The selection of fractional IMC filter structure has to be made considering the performance and robustness of the resulting fractional controller. The fractional IMC filter used in the IMC method plays a crucial role because tuning parameters in the IMC based controller are those associated with the fractional IMC filter. Till now, there is a little progress observed on design of fractional filter controllers. It is with this intention that the present work has been undertaken.

1.3 Objectives

For the performance enhancement of integer and non-integer order time delay systems, the fractional controllers based on IMC is the most effective method. The present research work aims at exploring the design and analysis of fractional filter PID/FOPID controller based on IMC scheme by the use of higher order fractional filter structure.

The objectives of this thesis are set as follows:

1. To develop fractional filter IMC-PID controller for enhanced performance of second order plus time delay processes
2. To design fractional filter IMC-PID controller for improved performance of integrating processes with time delay
3. To develop fractional filter fractional IMC-PID controller for enhanced performance of non-integer order plus time delay processes
4. To design fractional filter IMC-PID controller for cascade loops

All example systems used to demonstrate the proposed method are simulated in MATLAB (2014b) environment using FOMCON toolbox and Simulink.

1.4 Problem statement

The purpose of this work is to develop a systematic analytical method to evaluate the feasibility analysis and design of fractional filter IMC-PID controllers to enhance the closed loop performance. The methodology should output different designs for various classes of systems: second order plus time delay systems, integrating systems (integer order systems) and non-integer order plus time delay systems. In addition, design of fractional filter controllers for cascade loops consisting of integer order time delay systems has also been taken. To design the fractional filter controller, IMC design method has been used considering fractional IMC filter structure of different orders. It is also required to consider higher order Pade's approximation for time delay during the controller design. The major problem here is the identification of optimum fractional IMC filter structure. Hence, there is a need to develop systematic procedure for identification of optimum fractional IMC filter structure based on the robustness. The designed fractional filter controller shall be proved to give enhanced performance by using different performance measures for nominal process conditions; for perturbations in the process parameters and for noise in the measured output. Further, the performance of designed controllers need to be estimated for controller parametric uncertainties using fragility analysis.

1.5 Contributions of the scholar

- A systematic procedure is proposed based on robustness for identification of optimum fractional IMC filter structure
- The application of proposed fractional filter controller is generalised by checking the closed loop performance on broad class of case studies.
- The tuning parameters of the controller are exclusively associated with the fractional filter term of the controller
- The fragility of the proposed controllers is investigated for perturbations in the controller parameters.
- Numerical simulation of different classes of integer and non-integer order processes with time delay to illustrate the proposed methods.

1.6 Organization of the thesis

This thesis is organized in eight chapters.

Chapter 1 presents an overview of the state of current research in the area of fractional control with key objectives of the present research work.

Chapter 2 deals with the literature review related to the entire research work. Details of the work on controller design for SOPTD, IPTD and NIOPTD systems is reviewed in this chapter. It also presents the literature on controller design for cascade control loops and fragility analysis. The summary of the gaps identified in the literature are discussed.

Chapter 3 presents the fractional filter IMC-PID controller design using fractional IMC filter for second order plus time delay processes. Then, the application of fractional filter IMC-PID controller for an unstable inverted pendulum system is discussed.

In Chapter 4, an improved design of fractional filter IMC-PID controller is proposed for SOPTD processes using higher order fractional IMC filter. The optimum higher order fractional IMC filter structure is identified using systematic analytical design procedure. Also, the optimum M_s range is identified for robust performance of the closed loop system.

Chapter 5 highlights the need to control the integrating processes and the control of same using fractional filter IMC-PID controller. The fractional filter PID controller is designed for different integrating processes with time delay after identifying the optimum higher order fractional IMC filter structure according to the analytical design procedure. β versus IAE graphs are plotted for easy identification of optimum IMC filter structure. The controller fragility is estimated for uncertainties in the controller parameters.

Chapter 6 deals with the fractional filter fractional IMC-PID controller design for NIOPTD processes. It also focuses on the design of fractional filter fractional order PID controller for higher order systems approximated as NIOPTD systems. Also, the fragility of the controller is investigated in terms of robustness and performance for variation in the controller parameters. The effect of L/T ratio on the closed loop performance is studied for large changes in time delay.

Chapter 7 covers the design of fractional filter IMC-PID controller for cascade loops. The inner loop controller is designed using integer order IMC filter. The outer loop controller is designed using fractional IMC filter structure for different time delay systems. The robust stability

of overall cascade control loop is identified through magnitude plots using complementary sensitivity functions. Also, the fragility is studied for controller parameter variations

Chapter 8 draws the general conclusions and perspective of future work.

Appendix A covers the MATLAB code and Simulink block diagram for Example 1 used in chapter 3.

Appendix B includes MATLAB code and Simulink block diagram for closed loop response of Example 1 considered in chapter 4. Also, the MATLAB code is provided for magnitude plot.

Appendix C provides the MATLAB code and Simulink block diagram for obtaining the closed loop response of Example 1 studied in chapter 5.

Appendix D covers the MATLAB code and Simulink block diagram for Example 1 studied in chapter 6.

Appendix E contains the MATLAB code and Simulink block diagram for providing the closed loop response of cascade control loop (Example 1) considered in chapter 7.

Chapter 2

Literature review

2. Literature Review

The main purpose of a feedback control system is to assure the desired response characteristics of closed loop system under steady state and dynamic conditions. To ensure the response characteristics the system must satisfy the performance criteria: stable, minimal effect of disturbance, smooth response to set point change, no offset, no extra control action, robust to plant-model mismatch and ability to deal with constraints on inputs and outputs.

The performance of a closed loop system depends on the design and tuning of the controller used for control. In the process control industries, different transport delays, communication delays associated with sensors and transducers, computational time, time-delay effects are inevitable. Therefore, the design and application of controller which takes the time-delay into account are necessary.

The works on the controller design for various integer order plus time delay systems (second order plus time delay (SOPTD), integrating plus time delay (IPTD) systems) and noninteger order plus time delay (NIOPTD) systems are reviewed in the following sections. Also, the summary of literature on controller for cascade control loops and fragility analysis is presented.

2.1. Integer order plus time delay systems

2.1.1. Second order plus time delay (SOPTD) systems

Chen and Seborg (2002) designed a PI/PID controller analytically based on disturbance rejection using DS method. Setpoint weighting was used to suppress the overshoot in the servo response and derivative weighting was also used to handle the measurement noise. Rao et al. (2009) designed a DS based PID controller in series with lead-lag compensator, and they have used setpoint weighting to achieve better servo response. Srivastava et al. (2016) proposed a PID controller using linear quadratic regulator (LQR) and pole placement based approach. The PID parameters were calculated using the user defined values of closed loop damping ratio and natural frequency.

The IMC method has been the mostly used for designing the controller as the resulting tuning rules have only one tuning parameter. There are limited tuning rules of IMC - PID controller for SOPTD processes (Weigand and Kegerreis, 1972). However, the tuning rules are still evolving to ensure better disturbance rejection for SOPTD processes as the IMC-PID controller doesn't always give good disturbance rejection (sluggish response) (Vilanova and Visioli, 2012; Jeng et al., 2014; Lee et al., 2013). There was a work in literature addressing the implicit disturbance rejection capacity of closed loop controller (Alagoz et al., 2015). Lee et al. (1998) designed a PID controller based on IMC scheme and the controller parameters were obtained using Maclaurin series. Further, they have studied different IMC based PID tuning rules to control SOPTD processes. Panda et al. (2004) proposed a new PID tuning rule based on closed loop trajectory specification.

Shamsuzzoha and Lee (2007) used IMC method to design PID controller. In their work, an optimum IMC filter was identified by observing the closed loop response after designing the PID controller for different process models which gives minimum IAE for a specific M_s. In addition, guidelines were provided for selecting the closed loop time constant. Shamsuzzoha and Lee (2008) derived an IMC based PID controller cascaded with lead-lag compensator using analytical method for SOPTD processes. They have also used setpoint filter to minimize overshoot in the closed loop response. Shamsuzzoha (2015) designed an IMC - PID controller for disturbance rejection with an intention to have single tuning rule for different types of processes using second order IMC filter. Madhuranthakam et al. (2008) designed a PID controller whose parameters were optimized based on the minimization of IAE. Wang et al. (2016) designed an IMC-PID controller using pole-zero conversion with a unified IMC filter. An imaginary filter was used during the controller design to calculate the PID parameters. Also, setpoint weighting was used to minimize the overshoot.

The work on IMC-PID controller design for SOPTD systems is summarized in Table 2.1.

Table 2.1 Reported work on IMC based PID controller design for SOPTD systems

S.No.	Author	Description	Remarks
1	Lee et al. (1998)	PID parameters were obtained by approximating the controller in s-domain with a Maclaurin series	Improved closed loop response is observed with increase in dead time of the process
2	Shamsuzzoha and Lee (2007)	Optimum IMC filter structures were proposed to design PID controller for different process models to improve the disturbance rejection	Simulations are carried out for same degree of robustness (M_s). Better performance is observed for lag dominant processes
3	Shamsuzzoha and Lee (2008)	PIMC based PID controller cascaded with lead-lag compensator is proposed for improved disturbance rejection	Used set point filter to suppress the overshoot and simulation results are obtained for same degree of robustness
4	Shamsuzzoha (2015)	Unified tuning rule is proposed for different process models based on IMC for rejecting the disturbance	Suitable for lag dominant processes and used set point filter to reduce the overshoot
5	Wang et al. (2016)	Designed IMC based PID controller for different time delay models using an unique IMC filter and pole zero conversion	Improved performance is shown compared to the recent tuning methods

2.1.2. Integrating plus time delay (IPTD) systems

There have been several IMC based controllers for time delayed integrating processes. Rao and Sree (2010) reported a simple PID controller using IMC principles. Fruehauf et al. (1994) developed simplified rules to tune IMC-PID controller that resemble Ziegler-Nichols tuning rules to give a less aggressive response. An IMC-PID controller was designed for integrating processes approximated as an unstable model of first order with pole located close to origin (Lee et al., 2000; Shamsuzzoha and Lee, 2008). A PID controller with derivative filter (Rice and Cooper, 2002) and a PID with filter controllers were developed for integrating processes using IMC method (Arbogast

and Cooper, 2007). Shamsuzzoha and Lee (2008) developed an IMC-PID controller for a group of integrating processes using second order to fourth order IMC filter. They have also used set point filter to minimize overshoot. Panda (2009) proposed an IMC-PID controller for integrating unstable systems using integer order IMC filter.

Chia and Lefkowitz (2010) proposed an alternative IMC scheme for integrating processes by approximating the integrator by a lag filter of order one with a huge time constant. Liu and Gao (2011) developed a modified IMC based controller for rejecting different disturbances on the integrating process. Rao et al. (2011) developed a PID controller using direct synthesis method, IMC and stability analysis method followed by performance comparison. Zhao et al. (2011) proposed a sensitivity based IMC-PID controller for integrating processes approximated as a delayed first order model. Vanavil et al. (2014) developed an IMC based PID controller sequentially connected to a lead-lag filter. Jin and Liu (2014) proposed a 2Dof (degree of freedom) PID controller using IMC scheme. Further, a 1Dof controller was proposed with a trade-off between performance/robustness and servo/regulatory performance. Kumar and Sree (2016) proposed a PID plus lead-lag filter controller for a class of non-self-regulating processes using integer order IMC filter whose denominator order is chosen as one less than the numerator.

The reported work on IMC - PID controller for integrating systems is presented in Table 2.2.

Table 2.2 Description of the work on IMC based PID controller design for integrating systems

S.No.	**Author**	**Description**	**Remarks**
1	Fruehauf et al. (1994)	Proposed simple IMC-PID tuning rules for Chemical process loops. Also, proposed rules for setting filter action	Reported that derivative action and filter should not be used together as they cancel each other
2	Lee et al., 2000	IMC based PID controller is proposed for integrating process approximated as unstable FOPTD model. PID settings were obtained from Maclaurin series expansion	Improved performance was shown compared to the existing methods

3	Shamsuzzoha and Lee (2008)	Proposed PID controller cascaded with lead lag compensator using IMC method. Simulations are carried out by tuning the controller for same M_s	The integrating process was approximated as SOPTD model for application of proposed method
4	Chia and Lefkowitz (2010)	IMC based controller is proposed integrating model approximated as a first-order model with very large time constant.	Proposed design introduced a second tuning parameter that adds flexibility in obtaining the desired closed loop response
5	Liu and Gao (2011)	IMC based controller is developed for rejecting the step or ramp type disturbances	The proposed method can be used to reject step disturbance from input side in presence of unknown load disturbance
6	Zhao et al. (2011)	IMC based controller is designed for integrator approximated as first order model with time delay. Analytical approach is followed for obtaining the tuning parameter based on M_s.	Better performance is observed with the proposed method. But, the integrator is approximated as a first order model
7	Vanavil et al. (2014)	IMC based PID controller in series with lead-lag filter is proposed for integrating process approximated as unstable FOPTD model. Tuning parameter was chosen using M_s.	Tuning parameter was chosen as per a systematic procedure
8	Kumar and Sree (2016)	IMC - PID controller is designed for different integrating processes. Tuning parameter is chosen with a tradeoff between performance and robustness	Controllers are tuned for pre-defined M_s. Proposed controller is better in performance compa-red to recent tuning methods

2.1.3 Controller for cascade loops

Krishnaswamy et al. (1990) and Seborg et al. (2004) addresses that the Cascade control is an advanced control structure widely used in chemical process industry with flow, pressure, level and temperature control loops to attenuate the external disturbances for improved and rapid performance of the single feedback loop. This structure also handles nonlinearities in the process elements and ensures accurate control performance in presence of large time delays. The enhanced performance of cascade system depends on the effective tuning of these loops (Huang et al., 1998; Leva and Marinelli, 2009) and PID controllers are mostly used for the purpose due to their adopted structure and range of tuning methods available (Song et al., 2003; Brambilla and Semino, 1992; Veronesi, and Visioli, 2011; Vivek and Chidambaram, 2013).

Raja and Ali (2017) reviewed the different series cascade control structures available in the literature. Leva and Donida (2009) used IMC based tuning for cascade systems which offers flexibility in tuning. Azar and Serrano (2014) developed an IMC based PID controller for cascade loop: first the controller for inner loop is designed and after that the controller for outer loop is designed by considering the desired response of inner loop. Vu and Le Hieu Giang (2016) developed FOPI controller tuning rules for cascade control systems. The analytical controller design using fractional IMC filter produce a fractional filter PID controller in spite of conventional three term PID controller (Padula and Visioli, 2014).

The summary of work on controller design for cascade loops is presented in Table 2.3.

Table 2.3 Work summary on controller design for cascade loops

S.No.	Author	Description	Remarks
1	Huang et al., 1998	Cascade loop is tuned in terms of figures or simple equations. Perfo-rmance specifications are used for the selection of tuning parameters	Developed with simplicity for application
2	Song et al., 2003	The process parameters of both the loops are identified using relay feedback test. Established PID tuning rules are used to tune both the loops.	The method was simple and can be easily integrated into auto tuning systems

3	Leva and Donida (2009)	Proposed a tuning method for cascade control system based on single relay experiment and IMC	Proposed method is simple and involves less computations
4	Azar and Serrano (2014)	IMC based PID controller is designed for both the loops using integer order IMC filter and tuned for specific gain and phase margin	Low performance index values and good disturbance rejection
5	Vu and Le Hieu Giang (2016)	Analytical design of fractional order PI controller is proposed for cascade loop using fractional calculus and IMC	Improved performance is shown with the fractional controller

2.2 Noninteger order plus time delay (NIOPTD) systems

Oustaloup (1991) initiated the work on fractional order controllers and Podlubny (1999) proposed an FOPID or $PI^{\lambda}D^{\mu}$ controller with the help of fractional calculus. The $PI^{\lambda}D^{\mu}$ controller was developed for higher order systems approximated as lower order time delay systems (Monje et al., 2008; Padula and Visioli, 2011). Shah and Agashe (2016) reported several tuning rules for tuning the FOPID controller and fractional filter PID controller for integer order time delay systems (Sánchez et al., 2017).

Higher order models describe the process dynamics accurately than lower order models (Isaksson and Graebe, 1999; Malwatkar et al., 2009). An alternative to preserve the dynamics while ensuring satisfactory control is to approximate higher order models as NIOPTD models (Pan and Das, 2013). Bongulwar and Patre (2017) proposed a FOPID controller whose parameters are identified based on the stability regions of closed loop system. Das et al. (2011) proposed $PI^{\lambda}D^{\mu}$ controller tuning strategies in frequency domain and time domain for NIOPTD systems. Tavakoli-Kakhki and Haeri (2011) proposed an analytical tuning method of FOPID controller for fractional order systems after reducing the higher order fractional system by retaining its dynamics. A $PI^{\lambda}D^{\mu}$ controller was also designed using soft computing technique for delay free non-integer order systems (Liu et al., 2015) and by using optimization (Zeng et al., 2015). Vinopraba et al (2012) proposed. Maamar and Rachid (2014) proposed an IMC-PID fractional order filter controller for

integer order systems with and without time delay. It was extended to delay free, non-integer order processes and non-integer order time delay processes (Bettayeb and Mansouri, 2014). With respect to integer order systems, the simulations were performed on few delay free systems of second order and first order with added integrator. In both cases, the filter time constant and order were chosen depending on the phase margin and gain cross over frequency. Li et al. (2015) developed an IMC-PID controller for NIOPTD systems using integer order IMC filter.

The details of the work on IMC based FOPID controller for NIOPTD systems is summarized in Table 2.4.

Table 2.4 Summary of the work on IMC based FOPID controller design for NIOPTD systems

S.No.	Author	Description	Remarks
1	Das et al. (2011)	Proposed a procedure to reduce higher order models to NIOPTD-I and NIOPTD - II models. Compared the performance of FOPID controller using time domain and frequency domain approaches	Concluded that each FOPID controller tuning approach has its own strength and weakness and its usage depends on the nature of control problem
2	Tavakoli-Kakhki and Haeri (2011)	A new model reduction technique is proposed for approximating complicated fractional models into lower order fractional models. Then, an analytical design of FOPI/FOPID controller was proposed based on IMC	Proposed method was efficient for reduced fractional order models with the help of several simulation examples
3	Maamar and Rachid (2014)	Proposed an analytical PID fractional filter controller using fractional IMC filter structure for integer order systems	Proposed controllers using only Taylor series approximation and first order Pade's procedure for time delay

4	Bettayeb and Mansouri, 2014	Proposed fractional filter FOPID controller using fractional IMC filter structure	Taylor series approximation and first order Pade's procedure for time delay was used during the controller design
5	Li et al. (2015)	Analytical design of fractional IMC-PID controller is proposed based on maximum sensitivity	Simple controller structure and easier tuning method. IMC filter of integer order is used.

2.3 Fragility analysis

A prominent topic to be considered is the controller fragility to variations in the controller parameters. Keel and Bhattacharyya (1997) found out that the fragility analysis carried out for controllers designed using H_2, H_∞ and l_2 norms provide optimal and robust performance but highly fragile controller for minor changes in the controller parameters. The fragile nature of the controller would make the system unstable. There are several works on the design of nonfragile controllers (Ho M-T, 2000) and an index to estimate the fragility (Alfaro, 2007) of the controllers. This fragility is addressed in the context of not only the robustness but also the closed loop performance to produce robust and optimal closed loop system (Alfaro et al., 2009; Alfaro and Vilanova, 2012; Padula and Visioli, 2016). The reported work on fragility of the controller is given in Table 2.5.

Table 2.5 Reported work on controller fragility analysis

S.No.	**Author**	**Description**	**Remarks**
1	Keel and Bhattacharyya (1997)	Observed that higher order and highly fragile controllers were produced when designed under H_2, H_∞ and l_1 norms.	Deep understanding of many sophisticated issues is needed for controller design. Minimum change in controller parameters made the system unstable
2	Ho M-T, 2000	Designed a PID controller which gives stable response and tolerate controller parameter perturbations	Designed non-fragile PID controller

3	Alfaro, 2007	Proposed fragility index for PID controllers	Fragility of different controllers can be made for a specific perturbation in the controller parameters
4	Alfaro and Vilanova (2012)	Proposed an index for measuring the fragility in terms of robustness and performance	Controller fragility depends on both the tuning rule design considerations and controller implementation

2.4 Summary

It is observed from literature that there is more work on the design of PID controller using IMC method for integer order time delays systems (second order systems and integrating plus time delay systems). Moreover, integer order IMC filter structures have been used in the previous works. There is lack of work on the design of fractional filter controller using IMC method. The little work reported in the literature used lower order fractional IMC filter structure (Maamar and Rachid, 2014; Bettayeb and Mansouri, 2014; Li et al., 2015) to design controller for integer and noninteger order systems.

It is found that there is a gap on the design of fractional filter controller using higher order fractional IMC filter structures. In addition, it would be beneficial to include higher order Pade's approximation for time delay in the design. It would be good to develop a generalized systematic procedure for identifying the optimum fractional IMC filter structure and to identify the tuning parameters based on robustness (M_s). It was also found that the researchers are observing the closed loop performance for perturbations in the process parameters but not for perturbations in the controller parameters. Hence, the performance of proposed controller for perturbations in their parameters need to be studied. This can be achieved through the fragility analysis (Alfaro, 2007; Alfaro and Vilanova, 2012).

Chapter 3

Fractional filter IMC-PID controller design for SOPTD processes

3. Fractional filter IMC-PID controller design for SOPTD processes*

In this chapter, a simple method of designing a fractional filter IMC-PID controller is proposed for second order plus time delay (SOPTD) processes using IMC scheme. There has been limited number of tuning rules for SOPTD processes developed using direct synthesis method and IMC method. The proposed fractional filter IMC-PID controller using fractional IMC filter results in a controller structure composed of PID controller cascaded with fractional filter term. Simulations have been performed on several second order lag dominant and delay significant processes. Robustness checks are performed for variations in the process parameters and robustness analysis is carried out using sensitivity functions. The proposed controller results in an enhanced control performance for nominal process parameters and with parameter variations. In addition, the effect of measurement noise is also studied for set point tracking and load disturbance variations. A case study of inverted pendulum system is considered to validate the performance of proposed fractional filter PID controller. The system is stabilized by using a compensatory function to cancel out the unstable poles and zeros in the model. Now, the controller is designed for the stabilized model producing a PID controller along with fractional filter. The simulations are performed for set point tracking and disturbance rejection with nominal process model and with perturbations. The results show an improvement in the control performance. Further, robustness analysis is done to check the stability of the closed loop system for parameter uncertainties.

3.1. Fractional filter IMC-PID controller design for second order plus time delay processes

3.1.1. Introduction

Proportional Integral Derivative (PID) controller has been the main choice for industrial sector applications from centuries. In spite of the advancements in control, PID controller is still being

*This work is published in Cogent Engineering (Taylor Francis) - https://doi.org/10.1080/23311916.2017.1366888**;** the application in section 3.2 is published in IEEE explore – doi:10.1109/ICSTM.2017.8089195

used by 90% of the applications due to its ability to control wide range of industrial processes (Shamsuzzoha, 2013). Moreover, the simple structure and the availability of tuning rules contribute to the wider use of PID controller (Astrom and Hagglund, 1995; Skogestad, 2003). However, the controller tuning methods are still evolving to ensure improved closed loop performance of the processes as they are associated with time delays, external perturbations and non-linearities (Vilanova and Visioli, 2012; Silva et al., 2007; Lee et al., 2013; Jeng et al., 2014). The real processes need to be approximated as lower order models for the application of PID tuning rules. The SOPTD models represent better dynamics of the processes than FOPTD models. The PID tuning rules for SOPTD processes are less (Panda et al., 2004; Weigand et al., 1972) in number compared to FOPTD processes. Hence, the current work is carried out on SOPTD processes.

The direct synthesis (DS) method and internal model control (IMC) schemes are mostly used for designing the controller for SOPTD processes (Chen and Seborg, 2002; Lee et al., 1998; Panda et al., 2004). DS controllers are designed for the desired trajectory of the closed loop transfer function. But, the design not necessarily results in a PID form of controller. Direct synthesis controllers are suitable for set point tracking and don't give satisfactory performance for disturbance rejection. The IMC based design results in a PID controller structure by proper approximation of the process model. Several controller tuning methods based on IMC-PID method have been proposed for SOPTD processes. The design was based on the selection of optimum IMC filter and controller structure (Shamsuzzoha and Lee, 2008; Shamsuzzoha and Lee, 2007). An analytical method of designing IMC-PID controller was proposed for all kinds of time delay systems (Shamsuzzoha, 2015). For improved disturbance rejection a PID controller cascaded with lead-lag compensator has been used (Shamsuzzoha and Lee, 2008; Rao et al., 2009). Further, the overshoot in servo response was reduced by utilizing set point weighting. An optimal tuning method for SOPTD processes by optimizing IAE was also proposed (Madhuranthakam et al., 2008). A graphical method of obtaining PID controller parameters for SOPTD processes through dominant pole placement approach with assured gain margin and phase margin was also proposed (Srivastava and Pandit, 2016).

Some of the design methods presented above are suitable for set point tracking while others were exclusively designed for disturbance rejection. A few of the design procedures doesn’t guarantee the PID form of controller structure which is widely used in industries while still providing better closed loop performance. Though, the IMC based methods had only one tuning

parameter they have used set point weighting and set point filter along with controller to suppress the overshoot. So, there was a need to choose the weighting factor or filter parameter along with the controller settings. Recently, an IMC-PID controller was proposed using pole zero conversion with a unified IMC filter structure (Wang et al., 2016). The design also used derivative coefficient weighting along with pole zero conversion to obtain the controller settings for SOPTD processes. Also, the overshoot was minimized with set point weighting technique. Majority of the controllers designed for SOPTD processes were based on the use of higher order IMC filter (second to fourth order) and by using optimization. The current work focuses on the design of a simple IMC-PID controller using fractional IMC filter for SOPTD processes. The resulting controller structure consists of a PID in series with fractional filter. The performance metrics like ISE, IAE, %OS and M_s are used to estimate the closed loop performance of SOPTD processes. The effectiveness of the present method is illustrated with simulations carried out on over damped and critically damped SOPTD processes using MATLAB and Simulink. In addition, the simulation is carried out on a higher order process reduced to SOPTD process. The effects on process output performance in presence of parametric uncertainties and output noise have also been discussed.

3.1.2. Fractional filter IMC-PID controller design

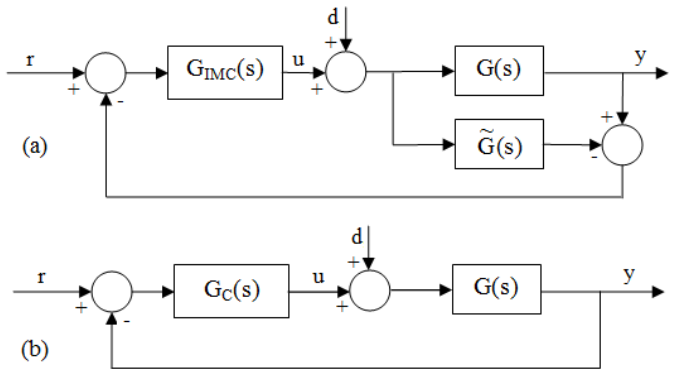

Fig 3.1 Block diagram: (a) IMC scheme (b) feedback control structure

The IMC scheme and feedback control loop with internal blocks are shown in Fig 3.1, where G(s), $\tilde{G}(s)$, $G_{IMC}(s)$ and $G_C(s)$ representing process, process model, IMC controller and transfer function of the traditional controller. Let r, y, u and d be the set point, controlled variable, control input and disturbance respectively.

The controller design using IMC method is given as follows:

1) Decompose the process model into non-invertible and invertible parts

$$\tilde{G}(s)=\tilde{G}^{+}(s)\tilde{G}^{-}(s) \tag{3.1}$$

Where $\tilde{G}^{+}(s)$ is non-invertible contains all time delays and unstable zeros. $\tilde{G}^{-}(s)$ is invertible and contains minimum phase elements.

2) The IMC controller is given by

$$G_{IMC}(s)=\frac{f(s)}{\tilde{G}^{-}(s)} \tag{3.2}$$

Where f(s) is the IMC filter

3) The equivalent feedback controller is

$$G_C(s)=\frac{G_{IMC}(s)}{1-G_{IMC}(s)\tilde{G}(s)} \tag{3.3}$$

3.1.2.1. Proposed fractional filter IMC-PID controller design

The proposed controller has the structure

$$G_c(s)=(\text{fractional filter})K_p\left(1+\frac{1}{T_i s}+T_d s\right) \tag{3.4}$$

Consider a SOPTD model

$$G(s)=\frac{Ke^{-Ls}}{(T_1 s+1)(T_2 s+1)} \tag{3.5}$$

The fractional IMC filter used is

$$f(s)=\frac{1}{\gamma s^{p}+1} \tag{3.6}$$

Now, the IMC controller according to eq. (3.2) is

$$G_{IMC}(s)=\frac{(T_1 s+1)(T_2 s+1)}{K}\left(\frac{1}{\gamma s^{p}+1}\right) \tag{3.7}$$

Finally, the fractional filter IMC-PID controller from (3.3), (3.5) & (3.7) is

$$G_C(s)=\frac{\left[\frac{(T_1 s+1)(T_2 s+1)}{K(\gamma s^{p}+1)}\right]}{1-\left[\frac{(T_1 s+1)(T_2 s+1)}{K(\gamma s^{p}+1)}\;\frac{Ke^{-Ls}}{(T_1 s+1)(T_2 s+1)}\right]} \tag{3.8}$$

$$G_C(s)=\frac{(T_1 s+1)(T_2 s+1)}{K[(\gamma s^{p}+1)-e^{-Ls}]} \tag{3.9}$$

The delay e^{-Ls} expressed as a first order fraction according to Pade's rule is

$$e^{-Ls}=\frac{1-0.5Ls}{1+0.5Ls} \tag{3.10}$$

Now, the controller becomes

$$G_C(s)=\frac{(T_1s+1)(T_2s+1)}{K\left[(\gamma s^p+1)-\left(\frac{1-0.5Ls}{1+0.5Ls}\right)\right]} \tag{3.11}$$

The above equation can be written as

$$G_C(s)=\left(\frac{0.5Ls+1}{0.5\gamma Ls^p+\gamma s^{p-1}+L}\right)\left(\frac{T_1+T_2}{K}\right)\left[1+\frac{1}{(T_1+T_2)s}+\left(\frac{T_1T_2}{T_1+T_2}\right)s\right] \tag{3.12}$$

Comparing eq. (3.4) and eq. (3.12), the controller settings are

$$K_p=\frac{T_1+T_2}{K};T_i=T_1+T_2;T_d=\frac{T_1T_2}{T_1+T_2} \tag{3.13}$$

and the fractional filter is

$$\text{filter}=\frac{0.5Ls+1}{0.5\gamma Ls^p+\gamma s^{p-1}+L} \tag{3.14}$$

The tuning parameters γ and p were chosen based on trial and error such that IAE is minimum.

3.1.2.2. Robustness analysis

The closed loop stability of system should be verified in presence of model uncertainties for robustness of the designed controller which is derived under nominal process conditions. The designed controller should be able to provide better closed loop performance (good servo response and regulatory response) irrespective of the perturbations in process parameters which are common in practice. The controller that ensures good response characteristics for perturbations in system gain, time delay and time constant is said to be robust. This robust stability of closed loop system can be verified with small gain theorem (Morari and Zafiriou, 1989; Maciejowski, 1989). According to this theorem, the closed loop system will be robustly stable if and only if

$$\|T(s)l_m(s)\|<1 \tag{3.15}$$

Where T(s) & $l_m(s)$ are the complementary sensitivity function and the bound on multiplicative uncertainty. They are defined as

$$T(s)=\frac{G(s)G_c(s)}{1+G(s)G_c(s)} \tag{3.16}$$

$$l_m(s)=\frac{G(s)-\tilde{G}(s)}{\tilde{G}(s)} \tag{3.17}$$

Where G(s) is the real process representing the nominal model (eq. (3.5)); $\tilde{G}(s)$ is the actual model of the process.

In addition to the condition for robust stability in eq. (3.15), the following inequality constraint must hold good to ensure robust closed loop performance

$$\|T(s)l_m(s)+S(s)W_m(s)\|<1 \quad (3.18)$$

Where S(s) is the sensitivity function which can be found from S(s) = 1-T(s) and $W_m(s)$ is the multiplicative uncertainty bound on the sensitivity function.

3.1.3. Results and Discussion

The performance of different SOPTD processes with the designed controller is analyzed and was compared with the control performance obtained from Wang et al. (2016) tuning method. Several SOPTD processes representing lag dominant and balanced/delay significant process dynamics are considered for simulation. In addition, the simulations are performed on a higher order process reduced to SOPTD model. The performance metrics ISE, IAE, TV and M_s used for comparison are defined as follows:

$$ISE=\int_0^\infty e^2(t)dt \quad (3.19)$$

$$IAE=\int_0^\infty |e(t)|dt \quad (3.20)$$

$$M_s=\max_{0<\omega<\infty}\left|\frac{1}{1+G(j\omega)G_c(j\omega)}\right| \quad (3.21)$$

$$TV=\sum_{i=0}^{\infty}|u_{i+1}-u_i| \quad (3.22)$$

The simulation scheme is shown in Fig 3.2. The closed loop response was observed for a step set point changes of unit magnitude with load disturbance. The quality of response was verified by introducing a white noise in the output. It is to be noted that the fractional term in fractional filter of the controller is approximated using Oustaloup method. The frequency range used for approximation is 0.01-100rad/s with an approximation order of 5.

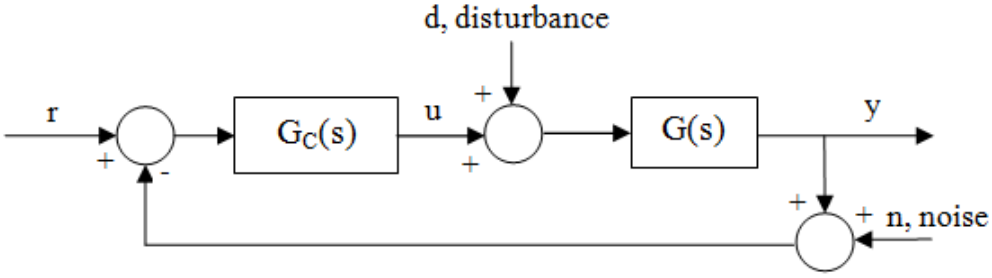

Fig 3.2 Simulation scheme

3.1.3.1. Example1

Consider the delay significant SOPTD process as studied in (Lee et al., 2013)

$$G_1(s)=\frac{e^{-2s}}{(s+1)(0.7s+1)} \tag{3.23}$$

The controller obtained for the above process with proposed method is given in eq. (3.24). The filter time constant was chosen as $\gamma=2$ and the fractional order $p=1.02$.

$$G_C(s)=\left(\frac{s+1}{2s^{1.02}+2s^{0.02}+2}\right)1.7\left[1+\frac{1}{1.7s}+0.4117s\right] \tag{3.24}$$

The controller settings as proposed in Wang et al. (2016) are $K_c=0.435$; $\tau_i=1.653$ and $\tau_d=0.4$. The weighting factor used to decrease the overshoot is 0.4. Fig 3.3 shows the servo response with step disturbance change of magnitude -0.5 applied at t=50s. The proposed controller results in a lower overshoot in the response without set point weighting which was used in Wang et al. (2016) method. Lower values of performance metrics ISE and IAE are observed with the proposed controller which are shown in Table 3.1. Fig 3.4 shows the closed loop response for perturbations of +10% in time delay and process gain. The effect of noise in the measurement is studied by introducing a white noise of zero mean and a variance of 0.0001. This is illustrated in Fig 3.5. The performance indices for noise rejection case are given in Table 3.2. Note that the TV value indicating the control effort is small with the proposed controller for the output mixed with noise. The values of M_s from Table 3.1 confirms the robustness of closed loop system for model uncertainties. Further, the robust stability of closed loop system is evaluated with a magnitude plot comprising complementary sensitivity function and an uncertainty of +10% in time delay. The robust stability characteristics are shown in Fig 3.6 and it confirms the stability condition given in eq. (3.15) making the system robustly stable.

Table 3.1 Comparison of closed loop performance of the examples

Process	**Method**	**Perfect case**			**Perturbed case**			**M_s**
		ISE	**IAE**	**%OS**	**ISE**	**IAE**	**%OS**	
G_1	Proposed	3.588	5.91	0.5	4.096	6.674	11.798	1.56
	Wang et al.	4.768	7.328	5.8	5.407	9.151	24.375	1.6
G_2	Proposed	2.563	3.991	0.5	2.787	4.508	8.152	1.77
	Wang et al.	3.025	5.034	0.55	3.323	5.893	19.88	1.787
G_3	Proposed	0.7197	1.427	0.52	0.68	1.322	0.505	1.156
	Wang et al.	0.8204	1.678	-0.18	0.7706	1.551	0.502	1.138
G_4	Proposed	5.638	8.255	0.64	6.305	10.16	11.992	2
	Wang et al.	6.822	11.43	24.37	7.919	14.67	18.476	2.16

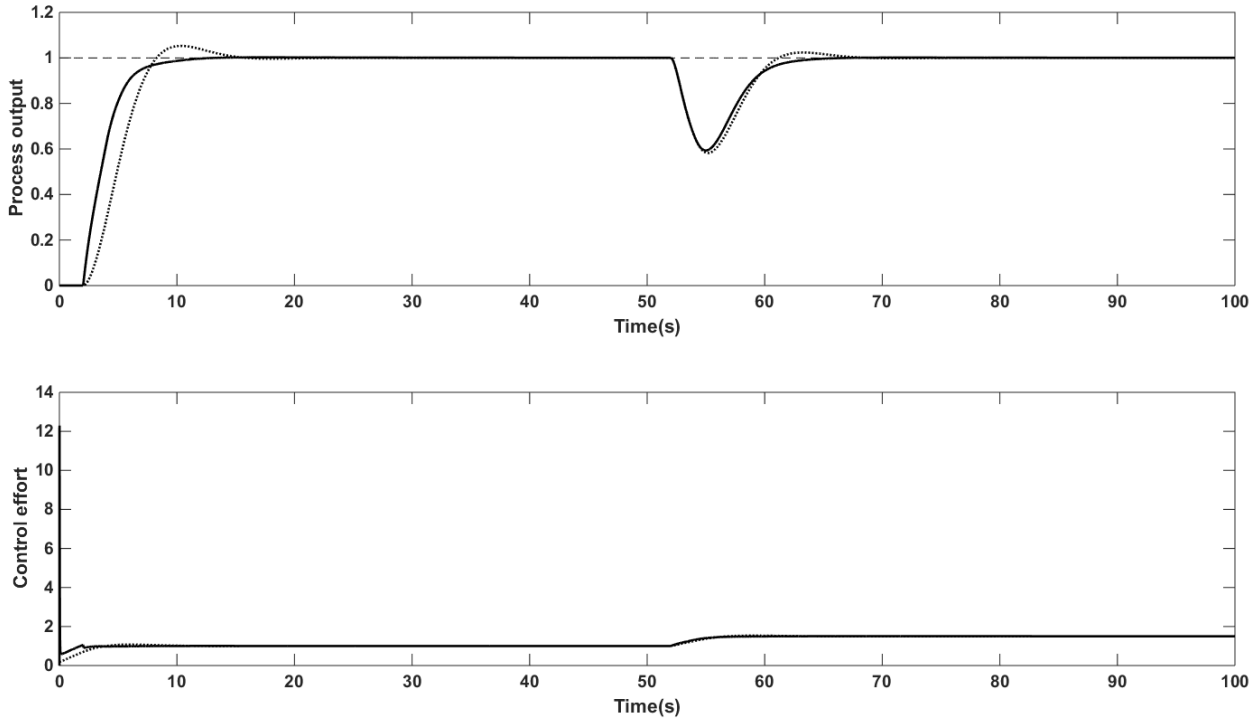

Fig 3.3 Closed loop response for G_1: Solid-Proposed, Dotted-Wang et al. (2016)

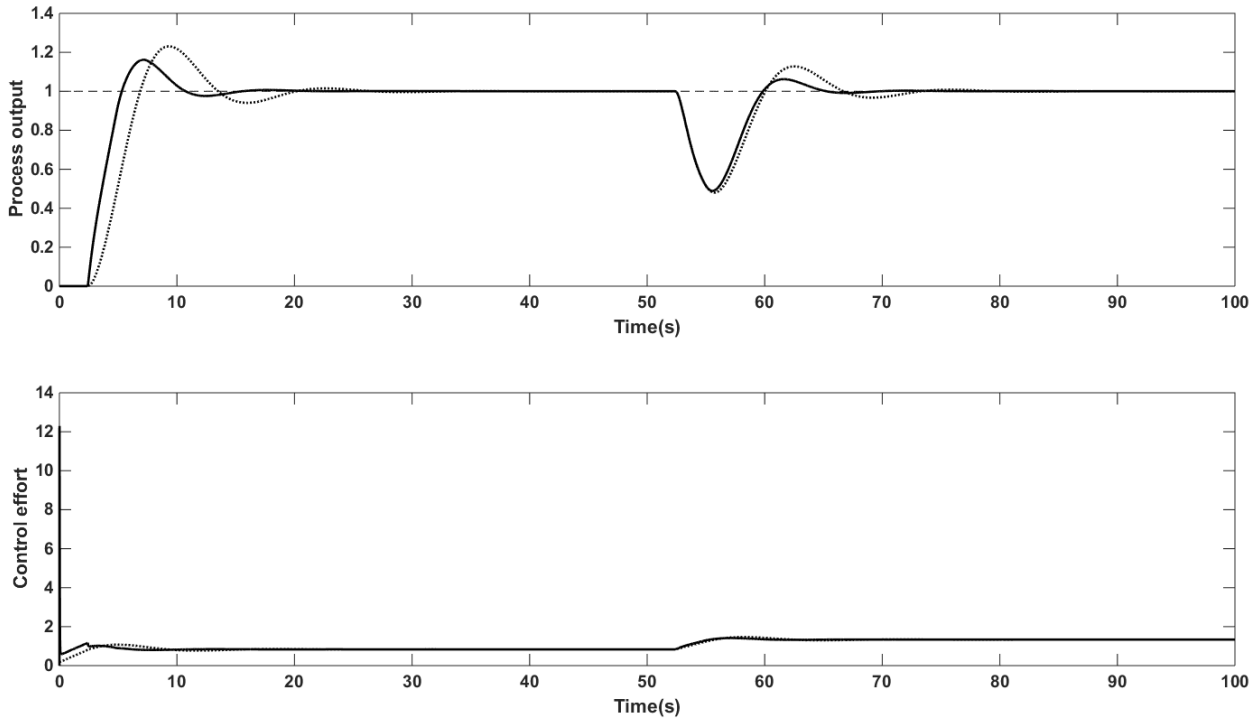

Fig 3.4 Perturbed response for G_1: Solid-Proposed, Dotted-Wang et al. (2016)

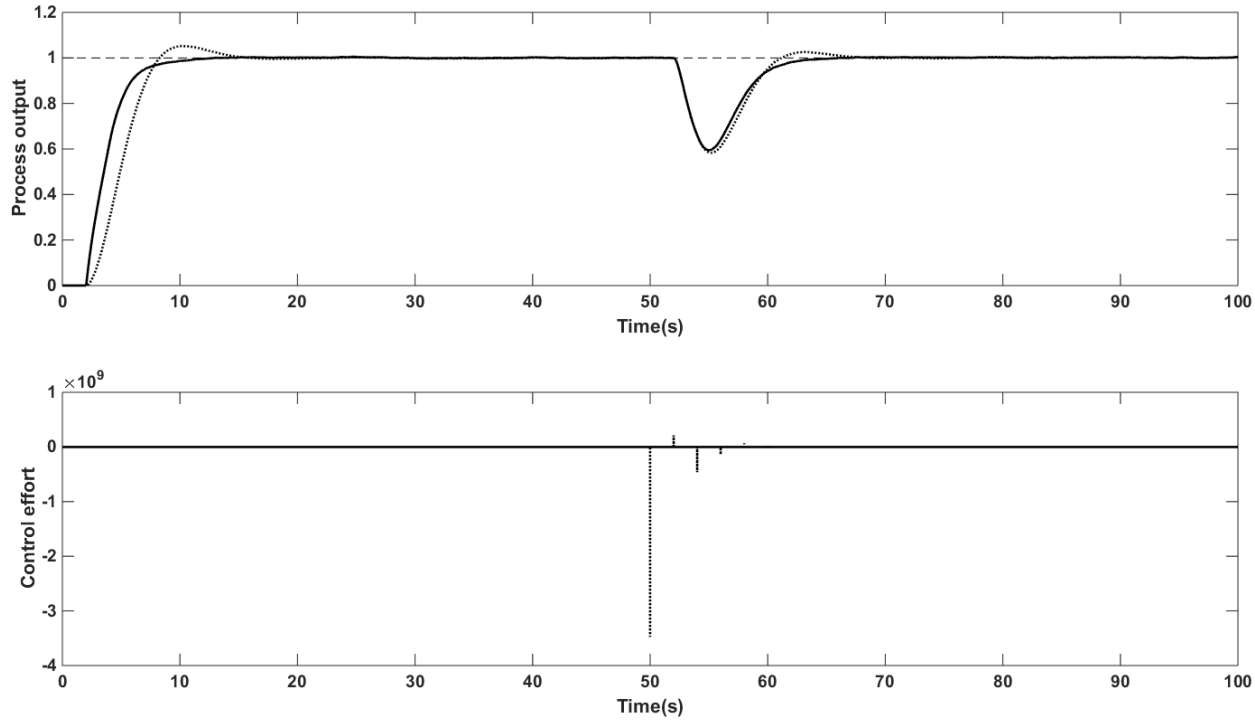

Fig 3.5 Response in presence of measurement noise for G_1: Solid-Proposed, Dotted-Wang et al. (2016)

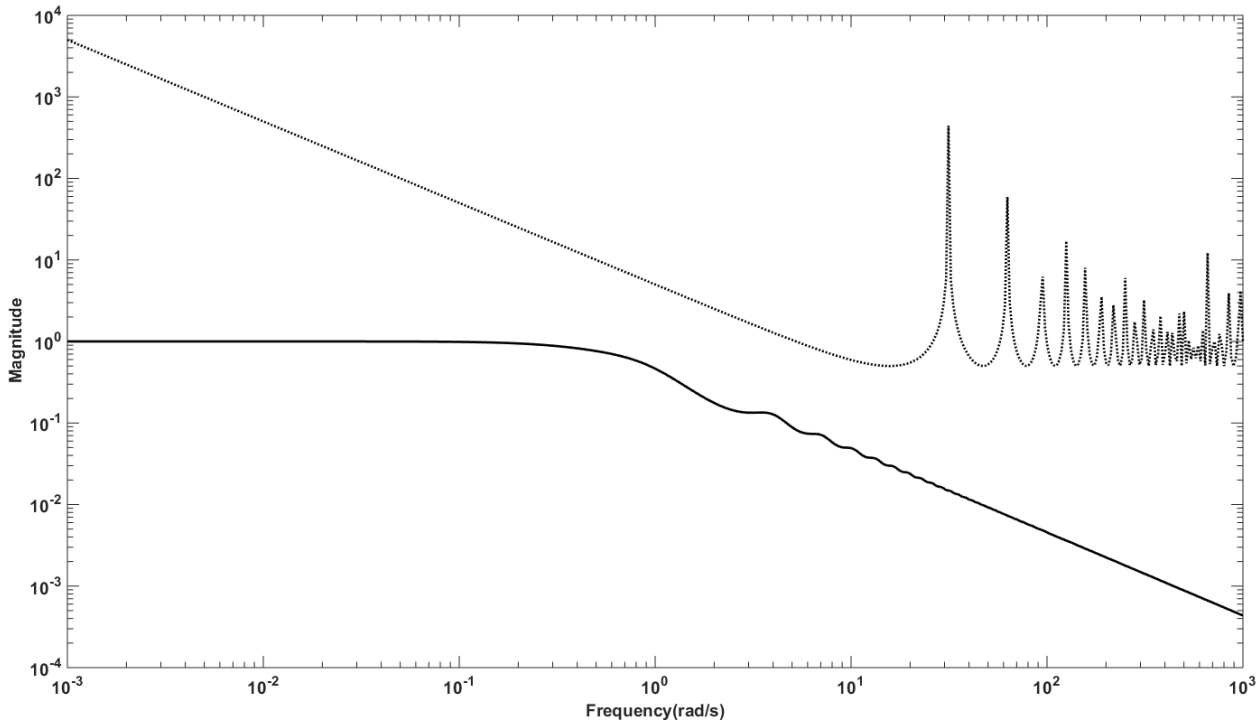

Fig 3.6 Magnitude plot for G_1: Solid-Complementary sensitivity function, Dotted-+10% uncertainty in L

3.1.3.2. Example2

The second example considered for performance comparison is as follows (Srivastava et al., 2016):

$$G_2(s)=\frac{e^{-1.64s}}{s^2+3s+2} \tag{3.25}$$

The proposed controller for this process is given in eq. (3.26) for a filter time constant of 1 and fractional order p is equal to 1.02.

$$G_C(s)=\left(\frac{0.82s+1}{0.82s^{1.02}+s^{0.02}+1.64}\right) 3\left[1+\frac{1}{1.5s}+0.3333s\right] \tag{3.26}$$

The controller used for comparison is having the settings: K_c =1.1069; τ_i =1.4995 and τ_d =0.3332. The servo response of the closed loop system is evaluated for step set point changes of unit magnitude and for step change in load applied at t=40s having a magnitude of -1. Fig 3.7 shows the response characteristics of the SOPTD process in (3.25) with the two controllers. The performance metrics are provided in Table 3.1 and an improved performance is resulted with the proposed controller. There is a reduction in the overshoot, ISE and IAE values which is clear from Table 3.1. Fig 3.8 shows the robust performance of the proposed controller for +10% change in time delay and process gain. An important observation here is that both the controllers give robust control performance as the M_s values are less than 2 which is evident from Table 3.1.

The impact of white noise having a mean value of zero and a variance of 0.0001 in the output was well rejected by both the controllers but the control effort is comparatively small with the proposed controller structure. Fig 3.9 and Table 3.2 shows the superior performance of the designed controller which is clear from smaller values of ISE and IAE.

Table 3.2 Performance comparison with measurement noise

Process	**Method**	**ISE**	**IAE**	**TV**
G_1	Proposed	3.592	6.478	311.225
	Wang et al.	4.771	7.903	87664
G_2	Proposed	2.572	4.484	721.749
	Wang et al.	3.034	5.793	749.317
G_3	Proposed	0.7201	1.658	408.651
	Wang et al.	0.8198	1.9	757.488
G_4	Proposed	5.649	8.955	1263.2
	Wang et al.	6.825	11.91	1745.5

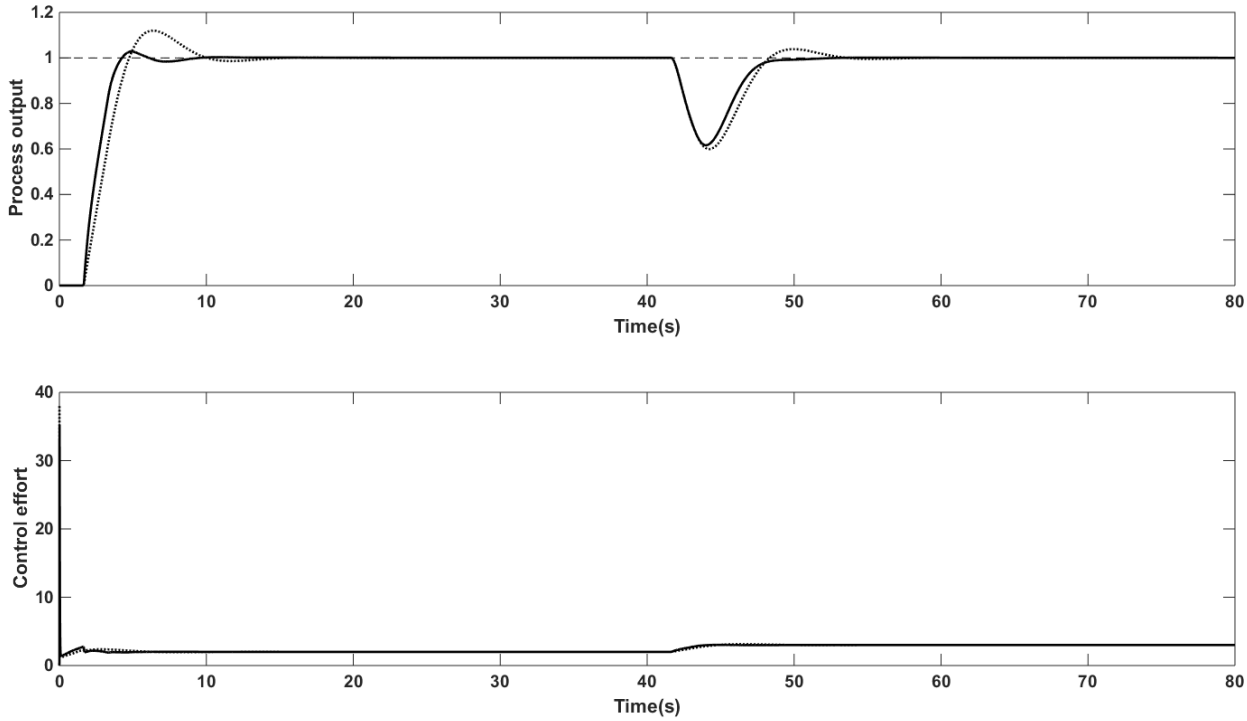

Fig 3.7 Closed loop response for G_2: Solid-Proposed, Dotted-Wang et al. (2016)

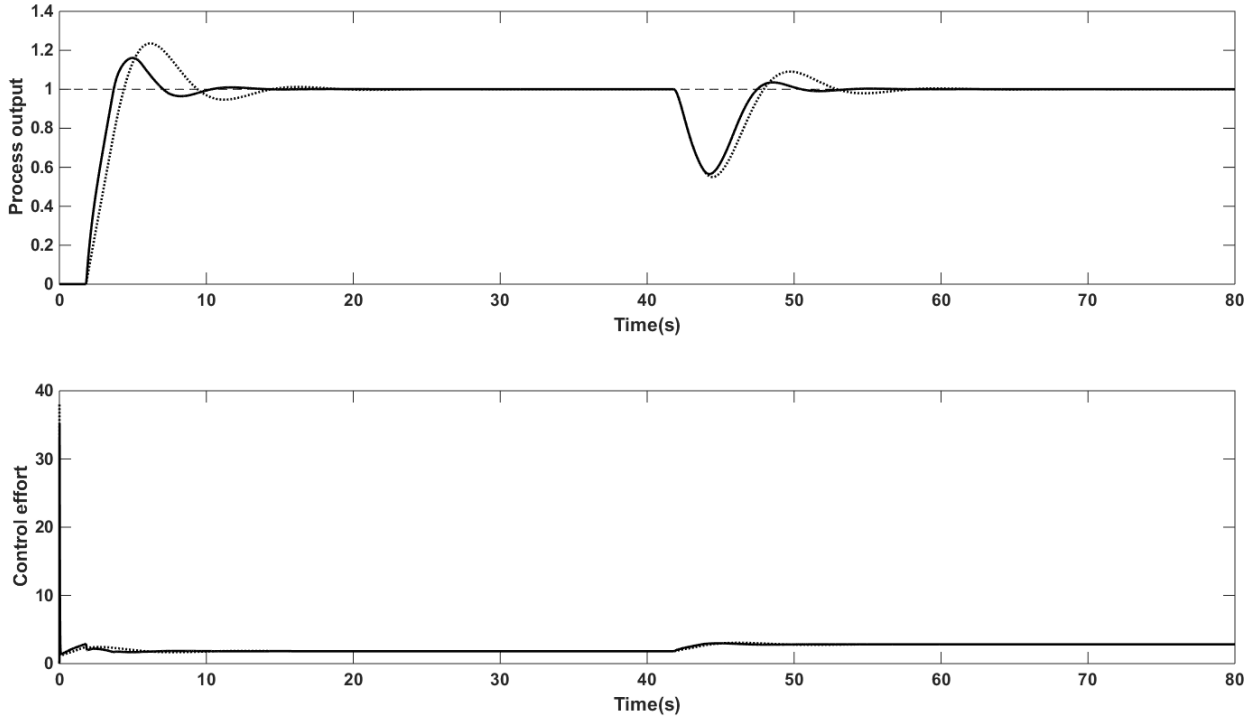

Fig 3.8 Perturbed response for G_2: Solid-Proposed, Dotted-Wang et al. (2016)

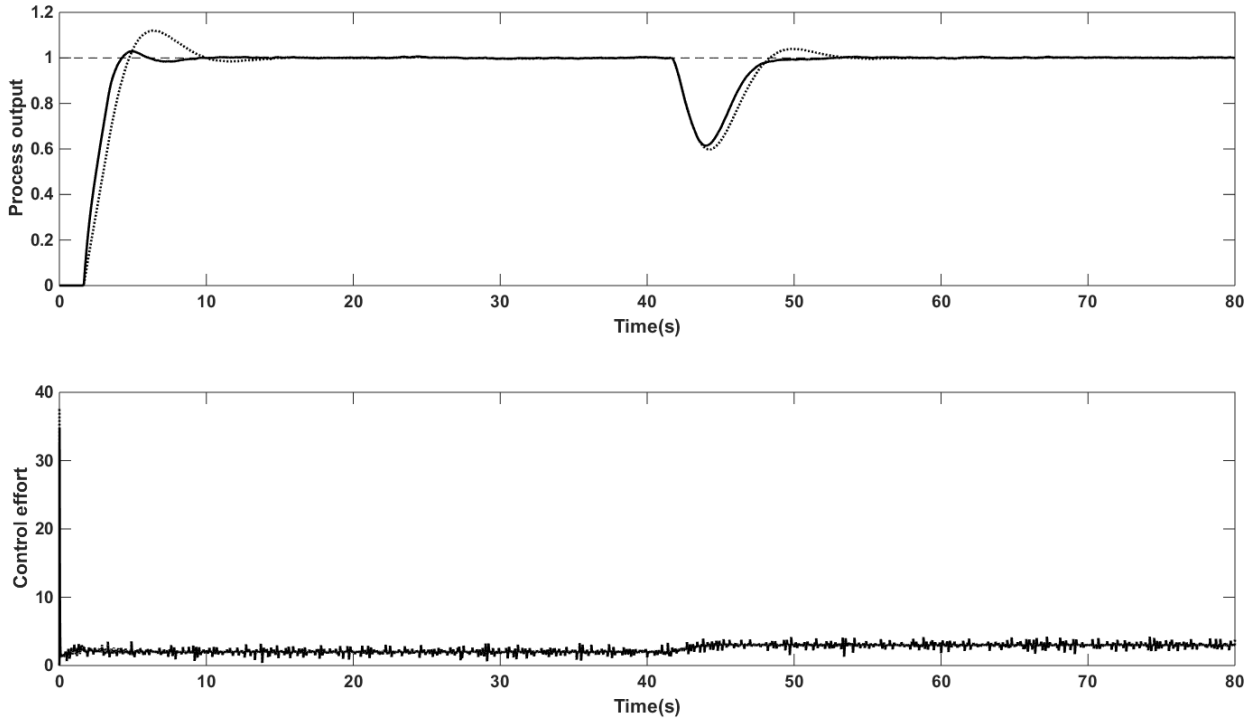

Fig 3.9 Response in presence of measurement noise for G_2: Solid-Proposed, Dotted-Wang et al. (2016)

Table 3.3 Performance comparison for G_2 with proposed method at different values of p

p	**ISE**	**IAE**
1.01	2.208	2.673
1.02	2.21	2.686
1.03	2.212	2.701
1.04	2.214	2.718
1.05	2.216	2.736
1.06	2.218	2.756
1.07	2.221	2.777
1.08	2.224	2.798
1.09	2.227	2.821
1.1	2.231	2.843

In addition, the servo responses with the proposed method at different values of p are compared and the characteristics are shown in Fig 3.10. The ISE and IAE values at each value of p are given in Table 3.3 which are less than ISE and IAE values used for comparison. Hence, the proposed method has flexibility that the fractional order p can be varied over a range producing lower values of ISE and IAE. The trend of T(s) satisfying the robustness bound is shown in Fig 3.11. The characteristics confirm the robust closed loop stability of the simulated system.

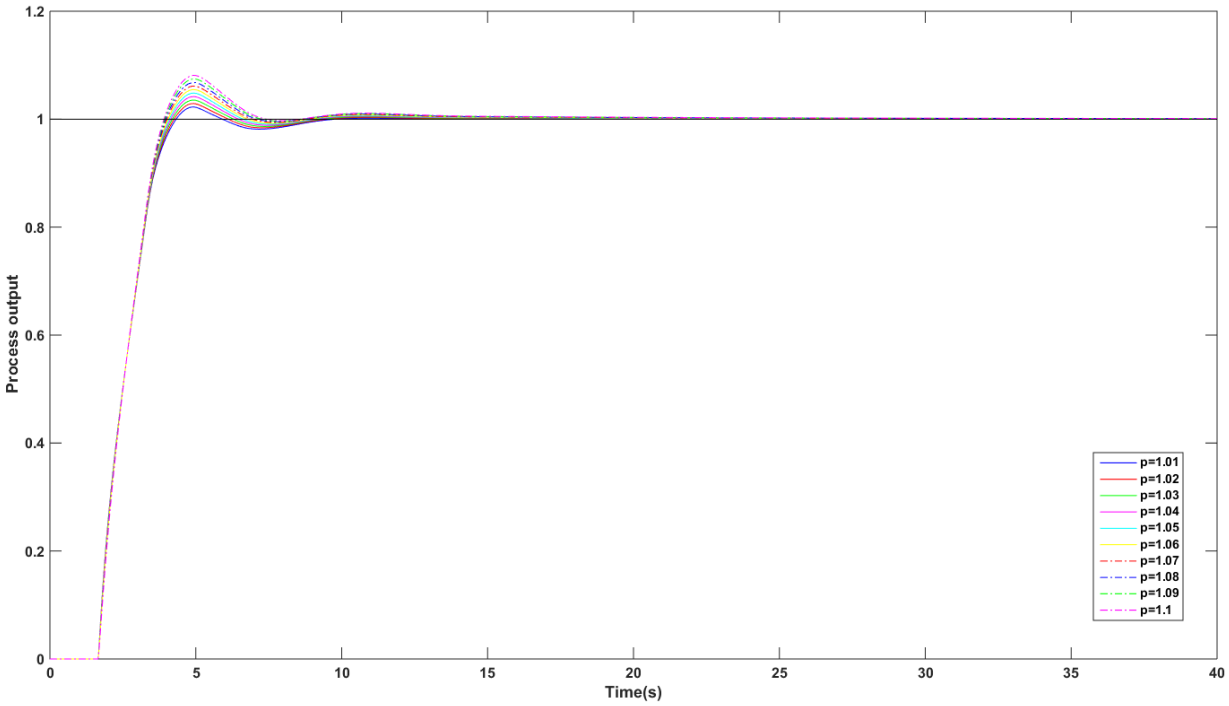

Fig 3.10 Comparison of closed loop response for process G_2 at different values of p

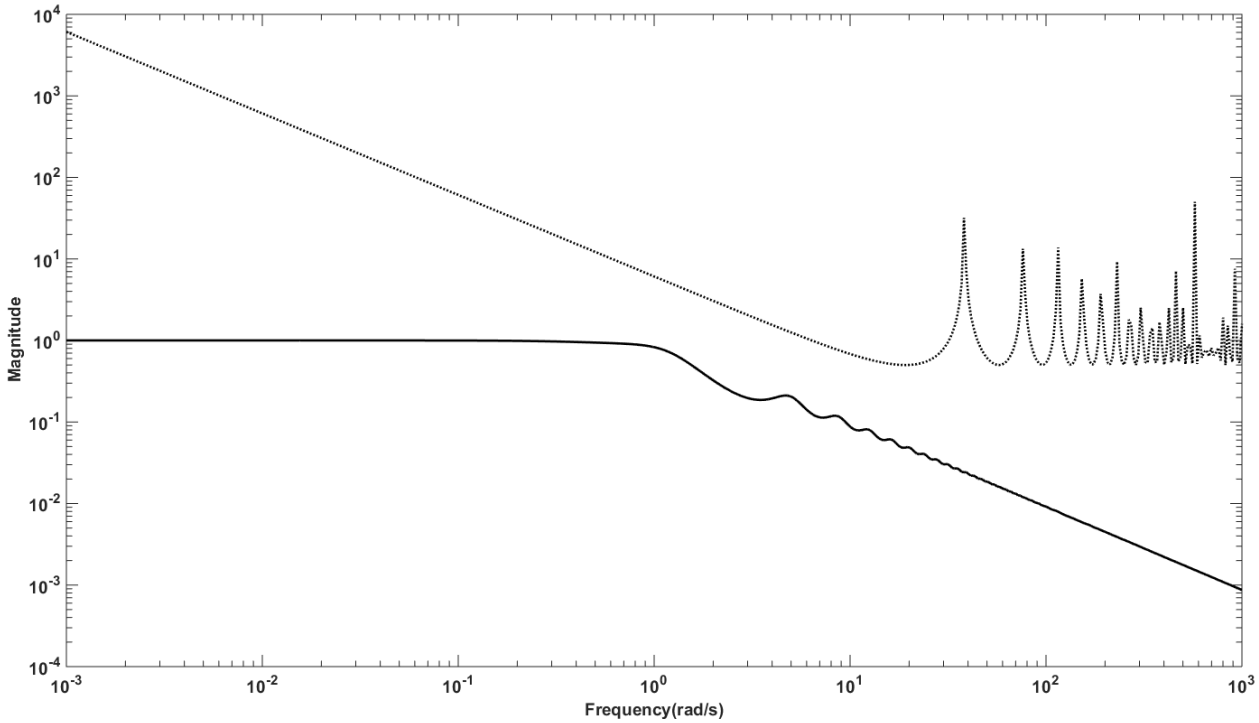

Fig 3.11 Magnitude plot for G_2: Solid-Complementary sensitivity function, Dotted-+10% uncertainty in L

3.1.3.3. Example3

Consider the second order lag dominant linear process (Dey and Mudi 2009) given by

$$G_3(s)=\frac{e^{-0.2s}}{(s+1)^2} \tag{3.27}$$

The controller designed according to the design rules in Wang et al. (2016) is used for comparison. The controller settings as per their method are: K_c=1.4247; τ_i=1.9924 and τ_d=0.498. The proposed controller with the filter parameters γ= 1 and p=1.01 is

$$G_C(s)=\left(\frac{0.1s+1}{0.1s^{1.01}+s^{0.01}+0.2}\right)2\left[1+\frac{1}{2s}+0.5s\right] \tag{3.28}$$

The set point tracking of closed loop system with a negative step disturbance of magnitude 0.2 applied at t=20s is shown in Fig 3.12 while the performance metrics are given in Table 3.1. There is negligible overshoot in the response for both the controllers but the error values are lesser with the proposed controller. The similar response holds even after introducing +10% variation in time delay and process gain which is evident from Fig 3.13 and Table 3.1. The M_s values for both methods are in the standard range of 1 to 2 which ensure robust control performance.

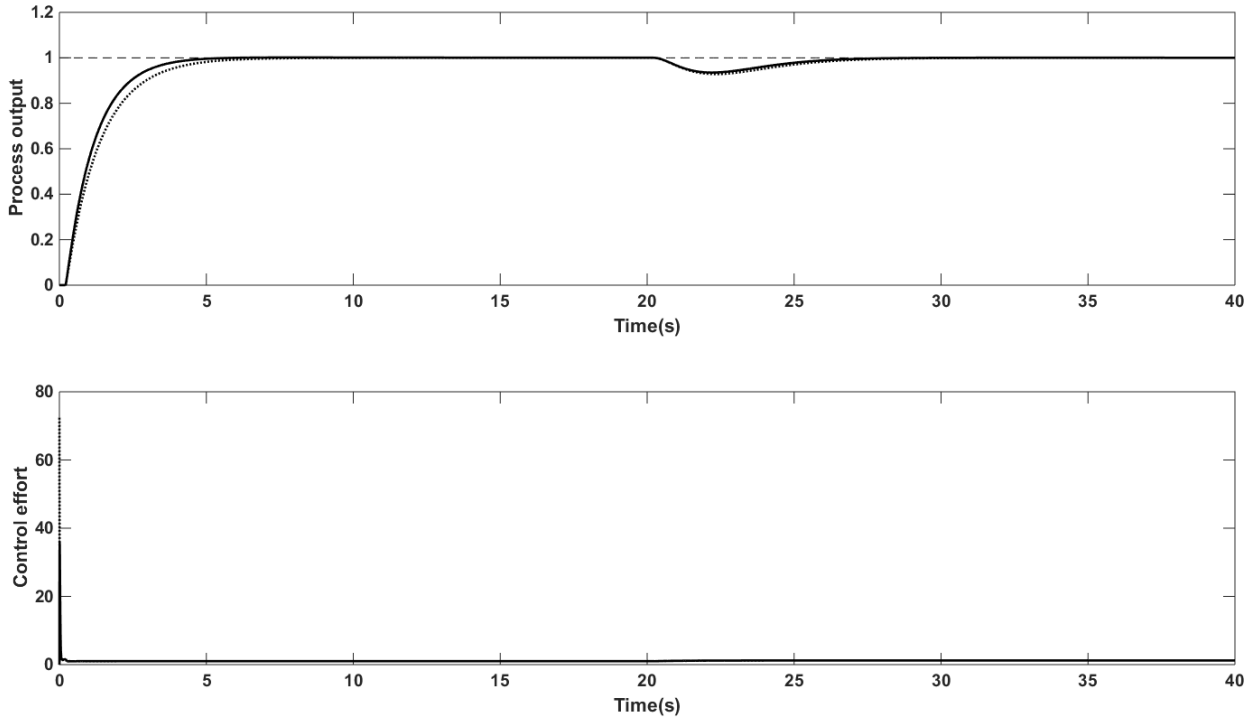

Fig 3.12 Closed loop response for G_3: Solid-Proposed, Dotted-Wang et al. (2016)

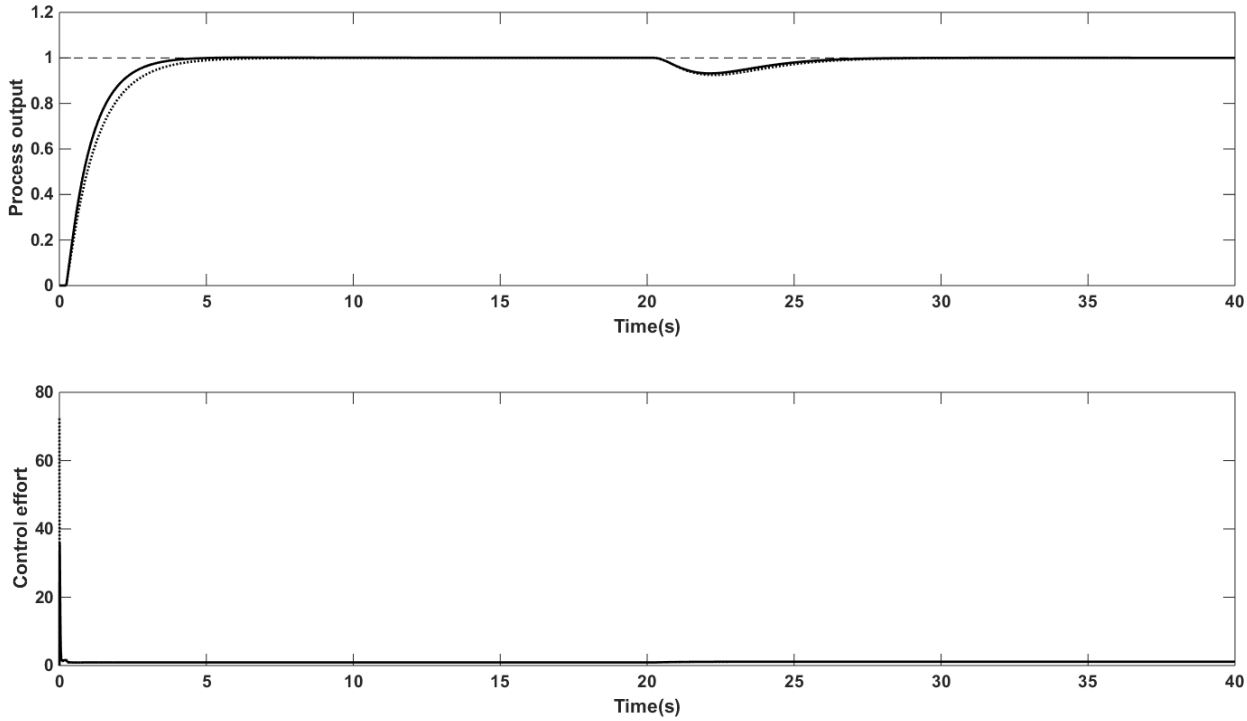

Fig 3.13 Perturbed response for G_3: Solid-Proposed, Dotted-Wang et al. (2016)

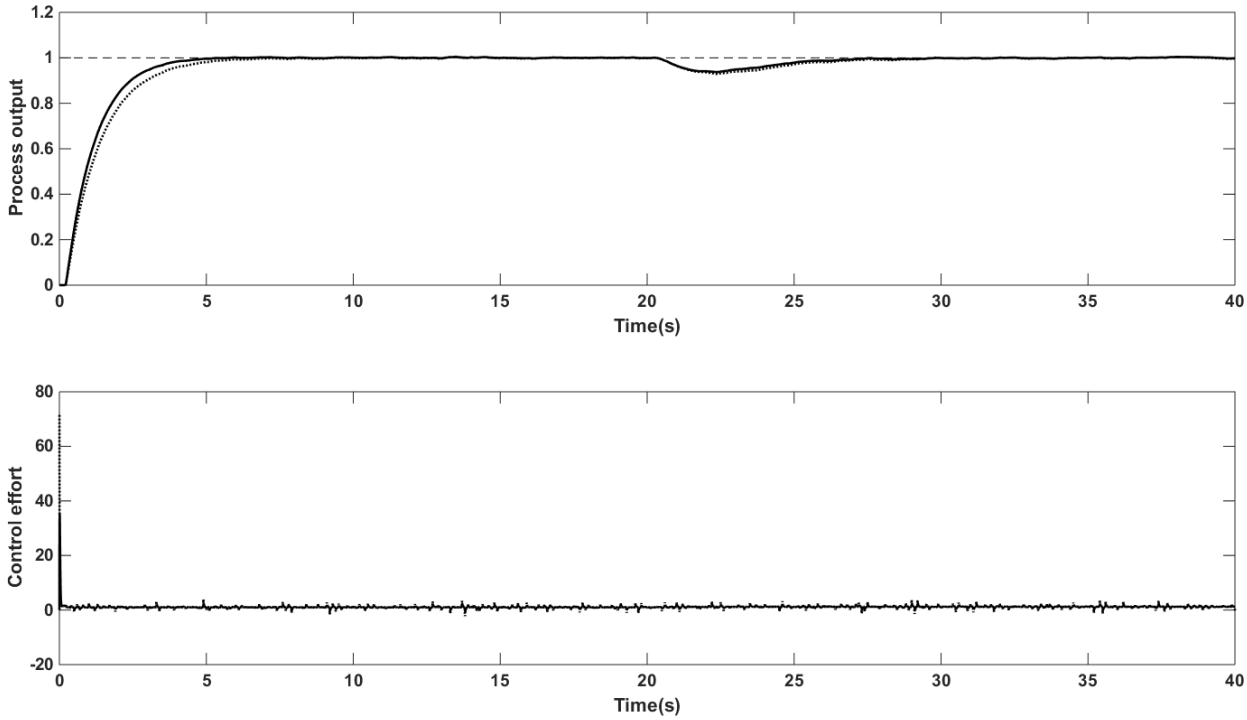

Fig 3.14 Response in presence of measurement noise for G_3: Solid-Proposed, Dotted-Wang et al. (2016)

The response of closed loop system with added noise is illustrated in Fig 3.14. The white noise used has a mean of zero and a variance of 0.0001. The control effort is significantly less with the proposed method against the method used for comparison. The ISE, IAE and TV values for this case are given in Table 3.2. The closed loop robust stability satisfying the stability condition in eq. (3.15) is shown in Fig 3.15. It is clear from the magnitude plot that the system is closed loop stable for parametric uncertainties.

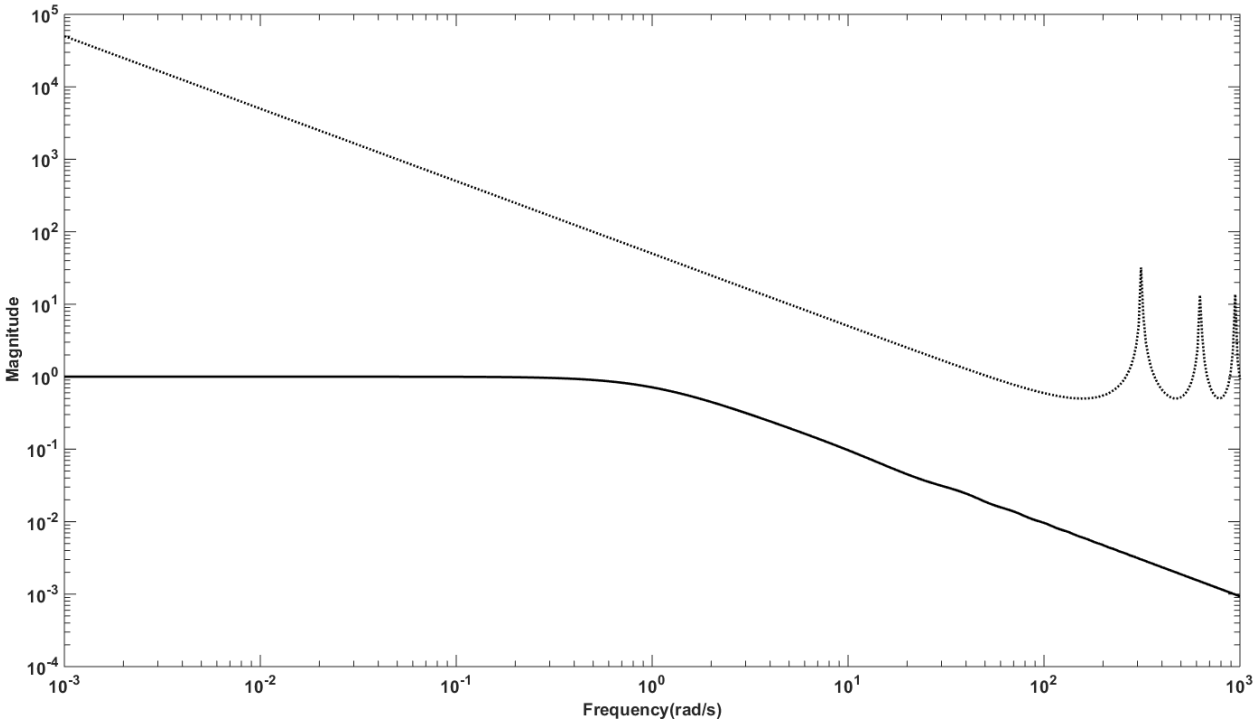

Fig 3.15 Magnitude plot for G_3: Solid-Complementary sensitivity function, Dotted-+10% uncertainty in L

3.1.3.4. Example4

Consider a higher order process (Astrom and Hagglund, 1995):

$$G_4(s)=\frac{1}{(s+1)^8} \tag{3.29}$$

The second order approximated model for the above process is

$$G_4(s)=\frac{0.336e^{-4.3s}}{s^2+1.3878s+0.336}=\frac{1.0002e^{-4.3s}}{(3.201s+1)(0.9299s+1)} \tag{3.30}$$

The proposed controller for this process with $\gamma=2$ and $p=1.1$ is

$$G_C(s)=\left(\frac{2.15s+1}{4.3s^{1.1}+2s^{0.1}+4.3}\right)4.13\left[1+\frac{1}{4.1309s}+0.7205s\right] \tag{3.31}$$

The settings of the controller used for comparison are: K_c=0.7086; τ_i=3.9987 and τ_d =0.7136. Fig 3.16 shows the servo response for step set point change of unit magnitude and step change in disturbance applied at t=70s having a magnitude of -0.2. The response for perturbed process model is shown in Fig 3.17 with +10% mismatch in time delay and process gain. The performance metrics are provided in Table 3.1. Clearly, the proposed controller outperforms the other one used for comparison. There is a drastic reduction in the overshoot.

Fig 3.18 shows the closed loop response with white noise in the measurement. The TV value of the proposed controller with added noise is low compared to the other value. Table 3.2 confirms the lower values of ISE, IAE and TV. The M_s value of closed loop system with the proposed controller is 2 where as it is 2.17 for the other method. The value of 2 is the higher limit in the standard M_s range. It means that both the controllers are likely to respond to model uncertainties and their impact could be seen the response.

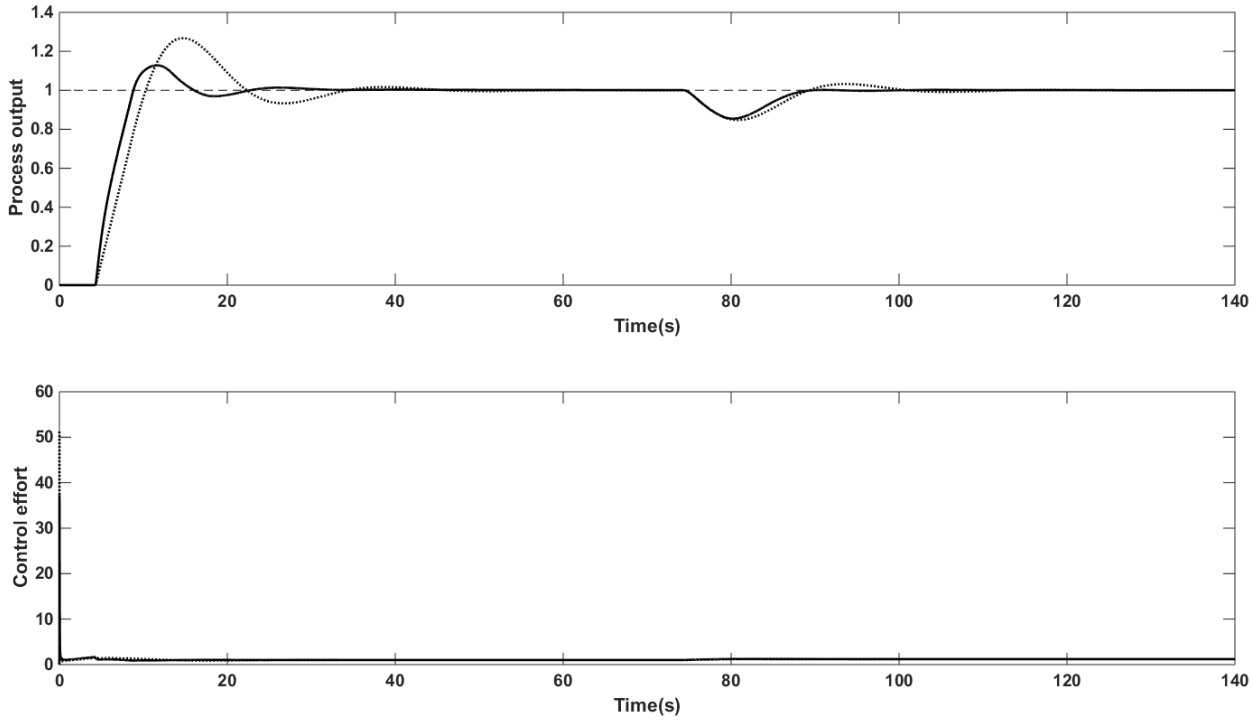

Fig 3.16 Closed loop response for G_4: Solid-Proposed, Dotted-Wang et al. (2016)

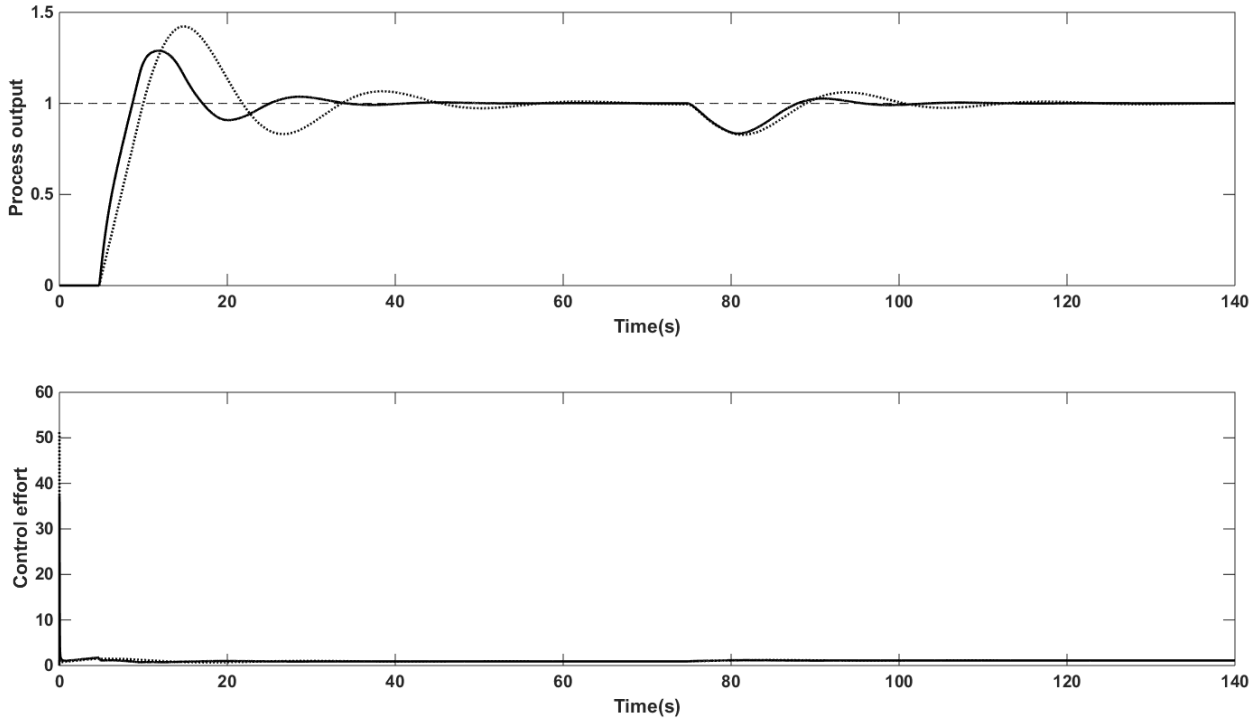

Fig 3.17 Perturbed response for G_4: Solid-Proposed, Dotted-Wang et al. (2016)

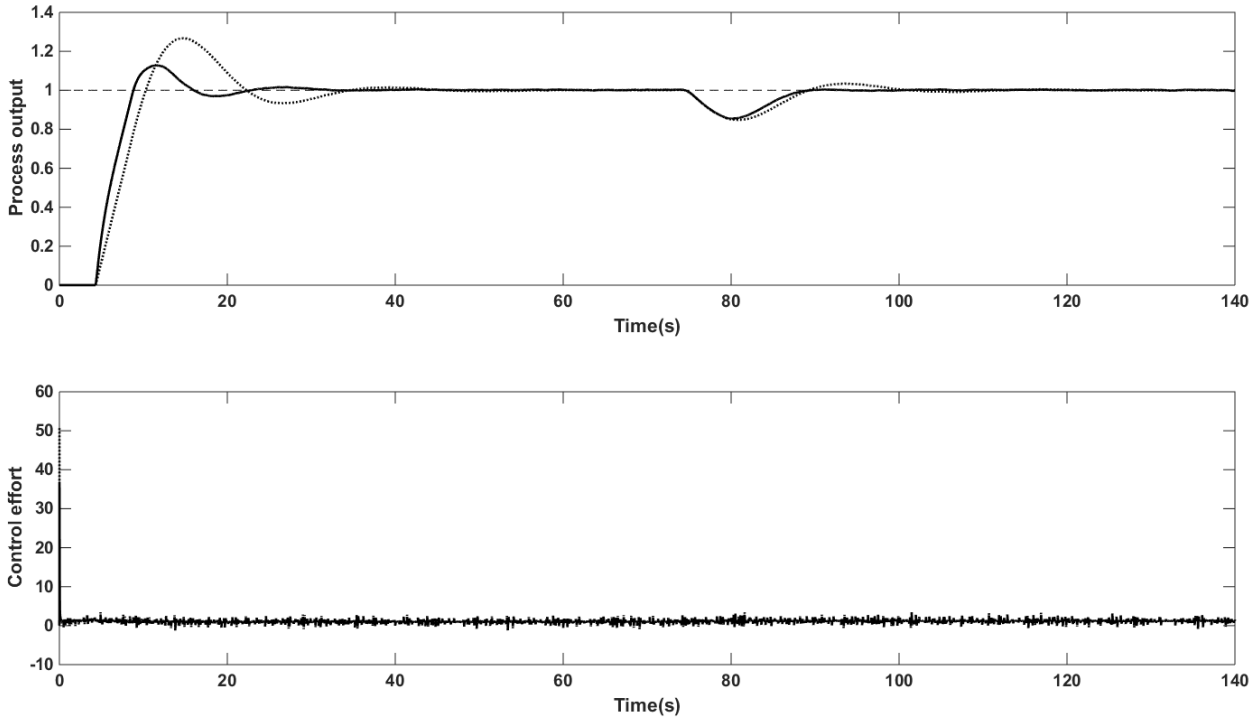

Fig 3.18 Response in presence of measurement noise for G_4: Solid-Proposed, Dotted-Wang et al. (2016)

Fig 3.19 shows the servo response of the process in (3.30) for the values of p=1.01,1.02,....1.1. The performance metrics ISE and IAE are provided in Table 3.4. Better performance is observed at every value of p. Also, the magnitude plot in Fig 3.20 tells that the complementary sensitivity function with +10% uncertainty in time delay obeys the robust stability condition. Hence, the closed loop system ensures robust and stable performance even with uncertainty in the process parameters.

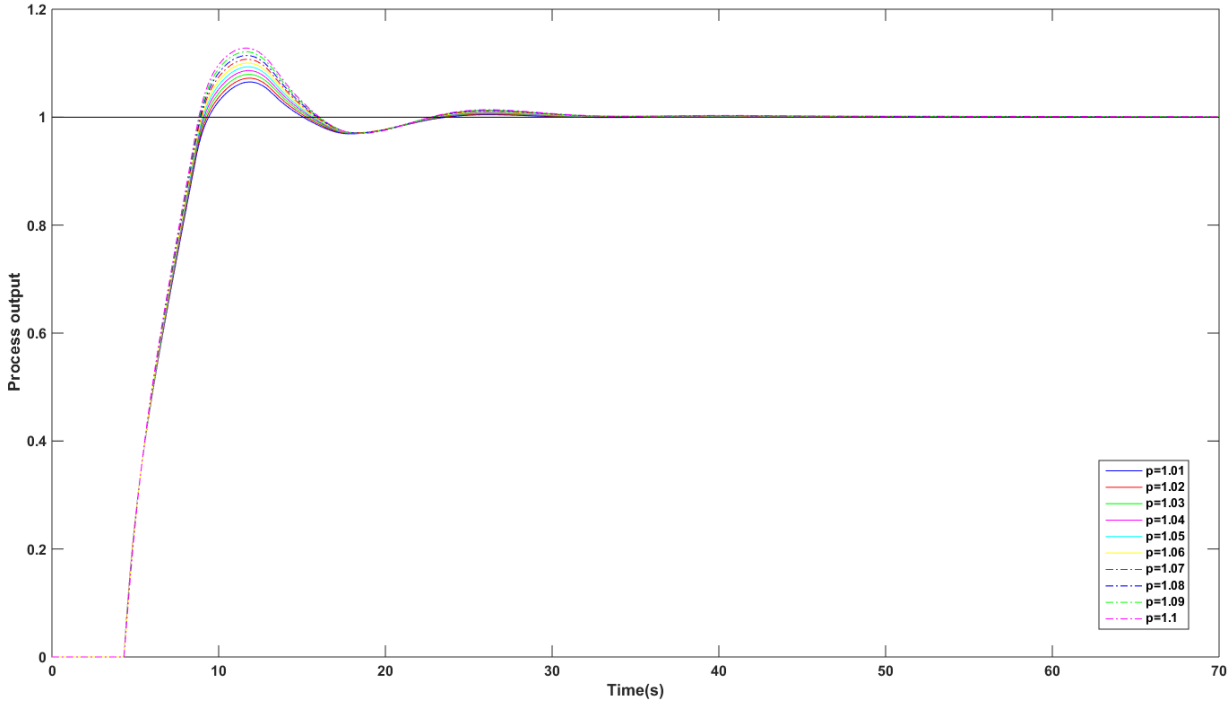

Fig 3.19 Comparison of closed loop response for process G_4 at different values of p

Table 3.4 Performance comparison for G_4 with proposed method at different values of p

p	**ISE**	**IAE**
1.01	5.501	6.729
1.02	5.5	6.76
1.03	5.5	6.796
1.04	5.501	6.833
1.05	5.502	6.872
1.06	5.503	6.944
1.07	5.506	6.951
1.08	5.509	6.991
1.09	5.512	7.032
1.1	5.516	7.072

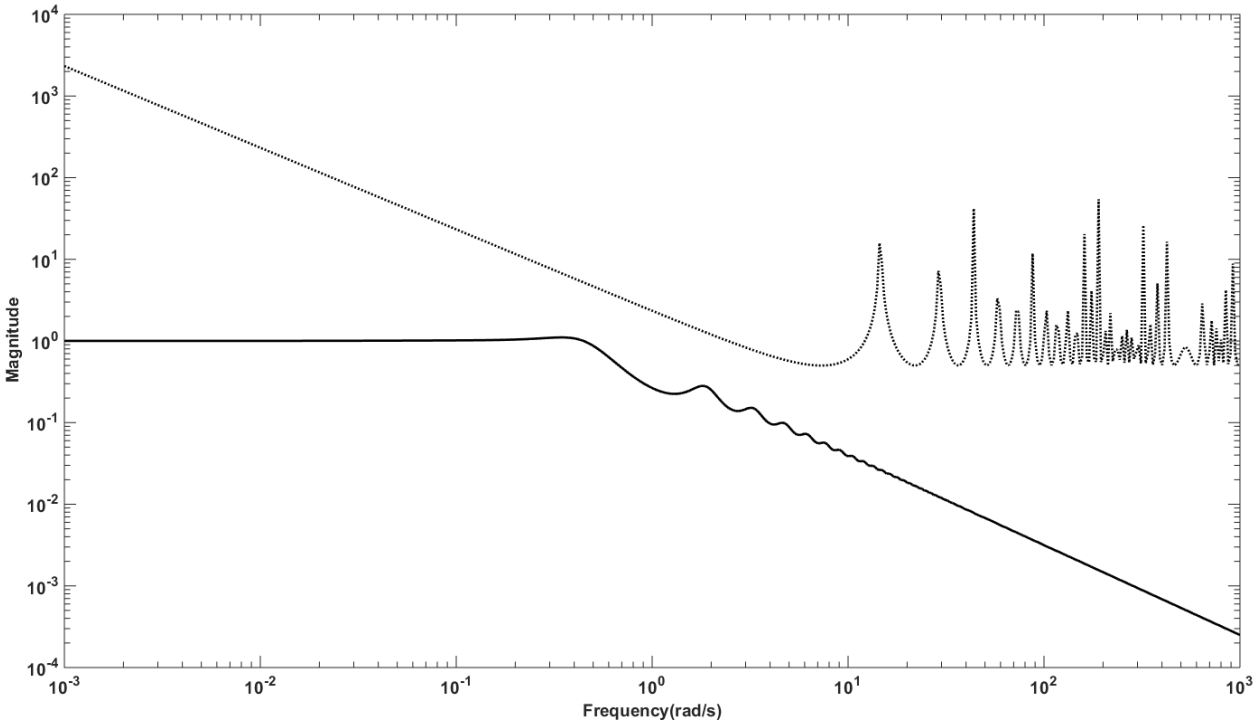

Fig 3.20 Magnitude plot for G_4: Solid-Complementary sensitivity function, Dotted-+10% uncertainty in L

The effect of fractional filter on the robustness of closed loop control system is explained with the help of parametric uncertainties. A better closed loop response is obtained compared to Wang et al. (2016) method for uncertainty in K and L for all the four examples which proves that the closed loop system gives robust performance for uncertainties with fractional filter PID controller. Further, the stability of closed loop system with the proposed controller is investigated for parametric uncertainties. It is proved that all the four systems used are satisfying robust stability condition and the illustrations are shown in Figs 3.6, 3.11, 3.15, 3.20. In addition, the closed loop system is robust for noise inputs and the proposed controller successfully attenuates the noise at high frequencies. This is clear from the magnitude of complementary sensitivity function which is approaching zero (Figs 3.6, 3.11, 3.15, 3.20) with increase in frequency for all the four systems.

3.1.4. Conclusion

A simple fractional filter IMC-PID controller is proposed for SOPTD processes using fractional IMC filter structure. Different case studies were analyzed for servo response and regulatory control. It can be concluded from the results that a good closed loop performance is obtained with nominal

model and actual model of the process with the proposed controller. The proposed controller resulted in a minimum overshoot in the response in absence of set point weighting. It was also shown that the effort of proposed controller is less for noise corrupted measurements. The robustness for parametric uncertainties is proved with robustness analysis using sensitivity functions. The work is in progress to extend the proposed method for unstable and non-minimum phase systems.

3.2. Fractional filter IMC-PID Controller design for an unstable inverted pendulum system

3.2.1. Introduction

The inverted pendulum system (Lundberg and Barton, 2010; Kwakernaak and Sivan, 1972; Khalil, 1996) is a benchmark example in the field of control and an extensive work has been carried out for controlling the inverted pendulum since the past half century. Many linear and non-linear control approaches have been proposed for this unstable, non-linear and highly perturbed system (Yang et al., 2009). But, the design procedures are still evolving due to the non-linear behavior of the system and stabilization issues.

The widely accepted PID controller was used to control the inverted pendulum system (Wang, 2011) because of the availability of vast range of tuning rules. Several other controllers based on soft computing techniques (Huang et al., 2011) are also reported in the literature but the simplest being PID controller due to the above advantage. But, the PID controller doesn't always ensure stable response of the inverted pendulum system due to its nonlinear behavior. Hence, an improved controller structure is required to enhance the closed loop response of inverted pendulum system dealing with the nonlinearities. The fractional order control (Chen et al., 2009) is the right choice to handle this problem. If a fractional order PID controller is used, the tuning becomes complex due to the increase in number of tuning parameters. Hence, a PID controller with minor changes is needed to avoid the tuning complexity.

Here, a fractional filter IMC-PID controller is proposed using fractional IMC filter in the controller design. The resulting controller has only two tuning parameters which are the fractional filter time constant and fractional order of the filter. The closed loop performance of the inverted pendulum system with the proposed controller is compared with the fractional order PID controller in Wang et al. (2016).

3.2.2. Modeling of inverted pendulum system

The inverted pendulum system consists of a moving cart to which pendulum is attached which can rotate freely when the cart moves along the track. The geometry of the inverted pendulum

system is shown in Fig 3.21 where M is the mass of cart; m is the mass of pendulum; l is the half length of pendulum; F is the driving force; ϕ and x are the angle of pendulum from upright position and cart position. The modeling equations of the system as in Wang et al. (2016) are given as follows:

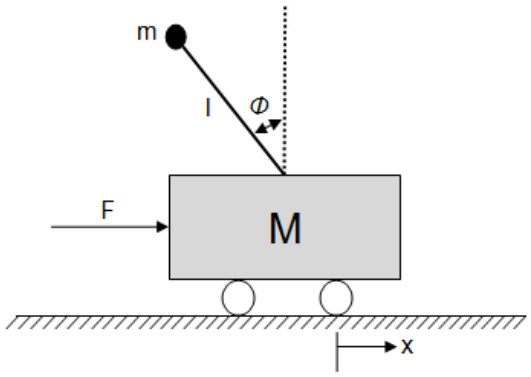

Fig 3.21 Geometrical diagram of the inverted pendulum system

The modeling equations of the system as in Wang et al. (2016) are given as follows:

$$mgl\ddot{x}=(I+ml^2)\ddot{\phi}-mgl\phi \quad (3.32)$$

$$u=(M+m)\ddot{x}+b\dot{x}-mgl\phi \quad (3.33)$$

The transfer function of the inverted pendulum system after applying Laplace transform and then substituting system parameters given in Table 3.5 (Wang et al., 2016) is

$$G(s)=\frac{4.5455s}{s^3+0.1818s^2-31.1818s-4.4545} \quad (3.34)$$

The pole-zero form of eq. (3.34) is

$$G(s)=\frac{4.5455s}{(s+5.604)(s+0.1428)(s-5.565)} \quad (3.35)$$

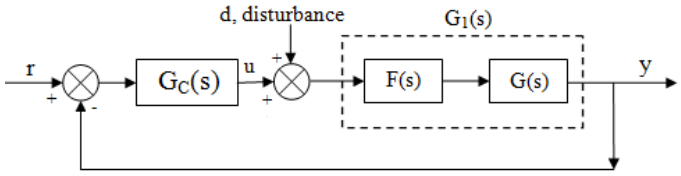

Fig 3.22 Stabilization block diagram of inverted pendulum system

Table 3.5 Inverted pendulum system parameters

M(kg)	m(kg)	l(m)	b	I(kgm^2)	g(m/s^2)
0.5	0.2	0.3	0.1	0.006	9.8

Fig 3.22 shows the block diagram of the closed loop with compensator unit F(s). The stabilized model of the inverted pendulum system after canceling the unstable pole and zero by choosing F(s) as $\frac{s-5.565}{s}$ (Wang et al., 2016) is

$$G_1(s)=F(S)G(s)=\frac{4.5455}{(s+5.604)(s+0.1428)} \tag{3.36}$$

That is,

$$G_1(s)=\frac{5.68}{(7.0028s+1)(0.1784s+1)} \tag{3.37}$$

3.2.3. Proposed fractional filter IMC-PID controller design

The structure of the proposed controller is

$$G_c(s)=(\text{fractional filter})\left[K_p\left(1+\frac{1}{\tau_i s}+\tau_d s\right)\right] \tag{3.38}$$

Consider the general transfer function of the stabilized inverted pendulum system with reference to eq. (3.37).

$$G(s)=\frac{K}{(T_1 s+1)(T_2 s+1)} \tag{3.39}$$

Where K is the system gain, T_1 and T_2 are the process time constants.

The fractional IMC filter used is

$$f(s)=\frac{1}{\gamma s^p+1} \tag{3.40}$$

Where γ is the time constant and p is the fractional order of f(s). Now, the IMC controller is

$$G_{IMC}(s)=\frac{(T_1 s+1)(T_2 s+1)}{K}\left(\frac{1}{\gamma s^p+1}\right) \tag{3.41}$$

Finally, the fractional filter IMC-PID controller is

$$G_c(s)=\frac{\frac{(T_1 s+1)(T_2 s+1)}{K(\gamma s^p+1)}}{1-\frac{(T_1 s+1)(T_2 s+1)}{K(\gamma s^p+1)}\frac{K}{(T_1 s+1)(T_2 s+1)}} \tag{3.42}$$

The above equation is simplified to

$$G_c(s)=\frac{(T_1 s+1)(T_2 s+1)}{K\gamma s^p} \tag{3.43}$$

Equation (3.43) can be written as

$$G_C(s)=\left(\frac{1}{\gamma s^{p-1}}\right)\left(\frac{T_1+T_2}{K}\right)\left[1+\frac{1}{(T_1+T_2)s}+\left(\frac{T_1T_2}{T_1+T_2}\right)s\right] \quad (3.44)$$

Comparing eq. (3.38) and eq. (3.44), the controller settings are

$$K_p=\frac{T_1+T_2}{K};\tau_i=T_1+T_2;\tau_d=\frac{T_1T_2}{T_1+T_2} \quad (3.45)$$

and the fractional filter term is

$$\text{filter}=\frac{1}{\gamma s^{p-1}} \quad (3.46)$$

The tuning parameters are the fractional filter time constant γ and fractional order of the filter p. The value of γ is chosen as the smallest of the process time constants. The value of p is identified iteratively such that the performance indices ISE and IAE are minimum.

3.2.4. Results and discussion

3.2.4.1. Example 1

Consider the inverted pendulum model in eq. (3.37)

$$G(s)=\frac{5.68}{(7.0028s+1)(0.1784s+1)} \quad (3.47)$$

The process parameters are: K=5.68, T_1=7.0028 and T_2=0.1784. The proposed controller is obtained according to eq. (3.44). The value of γ is chosen as 0.1 as it is approximately equal to the smallest process time constant 0.17. After several simulations the fractional order p is identified as 1.01. This optimum value identification is illustrated in Fig 3.23 and the ISE and IAE values are shown in Table 3.6. The proposed controller is given in eq. (3.48)

$$G_{proposed}(s)=\frac{1}{0.1s^{0.01}}\left[1.2462+\frac{0.176}{s}+0.2198s\right] \quad (3.48)$$

The other controllers designed in Wang et al. (2016) are

$$G_{PID}(s)=1.2467+\frac{0.4244}{s}+0.0132s \quad (3.49)$$

$$G_{FOPD}(s)=18.1655+1.8056s^{0.9537} \quad (3.50)$$

$$G_{FOPID}(s)=0.9997+\frac{0.3373}{s^{0.98}}+0.0095s^{0.953} \quad (3.51)$$

The servo response is observed for a unit step change in setpoint and the regulatory response for a step magnitude of 0.5. Fig 3.24 shows the servo response for nominal process conditions. The

ISE and IAE values with the proposed method are less compared to other three methods which can be observed from Table 3.7. The ISE and IAE values with the FOPD controller are close to proposed method. Usually, the sensitivity M_s values for unstable systems may not lie in the standard range of 1 to 2 to ensure robust performance. But, the M_s values in this case are in the range of 1 to 1.15 which means that they are close to the lower bound of standard range. So, the probability of ensuring robust closed loop performance is 0.5. Similarly, the regulatory response under nominal process conditions is shown in Fig 3.25 and performance indices are listed in Table 3.7. It is observed from Table 3.7 that the proposed method is giving superior performance which is evident in terms of smaller values of ISE, IAE and TV.

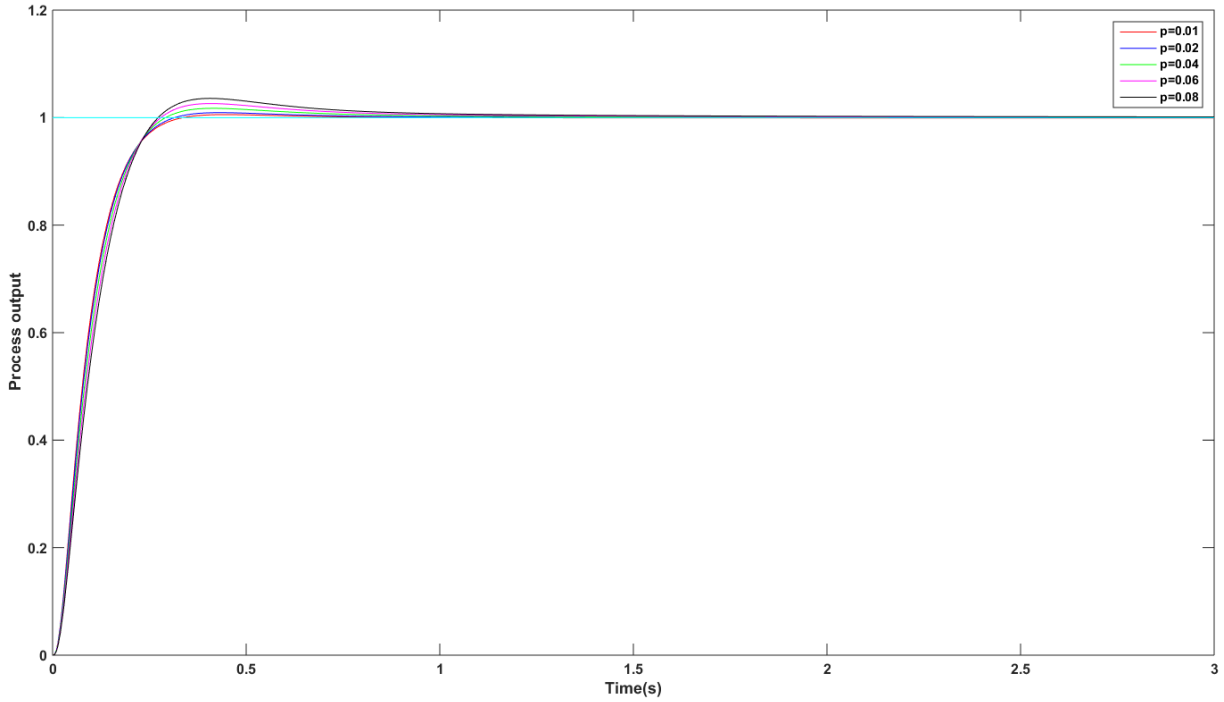

Fig 3.23 Servo response for variation of fractional order p

Table 3.6 Servo response for variation of fractional order p with proposed method

p	**ISE**	**IAE**
1.01	0.0585	0.0953
1.02	0.0597	0.0975
1.04	0.0622	0.1051
1.06	0.0649	0.1137
1.08	0.0677	0.1225

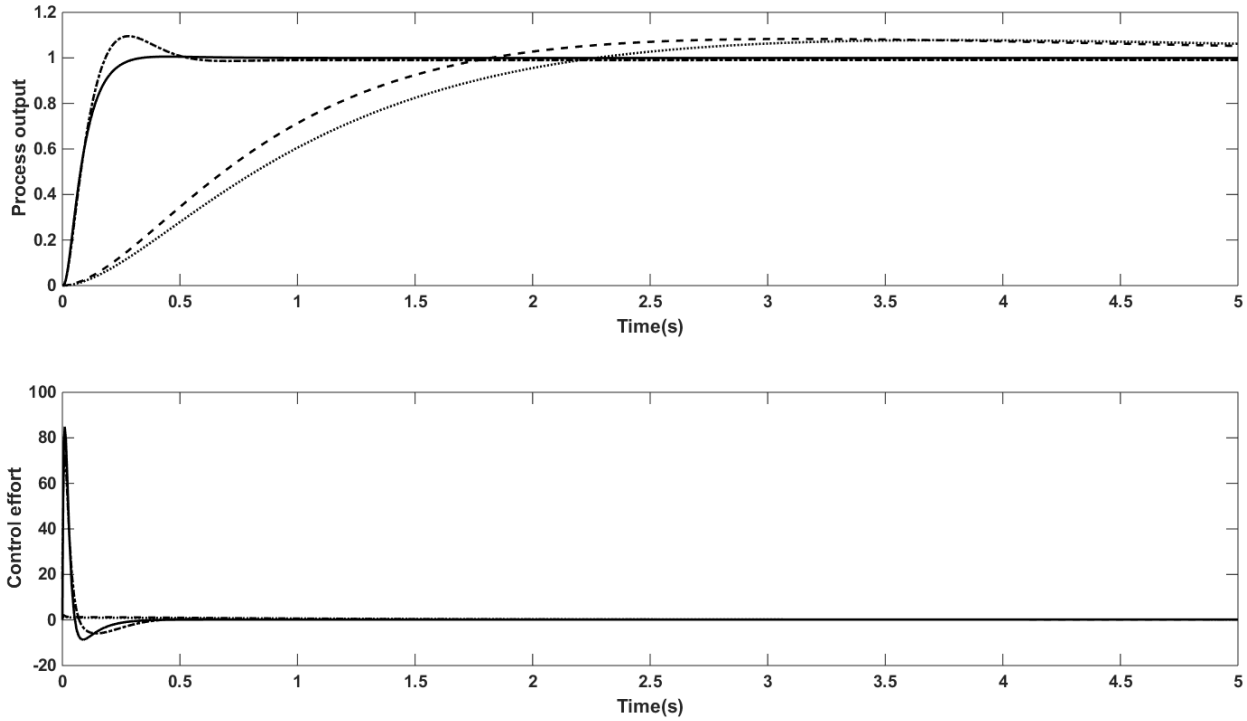

Fig 3.24 Servo response under nominal process conditions: solid - proposed, dashed - PID, dash dot - FOPD, dotted – FOPID

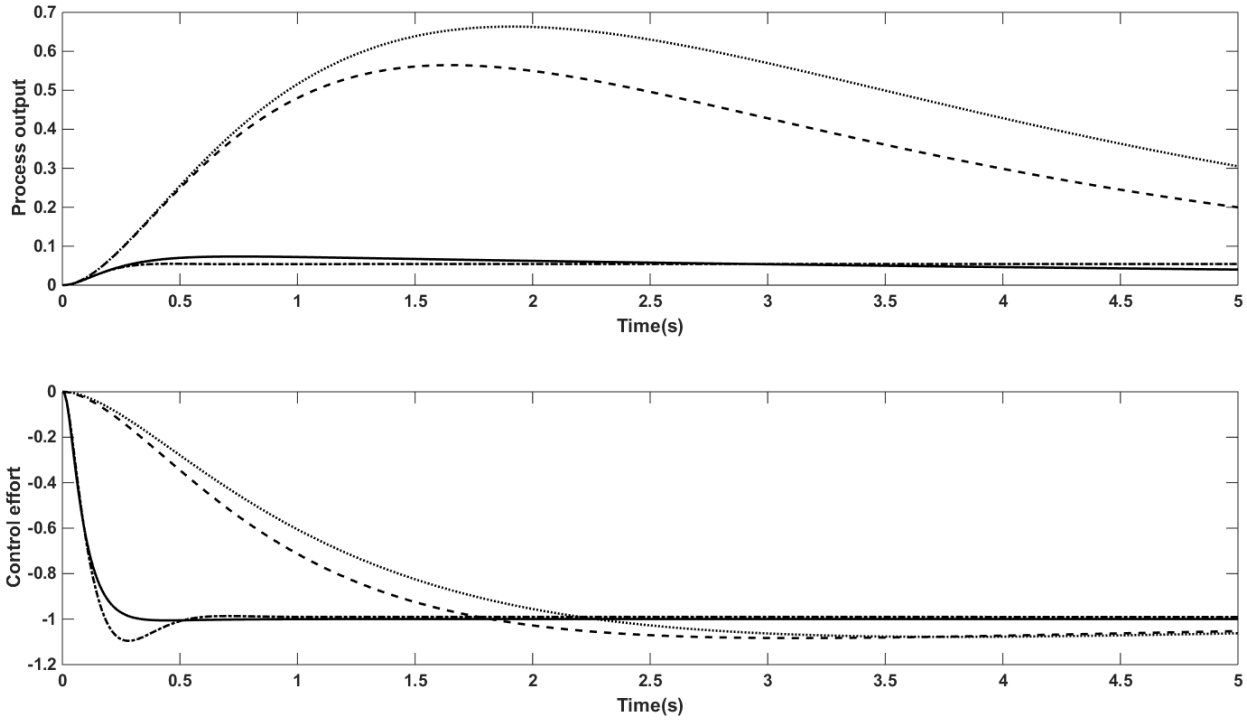

Fig 3.25 Regulatory response under nominal process conditions: solid - proposed, dashed - PID, dash dot - FOPD, dotted - FOPID

Table 3.7 Comparison of ISE, IAE and TV for nominal response

Method	**Servo response**			**Regulatory response**			**M_s**
	ISE	**IAE**	**TV**	**ISE**	**IAE**	**TV**	
Proposed	0.0585	0.0965	187.3219	0.004	0.1378	0.506	1
PID	0.5157	0.9641	2.4214	0.2047	0.9438	0.557	1.152
FOPD	0.06	0.146	140.0509	0.0035	0.1315	0.6045	1.052
FOPID	0.6104	1.086	1.4271	0.3141	1.181	0.5468	1.131

The closed loop performance for perturbation of +30% in K is shown in Fig 3.26 and Fig 3.27. It is clear from the figures that the proposed method is giving better servo and regulatory performance under perturbed process conditions. This is evident from the ISE, IAE and TV values in Table 3.8. The TV value for servo performance is high with the proposed method whereas the ISE and IAE values are low compared to the other three methods. In case of regulatory performance for perturbed case, the ISE and IAE values with the proposed method and FOPD method are almost same but the TV value is smaller than the other three methods.

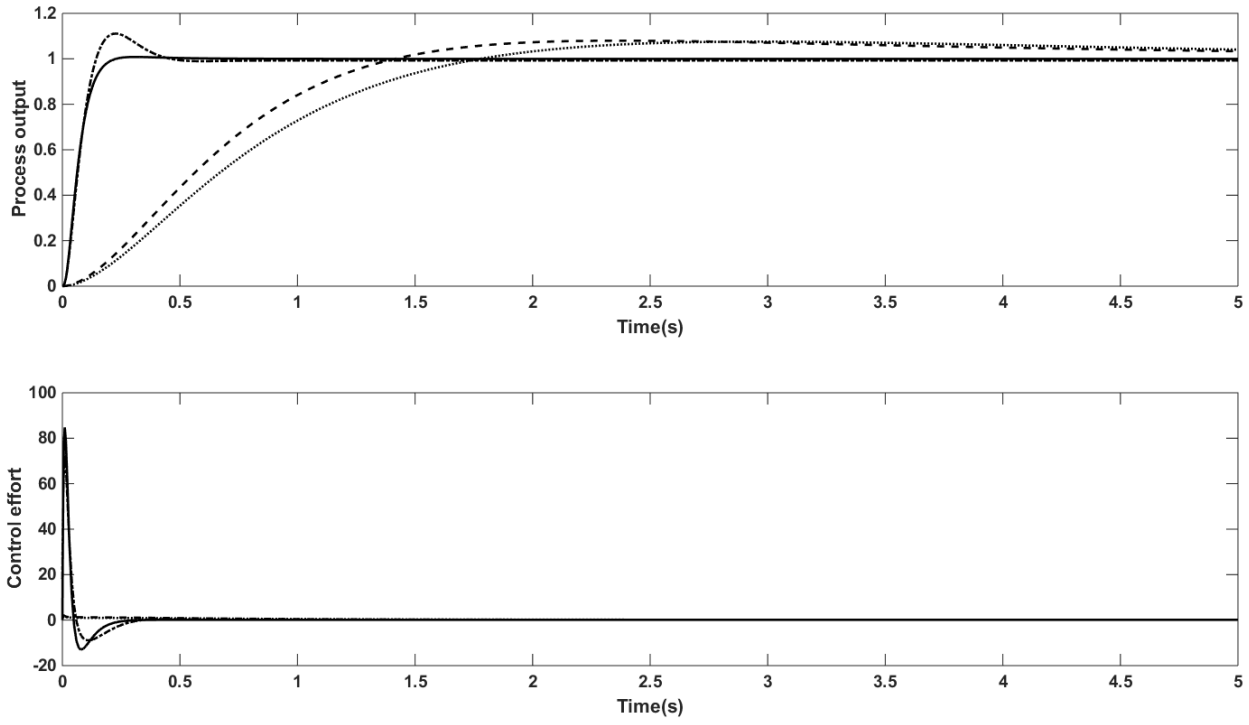

Fig 3.26 Servo response for perturbation: solid-proposed, dashed-PID, dash dot-FOPD, dotted-FOPID

Table 3.8 Comparison of ISE, IAE and TV for perturbed response

Method	Servo response			Regulatory response		
	ISE	IAE	TV	ISE	IAE	TV
Proposed	0.0478	0.076	195.7574	0.004	0.1382	0.5085
PID	0.4249	0.8132	2.465	0.213	0.9516	0.5631
FOPD	0.0504	0.1214	145.8854	0.0035	0.1322	0.6176
FOPID	0.502	0.923	1.4678	0.3328	1.206	0.5554

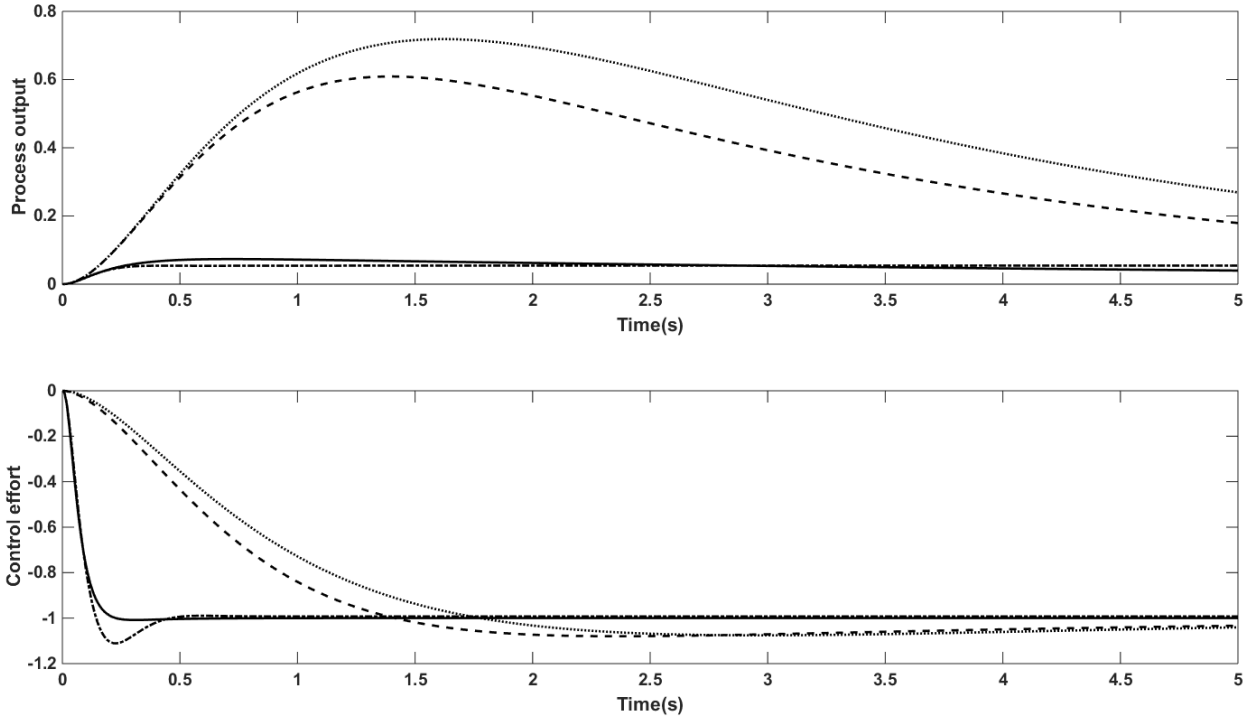

Fig 3.27 Regulatory response for perturbation: solid-proposed, dashed-PID, dash dot-FOPD, dotted-FOPID

The robust stability of the closed loop system is assessed for +20% uncertainty and +80% uncertainty in process time constant T_1 and is illustrated in Fig 3.28. All the four methods satisfy the robust stability condition provided in eq. (3.15). Further increase in uncertainty causes the four complementary sensitivity function lines to cross the uncertainty bound line and hence violating the stability condition. Therefore, +80% with a tolerance of +5% is the bound on multiplicative uncertainty. Finally, the closed loop system is robustly stable with all the four controllers which can be observed from the magnitude plot.

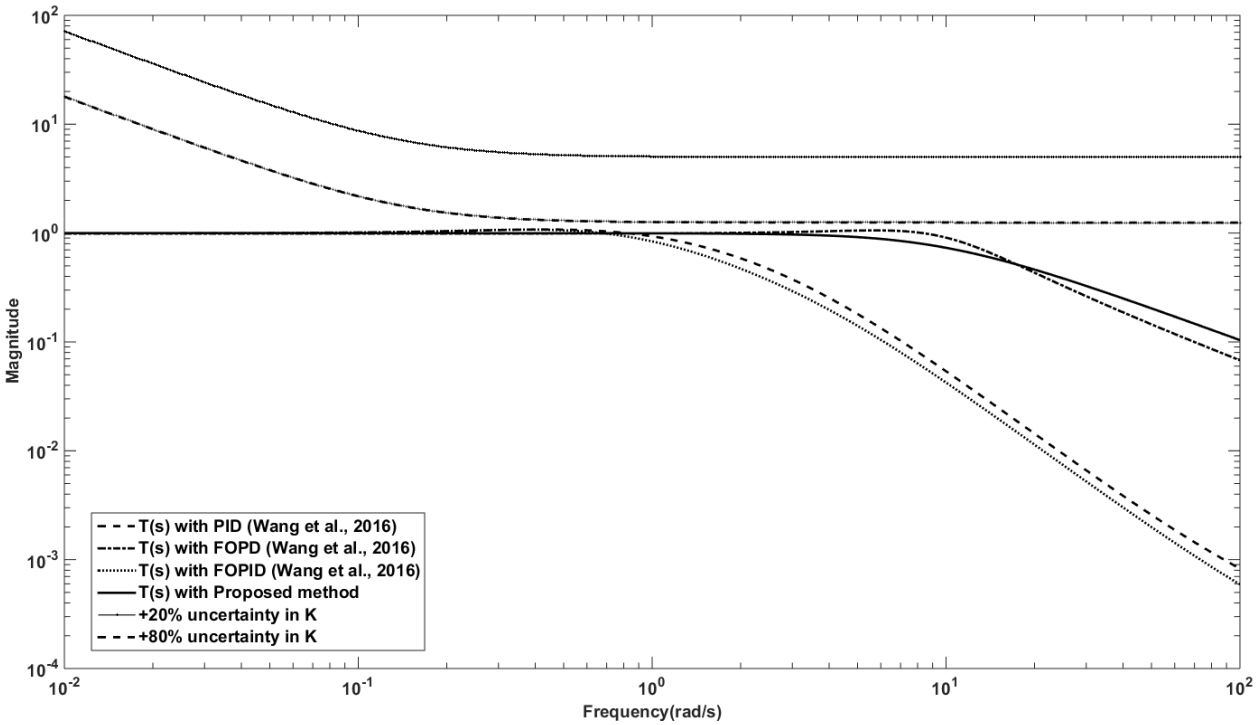

Fig 3.28 Magnitude plot

3.2.5. Conclusion

A fractional filter IMC-PID controller is proposed for inverted pendulum system after stabilizing its model by eliminating unstable poles and zeros. The design had used first order fractional IMC filter. The simulation results showed that the proposed method is giving superior servo and regulatory performance compared to the other three methods for nominal and perturbed process model. The control effort with the proposed method is less especially for disturbance rejection. The robust stability of the closed loop system is proved for parametric uncertainties.

Chapter 4

Enhanced fractional filter IMC-PID controller for improved disturbance rejection of SOPTD processes

4. Enhanced fractional filter IMC-PID controller for improved disturbance rejection of SOPTD processes*

A modified fractional internal model control (IMC) filter structure is proposed to design a fractional filter Proportional-Integral-Derivative (FFPID) controller for improved disturbance rejection of second order plus time delay (SOPTD) processes. The proposed method aims at improving the disturbance rejection of slow chemical processes as the tuning rules for such processes are limited. The present design also considers the higher order approximation for time delay as it gives improved response for higher order processes. There is an additional tuning parameter in the proposed IMC filter apart from the conventional IMC filter time constant, which is tuned according to the derived formula. The additional adjustable parameter achieves the disturbance rejection and the closed loop stability. The simulation results have been performed for the same degree of robustness (maximum sensitivity, M_s) for a fair comparison. The results show an improved disturbance rejection for lag dominant and delay significant SOPTD processes with the proposed controllers designed using higher order Pade's approximation of time delay than the proposed method using first order approximation and the conventional method. The closed loop robust performance is observed for perturbations in the process parameters and the performance is also observed for noise in the measurement. The robust stability analysis is carried out using sensitivity functions. In addition, the M_s range is also identified over which the system gives robust performance for the controllers designed using higher order pade's approximation of time delay compared to conventional method.

4.1. Introduction

The PID controller is still being extremely used in process control applications inspite of the availability of many advanced control algorithms (Shamsuzzoha, 2013; Silva et al., 2007). This is due to the fact that the PID controller has been provided with wide range of tuning rules and it is proved to give satisfactory performance (Astrom and Hagglund, 1995; Skogestad, 2003). The IMC method has been the mostly used for designing the controller as the resulting tuning rules have only

*The work is published in Chemical Product and Process Modeling (De Gruyter), doi: 10.1515/cppm-2018-0012

one tuning parameter. There are IMC based PID tuning rules for SOPTD processes but their number is limited (Weigand and Kegerreis, 1972). However, the tuning rules are still evolving to ensure better disturbance rejection for SOPTD processes as the IMC-PID controller doesn't always give good disturbance rejection (sluggish response) (Vilanova and Visioli, 2012; Jeng et al., 2014; Lee et al., 2013). There was a work in literature addressing the implicit disturbance rejection capacity of closed loop controller (Alagoz et al., 2015). Hence, the present work focuses on the design of controller for better disturbance rejection of SOPTD processes. The design uses fractional calculus that results in a fractional controller for precise monitoring of the closed loop system with the help of fractional order differentiation and integration (Miller and Ross, 1993). In practice, there is difficulty in adjusting the parameters of the PID controller as the industrial systems are often associated with parametric uncertainties, large transportation lags, nonlinearities and structural complexities. The performance of these integer order systems can be improved by using fractional order controller. Fractional order controller provides robust control with additional tuning parameters leading to complexity in tuning. Moreover, it was proved to give improved performance than integer order controllers (Podlubny, 1994; Das, 2011; Yeroglu and Tan, 2011; Monje et al., 2008). The fact is that the fractional derivative has the ability to model a vast range of dynamical systems and can control systems with higher orders and nonlinearities.

The dominant controller design methods used for SOPTD processes are DS method and IMC scheme. A PI/PID controller was designed analytically based on disturbance rejection using DS method. Setpoint weighting was used to suppress the overshoot in the servo response and derivative weighting was also used to handle the measurement noise (Chen and Seborg, 2002). A PID controller was designed based on IMC scheme and the controller parameters were obtained using Maclaurin series (Lee et al., 1998). Different PID tuning rules to control SOPTD processes was studied with most of them being designed using IMC method. A new PID tuning rule was also proposed based on closed loop trajectory specification (Panda et al., 2004). Controllers designed using DS method doesn't give satisfactory disturbance rejection and their structure may not always takes the PID form. A DS based PID controller in series with lead-lag compensator is reported (Rao et al., 2009), and they used setpoint weighting to achieve better servo response. The IMC based design always results in a PID form of the controller and there are several IMC-PID tuning methods available in literature for SOPTD processes. In Shamsuzzoha and Lee (2007), an optimum IMC filter was identified by observing the closed loop response after designing the PID controller

for different process models which gives minimum IAE for a specific M_s. In addition, guidelines were provided for selecting the closed loop time constant. A PID controller cascaded with lead-lag compensator was analytically derived for SOPTD processes using IMC method. Further, setpoint filter was used to reduce overshoot in the closed loop response (Shamsuzzoha and Lee, 2008). An IMC based PID controller was designed for disturbance rejection with an intention to have single tuning rule for different types of processes using second order IMC filter (Shamsuzzoha, 2015). A PID controller was designed whose parameters were optimized based on the minimization of IAE (Madhuranthakam et al., 2008). A linear quadratic regulator (LQR) and pole placement based approach for designing PID controller is proposed (Srivastava et al., 2016). The PID parameters were calculated using the user defined values of closed loop damping ratio and natural frequency. An IMC-PID controller using pole-zero conversion is designed with a unified IMC filter (Wang et al., 2016). An imaginary filter was used during the controller design to calculate the PID parameters. Also, setpoint weighting was used to minimize the overshoot.

The various IMC based PID controller design methods cited above have used integer order IMC filter for their design. Some of them were suitable for either setpoint tracking or disturbance rejection. Moreover, they have used setpoint weighting/setpoint filter for suppressing the overshoot to improve the servo response. Hence, there is a need to devise new tuning rules for improved closed loop performance of SOPTD processes especially disturbance rejection. Hence, the present work focuses on the design of controller using fractional IMC filter. The authors have proposed a fractional filter IMC-PID controller for SOPTD processes using first order fractional IMC filter in the earlier chapter. The tuning parameters were chosen iteratively such that ISE and IAE are minimum. The improved closed loop performance with the first order fractional IMC filter motivated to design FFPID controller using higher order fractional IMC filter structure. In the current work, a FFPID controller is designed using optimum higher order fractional IMC filter for a standard M_s as the higher order IMC filter was proved to give better performance for SOPTD processes. The novelty of the work lies in finding the optimum higher order fractional IMC filter structure and to observe the effect of time delay approximations used during the controller design on the closed loop response especially disturbance rejection. A systematic procedure is developed to find the optimum IMC filter structure for same robustness. The proposed method improves the disturbance rejection through the modified fractional IMC filter structure by cancelling the dominant pole in the process. The resulting controller has an additional adjustable parameter apart

from filter time constant which offer flexibility in controller tuning. Further, a higher order Pade's approximation i.e., the generally encountered second order approximation (Vajta, 2000; Kuo, 1991), 1/2 order approximation and 2/3 order approximation of time delay (the order of numerator is one less than that of denominator) which gives better step response is used during the design (Vu et al., 2017). The ISE, IAE, TV and M_s are used to assess the closed loop performance of SOPTD processes.

4.2. Fractional filter IMC-PID Controller design using fractional IMC filter

4.2.1. Internal model control

The IMC design procedure is same as given in Chapter 3 except for the use of higher order fractional IMC filter structure. The modified fractional IMC filter used here is given by,

$$f(s)=\frac{(\beta s+1)^n}{(\gamma s^p+1)^{n+1}} \tag{4.1}$$

The filter order 'n' must be large enough such that the IMC controller is realizable; γ is an adjustable parameter that affects the speed of response and β improves the disturbance rejection by cancelling the dominant pole of G_m which is determined by eq. (4.2)

$$(1-G_m C_{IMC})_{s=\frac{-1}{T_1}} = 0 \tag{4.2}$$

where T_1 is the dominant pole of G_m.

4.2.2. Proposed controller design using fractional IMC filter

The current work uses a fractional IMC filter (eq. (4.1)) with n=1 for designing the controller according to the IMC design procedure. The purpose of numerator term in the filter is to cancel out the system's dominant pole for effective disturbance rejection. The resulting structure consists of a PID term cascaded with fractional filter term. The resulting controller remains same for all the proposed methods (for different approximations of time delay) except for the variation in fractional filter term. The tuning of this fractional filter term is sufficient to assure improved closed loop response without having to use setpoint weighting/setpoint filter. The proposed controller is obtained as follows:

The proposed controller structure is

$$C(s)=(\text{fractional filter})K_p\left[1+\frac{1}{T_i s}+T_d s\right] \tag{4.3}$$

Consider a SOPTD model

$$G_m(s)=\frac{Ke^{-Ls}}{(T_1 s+1)(T_2 s+1)} \tag{4.4}$$

The optimum fractional IMC filter structure used is

$$f(s)=\frac{\beta s+1}{(\gamma s^p+1)^2} \tag{4.5}$$

Where γ is the fractional filter time constant, β additional degree of freedom. Now, the IMC controller is

$$C_{IMC}(s)=\left[\frac{(T_1 s+1)(T_2 s+1)}{K}\right]\left[\frac{\beta s+1}{(\gamma s^p+1)^2}\right] \tag{4.6}$$

Finally, the fractional filter IMC-PID controller according to equations (4.4) and (4.6) is

$$C(s)=\frac{\left[\frac{(T_1 s+1)(T_2 s+1)(\beta s+1)}{K(\gamma s^p+1)^2}\right]}{\left[1-\frac{(T_1 s+1)(T_2 s+1)(\beta s+1)}{K(\gamma s^p+1)^2}\right]\left[\frac{Ke^{-Ls}}{(T_1 s+1)(T_2 s+1)}\right]} \tag{4.7}$$

$$C(s)=\frac{(T_1 s+1)(T_2 s+1)(\beta s+1)}{K\left[(\gamma s^p+1)^2-(\beta s+1)e^{-Ls}\right]} \tag{4.8}$$

Now, the final controller expression can be obtained by approximating the delay term using Pade's approximation of different order. The first, second, 2/3 order and 1/2 order Pade's approximation of time delay are listed in Table 4.1. By using these approximations for time delay, the general controller structure obtained is

$$C(s)=(\text{fractional filter})\left(\frac{T_1+T_2}{K}\right)\left[1+\frac{1}{(T_1+T_2)s}+\left(\frac{T_1 T_2}{T_1+T_2}\right)s\right] \tag{4.9}$$

The proportional, integral and derivative terms for the four proposed methods are:

$$k_P=\frac{T_1+T_2}{K};T_i=T_1+T_2;T_d=\frac{T_1 T_2}{T_1+T_2} \tag{4.10}$$

Table 4.1 Pade's approximation of time delay term

Pade's approximation of e^{-LS}	
First order	$(1-0.5Ls)/(1+0.5Ls)$
Second order	$\left[1-(L/2)s+\left(L^2/12\right)s^2\right]/\left[1+(L/2)s+\left(L^2/12\right)s^2\right]$
2/3 order	$(60-24Ls+3L^2s^2)/(60+36Ls+9L^2s^2+L^3s^3)$
1/2 order	$(6-2Ls)/(6+4Ls+L^2s^2)$

The K_p, T_i and T_d expressions with the proposed method (proposed method in chapter 3 is termed as conventional/proposed in this chapter) are same as given in eq. (4.10). The fractional filter terms for the four proposed methods and the conventional method are given in Table 4.2 along with the tuning formula for parameter β. The controller settings K_p, T_i and T_d can be obtained from the process parameters according to the derived formulae. The remaining parameters to be tuned in all the proposed controllers are γ, β and p which are the IMC filter time constant; an extra degree of freedom that cancels out the dominant pole and fractional order of the IMC filter. The optimum values of these parameters are chosen for a predefined M_s. The proper selection of these parameters alters the filter term of the controller, which enhances the closed loop performance. Hereafter, the four proposed methods are referred to as Proposed1 (design using IMC filter $(\beta s+1)/(\gamma s^p+1)^2$ and with first order Pade's approximation of time delay); Proposed2 (design using IMC filter $(\beta s+1)/(\gamma s^p+1)^2$ and with second order Pade's approximation of time delay); Proposed3 (design using IMC filter $(\beta s+1)/(\gamma s^p+1)^2$ and with 2/3 Pade's approximation of time delay) and Proposed4 (design using IMC filter $(\beta s+1)/(\gamma s^p+1)^2$ and with 1/2 Pade's approximation of time delay).

Table 4.2 Fractional filter terms in the proposed controllers

Method	**Fractional filter term**
Proposed1	$\frac{0.5\beta L s^2+(\beta+0.5L)s+1}{0.5\gamma^2 L s^{2p}+\gamma^2 s^{2p-1}+\gamma L s^p+0.5\beta L s+2\gamma s^{p-1}+(L-\beta)}$
Proposed2	$\frac{\frac{\beta L^2}{12}s^3+\left(\frac{\beta L}{2}+\frac{L^2}{12}\right)s^2+\left(\frac{L}{2}+\beta\right)s+1}{\frac{\gamma^2 L^2}{12}s^{2p+1}+\frac{\gamma^2 L}{2}s^{2p}+\frac{\gamma L^2}{6}s^{p+1}+\frac{\beta L^2}{12}s^2+\gamma^2 s^{2p-1}+\gamma L s^p+\frac{\beta L}{2}s+2\gamma s^{p-1}+(L-\beta)}$
Proposed3	$\frac{\beta L^3 s^4+(L^3+9\beta L^2)s^3+(9L^2+36\beta L)s^2+(36L+60\beta)s+60}{\gamma^2 L^3 s^{2p+2}+9\gamma^2 L^2 s^{2p+1}+2\gamma L^3 s^{p+2}+36\gamma^2 L s^{2p}+18\gamma L^2 s^{p+1}+(L^3-3\beta L^2)s^2+60\gamma^2 s^{2p-1}+72\gamma L s^p+(6L^2+24\beta L)s+120\gamma s^{p-1}+(60L-60\beta)}$
Proposed4	$\frac{\beta L^2 s^3+(L^2+4\beta L)s^2+(4L+6\beta)s+6}{\gamma^2 L^2 s^{2p+1}+4\gamma^2 L s^{2p}+2\gamma L^2 s^{p+1}+6\gamma^2 s^{2p-1}+8\gamma L s^p+(L^2+2\beta L)s+12\gamma s^{p-1}+(6L-6\beta)}$
Proposed	$\frac{0.5Ls+1}{0.5\gamma L s^p+\gamma s^{p-1}+L}$

$$\beta=T_1\left\{1-\left[\gamma\left(\frac{-1}{T_1}\right)^p+1\right]^2 e^{\frac{-L}{T_1}}\right\}$$

4.3. Closed loop performance, robustness and fragility analysis

4.3.1. Performance analysis

The closed loop performance is observed for a unit step change in R and a step change in D of different magnitude. Also, the performance is observed for perturbations of +10% in time delay and gain. White noise with zero mean and a variance of 0.1 is introduced in the output to check the performance of closed loop system. The closed loop performance is assessed by using ISE, IAE, TV and M_s which are given in equations (4.11) - (4.14).

$$ISE= \int_0^\infty e^2(t)dt \tag{4.11}$$

$$IAE= \int_0^\infty |e(t)|dt \tag{4.12}$$

$$TV= \sum_{i=0}^{\infty} |u_{i+1} - u_i| \tag{4.13}$$

$$M_s= \max_{0<\omega<\infty} \left|\frac{1}{1+C(j\omega)G(j\omega)}\right| \tag{4.14}$$

4.3.2. Robustness analysis

The closed loop stability must be assessed for the nominal process conditions and with uncertainties as they practically exist in all the processes. Hence, the closed loop system must ensure a robust and stable control performance for parametric uncertainties with the proposed controller. This is verified with the following robust stability condition (Maciejowski, 1989; Morari and Zafiriou, 1989)

$$\|l_m(j\omega)T(j\omega)\|<1 \forall \omega \in (-\infty,\infty) \tag{4.15}$$

Where $T(s)_{s=j\omega}=\frac{C(s)G(s)}{1+C(s)G(s)}$ - the complementary sensitivity function;

$l_m(j\omega)= \left|\frac{G(j\omega)-G_m(j\omega)}{G_m(j\omega)}\right|$ - Process multiplicative uncertainty bound.

The controller must be tuned according to eq. (4.16) for uncertainty in time delay

$$\|T(j\omega)\|_\infty < \frac{1}{|e^{-\Delta L}-1|} \tag{4.16}$$

4.3.3. Controller fragility analysis

It is important to note that the closed loop system must be robust for changes in not just the process parameters but also the controller parameters. So, the fragility of the controller should be analyzed as their exactness is not guaranteed during implementation which degrades the performance of closed loop system. The controller fragility is checked using delta 20 fragility index (Alfaro, 2007) by varying all the controller parameters by +20%. The delta 20 fragility index ($FI_{\Delta 20}$) is defined as follows:

$$FI_{\Delta 20}=\frac{M_{s\Delta 20}}{M_s}-1 \quad (4.17)$$

Where $M_{s\Delta 20}$ is the maximum sensitivity for 20% variation in controller parameters and M_s is the nominal maximum sensitivity.

A controller is said to be fragile if $FI_{\Delta 20}>0.5$; nonfragile if $0.1<FI_{\Delta 20}\leq 0.5$ and resilient if $FI_{\Delta 20}\leq 0.1$.

In summary, the systematic steps involved in the design of proposed method are:

Step 1: Select an SOPTD system and derive controller into the form (fractional filter)×(PID)

Step 2: Derive controller expressions using different IMC filter structures and different Pade's approximation for time delay

Step 3: Select an IMC filter structure and derive the controller by choosing first order Pade's approximation of time delay

Step 4: Using the IMC filter structure chosen in step 3, derive controllers using second order Pade's approximation of time delay and 2/3 order Pade's approximation of time delay

Step 5: After steps 3 & 4, the PID terms remain same for all the controllers derived with a variation in the fractional filter term.

Step 6: Observe the parameters to be selected from the derived controllers

Step 7: K_p, T_i and T_d are obtained from the process parameters using the derived expressions

Step 8: Unknown parameters to be selected in the controller are γ, β and p

Step 9: Select an initial value for p (starting with 1.01) and γ

Observation: p should always be chosen as a value above 1. In the present algorithm, the initial value for p is chosen as 1.01. If the fractional value of p is increased, the overshoot increases and the errors (IAE) too. The authors have already presented it in their earlier work (previous chapter) about the effect of a change in p on the closed loop response.

Step 10: Obtain β according to the derived expression such that the M_s is equal to the predefined value

Step 11: If step 10 is not met, repeat steps 9 and 10

Step 12: Record the ISE and IAE values from the response with the selected controller parameters for one IMC filter structure

Step 13: Change the IMC filter structure and repeat steps 3 to 12

Step 14: Select the optimum IMC filter structure from the bar chart drawn using ISE and IAE values obtained from the response with all controllers designed using different IMC filter structures and different Pade's approximation of time delay

4.4. Simulation results and discussion

This section is dedicated to the selection of optimum fractional IMC filter structure and simulation study. The effectiveness of the proposed FFPID controller is examined by considering five different SOPTD processes. The simulations have been performed on several second order examples. The control scheme used for simulations is the standard feedback loop.

4.4.1. Optimum fractional IMC filter structure for fractional filter IMC-PID controller design

The selection of IMC filter is very important as it produces the best PID controller. The "best" here means minimizing performance measures ISE and IAE for a predefined M_s (Shamsuzzoha and Lee, 2007; Horn et al., 1993).

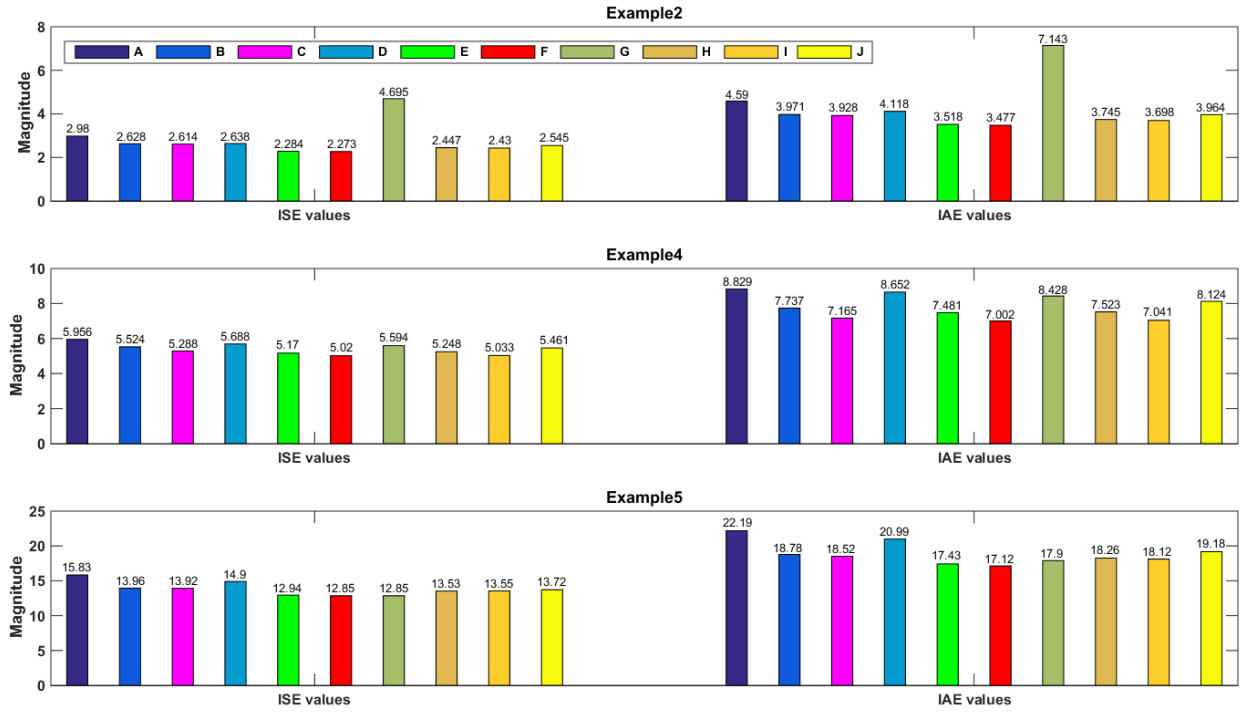

Fig 4.1 Comparison of ISE and IAE values for identification of optimum IMC filter: A - IMC filter $1/(\gamma s^p+1)^2$+first order pade's approximation of L; B - IMC filter $1/(\gamma s^p+1)^2$+second order Pade's approximation of L; C - IMC filter $1/(\gamma s^p+1)^2$+2/3 Pade's approximation of L; D - Proposed1; E - Proposed2; F - Proposed3; G - IMC filter $(\beta s+1)^2/(\gamma s^p+1)^3$+first order pade's approximation of L; H - IMC filter $(\beta s+1)^2/(\gamma s^p+1)^3$+second order pade's approximation of L; I - IMC filter $(\beta s+1)^2/(\gamma s^p+1)^3$+2/3 pade's approximation of L; J - Proposed method

The optimum fractional IMC filter structure used in the current paper is identified by comparing the closed loop performance of different SOPTD processes with the controllers designed using different IMC filters. The smallest values of ISE and IAE for a fixed M_s were used as measurements to identify the optimum filter structure and these values for different controllers are shown as a bar chart in Fig 4.1. It was found that the design using IMC filter (eq. (4.1) with n=1) along with second order Pade's approximation of time delay (Proposed2) and 2/3 order Pade's approximation of time delay (Proposed3) is better in terms of smaller ISE and IAE. Hence, the IMC filter in eq. (4.1) with n=1 is identified as optimum filter structure and simulation results were presented with the controllers designed using this optimum filter structure. Though the Proposed1 method is giving a poor performance (Fig 4.1), this case is still considered for closed loop performance comparison in the subsequent sections. But, this case (Proposed1) is not considered in identifying M_s range over which the system gives a robust performance.

4.4.2. Example 1

Consider the delay significant SOPTD process as studied in Lee et al. (2013)

$$G_m(s)=\frac{e^{-2s}}{(s+1)(0.7s+1)} \tag{4.18}$$

The PID controller settings for Proposed1, Proposed2, Proposed3, Proposed4 and proposed methods are K_p=1.7, T_i=1.7 and T_d=0.4117. The corresponding fractional filter terms are listed in Table 6.3. The controller settings according to Wang et al., (2016) are K_p=0.435; T_i=1.653 and T_d=0.4 and the setpoint weighting factor is 0.4. The disturbance input used is a step signal with a magnitude of -0.5.

Table 4.3 Tuning parameters and fractional filter terms for Example 1

Method	**γ**	**β**	**P**	**Fractional filter term**
Proposed1	1.165	0.366	1.02	$\frac{0.336s^2+1.366s+1}{1.357s^{2.04}+1.357s^{1.04}+2.33s^{1.02}+0.366s+2.33s^{0.02}+1.634}$
Proposed2	0.96	0.480	1.02	$\frac{0.16s^3+0.813s^2+1.48s+1}{0.307s^{3.04}+0.922s^{2.04}+0.64s^{2.02}-0.16s^2+0.922s^{1.04}+1.92s^{1.02}+0.48s+1.92s^{0.02}+1.52}$
Proposed3	0.95	0.485	1.02	$\frac{3.884s^4+25.478s^3+70.956s^2+101.13s+60}{7.22s^{4.04}+32.49s^{3.04}+15.2s^{3.02}+64.98s^{2.04}+68.4s^{2.02}+2.174s^2+54.15s^{1.04}+136.8s^{1.02}+47.304s+114s^{0.02}+90.87}$
Proposed4	1.03	0.442	1.02	$\frac{1.7696s^3+7.5392s^2+10.6544s+6}{4.2436s^{3.04}+8.4872s^{2.04}+8.24s^{2.02}+6.3654s^{1.04}+16.48s^{1.02}+5.7696s+12.36s^{0.02}+9.3456}$
Proposed	2	-	1.02	$\frac{s+1}{1.635s^{1.02}+1.635s^{0.02}+2}$

The servo and regulatory response for nominal process conditions is shown in Fig 4.2 and for perturbations in process parameters is shown in Fig 4.3. The system performance in the presence of output white noise is shown in Fig 4.4. The performance measures ISE, IAE and TV are recorded for unique M_s value of 1.64. These values for the above three input changes are presented in Tables 4.4-4.6.

Table 4.4 Performance measures of Example 1 for the perfect process model

Method	**Setpoint change**			**Load change**			**M_s**
	ISE	**IAE**	**TV**	**ISE**	**IAE**	**TV**	
Proposed1	3.161	3.915	12.229	0.577	1.946	0.511	1.64
Proposed2	2.786	3.443	23.736	0.480	1.709	0.506	1.64
Proposed3	2.771	3.424	24.183	0.476	1.697	0.506	1.64
Proposed4	2.905	3.612	18.739	0.511	1.798	0.507	1.64
Proposed	2.871	3.591	30.321	0.505	1.792	0.502	1.64
Wang et al. (2016)	4.148	5.231	0.982	0.621	2.097	0.570	1.64

Table 4.5 Performance measures of Example 1 for the perturbed process model

Method	**Setpoint change**			**Load change**		
	ISE	**IAE**	**TV**	**ISE**	**IAE**	**TV**
Proposed1	3.267	4.187	12.403	0.709	2.152	0.619
Proposed2	2.911	3.665	23.937	0.593	1.859	0.607
Proposed3	2.898	3.638	24.388	0.588	1.845	0.604
Proposed4	3.02	3.78	18.912	0.629	1.906	0.594
Proposed	2.981	3.745	30.493	0.62	1.906	0.609
Wang et al. (2016)	4.233	5.526	1.100	0.769	2.443	0.684

Table 4.6 Performance measures in the presence of output noise

Method	**Setpoint change**			**Load change**		
	ISE	**IAE**	**TV**	**ISE**	**IAE**	**TV**
Proposed1	8.201	15.55	2185.8	5.728	13.57	2182.9
Proposed2	7.812	15.21	4240.6	5.618	13.46	4234.8
Proposed3	7.8	15.21	4390.8	5.616	13.46	4384.9
Proposed4	7.931	15.31	3395.1	5.654	13.49	3390.5
Proposed	7.906	15.29	5488.1	5.65	13.49	5480.8
Wang et al. (2016)	9.092	16.26	6760.2	5.774	13.63	6693.1

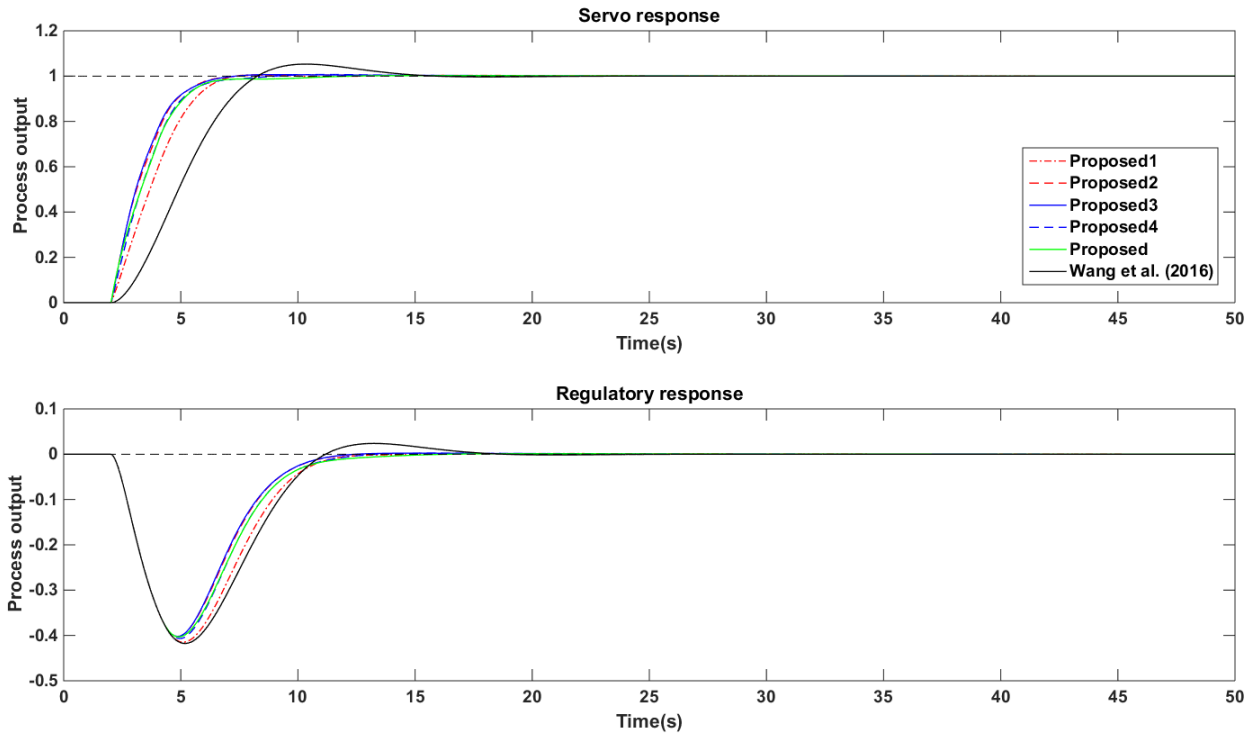

Fig 4.2 Closed loop response of Example 1 for nominal process conditions

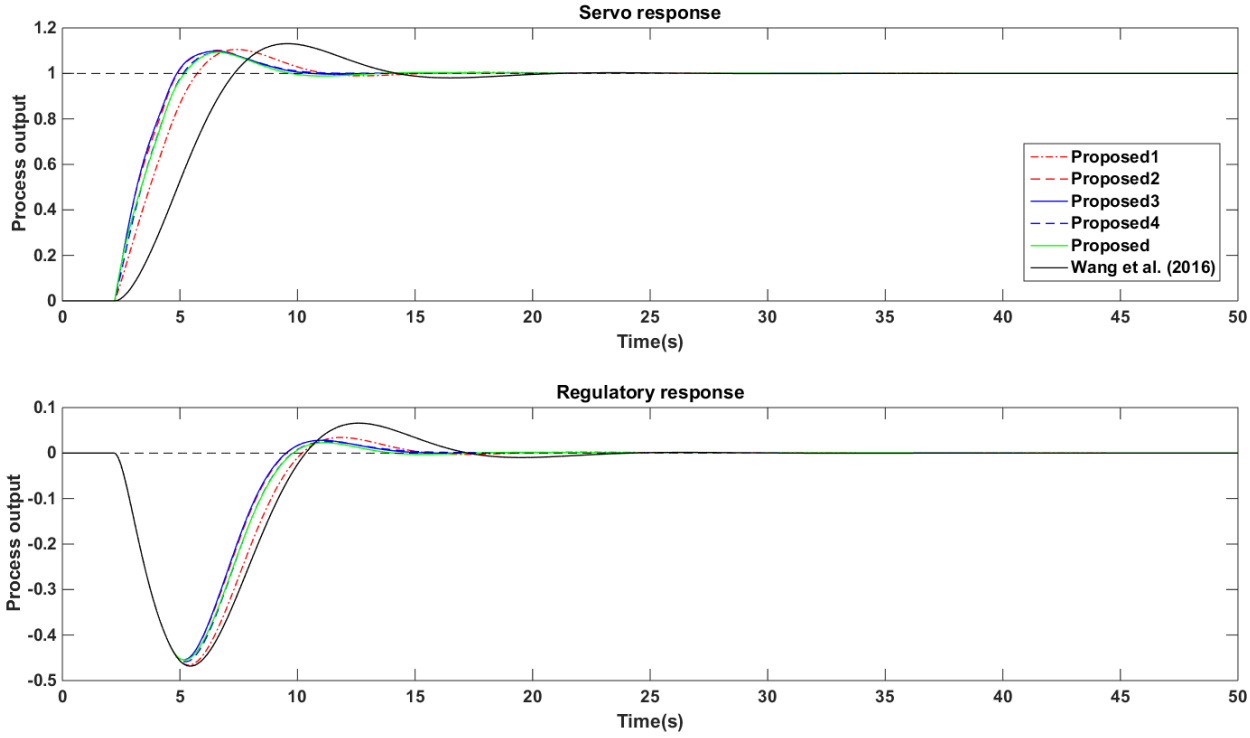

Fig 4.3 Closed loop response of Example 1 for perturbations

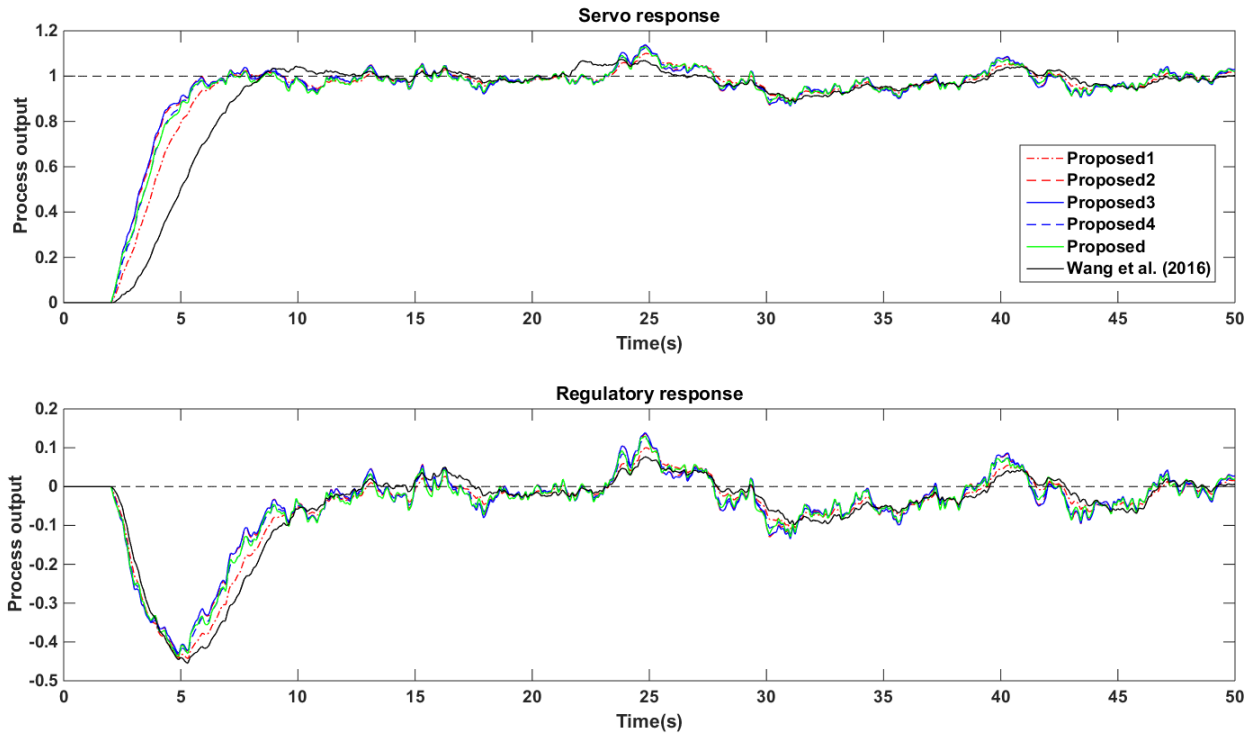

Fig 4.4 Closed loop response of Example 1 with measurement noise

It is evident from these results that the Proposed3 method is providing better performance with lower values of ISE and IAE. The TV value for nominal process conditions and perturbations is less with Proposed3 method especially for disturbance rejection. The TV value for noise case is slightly high compared to Proposed2 method while it is smaller compared to conventional method. It is observed that the ISE and IAE values are decreasing with the increase in the order of pade's approximation for servo and regulation while the TV is increasing for servo response.

The robust stability analysis is shown through magnitude plot in Fig 4.5 for +10% uncertainty in time delay. All the Proposed and old methods are stable by obeying the stability condition in eq. (4.16). The Proposed1 method is more robust compared to other methods. The effect of γ on the robust stability of closed loop system is also analyzed and is shown through magnitude plot in Fig 4.5. It can be observed that all the proposed methods are robustly stable. Further, the closed loop response for various M_s values are observed to know the range of M_s over which the response is robust. It was found that robust M_s range is 1.64-1.9 for Proposed2 and Proposed3 methods compared to conventional method. This M_s range is identified from the M_s versus ISE, IAE and TV graphs shown in Fig 4.6 and Fig 4.7. The Proposed3 method is superior in performance for this robust M_s range.

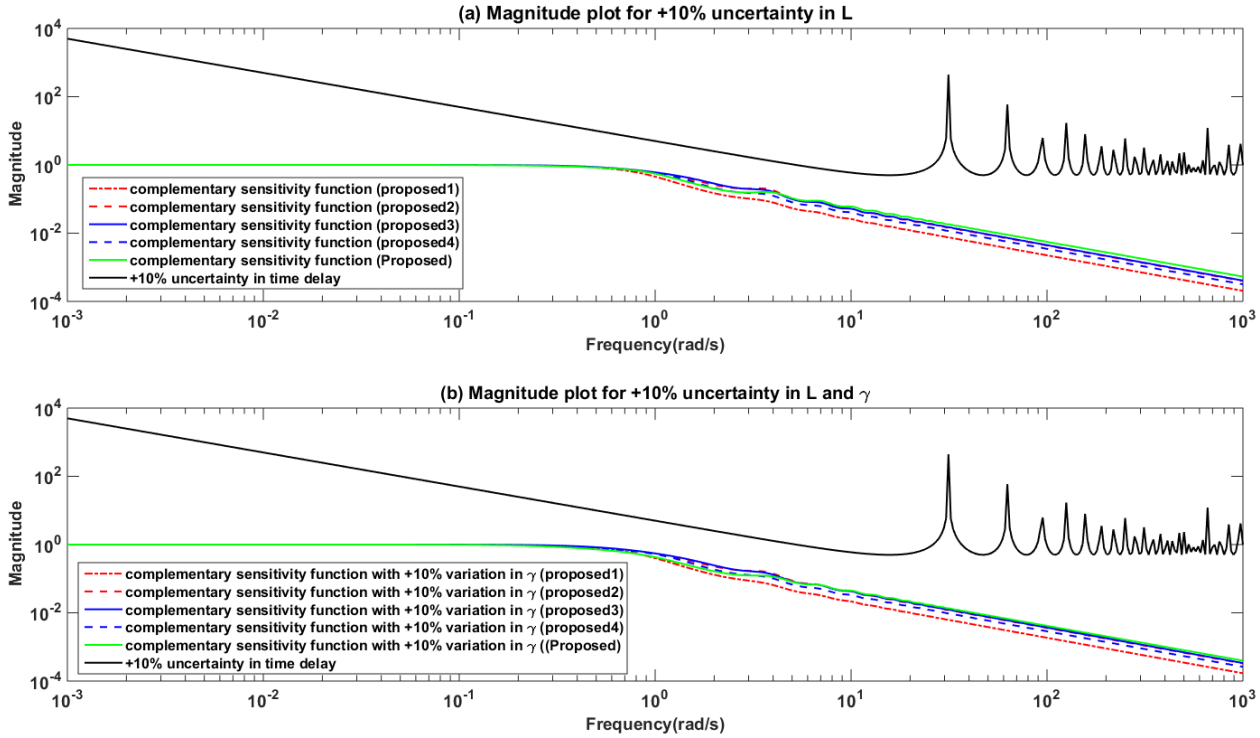

Fig 4.5 Example 1 Magnitude plot: (a) for +10% uncertainty in L (b) for +10% uncertainty in L and γ

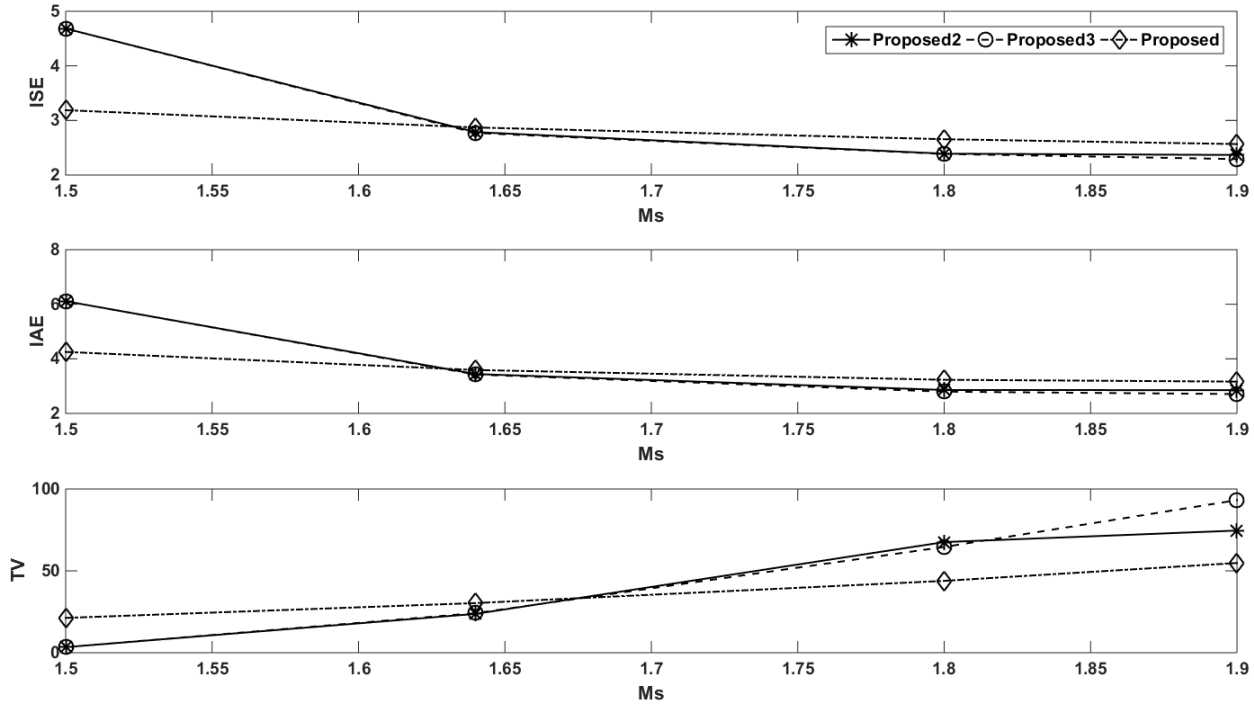

Fig 4.6 M_s versus ISE, IAE and TV for identification of robust servo performance of Example 1

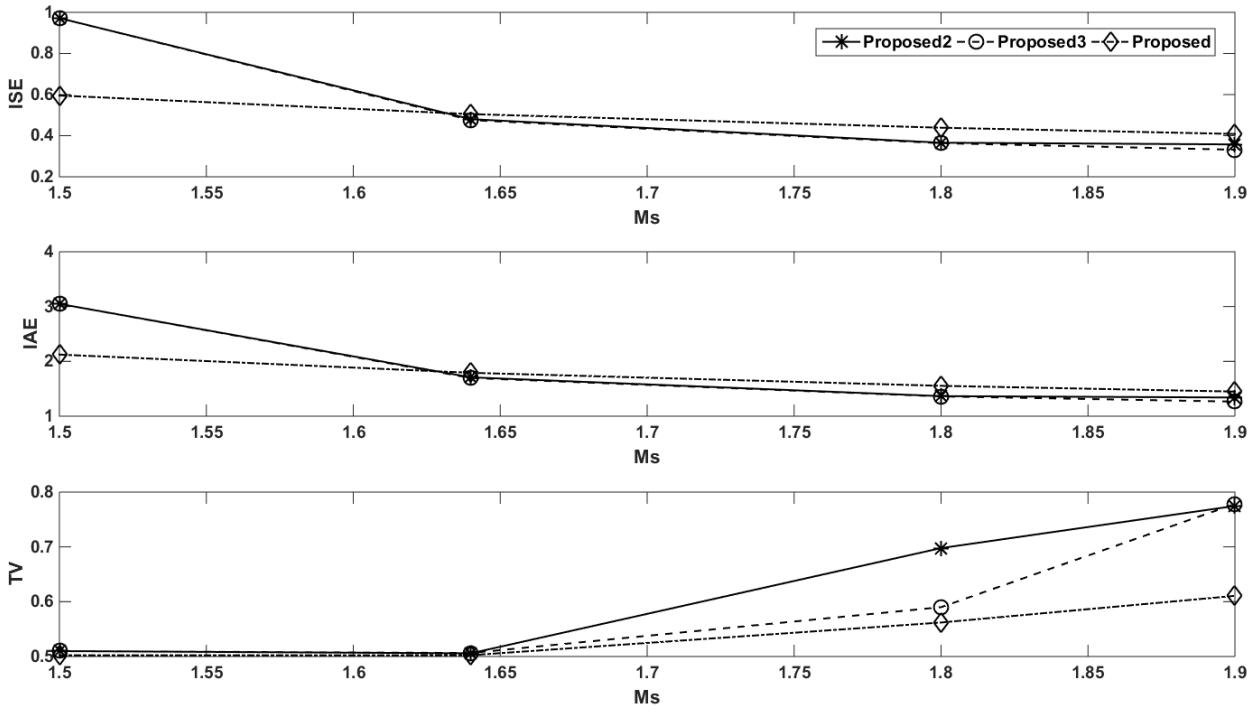

Fig 4.7 M_s versus ISE, IAE and TV for identification of robust regulatory performance of Example 1

4.4.3. Example 2

The second example (Srivastava et al., 2016) considered for performance comparison is as follows:

$$G_m(s)=\frac{e^{-1.64s}}{s^2+3s+2} \tag{4.19}$$

The PID controller settings for all the proposed methods and conventional method are K_p=3, T_i=1.5 and T_d=0.3333. The associated fractional filter terms are shown in Table 4.7 respectively. The disturbance input used is a step signal of magnitude -1. The closed loop response for different input changes are presented in Figs 4.8-4.10 for fixed M_s of 1.7 and the respective ISE, IAE and TV values are listed in Tables 4.8-4.10. The Proposed3 method is identified to be better both for servo and regulation followed by Proposed2 method. All the Proposed methods are robust which is shown through magnitude plot in Fig 4.11.

Table 4.7 Tuning parameters and fractional filter terms for Example 2

Method	**γ**	**β**	**P**	**Fractional filter term**
Proposed1	0.835	0.347	1.02	$\frac{0.2846s^{2}+1.1671s+1}{0.572s^{2.04}+0.697s^{1.04}+1.369s^{1.02}+0.285s+1.67s^{0.02}+1.293}$
Proposed2	0.68	0.453	1.02	$\frac{0.1015s^{3}+0.5953s^{2}+1.2727s+1}{0.104s^{3.04}+0.379s^{2.04}+0.305s^{2.02}-0.101s^{2}+0.462s^{1.04}+1.115s^{1.02}+0.371s+1.36s^{0.02}+1.187}$
Proposed3	0.67	0.459	1.02	$\frac{2.025s^{4}+15.526s^{3}+51.318s^{2}+86.592s+60}{1.98s^{4.04}+10.866s^{3.04}+5.91s^{3.02}+26.503s^{2.04}+32.437s^{2.02}+0.706s^{2}+26.934s^{1.04}+79.114s^{1.02}+34.212s+80.4s^{0.02}+70.848}$
Proposed4	0.75	0.406	1.02	$\frac{1.0925s^{3}+5.3542s^{2}+8.9972s+6}{1.5129s^{3.04}+3.69s^{2.04}+4.0344s^{2.02}+3.375s^{1.04}+9.84s^{1.02}+4.0219s+9s^{0.02}+7.4028}$
Proposed	1.16	-	1.02	$\frac{0.82s+1}{0.951s^{1.02}+1.16s^{0.02}+1.61}$

Table 4.8 Performance measures of Example 2 for the perfect process model

Method	**Setpoint change**			**Load change**			**M_s**
	ISE	**IAE**	**TV**	**ISE**	**IAE**	**TV**	
Proposed1	2.427	2.979	32.472	0.411	1.459	1.055	1.7
Proposed2	2.127	2.566	66.602	0.334	1.267	1.029	1.7
Proposed3	2.113	2.544	67.714	0.330	1.254	1.016	1.7
Proposed4	2.248	2.743	47.037	0.366	1.361	1.020	1.7
Proposed	2.279	2.781	61.739	0.375	1.385	1.036	1.7

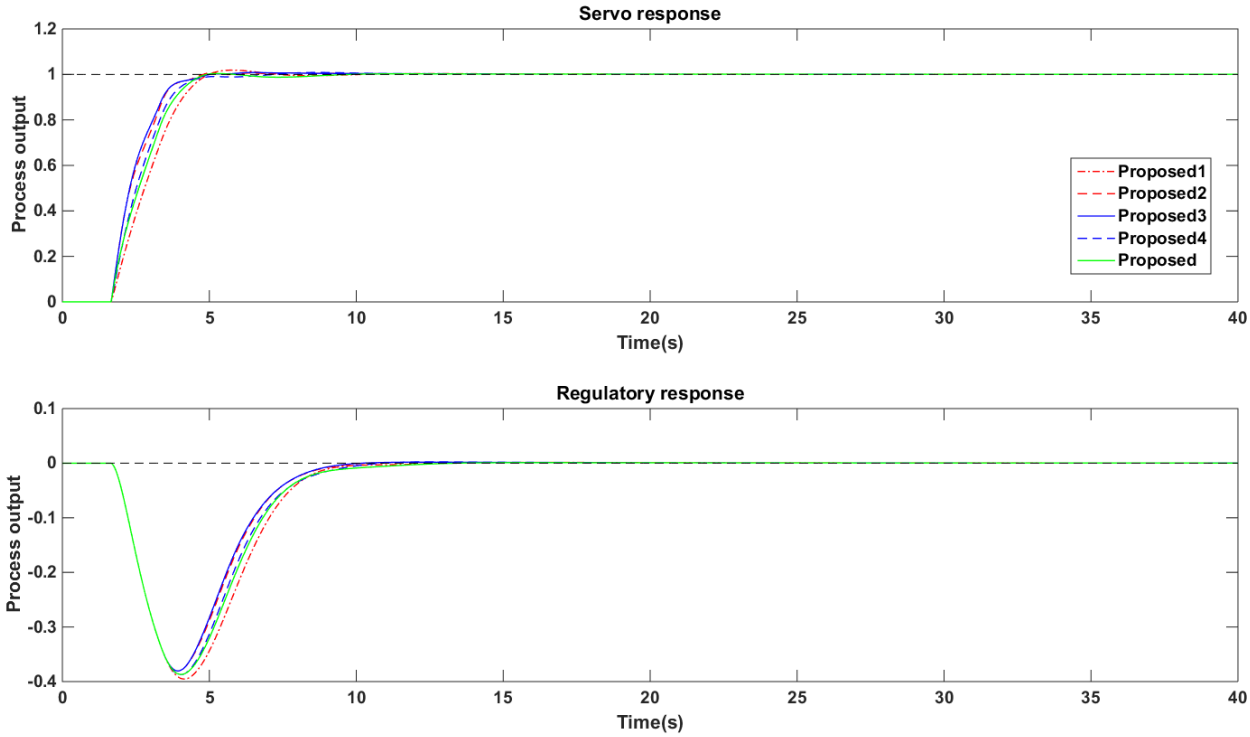

Fig 4.8 Closed loop response of Example 2 for nominal process conditions

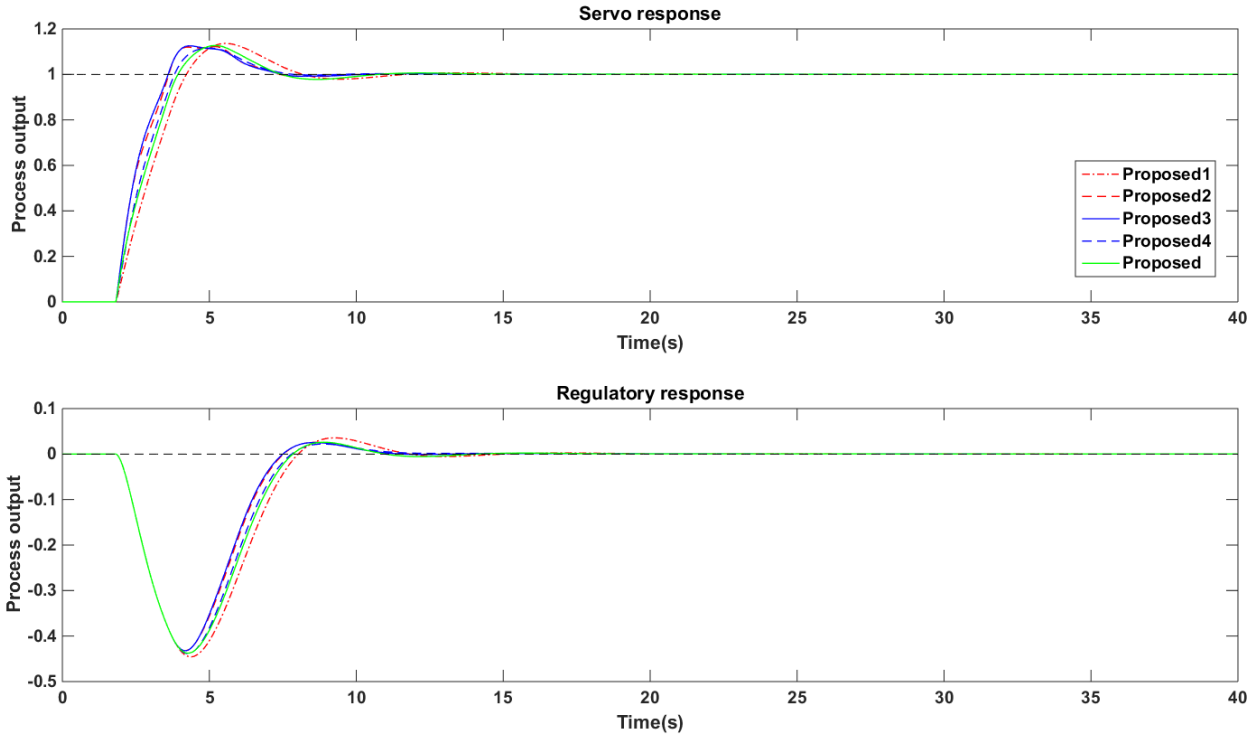

Fig 4.9 Closed loop response of Example 2 for perturbations

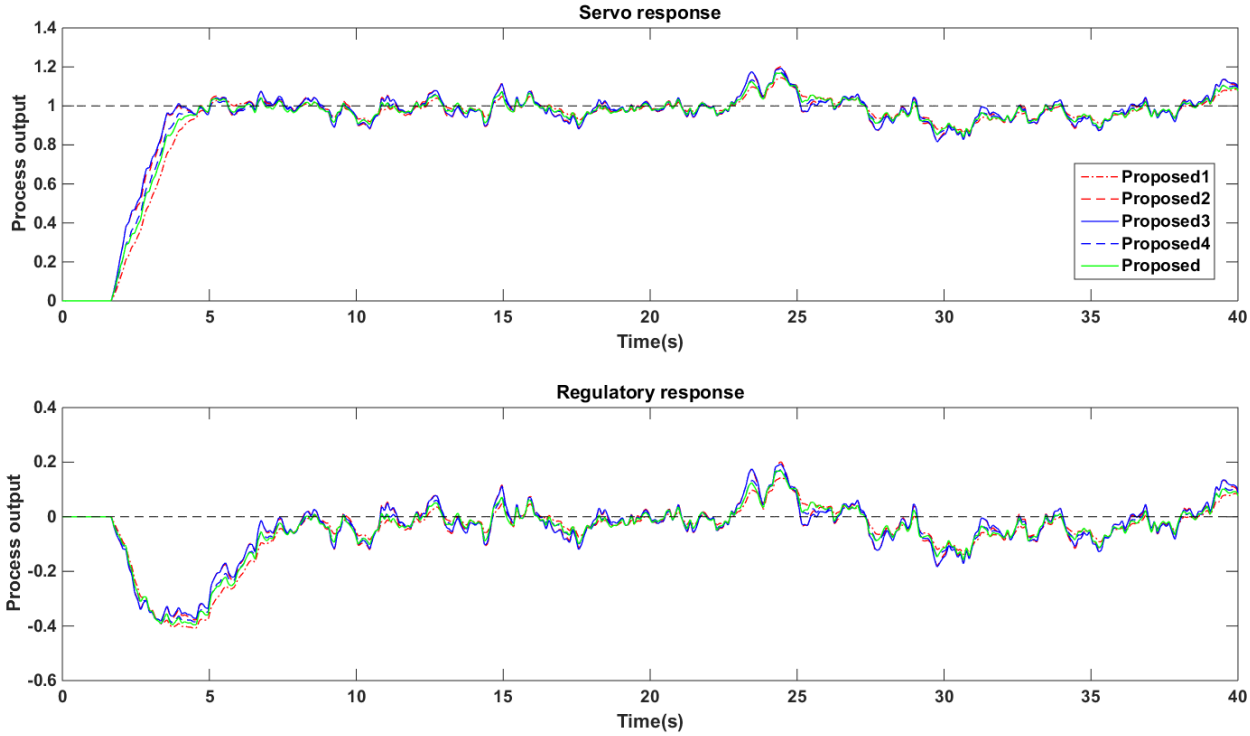

Fig 4.10 Closed loop response of Example 2 with measurement noise

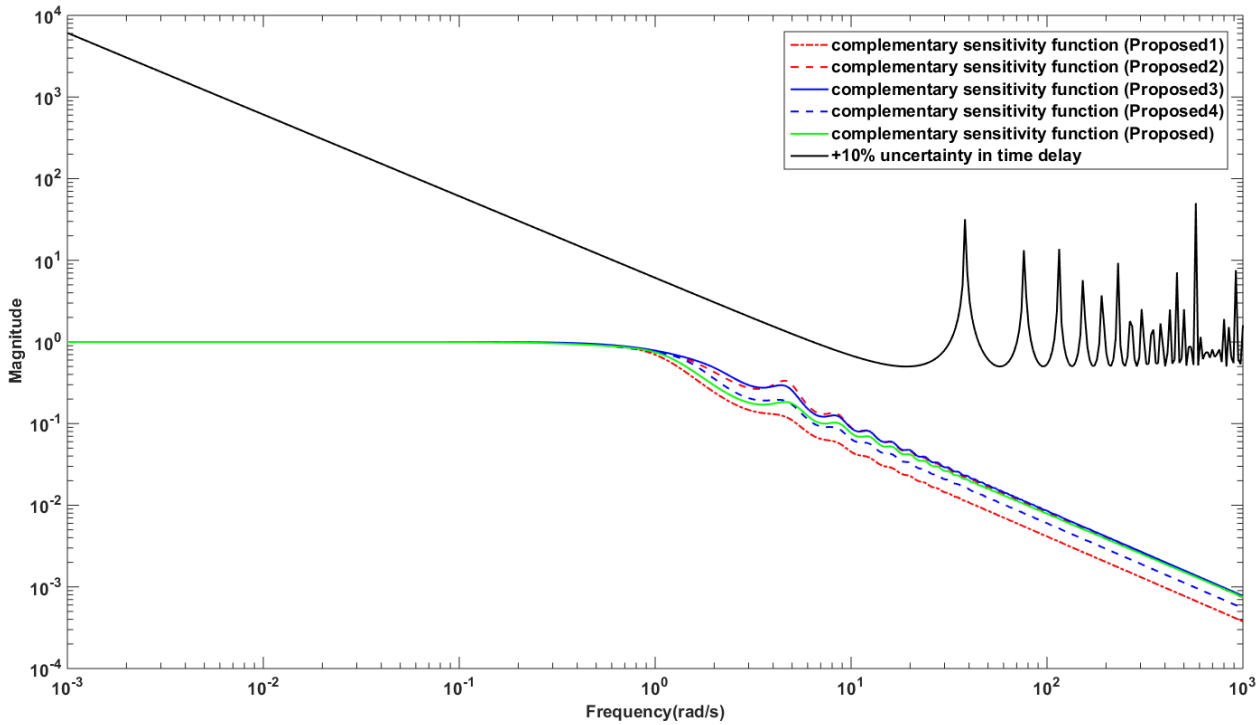

Fig 4.11 Magnitude plot for Example 2

Table 4.9 Performance measures of Example 2 for the perturbed process model

Method	**Setpoint change**			**Load change**		
	ISE	**IAE**	**TV**	**ISE**	**IAE**	**TV**
Proposed1	2.54	3.293	33	0.507	1.618	1.328
Proposed2	2.255	2.856	67.55	0.415	1.367	1.276
Proposed3	2.243	2.822	68.526	0.41	1.352	1.273
Proposed4	2.364	2.957	47.406	0.452	1.452	1.242
Proposed	2.392	3.055	62.207	0.463	1.486	1.311

Table 4.10 Performance measures in the presence of output noise

Method	**Setpoint change**			**Load change**		
	ISE	**IAE**	**TV**	**ISE**	**IAE**	**TV**
Proposed1	6.56	12.4	4718.9	4.68	10.93	4711.2
Proposed2	6.357	12.18	9306.9	4.69	10.92	9290.9
Proposed3	6.334	12.16	9763.1	4.674	10.91	9746.9
Proposed4	6.416	12.24	6862.9	4.66	10.9	6851.4
Proposed	6.457	12.28	9027.9	4.688	10.93	9013.3

4.4.4. Example 3

Consider the second order lag dominant linear process (Dey and Mudi, 2009) given by

$$G_m(s)=\frac{e^{-0.2s}}{(s+1)^2} \tag{4.20}$$

The PID settings for all the methods are K_p=2, T_i=2 and T_d=0.5 and their corresponding fractional filter terms along with tuning parameters are given in Table 4.11. The regulatory response is observed for a step change in disturbance of magnitude -0.2. The behavior of closed loop system is illustrated in Figs 4.12-4.14 and the performance measures are listed in Tables 4.12-4.14 for a M_s of 1.7. The Proposed3 method continues to give superior performance for servo and regulation compared to the other methods with lower values of ISE and IAE. All the four methods used for comparison are stable for +10% uncertainty in L obeying the robust stability condition in eq. (4.16) which is illustrated in Fig 4.15.

Table 4.11 Tuning parameters and fractional filter terms for Example 3

Method	**γ**	**β**	**P**	**Fractional filter term**
Proposed1	0.095	0.017	1.02	$\frac{0.0018s^2+0.1176s+1}{0.00091s^{2.04}+0.0091s^{1.04}+0.0191s^{1.02}+0.0018s+0.191s^{0.02}+0.182}$
Proposed2	0.077	0.049	1.02	$\frac{0.000165s^3+0.0083s^2+0.149s+1}{0.0000199s^{3.04}+0.000599s^{2.04}+0.00052s^{2.04}-0.00016s^2+0.006s^{1.04}+0.0155s^{1.02}+0.005s+0.1548s^{0.02}+0.1503}$
Proposed3	0.076	0.051	1.02	$\frac{0.00041s^4+0.026s^3+0.729s^2+10.272s+60}{0.0000468s^{4.04}+0.002s^{3.04}+0.0012s^{3.02}+0.042s^{2.04}+0.055s^{2.02}+0.0019s^2+0.351s^{1.04}+1.102s^{1.02}+0.486s+9.18s^{0.02}+8.928}$
Proposed4	0.085	0.036	1.02	$\frac{0.001448s^3+0.0689s^2+1.0172s+6}{0.000289s^{3.04}+0.00578s^{2.04}+0.0068s^{2.02}+0.0433s^{1.04}+0.136s^{1.02}+0.0545s+1.02s^{0.02}+0.9828}$
Proposed	0.135	-	1.02	$\frac{0.1s+1}{0.0135s^{1.02}+0.135s^{0.02}+0.2}$

Table 4.12 Performance measures of Example 3 for the perfect process model

Method	**Setpoint change**			**Load change**			**M_s**
	ISE	**IAE**	**TV**	**ISE**	**IAE**	**TV**	
Proposed1	0.330	0.419	178.005	0.00135	0.073	0.234	1.7
Proposed2	0.278	0.345	761.273	0.00091	0.06	0.229	1.7
Proposed3	0.275	0.341	720.174	0.00089	0.059	0.227	1.7
Proposed4	0.297	0.367	389.478	0.00108	0.065	0.222	1.7
Proposed	0.294	0.367	560.094	0.001	0.066	0.232	1.7

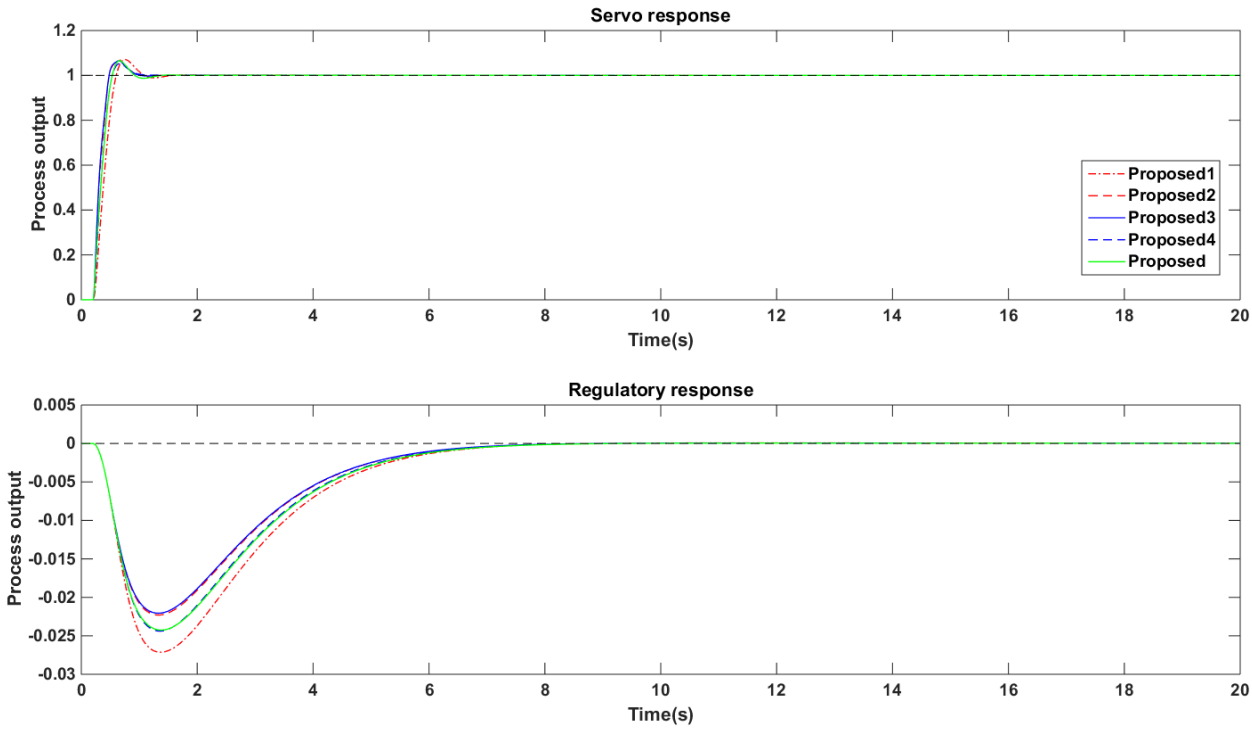

Fig 4.12 Closed loop response of Example 3 for nominal process conditions

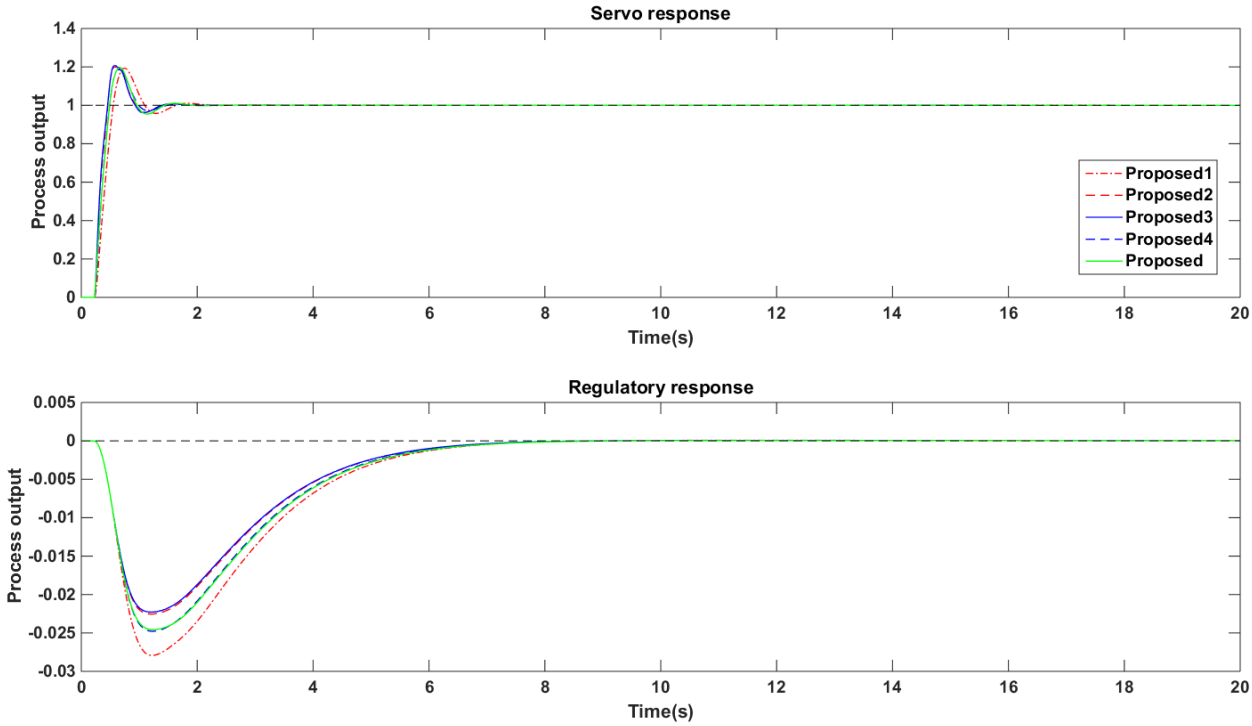

Fig 4.13 Closed loop response of Example 3 for perturbations

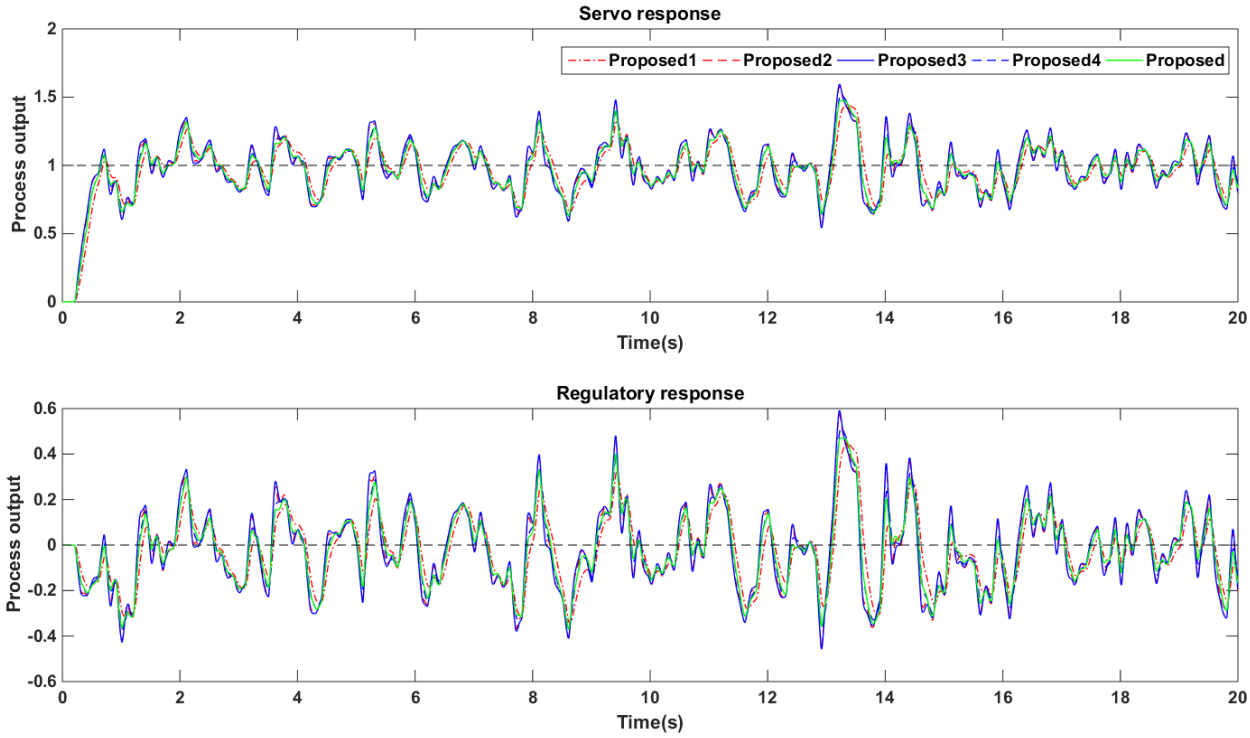

Fig 4.14 Closed loop response of Example 3 with measurement noise

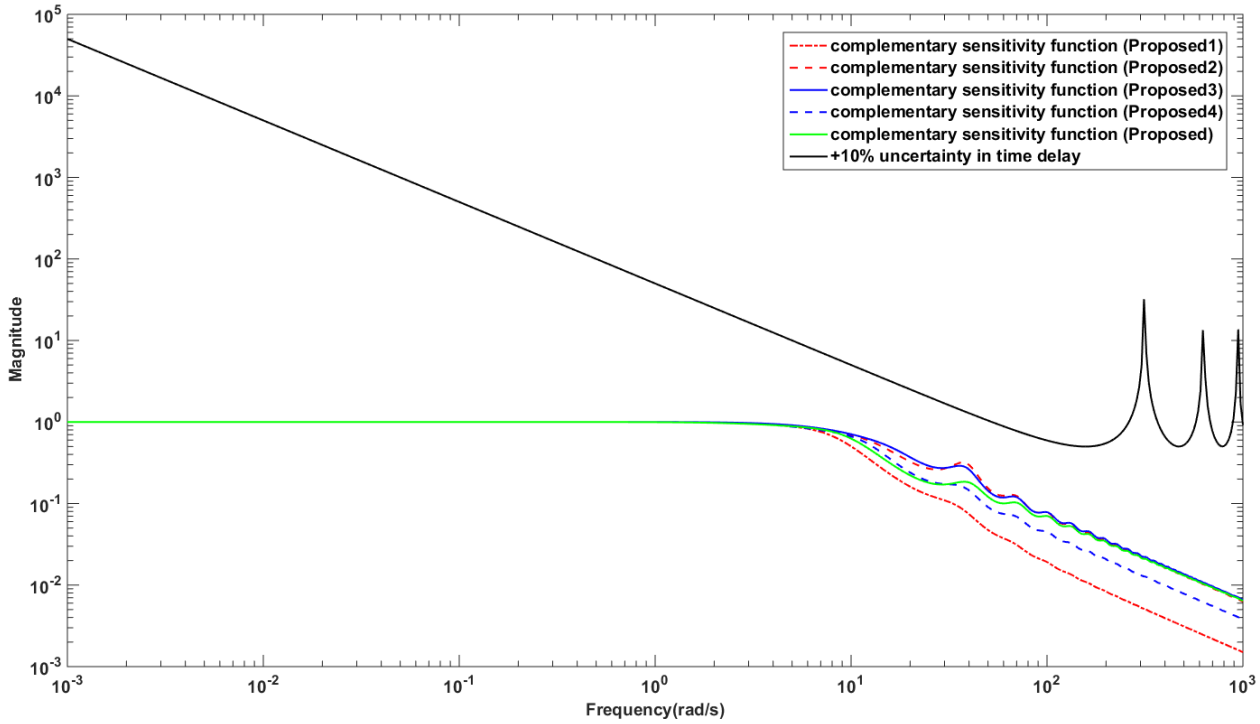

Fig 4.15 Magnitude plot for Example 3

Table 4.13 Performance measures of Example 3 for the perturbed process model

Method	Setpoint change			Load change		
	ISE	IAE	TV	ISE	IAE	TV
Proposed1	0.349	0.476	184.958	0.00137	0.073	0.299
Proposed2	0.299	0.405	799.276	0.00092	0.06	0.297
Proposed3	0.297	0.400	764.142	0.00090	0.059	0.302
Proposed4	0.317	0.421	401.824	0.0011	0.065	0.288
Proposed	0.314	0.425	570.906	0.0011	0.066	0.302

Table 4.14 Performance measures in the presence of output noise

Method	Setpoint change			Load change		
	ISE	IAE	TV	ISE	IAE	TV
Proposed1	2.926	6.096	11617	2.686	5.836	11567
Proposed2	3.079	6.224	47927	2.89	6.01	47743
Proposed3	3.103	6.243	47292	2.916	6.032	47103
Proposed4	2.995	6.158	26743	2.787	5.925	26635
Proposed	2.975	6.123	38543	2.766	5.887	38384

4.4.5. Example 4

Consider a higher order process approximated as SOPTD system (Astrom and Hagglund, 1995):

$$G_m(s)=\frac{1}{(s+1)^8}=\frac{0.336e^{-4.3s}}{s^2+1.3878s+0.336} \tag{4.21}$$

The PID settings for the proposed methods and conventional method are K_p=4.13, T_i=4.1312 and T_d=0.7204 and their respective filter terms in the resulting controller structure are given in Table 4.15. The disturbance input used in the closed loop system has a magnitude of -0.2.

Table 4.15 Tuning parameters and fractional filter terms for Example 4

Method	γ	β	P	Fractional filter term
Proposed1	2.55	0.761	1.1	$\frac{1.637s^2+2.911s+1}{13.98s^{2.2}+6.502s^{1.2}+10.965s^{1.1}+1.637s+5.1s^{0.1}+3.539}$
Proposed2	2.01	1.171	1.1	$\frac{1.805s^3+4.059s^2+3.321s+1}{6.225s^{3.2}+8.686s^{2.2}+6.194s^{2.1}-1.805s^2+4.04s^{1.2}+8.643s^{1.1}+2.518s+4.02s^{0.1}+3.129}$
Proposed3	2	1.178	1.1	$\frac{93.699s^4+275.621s^3+348.843s^2+225.51s+60}{318.028s^{4.2}+665.64s^{3.2}+318.028s^{3.1}+619.2s^{2.2}+665.64s^{2.1}+14.136s^2+240s^{1.2}+619.2s^{1.1}+232.561s+240s^{0.1}+187.29}$
Proposed4	2.06	1.135	1.1	$\frac{20.9843s^3+38.0103s^2+24.0094s+6}{78.4641s^{3.2}+72.9899s^{2.2}+76.1788s^{2.1}+25.4616s^{1.1}+70.864s^{1.1}+28.2501s+24.72s^{0.1}+18.9906}$
Proposed	3.1	-	1.1	$\frac{2.15s+1}{6.665s^{1.1}+3.1s^{0.1}+4.3}$

Figs 4.16-4.18 presents the response of closed loop system for a M_s of 1.8 and the associated ISE, IAE and TV values are listed in Tables 4.16-4.18. It is clear from all the Figs and Tables that the Proposed3 method is superior in performance followed by Proposed2 method. The robust stability is proved through the illustration in Fig 4.19 according to condition in eq. (4.16).

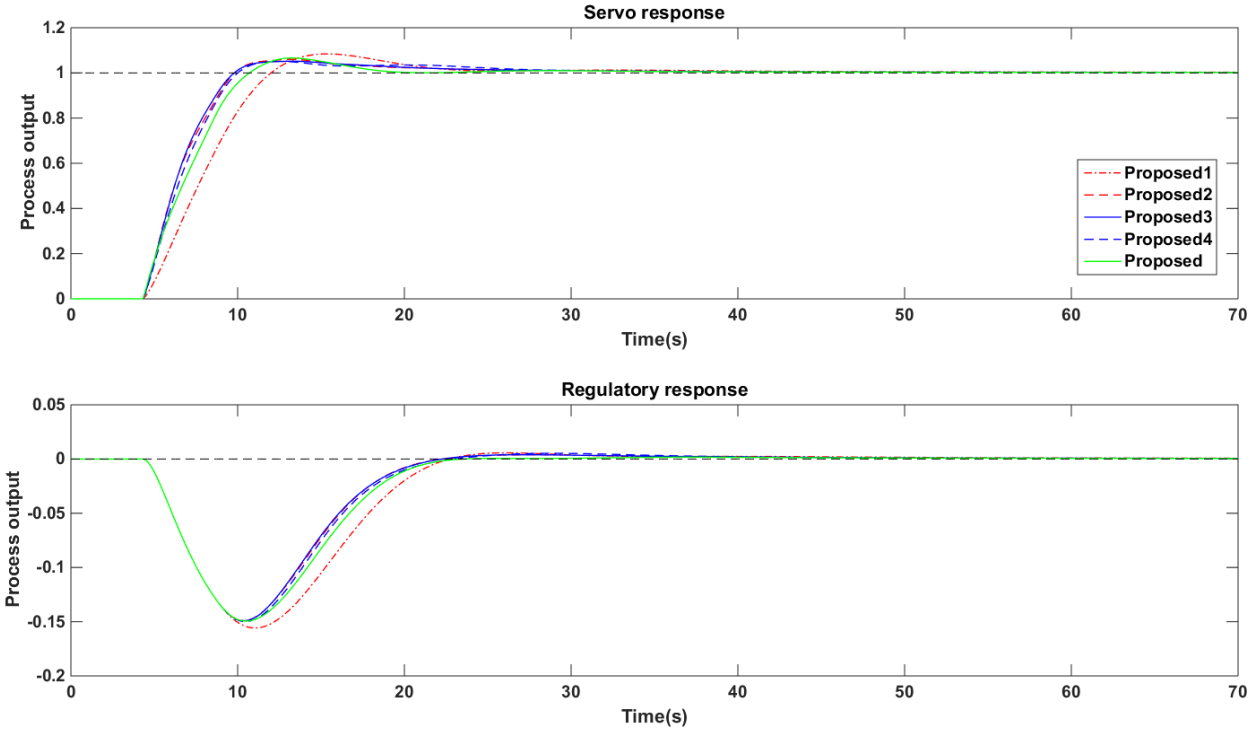

Fig 4.16 Closed loop response of Example 4 for nominal process conditions

Table 4.16 Performance measures of Example 4 for the perfect process model

Method	Setpoint change			Load change			M_s
	ISE	IAE	TV	ISE	IAE	TV	
Proposed1	6.658	8.665	11.658	0.172	1.584	0.235	1.8
Proposed2	5.693	7.268	28.882	0.134	1.318	0.223	1.8
Proposed3	5.683	7.21	28.968	0.133	1.315	0.220	1.8
Proposed4	5.809	7.439	26.293	0.138	1.366	0.222	1.8
Proposed	5.904	7.42	48.219	0.144	1.355	0.230	1.8

Table 4.17 Performance measures of Example 4 for the perturbed process model

Method	Setpoint change			Load change		
	ISE	IAE	TV	ISE	IAE	TV
Proposed1	7.089	9.688	11.967	0.216	1.821	0.301
Proposed2	6.163	8.198	29.297	0.169	1.485	0.293
Proposed3	6.153	8.135	29.356	0.168	1.477	0.291
Proposed4	6.257	8.276	26.547	0.174	1.527	0.281
Proposed	6.334	8.532	48.579	0.180	1.548	0.23

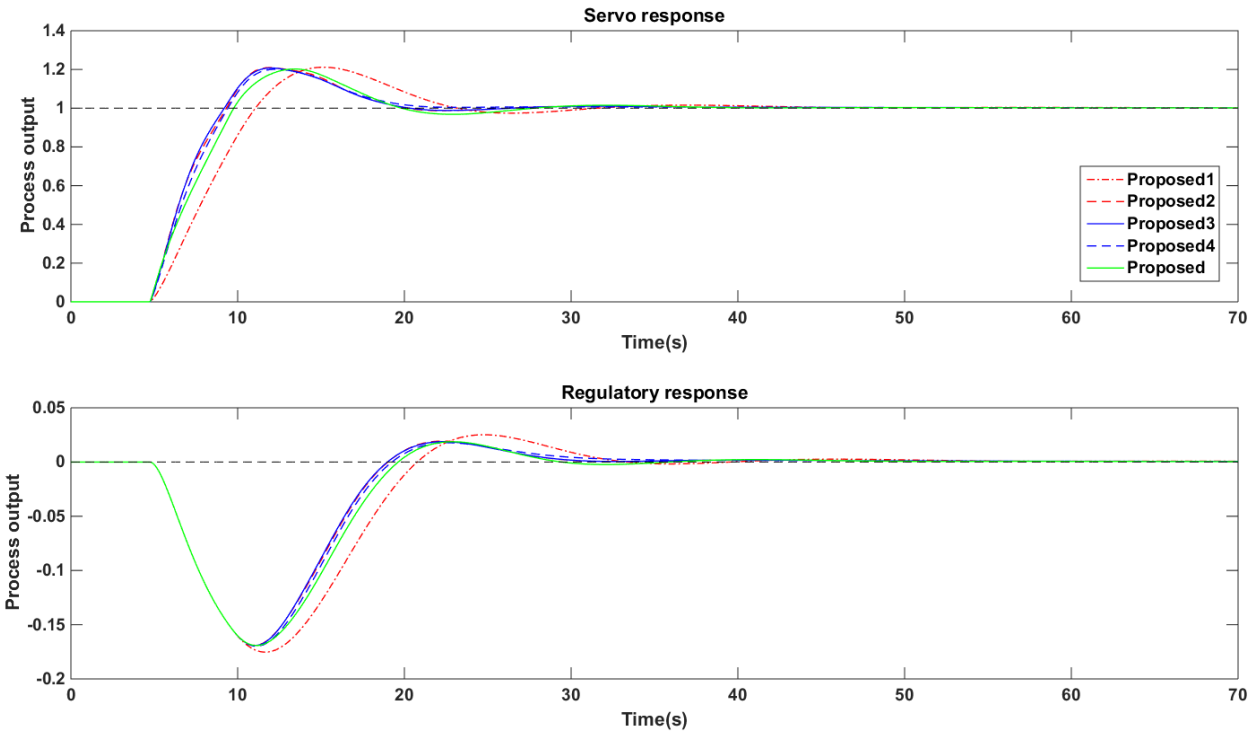

Fig 4.17 Closed loop response of Example 4 for perturbations

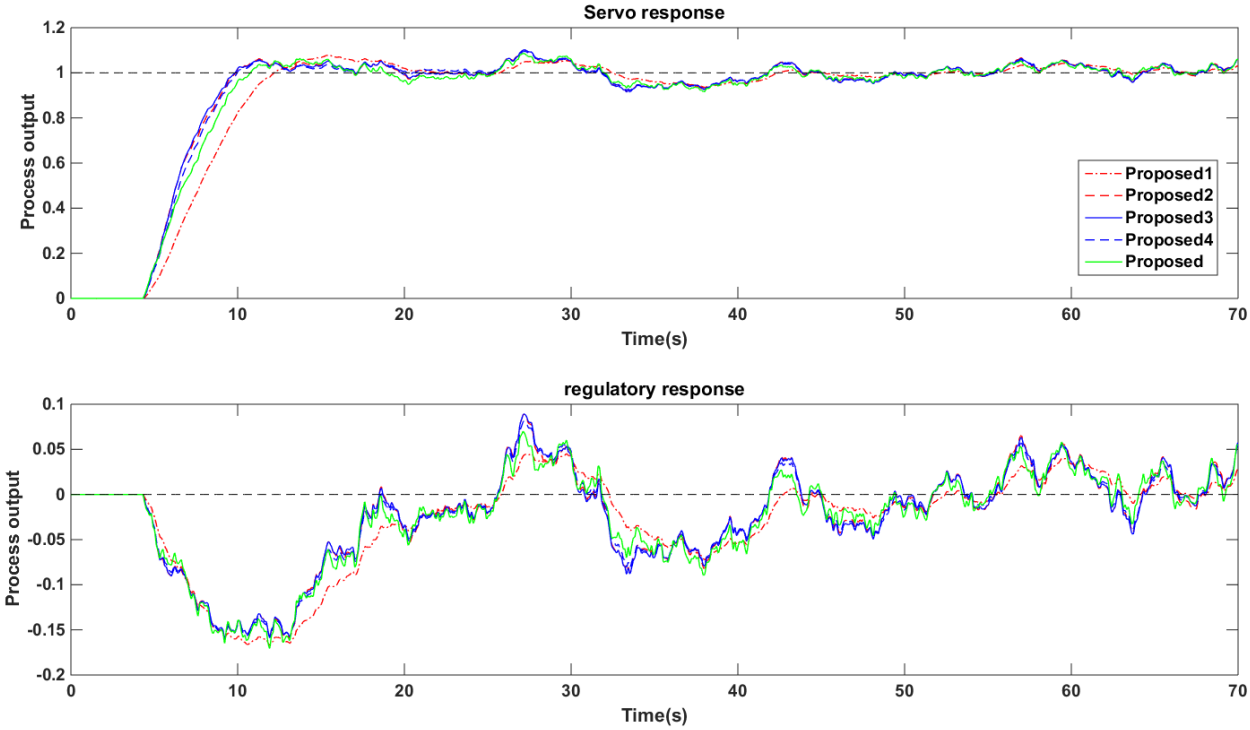

Fig 4.18 Closed loop response of Example 4 with measurement noise

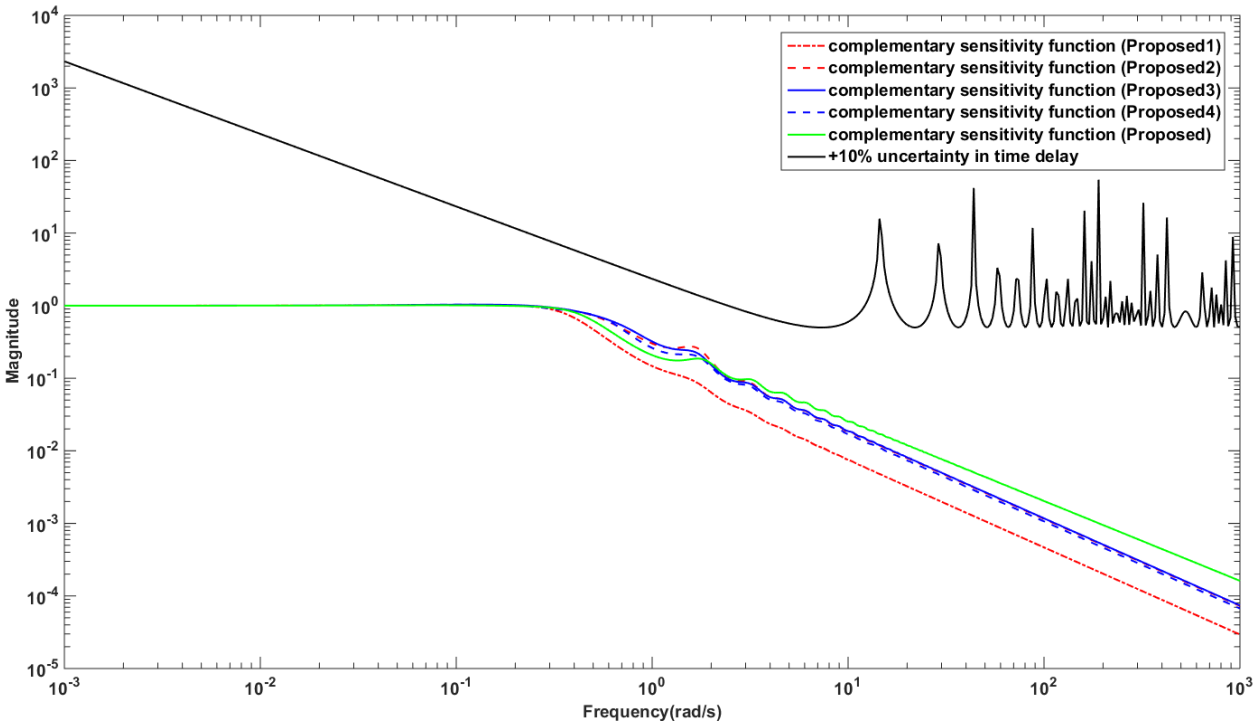

Fig 4.19 Magnitude plot for Example 4

Table 4.18 Performance measures in the presence of output noise

Method	Setpoint change			Load change		
	ISE	IAE	TV	ISE	IAE	TV
Proposed1	13.78	23.51	2807.4	7.493	18.38	2806.4
Proposed2	12.9	22.81	6986.2	7.482	18.37	6983.7
Proposed3	12.9	22.8	7117.9	7.483	18.36	7115.3
Proposed4	13	22.89	6456.1	7.483	18.37	6453.8
Proposed	13.1	23	12198	7.468	18.35	12195

4.4.6. Example 5

$$G_m(s)=\frac{e^{-10s}}{s^2+2s+1} \tag{4.22}$$

Consider a delay dominant process (Thyagarajan and Yu, 2003) given in eq. (4.22). The derived PID controller parameter values are K_p=2, T_i=2 and T_d=0.5 applicable for the four proposed methods and for the conventional (proposed) method. The corresponding fractional filter terms and their associated tuning parameters are given in Table 4.19. The performance graphs and performance measures are presented in Figs 4.20-4.22 and Tables 4.20-4.22 for M_s value of 1.8. The Proposed3 method is found to be better in terms of low ISE, IAE and TV for regulation and servo response followed by Proposed2 method.

Table 4.19 Tuning parameters and fractional filter terms for Example 5

Method	**γ**	**β**	**P**	**Fractional filter term**
Proposed1	4.1	0.999	1.02	$\frac{4.994s^2+5.999s+1}{84.5s^{2.04}+16.81s^{1.04}+41s^{1.02}+4.994s+8.2s^{0.02}+9.0012}$
Proposed2	2.78	0.999	1.02	$\frac{8.328s^3+13.33s^2+5.999s+1}{64.403s^{3.04}+38.642s^{2.04}+46.333s^{2.02}-8.328s^2+7.728s^{1.04}+27.8s^{1.02}+4.997s+5.56s^{0.02}+9.001}$
Proposed3	2.7	0.999	1.02	$\frac{999.4s^4+1899.5s^3+1259.8s^2+419.964s+60}{7290s^{4.04}+6561s^{3.04}+5400s^{3.02}+2624.4s^{2.04}+4860s^{2.02}+700.18s^2+437.4s^{1.04}+1944s^{1.02}+839.856s+324s^{0.02}+540.036}$
Proposed4	3.5	0.9991	1.02	$\frac{99.91s^3+139.964s^2+45.994s+6}{1225s^{3.04}+490s^{2.04}+700s^{2.02}+73.5s^{1.04}+280s^{1.02}+119.982s+42s^{0.02}+54.0054}$
Proposed	5.88	-	1.02	$\frac{5s+1}{29.4s^{1.02}+5.88s^{0.02}+10}$

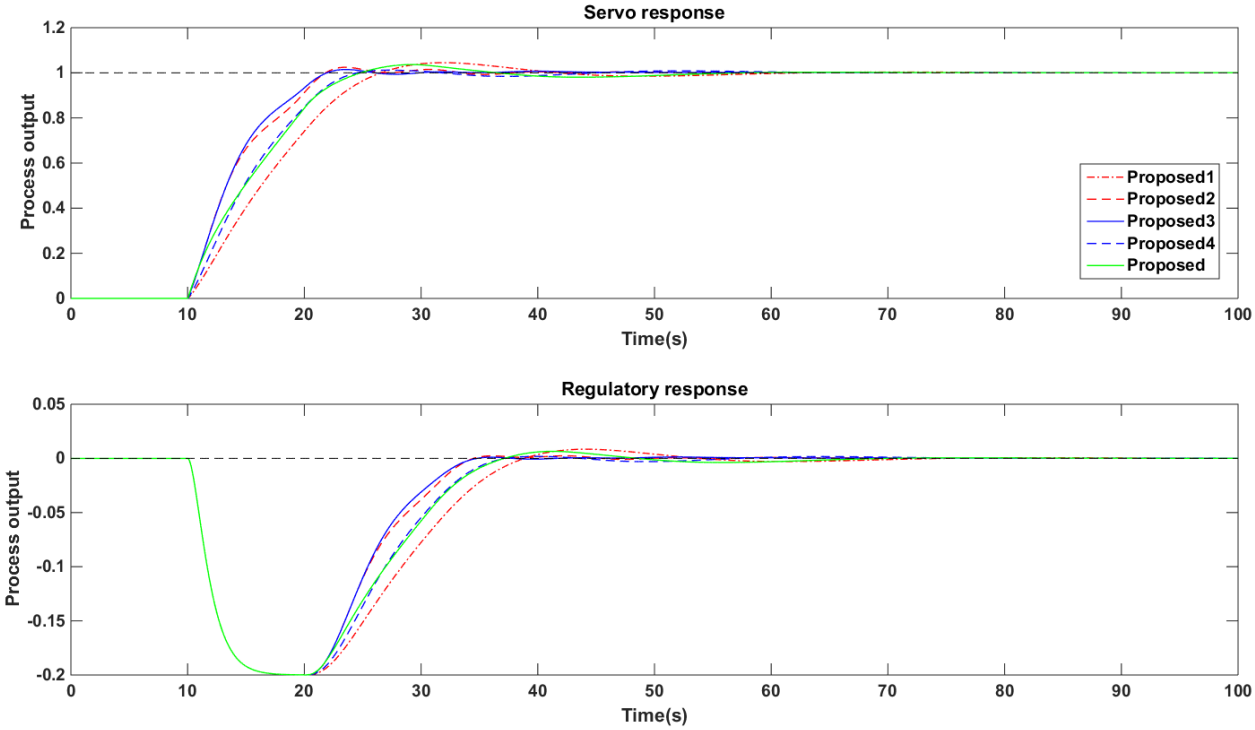

Fig 4.20 Closed loop response of Example 5 for nominal process conditions

Table 4.20 Performance measures of Example 5 for the perfect process model

Method	**Setpoint change**			**Load change**			**M_s**
	ISE	**IAE**	**TV**	**ISE**	**IAE**	**TV**	
Proposed1	14.36	17.47	4.640	0.539	3.482	0.225	1.8
Proposed2	12.48	14.54	8.915	0.462	2.889	0.223	1.8
Proposed3	12.4	14.28	9.329	0.458	2.842	0.213	1.8
Proposed4	13.41	15.82	5.9334	0.500	3.155	0.215	1.8
Proposed	13.23	16	12.466	0.493	3.187	0.223	1.8

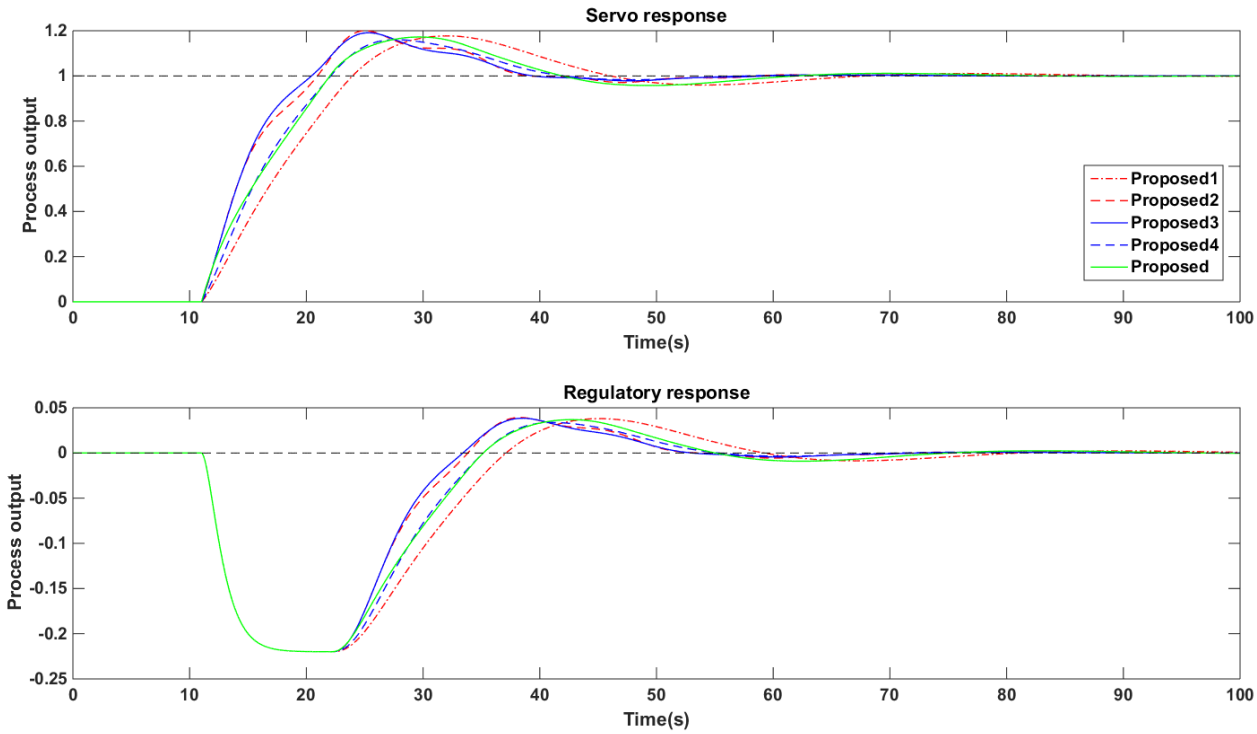

Fig 4.21 Closed loop response of Example 5 for perturbations

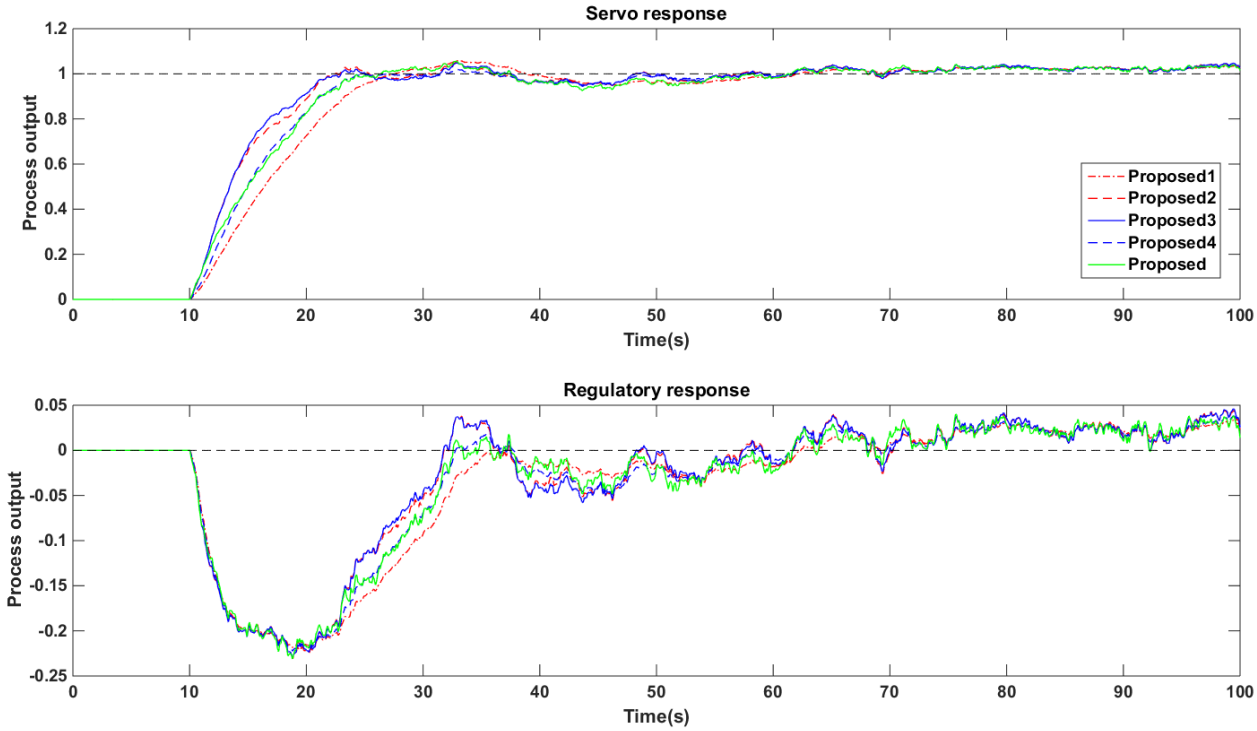

Fig 4.22 Closed loop response of Example 5 with measurement noise

Table 4.21 Performance measures of Example 5 for the perturbed process model

Method	Setpoint change			Load change		
	ISE	IAE	TV	ISE	IAE	TV
Proposed1	15.26	20.07	4.845	0.694	4.381	0.291
Proposed2	13.44	16.94	9.177	0.603	3.696	0.296
Proposed3	13.37	16.65	9.566	0.599	3.637	0.287
Proposed4	14.27	17.88	6.109	0.645	3.901	0.273
Proposed	14.13	18.51	12.681	0.638	4.031	0.291

Table 4.22 Performance measures in the presence of output noise

Method	Setpoint change			Load change		
	ISE	IAE	TV	ISE	IAE	TV
Proposed1	24.68	37.68	1400.1	11.17	27.15	1399.8
Proposed2	22.74	36.06	3065	11.15	27.08	3064.3
Proposed3	22.65	35.95	3253.3	11.14	27.08	3252.5
Proposed4	23.66	36.79	1932.7	11.16	27.11	1932.2
Proposed	23.52	36.77	4420.1	11.14	27.12	4419.1

Fig 4.23 shows the magnitude plot which proves the robust stability of closed loop system. All five methods are robustly stable but the Proposed1 method is more robust compared to the other three methods. The M_s range over which the system is giving robust performance is 1.7-1.9. This is depicted through M_s versus ISE, IAE and TV plots for servo and regulation in Fig 4.24.

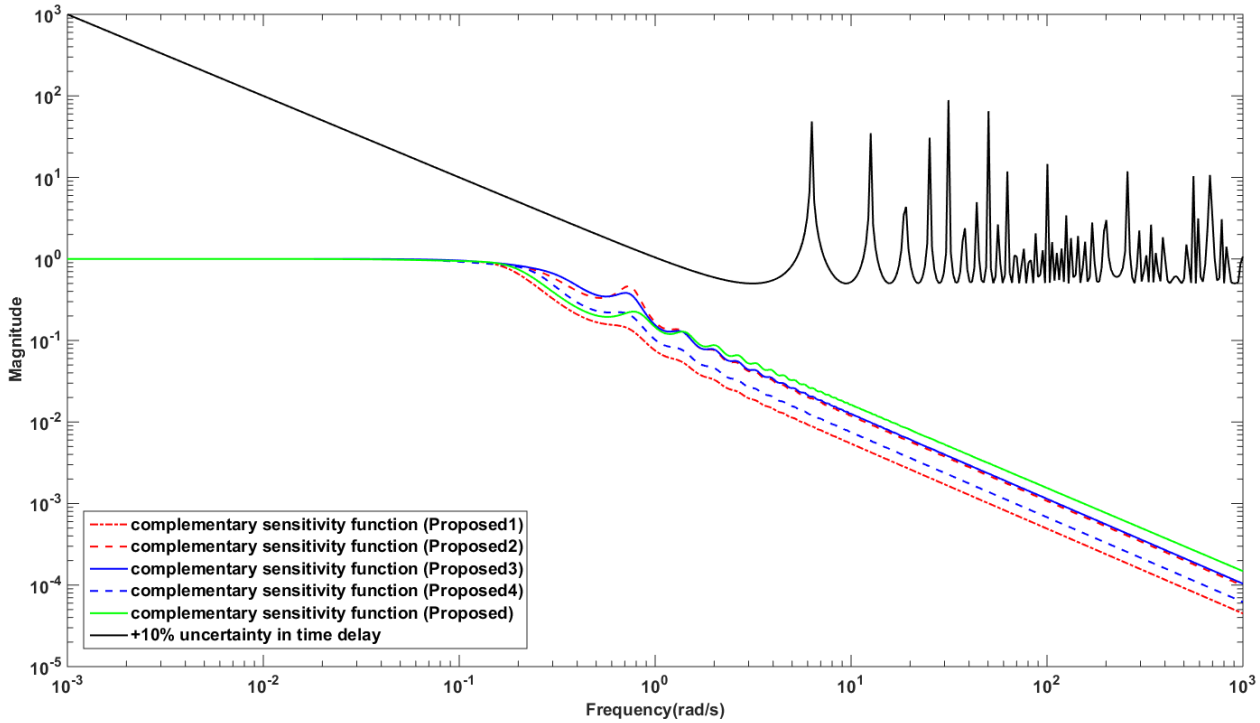

Fig 4.23 Magnitude plot for Example 5

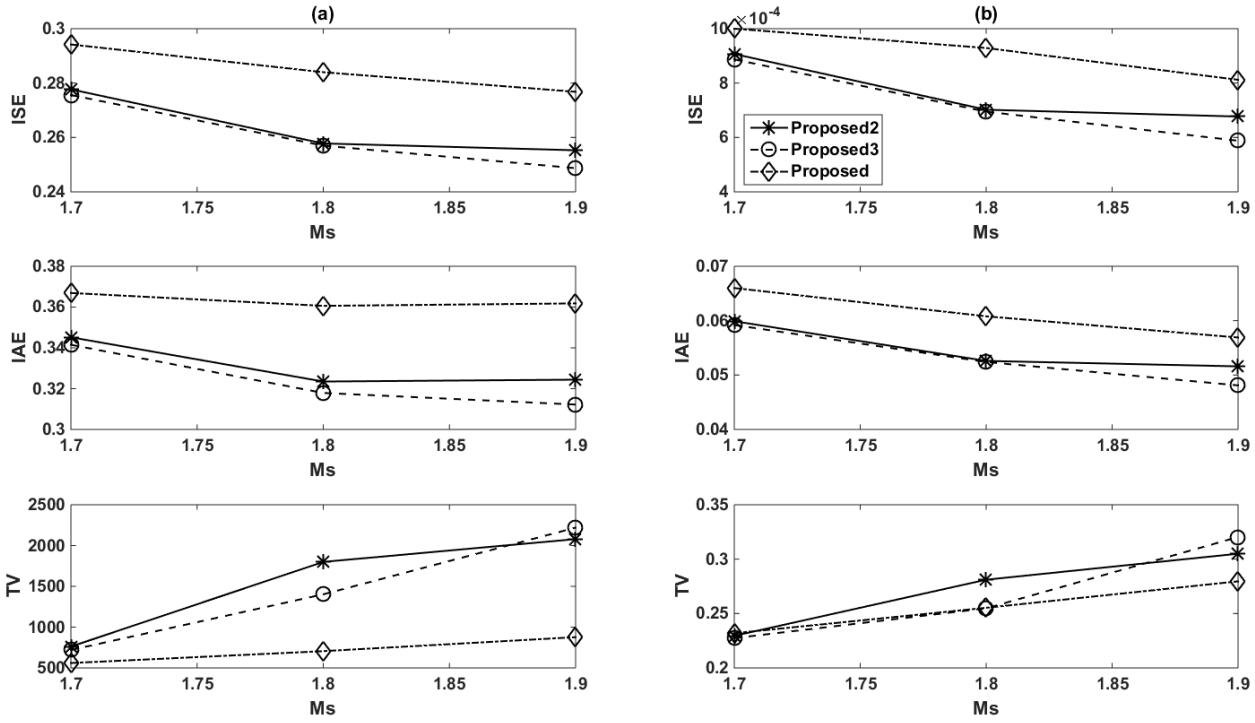

Fig 4.24 M_s versus ISE, IAE and TV for (a) identification of robust servo performance of Example 5 (b) identification of robust regulatory performance of Example 5

4.4.7. Controller fragility

Fig 4.25 shows the variation of delta epsilon fragility index for Example 2 and Example 3. It can be observed from Fig 4.25 and Table 4.23 that all the proposed controllers and the controllers used for comparison are nonfragile for +20% change in controller parameters. It means a change of +20% in controller parameters is acceptable as the loss of robustness is less than 50%. It is evident from Fig 4.25 that the Proposed1 and conventional controllers are resilient in case of Example 2 meaning that they lose only 10% of its robustness for +20% change in controller parameters. It is also observed from Fig 4.25 that all the controllers are nonfragile in case of Example 3. Further, the delta 20 fragility index ($FI_{\Delta 20}$) for Example 1, Example 4 and Example 5 is presented in Table 4.23. All the controllers are resilient in case of Example 1 and Example 5. In the case of Example 4, Proposed1 and conventional are resilient and Proposed2, Proposed3 and Proposed4 are nonfragile. Hence, all the proposed controllers and the controllers used for comparison are either resilient or nonfragile and thus assuring robust closed loop performance.

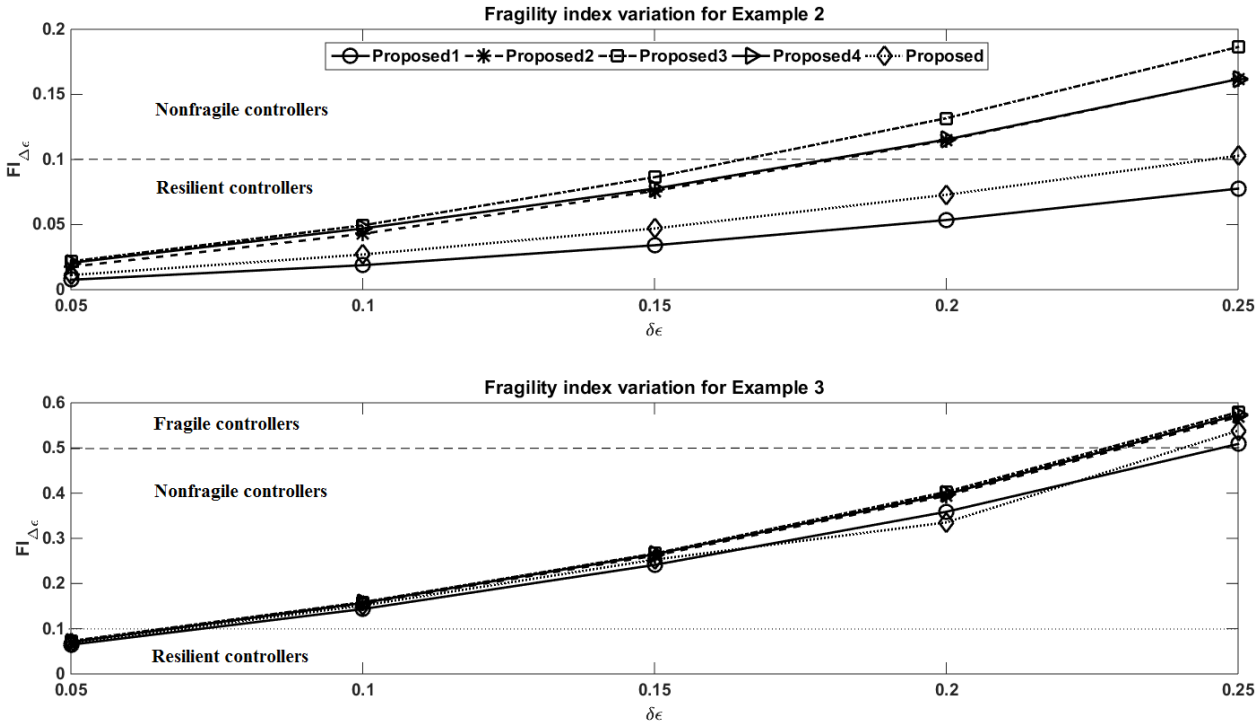

Fig 4.25 Fragility index variation for Example 2 and Example 3

Table 4.23 Controllers delta 20 fragility index ($FI_{\Delta 20}$) for all the examples

Method	**Example 1**	**Example 2**	**Example 3**	**Example 4**	**Example 5**
Proposed1	0.03	0.05	0.36	0.05	-0.013
Proposed2	0.07	0.11	0.39	0.12	-0.002
Proposed3	0.08	0.13	0.40	0.12	0.005
Proposed4	0.08	0.11	0.39	0.14	0.004
Proposed	-0.016	0.07	0.33	0.08	-0.012
Wang et al. (2016)	-0.016	-	-	-	-

4.6. Conclusions

An optimum fractional IMC filter of higher order is identified based on the lower values of ISE and IAE for same robustness (M_s). A FFPID controller is designed for SOPTD processes using this optimum filter and higher order Pade's approximation of time delay namely 1/2 order, second order and 2/3 order. Closed loop response for five different SOPTD systems is presented for changes in different inputs acting on the system and for parametric uncertainties. The simulation results demonstrate the superiority of the proposed method when various controllers are tuned to have the same degree of robustness in terms of M_s. Improved disturbance rejection and servo response is

observed with the controllers designed using optimum filter structure and 2/3 order Pade's approximation for time delay. This is evident even with perturbations in process parameters and in presence of measurement noise. It can be observed that the error values are decreasing with increase in the order of Pade's approximation but the control effort is slightly increasing. Hence, there is a compromise on the control effort to have better ISE and IAE values. The robust stability of the closed loop systems is verified for parametric uncertainty. The M_s range is identified over which the closed loop system gives robust performance. Fragility analysis is carried out for uncertainties in controller parameters and it is found that all the proposed controllers are either resilient or nonfragile for up to an uncertainty of +20% in the controller parameters for all the systems.

Chapter 5

Design of fractional filter IMC-PID controller for enhanced performance of integrating processes with time delay

5. Design of fractional filter IMC-PID controller for enhanced performance of integrating processes with time delay*

An improved fractional filter IMC-PID controller is proposed to enhance the performance of integrating processes after identifying the optimum higher order fractional IMC filter structure. The identification involves a systematic design procedure based on the minimization of IAE. The present design also considers different approximations for time delay. The tuning parameters are obtained based on the prefixed robustness (M_s). The present method is compared with recent methods in the literature and its superiority is demonstrated with performance measures IAE and TV. Enhanced output performance is obtained in terms of servo control and disturbance rejection for nominal process conditions; process parameter variations; and for noise in the measurement. Robustness analysis is performed using complementary sensitivity function and parametric uncertainty bounds. Also, the fragility analysis is carried out to check the sensitivity of closed loop system for variation in controller parameters.

5.1. Introduction

Maximum number of industrial processes are integrating (non-self-regulating) in nature, though there are many self-regulating processes. The integrating nature of the processes is usually found in level control systems, distillation columns, reactors, batch processes, power plants, aerospace control and oil industries. If the input or process conditions of such processes are varied, the output becomes unbounded i.e., output varies quickly and it will be difficult to revert the process to its operating point. Process industries predominantly use PID controllers due to the availability of a wide range of tuning rules to control broad class of process problems (Vilanova and Visioli, 2012).

Many IMC based controllers have been there for time delayed integrating processes. A simple PID controller using IMC principles was reported for integrating processes (Rao and Sree, 2010). Fruehauf et al. (1994) developed simplified rules to tune IMC-PID controller that resemble Ziegler-Nichols tuning rules to give a less aggressive response. An IMC-PID controller was designed for integrating processes approximated as an unstable model of first order with pole located close to

* This work got published in the journal Indian Chemical Engineer - https://doi.org/10.1080/00194506.2019.1656553

origin (Lee et al., 2000; Shamsuzzoha and Lee, 2008). A PID controller with derivative filter and a PID with filter controllers were developed for integrating processes using IMC method (Rice and Cooper, 2002; Arbogast and Cooper, 2007). An IMC-PID controller was developed for a group of integrating processes using second order to fourth order IMC filter (Shamsuzzoha and Lee, 2008). Further, they have used set point filter to minimize overshoot. Panda (2009) proposed an IMC-PID controller for integrating unstable systems using integer order IMC filter. An alternative IMC scheme was proposed for integrating processes by approximating the integrator by a lag filter of order one with a huge time constant (Chia and Lefkowitz, 2010). A modified IMC based controller (Liu and Gao, 2011) was also developed for rejecting different disturbances on the integrating process. There was a PID controller developed using direct synthesis method, IMC and stability analysis method (Rao et al., 2011) followed by performance comparison. A sensitivity based IMC-PID controller (Zhao et al., 2011) was proposed for integrating processes approximated as a delayed first order model. A PID controller sequentially connected to a lead-lag filter (Vanavil et al., 2014) was developed using IMC. Also, a 2Dof PID controller (Jin and Liu, 2014) was proposed using IMC scheme. Further, a 1Dof controller was proposed with a trade-off between performance/robustness and servo/regulatory performance. Recently, a PID controller in series with lead-lag filter was proposed for a class of non-self-regulating processes (Kumar and Sree, 2016) using integer order IMC filter whose denominator order is chosen as one less than the numerator.

Fractional order control has become the research interest to control processes with long time delays and nonlinearities. Further, several fractional order controller tuning rules (Padula and Visioli, 2015; Yeroglu and Tan, 2011; Muresan et al., 2016) are also developed for different time delay systems. The PID controller design employing fractional IMC filter for integer order systems and non-integer order systems has been in focus from the past few years. Recently, an IMC-PID fractional order filter controller (Maâmar and Rachid, 2014) was proposed for integer order systems with and without time delay. It was extended to delay free, non-integer order processes and non-integer order time delay processes (Bettayeb and Mansouri, 2014). With respect to integer order systems, the simulations were performed on few delay free systems of second order and first order with added integrator. In both cases, the filter time constant and order were chosen depending on the phase margin and gain cross over frequency. Further, an integer order IMC filter was used to develop an IMC-PID controller for non-integer order systems (Li et al., 2015).

It is observed from the literature that IMC based methods have used integer order IMC filter of the order one and higher. Most Smith predictor based control schemes used two controllers in their structure. In addition, Smith Predictor cannot be recommended for open-loop unstable processes as it cannot eliminate steady-state error in the response for load disturbances (García and Albertos, 2013). Many controller structures have filter in their design which should be carefully designed because the filter and derivative action cancel each other if they are used together (Fruehauf et al., 1994). Some of the developed controllers have more tuning parameters. All the controllers may not assure performance and robustness. Though, there are few controllers which can provide improved performance, there is always a scope to improve the controller design. There has been limited work on the IMC-PID controller design using a fractional IMC filter. In the above work (Maâmar and Rachid, 2014; Bettayeb and Mansouri, 2014), the phase margin and gain crossover frequency should be properly selected for better performance as they decide the optimum parameters of the filter.

Here, a fractional filter IMC-PID controller is designed using a fractional IMC filter for a class of integrating processes. Primarily, an optimum fractional IMC filter structure is identified based on systematic design procedure minimizing IAE for a fixed M_s. The designed controller consists of a PID term cascaded with a fractional filter term that prevents the need to use setpoint filter. The proposed controller offers flexibility in tuning with additional degree of freedom thereby enhance the system's performance. The parameters of PID term are directly obtained from process parameters according to the derived relations and the parameters need to be tuned are associated with the fractional filter term. These tuning parameters are chosen such that M_s is equal to a predefined value based on the systematic procedure. The simulations have been performed on several examples representing different integrating processes. The robust stability is assessed using complementary sensitivity functions under uncertainties. The simulation results show that the proposed method gives fairly better results compared to the recent methods. Also, the controller fragility analysis is carried out for uncertainties in controller parameters.

5.2. Proposed Fractional filter IMC-PID controller design

The controller is designed for different integrating plus time delay processes whose process models are given below:

Integrating plus time delay (IPTD) process,

$$G(s)=\frac{K}{s}e^{-Ls} \tag{5.1}$$

Integrating first order plus time delay (IFPTD) process,

$$G(s)=\frac{K}{s(Ts+1)}e^{-Ls} \tag{5.2}$$

Double integrating plus time delay (DIPTD) process,

$$G(s)=\frac{K}{s^2}e^{-Ls} \tag{5.3}$$

The parameters in the above processes are system gain (K), time delay (L) and time constant (T). The proposed structure of the IMC-PID controller using fractional IMC filter is

$$C(s)=(\text{fractional filter})K_p\left[1+\frac{1}{T_i s}+T_d s\right] \tag{5.4}$$

The designed controller must give a robust and stable closed loop performance. According to the IMC method (Morari and Zafiriou, 1989), the feedback loop controller is

$$C(s)=\frac{C_{IMC}(s)}{1-C_{IMC}(s)G(s)} \tag{5.5}$$

Where $C_{IMC}(s)$ is the IMC controller and G(s) is the process model. The $C_{IMC}(s)$ is

$$C_{IMC}(s)=\frac{1}{G^{-}(s)}F(s) \tag{5.6}$$

Where $G^{-}(s)$ is the invertible part of G(s) and F(s) is the IMC filter which makes a realizable IMC controller. The fractional IMC filter structures used in this paper are:

$$F(s)=\frac{1}{(\gamma s^p+1)^n};\ n=1,2,3 \tag{5.7}$$

$$F(s)=\frac{\beta s+1}{(\gamma s^p+1)^{n+1}};\ n=1,2 \tag{5.8}$$

$$F(s)=\frac{(\beta s+1)^2}{(\gamma s^p+1)^{n+2}};\ n=1,2 \tag{5.9}$$

'β' is the additional degree of freedom in equations (5.8) & (5.9). The proposed controllers for different integrating processes are explained in the successive sections.

5.2.1. Design for IPTD model

Consider the process model given in eq. (5.1). The invertible portion of G(s) is

$$G^{-}(s)=\frac{K}{s} \tag{5.10}$$

The fractional IMC filter used for the design is

$$F(s)=\frac{1}{(\gamma s^{p}+1)^{n}} \tag{5.11}$$

Where γ is the filter time constant and p is the fractional order of the filter. The IMC controller utilizing equations (5.6), (5.10) & (5.11) is

$$C_{IMC}(s)=\frac{s}{K}\frac{1}{(\gamma s^{p}+1)^{n}} \tag{5.12}$$

The final controller according to equations (5.1), (5.5) & (5.12) is

$$C(s)=\frac{\left[\frac{s}{K}\frac{1}{(\gamma s^{p}+1)^{n}}\right]}{\left[1-\frac{s}{K}\frac{1}{(\gamma s^{p}+1)^{n}}\frac{K}{s}e^{-Ls}\right]} \tag{5.13}$$

Eq. (5.13) can be rearranged as

$$C(s)=\frac{s}{K[(\gamma s^{p}+1)^{n}-e^{-Ls}]} \tag{5.14}$$

Similarly, C(s) for fractional IMC filter structure F(s) given in eq. (5.8) is,

$$C(s)=\frac{s(\beta s+1)}{K\left[(\gamma s^{p}+1)^{n+1}-(\beta s+1)e^{-Ls}\right]} \tag{5.15}$$

Similarly, C(s) for fractional IMC filter structure F(s) given in eq. (5.9) is,

$$C(s)=\frac{s(\beta s+1)^{2}}{K\left[(\gamma s^{p}+1)^{n+2}-(\beta s+1)^{2}e^{-Ls}\right]} \tag{5.16}$$

Using equations (5.14) - (5.16) and by using Pade's procedure for time delay (Table 5.1) the derived expressions for controller are given in Table 5.2. The controller settings given in Table 5.2 are same for all the IMC filter structures but the difference is only in the fractional filter term.

Table 5.1 Pade's approximation of time delay term

Approximation order	**Equivalent term for e^{-Ls}**
1st order	$(1-0.5Ls)/(1+0.5Ls)$
1/2 order	$(6-2Ls)/(6+4Ls+L^{2}s^{2})$
2nd order	$\left[1-(L/2)s+(L^{2}/12)s^{2}\right]/\left[1+(L/2)s+(L^{2}/12)s^{2}\right]$
2/3 order	$(60-24Ls+3L^{2}s^{2})/(60+36Ls+9L^{2}s^{2}+L^{3}s^{3})$

Table 5.2 Controller settings for IPTD process

Pade's approximation	**C(s)**
1st order	(fractional filter term) $\left(\frac{1}{K}\right)[1+0.5Ls]$
1/2 order	(fractional filter term) $\left(\frac{4L}{K}\right)\left[1+\frac{1}{0.6667Ls}+0.25Ls\right]$
2nd order	(fractional filter term) $\left(\frac{L}{2K}\right)\left[1+\frac{1}{(L/2)s}+\left(\frac{L}{6}\right)s\right]$

5.2.2. Design for IFPTD model

Considering the model in eq. (5.2) and IMC filter in eq. (5.7), the IMC controller is

$$C_{IMC}(s)=\frac{s(Ts+1)}{K}\frac{1}{(\gamma s^p+1)^n} \tag{5.17}$$

The final controller transfer function obtained using the equations (5.2), (5.5) & (5.17) is

$$C(s)=\frac{\left[\frac{s(Ts+1)}{K}\frac{1}{(\gamma s^p+1)^n}\right]}{\left[1\frac{s(Ts+1)}{K(\gamma s^p+1)^n}\frac{K}{s(Ts+1)}e^{-Ls}\right]} \tag{5.18}$$

Eq. (5.18) can be modified as follows

$$C(s)=\frac{s(Ts+1)}{K[(\gamma s^p+1)^n-e^{-Ls}]} \tag{5.19}$$

Similarly, the C(s) expressions using eq. (5.8) and eq. (5.9) are given by eq. (5.20) and eq. (5.21).

$$C(s)=\frac{s(Ts+1)(\beta s+1)}{K\left[(\gamma s^p+1)^{n+1}-(\beta s+1)e^{-Ls}\right]} \tag{5.20}$$

$$C(s)=\frac{s(Ts+1)(\beta s+1)^2}{K\left[(\gamma s^p+1)^{n+2}-(\beta s+1)^2e^{-Ls}\right]} \tag{5.21}$$

Using equations (5.19) - (5.21) and by using Table 5.1 the expressions for controller are given in Table 5.3. All the derived controllers differ only in the fractional filter term.

Table 5.3 Controller settings for IFPTD process

Pade's approximation	**C(s)**
1st order	(fractional filter term) $\left(\frac{T+0.5L}{K}\right)\left[1+\frac{1}{(T+0.5L)s}+\left(\frac{0.5TL}{T+0.5L}\right)s\right]$
1/2 order	(fractional filter term) $\left(\frac{4L}{K}\right)\left[1+\frac{1}{0.6667Ls}+0.25Ls\right]$
2nd order	(fractional filter term) $\left(\frac{L}{2K}\right)\left[1+\frac{1}{(L/2)s}+\left(\frac{L}{6}\right)s\right]$
2/3 order	(fractional filter term) $\left(\frac{1}{K}\right)[1+Ts]$ (or) (fractional filter term) $\left(\frac{T}{K}\right)\left[1+\frac{1}{Ts}\right]$

5.2.3. Design for DIPTD model

Similarly, the controller for DIPTD process in eq. (5.3) using equations (5.5), (5.6) & (5.7) is

$$C(s)=\frac{\left[\frac{s^2}{K(\gamma s^p+1)^n}\right]}{\left[1-\frac{s^2}{K(\gamma s^p+1)^n}\frac{K}{s^2}e^{-Ls}\right]} \tag{5.22}$$

The above equation can be modified as

$$C(s)=\frac{s^2}{K[(\gamma s^p+1)^n-e^{-Ls}]} \tag{5.23}$$

Similarly, by using F(s) in eq. (5.8) and eq. (5.9) the expressions for C(s) are:

$$C(s)=\frac{s^2(\beta s+1)}{K[(\gamma s^p+1)^{n+1}-(\beta s+1)e^{-Ls}]} \tag{5.24}$$

$$C(s)=\frac{s^2(\beta s+1)^2}{K\left[(\gamma s^p+1)^{n+2}-(\beta s+1)^2e^{-Ls}\right]} \tag{5.25}$$

The final controller expressions using Table 5.1 are same as given in Table 5.2 but with a difference in the fractional filter term.

5.3. Closed loop performance, robustness and fragility analysis

5.3.1. Closed loop performance analysis

The closed loop response is observed with the controllers designed using optimum fractional IMC filter structures identified according to the flowchart given in Fig 5.1. Two optimum fractional IMC filter structures are identified for each of the three integrating processes. One is the conventional first order fractional IMC filter structure (eq. (5.7) with n=1) and the second is the higher order fractional filter structure (any one from eq. (5.7), eq. (5.8) and eq. (5.9)). The only exception is that the conventional first order fractional IMC filter structure doesn't result in a realizable controller with DIPTD process. Hence, a higher order fractional IMC filter structure (eq. (5.7) with n=3) is used for DIPTD process. After obtaining the optimum fractional IMC filter structures, the system's step response is observed with the optimum controllers. Also, the performance is observed for perturbations in the process parameters and for noise in the output. The performance is assessed by using IAE, TV and M_s which are given in Table 5.4.

Table 5.4 Closed loop performance measures

IAE	TV	M_s
$\int_0^\infty \lvert e(t)\rvert dt$	$\sum_{i=0}^{\infty} \lvert u_{i+1}-u_i\rvert$	$\max_{0<\omega<\infty} \left\lvert \frac{1}{1+C(j\omega)G(j\omega)} \right\rvert$

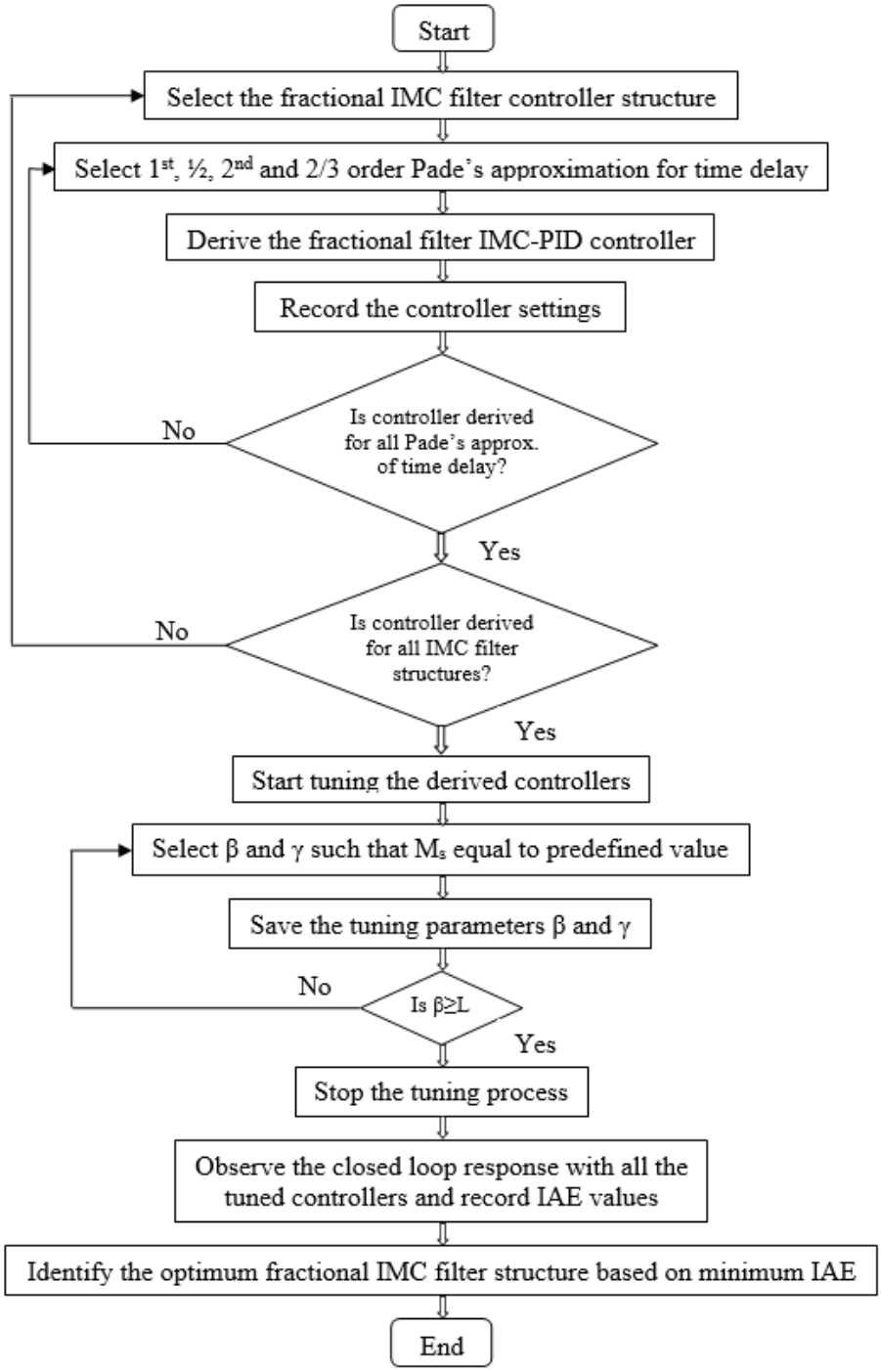

Fig 5.1 Systematic design procedure for identification of optimum fractional IMC filter structure

5.3.2. Robustness analysis

The controller that is designed for the process assumes that the model used captures the complete dynamics of the process. But, there always exists, an error in the model approximating only the true dynamics of the process. Thus, the system with feedback must be analysed for robust stability with uncertainties present in the parameters and for load changes. The robust stability condition (Morari and Zafiriou, 1989) is

$$\|l_m(j\omega)T(j\omega)\|<1 \forall \omega \in (-\infty,\infty) \quad (5.26)$$

Where $T(s)_{s=j\omega}=\frac{C(s)G(s)}{1+C(s)G(s)}$ is the complementary sensitivity function and $l_m(j\omega)=\left|\frac{G(j\omega)-G_m(j\omega)}{G_m(j\omega)}\right|$ is the bound on the process multiplicative uncertainty.

The controller must be tuned to satisfy eq. (5.27) for uncertainty in time delay

$$\|T(j\omega)\|_\infty<\frac{1}{|e^{-\Delta L}-1|} \quad (5.27)$$

Similarly, if there is uncertainty in K and L, the controller should be tuned to satisfy the relation

$$\|T(j\omega)\|_\infty<\frac{1}{\left|\left(\frac{\Delta K}{K}+1\right)e^{-\Delta L}-1\right|} \quad (5.28)$$

Also, another constraint to be satisfied for robust closed loop performance is

$$\|l_m(j\omega)T(j\omega)+w_m(j\omega)(1-T(j\omega))\|<1 \quad (5.29)$$

Where $w_m(j\omega)$is the uncertainty bound on the sensitivity function $(1-T(j\omega))$.

5.3.3. Fragility analysis

The sensitivity of the closed loop system to give robust performance must be analysed through fragility analysis (Alfaro, 2007) for changes in the controller parameters. The fragility is analysed through loss of robustness using delta 20 fragility index ($FI_{\Delta 20}$). The $FI_{\Delta 20}$ is defined as follows:

$$FI_{\Delta 20}=\frac{M_{s\Delta 20}}{M_s}-1 \quad (5.30)$$

Where $M_{s\Delta 20}$ - maximum sensitivity for +20% variation in controller parameters; M_s - nominal maximum sensitivity.

Any controller is said to be resilient if $FI_{\Delta 20}\leq 0.1$; nonfragile if $0.1<FI_{\Delta 20}\leq 0.5$ and fragile if $FI_{\Delta 20}>0.5$.

5.4. Simulation results and discussion

In this section, the optimum controller settings identified using the optimum fractional IMC filter structure according to the procedure described in section 5.3.1 are discussed. Then, numerous integrating time delay systems representing IPTD, IFPTD and DIPTD processes are simulated and their performance with the proposed method is analysed with the recent methods (Kumar and Sree, 2016). The step response is obtained for nominal process conditions; for perturbations of +5% in L and -10% in K and with a white noise (mean=0 and variance=0.1). The robust stability analysis is carried out for uncertainty of +10% in both L and K. The performance of the closed loop is measured with IAE. Total variation (TV) is used to identify the smooth working of the controller.

5.4.1. Identified optimum fractional filter IMC-PID controller settings

The optimum fractional filter IMC-PID controller settings for each of the three integrating processes studied in this work are identified using the procedure given in flowchart (Fig 5.1). An important point to note here is that 2/3 order Pade's approximation is not used with IPTD and DIPTD processes as the resulting controller structure doesn't comply with the one (eq. (5.4)) prescribed in this paper. The optimum proposed methods for the three processes are further referred to as Proposed1 ($(\beta s+1/(\gamma s^p+1)^2)$+ 2nd order Pade's approximation of e^{-Ls}); Proposed2 ($(1/\gamma s^p+1)$+ 2nd order Pade's approximation of e^{-Ls}); Proposed3 ($(\beta s+1/(\gamma s^p+1)^3)$+ 2/3 order Pade's approximation of e^{-Ls}); Proposed4 ($(1/\gamma s^p+1)$ + 2/3 order Pade's approximation of e^{-Ls}); Proposed5 ($(\beta s+1/(\gamma s^p+1)^3)$+ 2nd order Pade's approximation of e^{-Ls}) and Proposed6 ($(1/(\gamma s^p+1)^3)$ + 2nd order Pade's approximation of e^{-Ls}). The parameters of the PID term for IPTD, IFPTD and DIPTD processes remain same as given in Table 5.2, Table 5.3 and Table 5.2 respectively. The respective fractional filter terms of the optimum controllers for the above three processes are given in Table 5.5. These are identified based on minimum IAE for a fixed M_s as per the trends of IAE versus β shown in Figs 5.2-5.4.

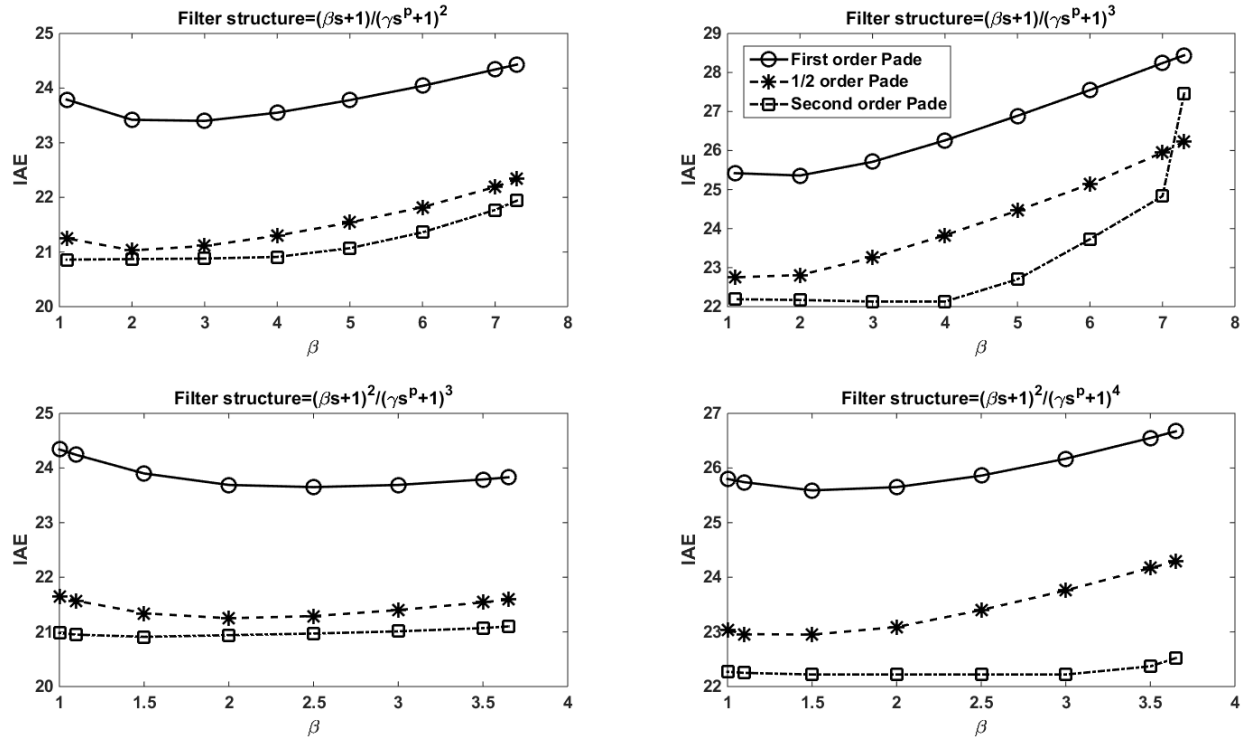

Fig 5.2 β versus IAE graphs for Example 1

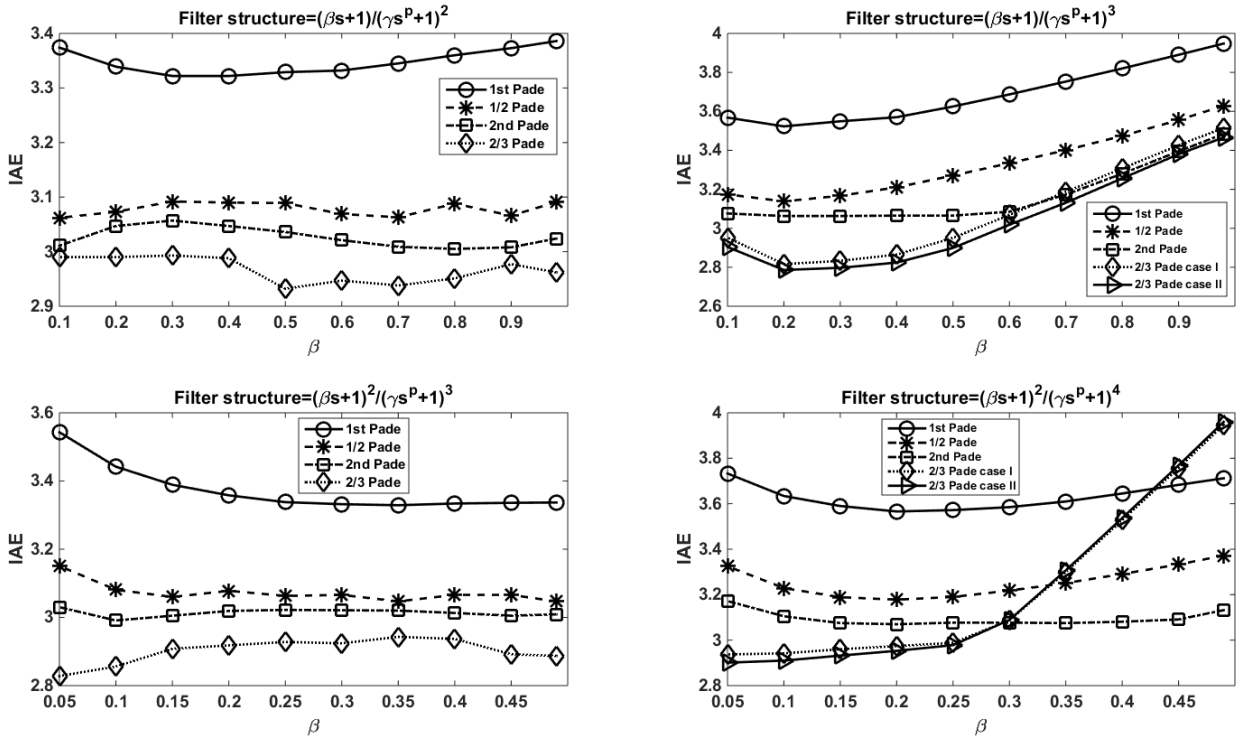

Fig 5.3 β versus IAE graphs for Example 2

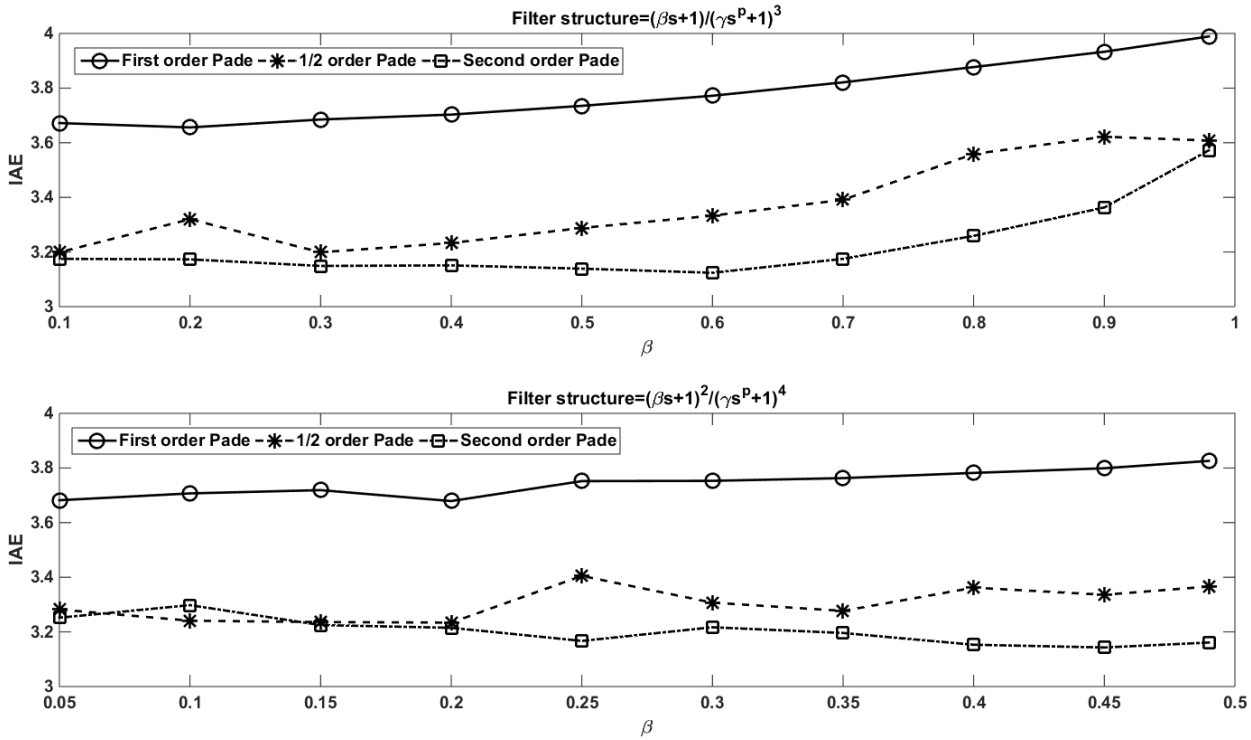

Fig 5.4 β versus IAE graphs for Example 3

Table 5.5 Fractional filter terms of the optimum controllers

Process	Method	Fractional filter term
IPTD	Proposed1	$\frac{\beta s^2+s}{\frac{\gamma^2L^2}{12}s^{2p+1}+\frac{\gamma^2L}{2}s^{2p}+\frac{\gamma L^2}{6}s^{p+1}-\frac{\beta L^2}{12}s^2+\gamma^2s^{2p-1}+\gamma Ls^p+\frac{\beta L}{2}s+2\gamma s^{p-1}+(L-\beta)}$
	Proposed2	$\frac{s}{\frac{\gamma L^2}{12}s^{p+1}+\frac{\gamma L}{2}s^p+\gamma s^{p-1}+L}$
IFPTD	Proposed3	$\frac{\beta L^3s^5+(9\beta L^2+L^3)s^4+(36\beta L+9L^2)s^3+(36L+60\beta)s^2+60s}{[\gamma^3L^3s^{3p+2}+9\gamma^2L^3s^{3p+1}+3\gamma^2L^3s^{2p+2}+36\gamma^3Ls^{3p}+27\gamma^2L^2s^{2p+1}+3\gamma L^3s^{p+2}+60\gamma^3s^{3p-1}+108\gamma^2Ls^{2p}+27\gamma L^2s^{p+1}+(L^3-3\beta L^2)s^2+180\gamma^2s^{2p-1}+108\gamma Ls^p+(24\beta L+6L^2)s+180\gamma s^{p-1}+(60L-60\beta)]}$
	Proposed4	$\frac{L^3s^3+9L^2s^2+36Ls+60}{\gamma L^3s^{p+2}+9\gamma L^2s^{p+1}+L^3s^2+36\gamma Ls^p+6L^2s+60\gamma s^{p-1}+60L}$
DIPTD	Proposed5	$\frac{\beta s^3+s^2}{\frac{\gamma^3L^2}{12}s^{3p+1}+\frac{\gamma^3L}{2}s^{3p}+\frac{\gamma^2L^2}{4}s^{2p+1}+\gamma^3s^{3p-1}+\frac{3\gamma^2L}{2}s^{2p}+\frac{\gamma L^2}{4}s^{p+1}-\frac{\beta L^2}{12}s^2+3\gamma^2s^{2p-1}+\frac{3\gamma L}{2}s^p+\frac{\beta L}{2}s+3\gamma s^{p-1}+(L-\beta)}$
	Proposed6	$\frac{s^2}{\frac{\gamma^3L^2}{12}s^{3p+1}+\frac{\gamma^3L}{2}s^{3p}+\frac{\gamma^2L^2}{4}s^{2p+1}+\gamma^3s^{3p-1}+\frac{3\gamma^2L}{2}s^{2p}+\frac{\gamma L^2}{4}s^{p+1}+3\gamma^2s^{2p-1}+\frac{3\gamma L}{2}s^p+3\gamma s^{p-1}+L}$

5.4.2. Example 1

Consider the distillation column bottom level control system (Chen and Seborg, 2002) modelled as an IPTD system

$$G(s)=\frac{0.2\,e^{-7.4s}}{s} \qquad (5.31)$$

The Proposed1 and Proposed2 controller settings are given in Table 5.6. The controller equation for Kumar and Sree (2016) method is $C(s)=\left(\frac{1}{1+1.4836s}\right)0.5169\left(1+\frac{1}{34.1s}+3.2985s\right)$. The step response for a unit step disturbance applied at t=150s is shown in Fig 5.5 and the corresponding IAE, TV values are listed in Table 5.7. The perturbed response and the response for measurement noise is shown in Fig 5.6 and Fig 5.7. The associated IAE and TV values are listed in Table 5.7. It is evident from these figures and Table 5.7 that the Proposed1 method is better with low IAE followed by Proposed2 method compared to Kumar and Sree (2016) method.

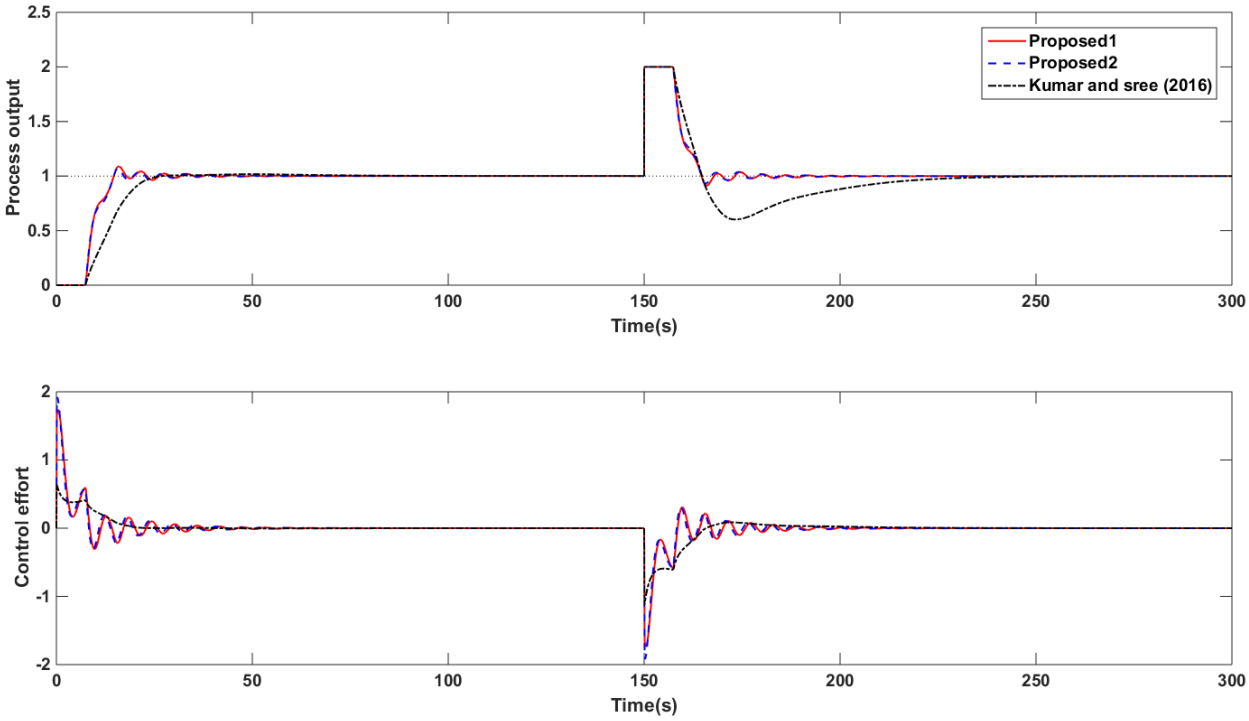

Fig 5.5 Nominal response of Example 1

Table 5.6 Controller settings for the proposed methods of all the Examples

Examples	Method	K_p	T_i	T_d	β	γ	p
Example 1	Proposed1	18.5	3.7	1.23	1.1	1.78	1.02
	Proposed2	18.5	3.7	1.23	-	2.54	1.02
Example 2	Proposed3	20	4	-	0.2	0.16	1.02
	Proposed4	5	-	4	-	0.25	1.02
Example 3	Proposed5	0.5	0.5	0.17	0.6	0.3	1.02
	Proposed6	0.5	0.5	0.17	-	0.14	1.02

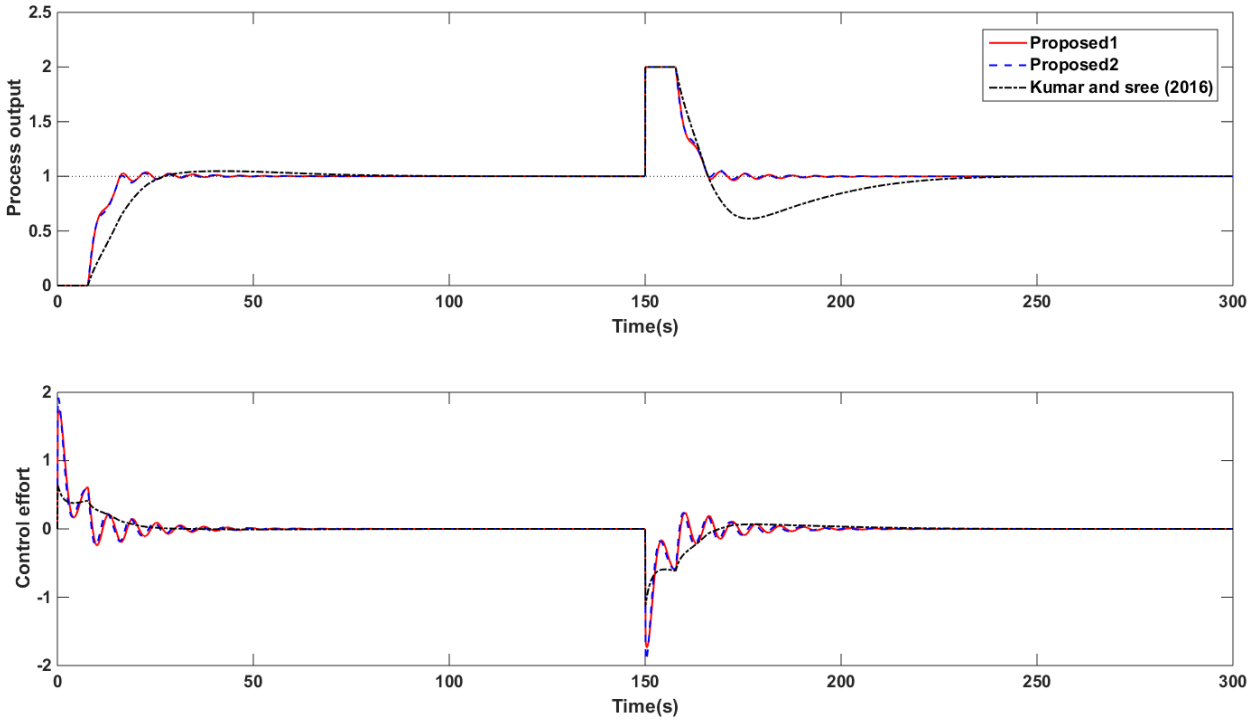

Fig 5.6 Perturbed response of Example 1

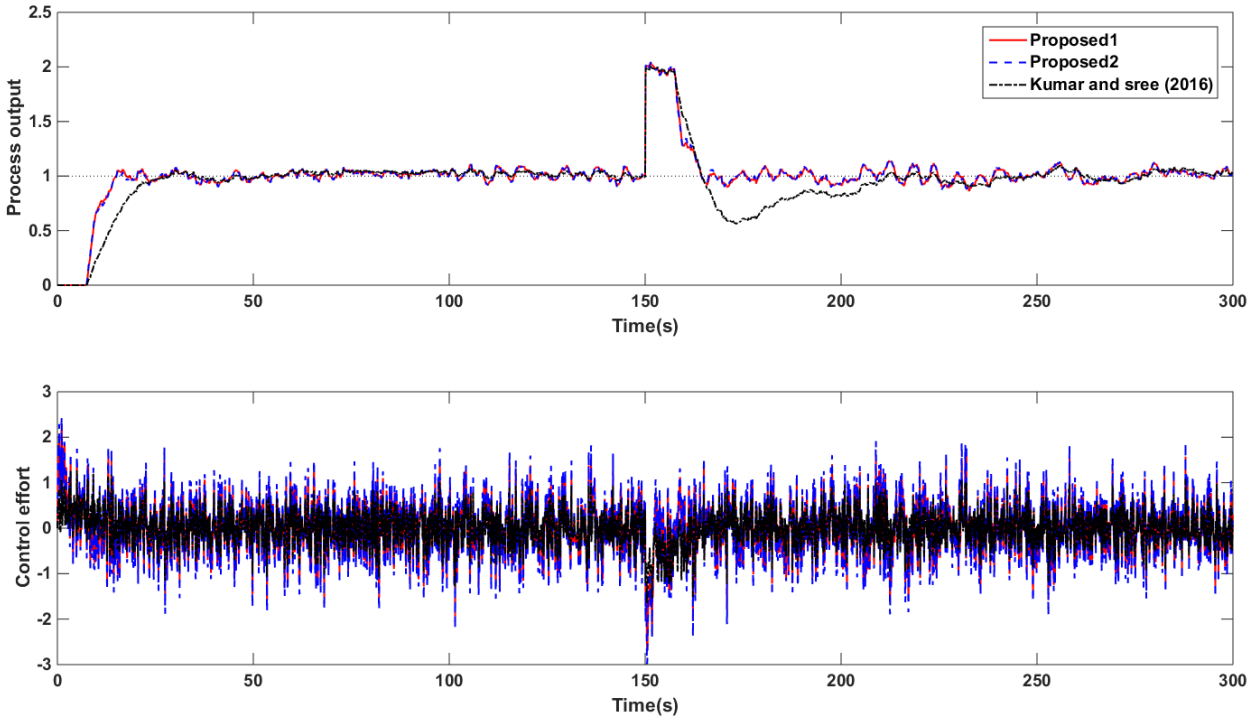

Fig 5.7 Response of Example 1 with measurement noise

The magnitude plot of T(s) for variation in γ is shown in Fig 5.8 which confirms that the Proposed1 is more robust compared to Proposed2 for an uncertainty of +10% in L and K. It can be observed

that the stability margin increases with increase in γ from +10% to +70% obeying the robust stability condition (eq. (5.28)).

Table 5.7 Comparison of IAE and TV values for Example 1

Method	**Nominal case**		**Perturbed case**		**Noise case**		**M_s**
	IAE	**TV**	**IAE**	**TV**	**IAE**	**TV**	
Proposed1	20.86	14.50	22.4	14.03	91.04	1775.3	2
Proposed2	20.82	15.31	22.44	14.56	91.07	2109.4	2
Kumar and Sree (2016)	36.13	3.82	39.19	3.81	92.57	1281.2	2

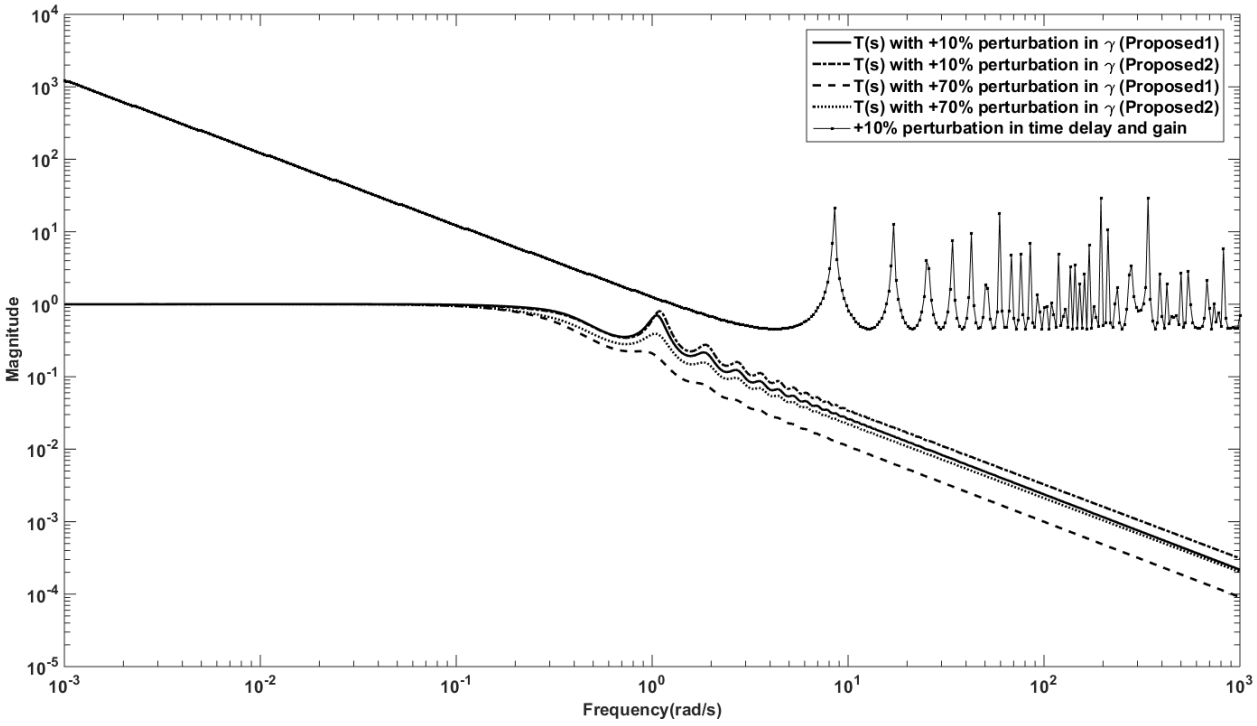

Fig 5.8 Example 1 magnitude plot

5.4.3. Example 2

The IFPTD system studied by Jin and Liu (2014) is considered as a second example

$$G(s)=\frac{0.2\,e^{-s}}{s(4s+1)} \tag{5.32}$$

The Proposed3 and Proposed4 controller parameters are listed in Table 5.6 and the controller for Kumar and Sree (2016) method is $C(s)=\left(\frac{1+0.5s}{1+0.1863s}\right)7.415\left(1+\frac{1}{7.8s}+1.9487s\right)$. The closed loop step response with a disturbance applied at t=20s is shown in Fig 5.9. Fig 5.10 and Fig 5.11 presents

the perturbed response and the response for noise in the measured output. The IAE and TV values for the three input changes are given in Table 5.8. It is evident that the Proposed3 method is superior in performance for all the three cases with low values of IAE and TV for an M_s of 1.98 followed by Proposed4 method (low IAE). It can be observed from magnitude plot (Fig 5.12) that the robust stability increases with Proposed3 method for variation of γ in T(s). The robust stability condition (eq. 5.28) is obeyed by both the methods (Proposed3, Proposed4) for uncertainty in L and K.

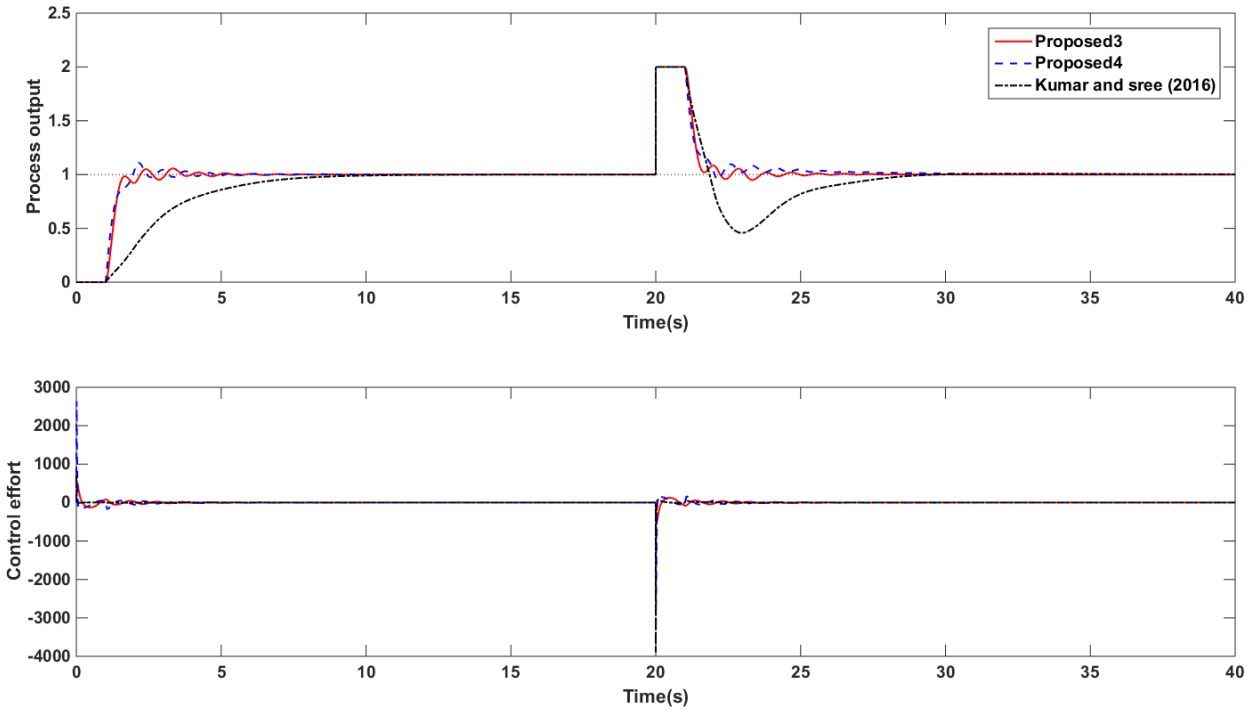

Fig 5.9 Nominal response of Example 2

Table 5.8 Comparison of IAE and TV values for Example 2

Method	**Nominal case**		**Perturbed case**		**Noise case**		**M_s**
	IAE	**TV**	**IAE**	**TV**	**IAE**	**TV**	
Proposed3	2.78	3993	3.08	4214.8	12.7	1.294×10^5	1.98
Proposed4	2.95	13191	3.19	13043	13.04	8.287×10^5	1.98
Kumar and Sree (2016)	4.22	8847.8	4.64	8829.5	15.07	1.202×10^6	1.98

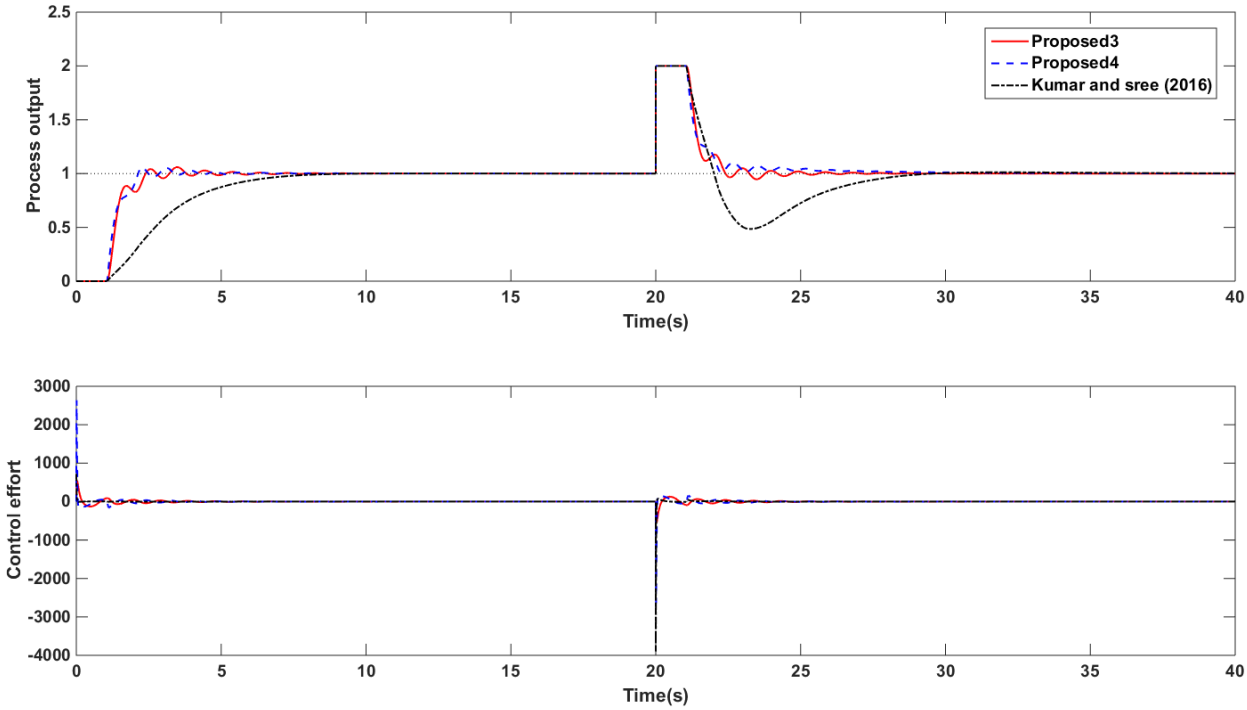

Fig 5.10 Perturbed response of Example 2

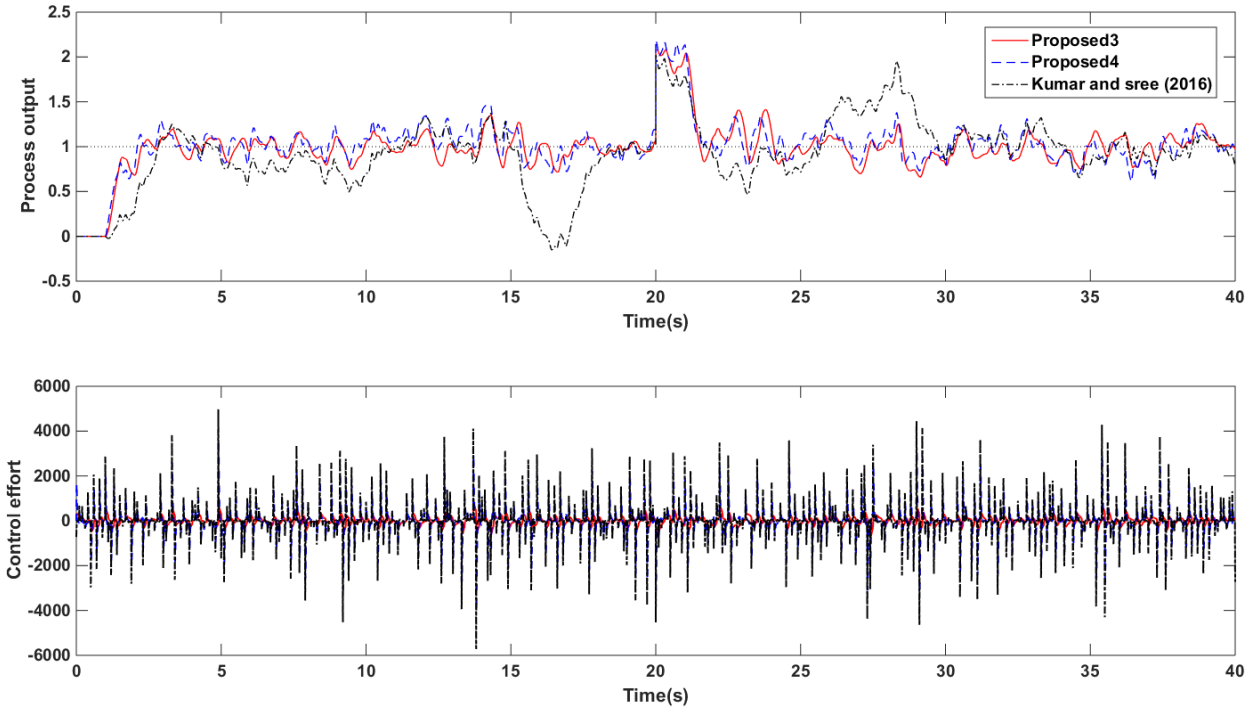

Fig 5.11 Response of Example 2 with measurement noise

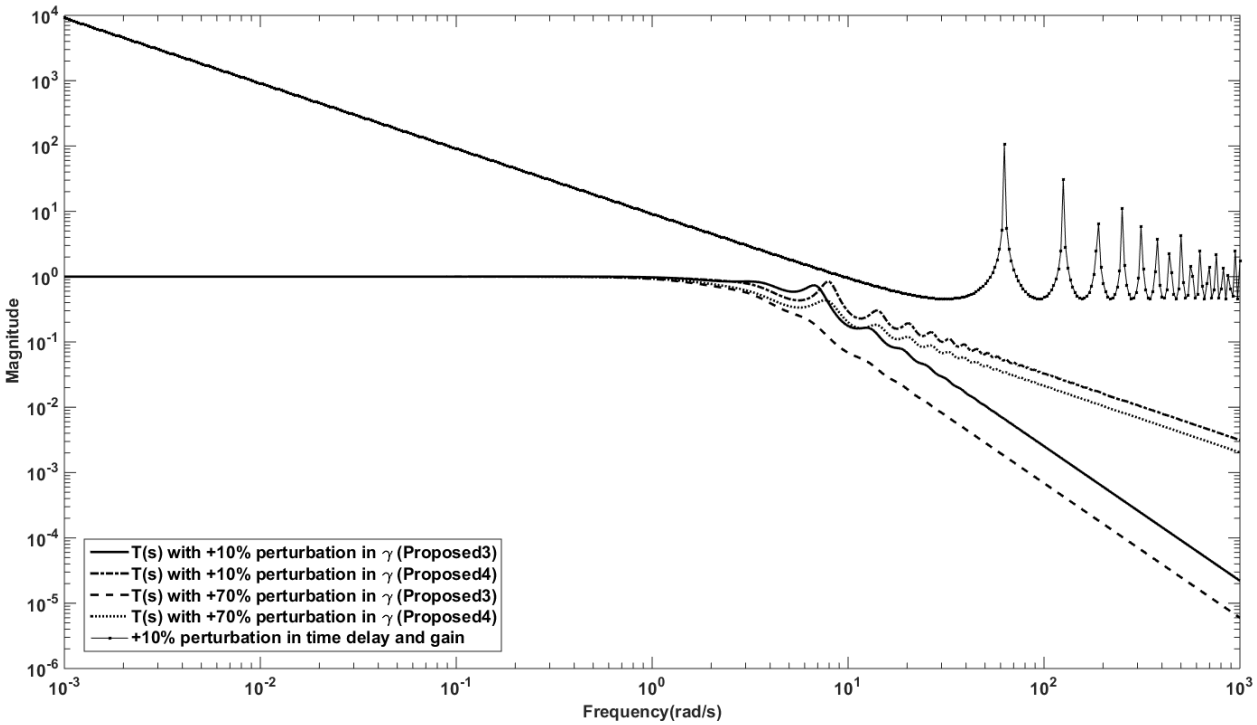

Fig 5.12 Example 2 magnitude plot

5.4.4. Example 3

The following DIPTD model is used for the simulation study (Lee et al., 2013)

$$G(s)=\frac{e^{-s}}{s^2} \tag{5.33}$$

The closed loop step response for nominal process conditions; for perturbations and for measurement noise is shown in Figs 5.13-5.15. The corresponding performance measures IAE and TV are listed in Table 5.9. It is clear that the Proposed5 method is giving improved performance with lower values of IAE and TV followed by Proposed6 method compared to Kumar and Sree (2016) method. Both the proposed methods are obeying the robust stability condition for an uncertainty in L and K.

Table 5.9 Comparison of IAE and TV values for Example 3

Method	**Nominal case**		**Perturbed case**		**Noise case**		**M_s**
	IAE	**TV**	**IAE**	**TV**	**IAE**	**TV**	
Proposed5	3.13	139.60	3.34	144.55	21.08	5517.9	2.01
Proposed6	3.22	144.81	3.49	154.31	21.08	3385.8	2.01
Kumar and Sree (2016)	6.05	342.70	6.75	342.25	27.95	78943	2.01

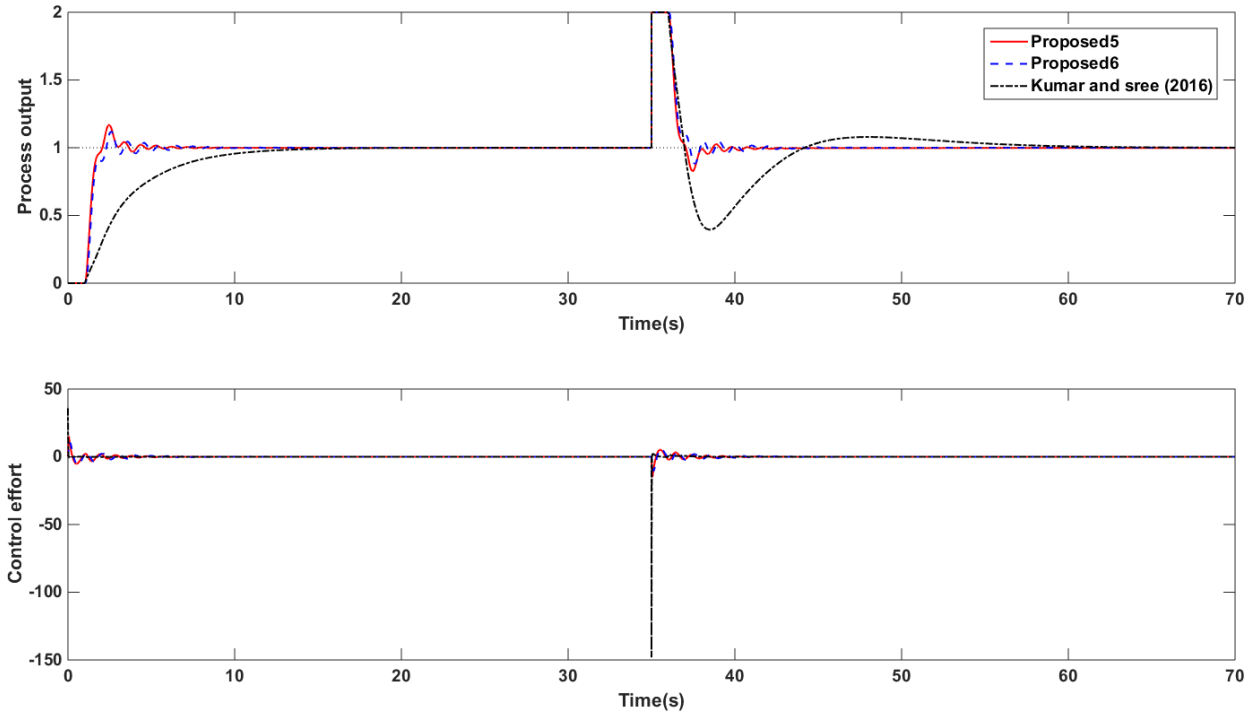

Fig 5.13 Nominal response of Example 3

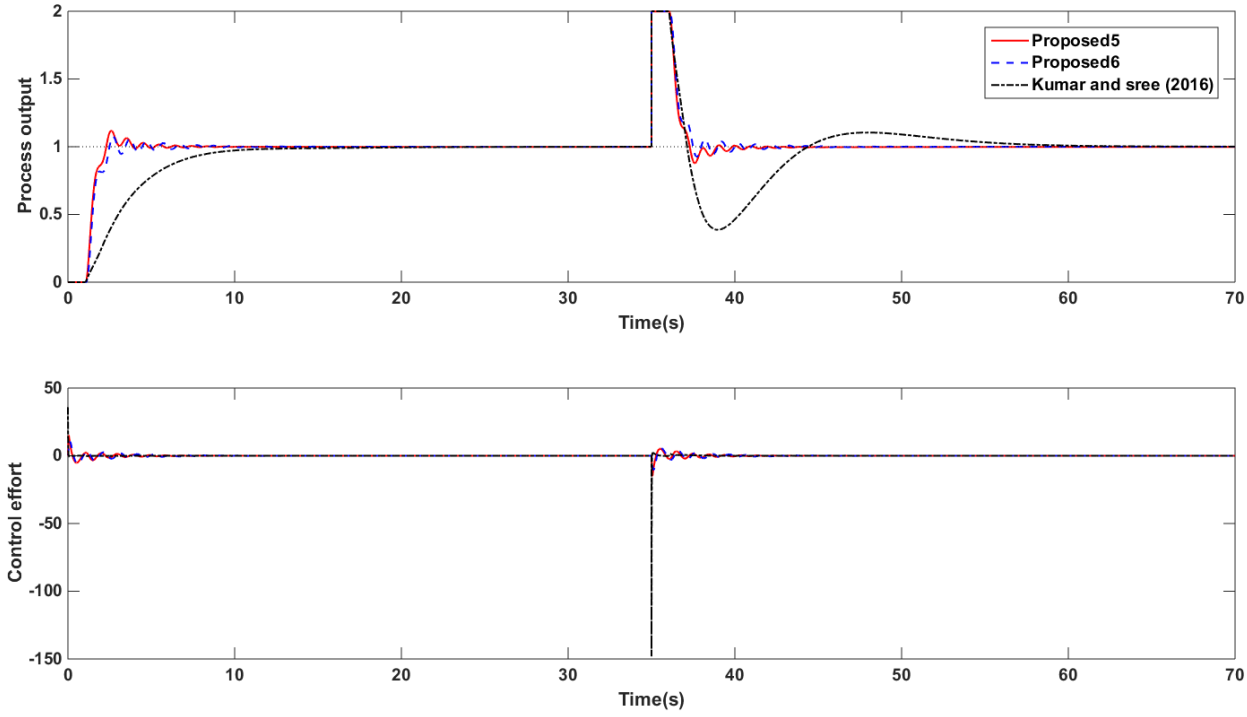

Fig 5.14 Perturbed response of Example 3

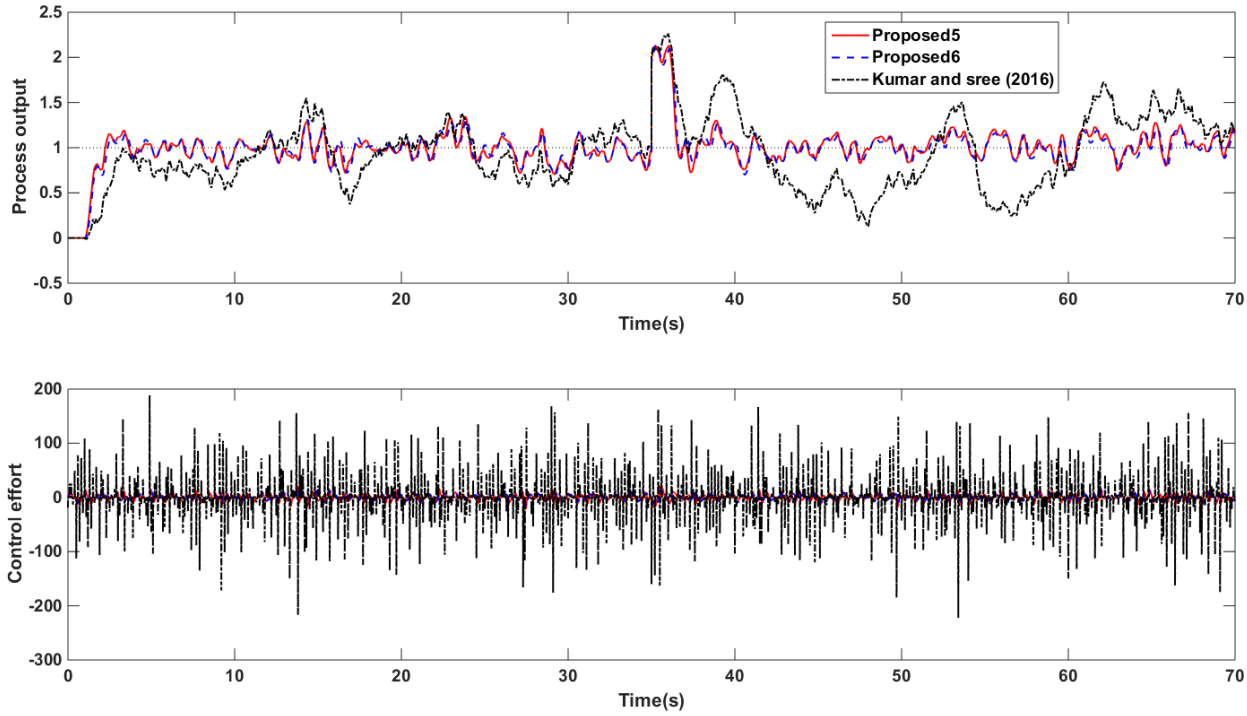

Fig 5.15 Response of Example 3 with measurement noise

5.4.5. Fragility analysis

The delta 20 fragility index ($FI_{\Delta 20}$) for all the examples with the proposed and Kumar and Sree (2016) methods is given in Table 5.10. The variation of delta epsilon fragility index (ε=0.05, 0.1….0.25, 'ε' is the percentage of variation in controller parameters) for all the examples is presented in Fig 5.16. The controller with Proposed1 method is resilient with respect to Example 1 as it doesn't lose 10% of its robustness whereas Proposed2 and Kumar and Sree (2016) methods are nonfragile which needs a careful tuning for variation in controller parameters. In case of Example 2, Proposed3 and Proposed4 methods are nonfragile whereas the Kumar and Sree (2016) method is fragile as it lose more than 50% of its robustness and is difficult to tune for changes in controller parameters. The controllers with Proposed5 and Proposed6 methods are resilient with respect to Example 3 and Kumar and Sree (2016) method is fragile.

Table 5.10 Controller Fragility indices ($FI_{\Delta 20}$) for all the examples

Example 1		**Example 2**		**Example 3**	
Method	**$FI_{\Delta 20}$**	**Method**	**$FI_{\Delta 20}$**	**Method**	**$FI_{\Delta 20}$**
Proposed1	0.069	Proposed3	0.136	Proposed5	0.071
Proposed2	0.113	Proposed4	0.439	Proposed6	0.013
Kumar and Sree (2016)	0.313	Kumar and Sree (2016)	1.207	Kumar and Sree (2016)	0.696

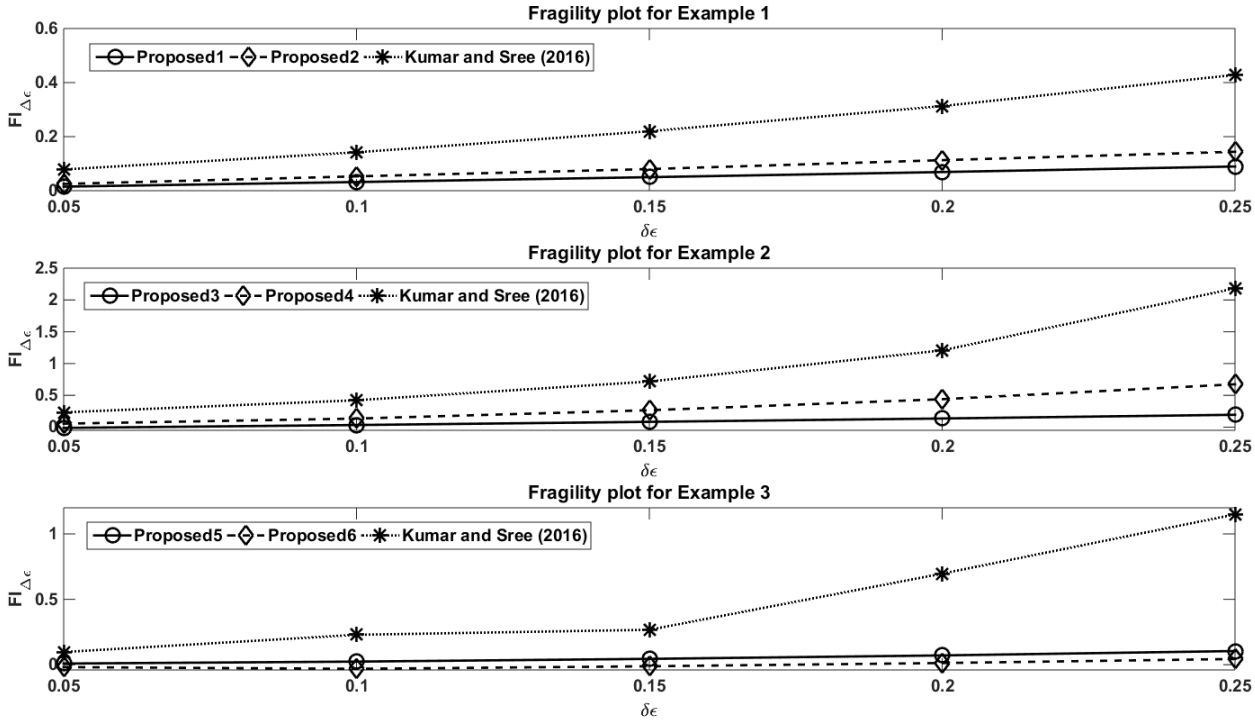

Fig 5.16 Fragility plots for the three examples

5.5. Conclusions

In this work, an optimum higher order fractional IMC filter structure is identified based on minimum IAE for a prefixed M_s. A fractional filter IMC-PID controller is designed for different integrating processes using the optimum higher order fractional IMC filter structure and different Pade's approximation for time delay. The proposed method provides more flexibility in the controller design with additional tuning parameters and enhance the system's performance. The step response of three integrating processes is presented for changes in different inputs acting on the closed loop system. Enhanced closed loop performance is observed with the controller designed using higher order fractional IMC filter structure plus 2nd order Pade's approximation of time delay for IPTD and DIPTD processes. Improved performance of IFPTD process is observed with the controller designed using higher order fractional IMC filter structure plus 2/3 order Pade's approximation of time delay. It is observed that the IAE and TV values are decreasing with increase in the order of fractional IMC filter structure for IFPTD process and DIPTD process whereas TV values are increasing for IPTD process for different process conditions. All the proposed methods are robustly stable for parametric uncertainty and for variation in γ. It is found from controller

fragility analysis for controller parametric uncertainties that all the proposed methods are either resilient (Proposed1, Proposed5 and Proposed6) or nonfragile (Proposed2, Proposed3 and Proposed4) and the stability margin is increasing with increase in the uncertainty.

Chapter 6

Fractional filter fractional IMC-PID controller design for non-integer order plus time delay (NIOPTD) processes

6. Fractional filter fractional IMC-PID controller design for non-integer order plus time delay (NIOPTD) processes*

A fractional filter fractional order PID (FFFOPID) controller is designed for Non-integer order plus time delay (NIOPTD) systems using fractional IMC filter structure. The novelty of the work lies in identifying the higher order fractional IMC filter structure using a systematic design procedure based on the minimization of IAE. The design includes different approximation for time delay term. The resulting controller consists of a fractional filter term and a fractional PID controller. The tuning parameters are identified based on the minimum value IAE for a fixed robustness (M_s). Simulations are carried out for servo response and regulatory response and an enhanced performance is observed with the proposed controller. Uncertainties in the process parameters are considered to check the robustness of the system and the stability is assessed with robust stability analysis. In addition, fragility analysis has been done for uncertainties in the controller parameters.

In the second part, FFFOPID controller design method is proposed for higher order systems approximated as NIOPTD models. An analytical tuning method is followed for identification of optimum controller settings. Simulation results on different systems shows that the proposed method is giving better output performance for set point tracking, disturbance rejection, parameter variations and for measurement noise in the output. The robust stability of the system for process parametric uncertainties is verified with robustness analysis. Controllability index analysis is also accomplished to know the closed loop system performance and robustness.

The third part of this chapter focuses on the fragility of FFFOPID controllers for higher order systems approximated as non-integer order plus time delay systems. The fragility of the controller is plotted for individual parameter variations to observe the effect on closed loop performance and robustness. Further, the fragility balance of the controller is estimated and the most influencing parameter on the fragility is identified. Two examples are used to illustrate the fragility plots and results show that this type of controller is nonfragile assuring the stable performance through fine tuning of the controller.

*This work has been published in European Journal of Electrical Engineering - https://doi.org/10.18280/ejee.210203; the second section has been published as a book chapter in CRC press; the third portion of this chapter is presented in an international conference at NIT Warangal.

6.1. Fractional filter fractional IMC-PID controller design for NIOPTD processes

6.1.1. Introduction

The fractional order controllers are gaining wide acceptance in the industrial sector and among the scientific community to control the processes modeled as higher order systems. Higher order models capture the subtleties of the processes and better represent the dynamics of nonlinear processes in a precise manner. It is difficult to control the higher order process models and more challenging if they are associated with time delays. The control performance of such systems degrades if the standard PID controller is used (Vilanova and Visioli, 2012). This is the concern of many researchers from the last twenty years and this fact resulted in the design and application of FOPID controller to improve the closed loop response of time delay systems.

The primary work on fractional order controllers was by Oustaloup in 1991 and subsequently Podlubny (1999) proposed an FOPID or $PI^{\lambda}D^{\mu}$ controller with the help of fractional calculus. The structure of FOPID controller is such that it becomes a PID controller by setting the fractional powers of integrator and differentiator to unity. This flexibility in the controller structure ensures robust performance of integer order systems and non-integer order systems. Hence, FOPID controller can enhance the closed loop performance of higher order systems. The $PI^{\lambda}D^{\mu}$ controller for such systems was developed by approximating higher order systems by lower order time delay systems (Monje et al., 2008; Padula and Visioli, 2011). Further, the FOPID controller was developed for non-integer order time delay systems as they represent the system dynamics in a better way than integer order systems. Thus, the fractional order PI/PID controller improves the closed loop performance of higher order processes. However, this structure of FOPID controller complicates the tuning with the additional tuning parameters. There are several tuning methods reported in the literature (Shah and Agashe, 2016) for tuning the FOPID controller and fractional filter PID controller for integer order time delay systems (Sánchez et al., 2017; Padula and Visioli, 2013).

The tuning methods of FOPID controller for fractional order systems gained momentum in the last decade. It has been identified that higher order processes need to be brought to the lower order, preferably of first and second order for frequency domain tuning and time domain tuning of the

FOPID controller. Based on this, $PI^{\lambda}D^{\mu}$ controller tuning strategies in frequency domain and time domain were proposed for NIOPTD systems (Das et al., 2011). An analytical tuning method of FOPID controller for fractional order systems was proposed after reducing the higher order fractional system by retaining its dynamics (Tavakoli-Kakhki and Haeri, 2011). A $PI^{\lambda}D^{\mu}$ controller was also designed using soft computing technique for delay free non-integer order systems (Liu et al., 2015) and by using optimization (Zeng et al., 2015). The use of IMC (Shamsuzzoha et al., 2012) method was predominant in the design of FOPID controller for NIOPTD systems (Vinopraba et al., 2012; Bettayeb and Mansouri, 2014; Li et al., 2015). The IMC filter used in the IMC method plays a crucial role because the tuning parameters in the IMC based controller are those associated with the IMC filter. The controller in Bettayeb and Mansouri (2014) was tuned to meet the specifications such as phase margin, flat phase, gain crossover frequency and infinite gain margin. The controller designed using the method in Li et al., (2015) was tuned based on maximum sensitivity. The aim of the present work is to propose a simple and improved method of designing the fractional filter fractional IMC-PID controller using fractional IMC filter for NIOPTD systems. The design also includes different approximation for time delay term using Pade's procedure. The resulting structure of the controller consists of a fractional order PID preceded by fractional filter to provide robust control. The tuning parameters in the controller are associated with fractional filter which are identified through the systematic procedure based on the minimum values of IAE and TV and to meet the maximum sensitivity, M_s specification for fair comparison.

6.1.2. Fractional order system

The dynamics of real time systems are better represented by non-integer order mathematical models using the fractional calculus with the help of fractional integration and differentiation. The fractional order systems are often described by the following fractional order differential equation:

$$a_0 y(t) + \sum_{i=1}^{n} a_i D^{\alpha_i} y(t) = b_0 u(t-L) + \sum_{i=1}^{m} b_i D^{\beta_i} u(t-L) \quad (6.1)$$

Where D is the fractional operator; a_i, b_i are the real coefficients; α_i, β_i are the real (R+) orders of fractional derivative; u(t) and y(t) are the real input and output; L is the time delay of the system. The Laplace transform of eq. (9.1) produces a fractional order transfer function

$$a_0 Y(s) + \sum_{i=1}^{n} a_i S^{\alpha_i} Y(s) = b_0 U(s) e^{-Ls} + \sum_{i=1}^{m} b_i S^{\beta_i} U(s) e^{-Ls} \quad (6.2)$$

Where $S^{\alpha_i}Y(s)$ and $S^{\beta_i}U(s)$ are the Laplace transform of $D^{\alpha_i}y(t)$ and $D^{\beta_i}u(t)$ respectively. Then, the transfer function of non-integer order system is

$$G(s)=\frac{Y(s)}{U(s)}=\frac{b_0+\sum_{i=1}^{m} b_i S^{\beta_i}}{a_0+\sum_{i=1}^{n} a_i S^{\alpha_i}} e^{-Ls} \tag{6.3}$$

The fractional operators S^{α_i} and S^{β_i} are difficult to program for simulations and for practical implementation in the hardware. Though, there are several means of practical implementation of fractional operators the most widely used one is the approximation of the fractional operator by integer order transfer function. The popular approximation used for fractional operator s^{ν} was by Oustaloup recursive filter (Oustaloup, 1991) which is based on the recursive distribution of poles and zeros over a frequency range $[\omega_l, \omega_h]$. This filter is given by

$$s^{\nu}=K\prod_{k=-N}^{N}\frac{s+\omega_k^{'}}{s+\omega_k} \tag{6.4}$$

Where N is the number of poles and zeros. Selection of N is crucial for the approximation; smaller values of N results in ripples in the gain and phase behavior, but they are minimized for higher values of N causing an increase in the computational load. The poles, zeros and gain are evaluated using the following equations:

$$\omega_k^{'}=\omega_l\left(\frac{\omega_h}{\omega_l}\right)^{\left(k+N+\frac{1-\nu}{2}\right)/(2N+1)} \tag{6.5.a}$$

$$\omega_k=\omega_l\left(\frac{\omega_h}{\omega_l}\right)^{\left(k+N+\frac{1+\nu}{2}\right)/(2N+1)} \tag{6.5.b}$$

$$K=\omega_h^{\nu} \tag{6.5.c}$$

The non-integer order process models used for the design of FOPID controller are:

(a) One non-integer order plus time delay (NIOPTD-I) system

$$G_m(s)=\frac{K}{Ts^{\alpha}+1}e^{-Ls} \tag{6.6}$$

Two cases of NIOPTD-I process (Li et al., 2015) are possible based on the value of α: case I ($0<\alpha<1$); case II ($1\leq\alpha<2$).

(b) Two non-integer order plus time delay (NIOPTD-II) system

$$G_m(s)=\frac{K}{s^{\alpha}+2\zeta\omega_n s^{\beta}+\omega_n^2}e^{-Ls} \tag{6.7}$$

Where α and β are the flexible system orders. This flexibility allows the accurate modeling of the processes with minimum modeling error compared to first order and second order time delay

(FOPTD and SOPTD) models. The two cases of NIOPTD-II process based on the value of α and β are: case I ($1<\alpha<2$, $\alpha>\beta$) and case II ($2\leq\alpha<3$, $\alpha>\beta$).

6.1.3. Proposed fractional filter fractional IMC-PID controller design

The proposed fractional filter fractional order PID controller structure is

$$C(s)=(\text{fractional filter term})K_p\left[1+\frac{1}{T_i s^{\lambda}}+T_d s^{\mu}\right] \tag{6.8}$$

The fractional IMC filter structures used in the present design are:

$$f(s)=\frac{1}{(\gamma s^p+1)^n};\ n=1,2,3 \tag{6.9}$$

$$f(s)=\frac{\eta s+1}{(\gamma s^p+1)^{n+1}};\ n=1,2 \tag{6.10}$$

$$f(s)=\frac{(\eta s+1)^2}{(\gamma s^p+1)^{n+2}};\ n=1,2 \tag{6.11}$$

γ is the filter time constant, p is the fractional order and η is the additional degree of freedom.
The fractional IMC filter controller for the NIOPTD-I system defined in eq. (6.6) and by using fractional IMC filter structure defined in eq. (6.9) is

$$C_{IMC}(s)=\left(\frac{Ts^{\alpha}+1}{K}\right)\frac{1}{(\gamma s^p+1)^n} \tag{6.12}$$

The feedback controller using fractional IMC filter is

$$C(s)=\frac{Ts^{\alpha}+1}{K[(\gamma s^p+1)^n-e^{-Ls}]} \tag{6.13}$$

Now, by using Pade's procedure for e^{-Ls} (Table 6.1), the general expression for C(s) is

$$C(s)=(\text{fractional filter term})\left(\frac{T}{K}\right)\left(1+\frac{1}{Ts^{\alpha}}\right) \tag{6.14}$$

It can be observed from eq. (6.14) that the controller is composed of fractional PI term in series with fractional filter term. Similarly, the controller is derived for other fractional IMC filter structures (eqs. (6.10) & (6.11)) by following the above design procedure (steps). The resulting controller takes the form given in eq. (6.14). All the controllers derived using different fractional IMC filter structures differ only in the fractional filter term.

Table 6.1 Equivalent term of e^{-Ls} using Pade's procedure

1st order Pade	**1/2 order Pade**	**2nd order Pade**	**2/3 order Pade**
(1-0.5Ls)/(1+0.5Ls)	(6-2Ls)/(6+4Ls+L^2s^2)	$\frac{1-(L/2)s+(L^2/12)s^2}{1+(L/2)s+(L^2/12)s^2}$	$\frac{60-24Ls+3L^2s^2}{60+36Ls+9L^2s^2+L^3s^3}$

The feedback controller for NIOPTD-II process can be obtained by applying the same procedure used for NIOPTD-I process. The generalized controller equation for all fractional IMC filter structures is

$$C(s)=(\text{fractional filter term})\left(\frac{2\zeta\omega_n}{K}\right)\left(1+\frac{\omega_n}{2\zeta s^{\beta}}+\frac{1}{2\zeta\omega_n}s^{\alpha-\beta}\right) \quad (6.15)$$

The feedback controller C(s) consists of a fractional PID term in series with fractional filter term. The controller settings K_p, T_i, T_d, λ and μ can be obtained from the process parameters according to the derived formulae. The remaining parameters to be tuned in all the four controllers are associated with the fractional filter term which are γ, η and p. They are chosen according the tuning procedure given the flowchart (Fig 6.1). The proper selection of these parameters alters the filter term of the controller, which enhances the closed loop performance.

6.1.4. Robustness and fragility analysis

6.1.4.1. Robustness analysis

The closed loop stability must be assessed for the nominal process conditions and with uncertainties in the processes. This is verified with a robust stability condition (Morari and Zafiriou, 1989).

$$\|l_m(j\omega)T(j\omega)\|<1\forall\omega\in(-\infty,\infty) \quad (6.16)$$

Where $T(s)_{s=j\omega}=\frac{C(s)G(s)}{1+C(s)G(s)}$ - the complementary sensitivity function; $l_m(j\omega)=\left|\frac{G(j\omega)-G_m(j\omega)}{G_m(j\omega)}\right|$ - Process multiplicative uncertainty bound.

Using robust stability analysis, one can know the amount of uncertainty that can be introduced into the process parameters for the robust performance once the controller is designed. The controller must be tuned according to eq. (6.17) for uncertainty in L

$$\|T(j\omega)\|_{\infty}<\frac{1}{|e^{-\Delta L}-1|} \quad (6.17)$$

6.1.4.2. Fragility analysis

The robust performance of the closed loop system should also be observed for changes in controller parameters. This is found through loss of robustness (M_s) of the system using fragility analysis (Alfaro and Vilanova, 2012). The degree of controller fragility is decided based on robustness delta 20 fragility index ($RFI_{\Delta 20}$) which is defined in eq. (6.18)

$$RFI_{\Delta 20} = \frac{M_{s\Delta 20}}{M_s} - 1 \tag{6.18}$$

$M_{s\Delta 20}$ is the M_s for 20% variation in all parameters of the controller and M_s in the nominal maximum sensitivity. Any controller is said to be resilient if $RFI_{\Delta 20} \leq 0.1$; nonfragile if $0.1 < RFI_{\Delta 20} \leq 0.5$ and fragile if $RFI_{\Delta 20} > 0.5$.

6.1.5. Simulation results

The effectiveness of the proposed fractional filter FOPID controller is explained with four examples representing all cases of NIOPTD system. The simulations have been performed for a step change in set point and disturbance. The system's performance is also observed for perturbations (-20% in K and +10% in L) in the process parameters and for Gaussian noise in the output. The closed loop performance of the NIOPTD system is assessed by using the performance measures given in Table 6.2.

Table 6.2 Performance measures

IAE	**ITAE**	**TV**	**M_s**
$\int_0^\infty \lvert e(t)\rvert dt$	$\int_0^\infty t\lvert e(t)\rvert dt$	$\sum_{i=0}^{\infty} \lvert u_{i+1}-u_i\rvert$	$\max_{0<\omega<\infty} \left\lvert \frac{1}{1+C(j\omega)G(j\omega)} \right\rvert$

6.1.5.1. Identified fractional IMC filter structure

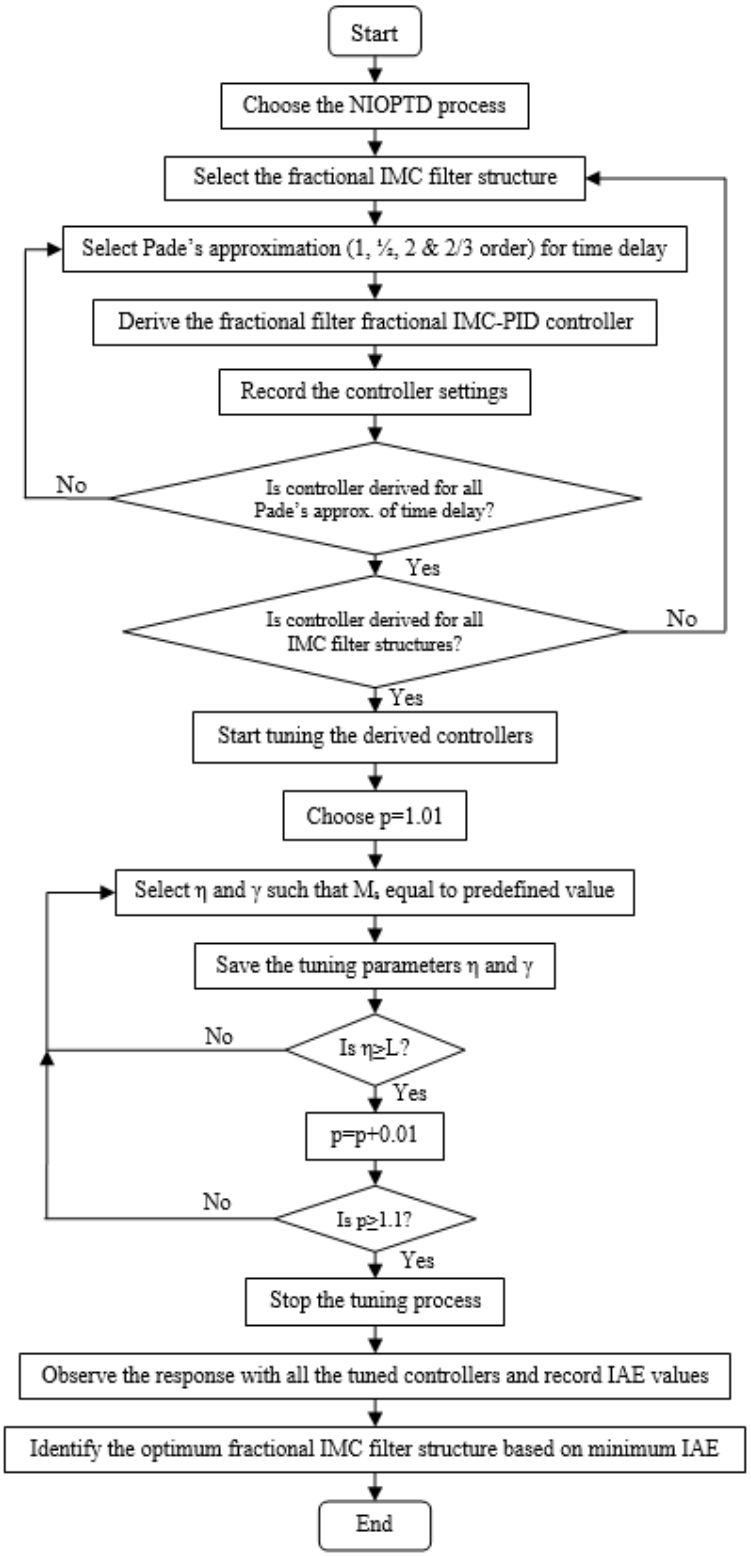

Fig 6.1 Systematic procedure for identification of optimum fractional IMC filter structure

The optimum fractional filter fractional IMC-PID controller settings for all the NIOPTD processes are identified according to the flowchart (Fig 6.1). A point to be noted here is that the tuning becomes difficult for controllers designed using higher order fractional IMC filter for case I of NIOPTD processes. Hence, a conventional fractional IMC filter is considered during the controller design for case I of NIOPTD processes. The FOPI and FOPID controller settings for NIOPTD-I and NIOPTD-II processes remain same as given in eq. (6.14) and eq. (6.15). The fractional filter terms of the optimum controllers are given in Table 6.3. Hereafter, the optimum proposed methods of the NIOPTD processes are referred to as Proposed1 (NIOPTD-I case I): $(1/\gamma s^p+1)$+ 2/3 Pade's approximation of e^{-Ls}; Proposed2 (NIOPTD-I case II): $((\eta s+1)^2/(\gamma s^p+1)^3)$+ 2/3 Pade's approximation of e^{-Ls}; Proposed3 (NIOPTD-II case I): $(1/\gamma s^p+1)$+ 2/3 Pade's approximation of e^{-Ls}; Proposed4 (NIOPTD-II case II): $(\eta s+1/(\gamma s^p+1)^3)$+ 2/3 Pade's approximation of e^{-Ls}.

Table 6.3 Fractional filter terms of the optimum controller

Process	**Fractional filter term**
NIOPTD-I (case I)	$\frac{L^3s^3+9L^2s^2+36Ls+60}{\left(\gamma L^3s^{p+2}+9\gamma L^2s^{p+1}+L^3s^2+36\gamma Ls^p+6L^2s+60\gamma s^{p-1}+60L\right)s^{1-\alpha}}$
NIOPTD-I (case II)	$\frac{\eta^3L^3s^5+(9\eta^2L^2+2\eta L^3)s^4+(36\eta^2L+18\eta L^2+L^3)s^3+(60\eta^2+72\eta L+9L^2)s^2+(36L+120\eta)s+60}{\left(\begin{array}{c}\gamma^3L^3s^{3p+2}+9\gamma^3L^2s^{3p+1}+3\gamma^2L^3s^{2p+2}+36\gamma^3Ls^{3p}+27\gamma^2L^2s^{2p+1}+3\gamma L^3s^{p+2}-3\eta^2L^2s^3+60\gamma^3s^{3p-1}+108\gamma^2Ls^{2p}\\ +27\gamma L^2s^{p+1}+(L^3+24\eta^2L-6\eta L^2)s^2+180\gamma^2s^{2p-1}+108\gamma Ls^p+(48\eta L+6L^2-60\eta^2)s+180\gamma s^{p-1}+(60L-120\eta)\end{array}\right)s^{1-\alpha}}$
NIOPTD-II (case I)	$\frac{L^3s^3+9L^2s^2+36Ls+60}{\left(\gamma L^3s^{p+2}+9\gamma L^2s^{p+1}+L^3s^2+36\gamma Ls^p+6L^2s+60\gamma s^{p-1}+60L\right)s^{1-\beta}}$
NIOPTD-II (case II)	$\frac{\eta L^3s^4+(9\eta L^2+L^3)s^3+(36\eta L+9L^2)s^2+(36L+60\eta)s+60}{\left(\begin{array}{c}\gamma^3L^3s^{3p+2}+9\gamma^3L^2s^{3p+1}+3\gamma^2L^3s^{2p+2}+36\gamma^3Ls^{3p}+27\gamma^2L^2s^{2p+1}+3\gamma L^3s^{p+2}+60\gamma^3s^{3p-1}+108\gamma^2Ls^{2p}\\ +27\gamma L^2s^{p+1}+(L^3-3\eta L^2)s^2+180\gamma^2s^{2p-1}+108\gamma Ls^p+(24\eta L+6L^2)s+180\gamma s^{p-1}+(60L-60\eta)\end{array}\right)s^{1-\beta}}$

6.1.5.2. Example 1

The fractional order model of a heat flow experiment (Malek et al., 2013) is considered for the current study:

$$G_m(s)=\frac{66.16}{12.72s^{0.5}+1}e^{-1.93s} \tag{6.19}$$

The value of α=0.5 which represents case I of NIOPTD-I system. The FOPID controller according to the Li et al. (2015) method is

$$C(s)=\left(\frac{0.96s+1}{4.53s^{1.5}+10.99s^{0.5}}\right)\left(0.19+\frac{0.015}{s^{0.5}}\right) \tag{6.20}$$

The frequency used for Oustaloup filter approximation of fractional operator is 0.001-1000rad/s. The Proposed1 controller settings are listed in Table 6.4. The closed loop step response with a disturbance of magnitude -1 applied at t=100s is shown in Fig 6.2. The corresponding performance measures are given in Table 6.5. It is evident that the Proposed1 method gives improved performance with low IAE, ITAE and TV compared to Li et al. (2015) method. The perturbed response and the associated performance measures are presented in Fig 6.3 and Table 6.6. The Proposed1 method clearly gives better result than the method used for comparison. The IAE and ITAE values for the response in presence of output noise of variance 10 given in Table 6.7 are close to each other for both the methods but the TV value is low with the Proposed1 method. The robust stability with the magnitude plot for T(s) is shown in Fig 6.4. It is found that both the methods are robustly stable up to +90% uncertainty in L obeying the stability condition (eq. 6.17).

Table 6.4 Controller settings for proposed methods of all the examples

Example	$\mathbf{K_p}$	$\mathbf{T_i}$	$\boldsymbol{\lambda}$	$\mathbf{T_d}$	$\boldsymbol{\mu}$	$\boldsymbol{\eta}$	$\boldsymbol{\gamma}$	**p**	$\mathbf{M_s}$
Example 1	0.19	12.72	0.5	-	-	-	11.1	1.05	1.15
Example 2	0.3	1.5	1.5	-	-	0.2	0.66	1.01	1.51
Example 3	1.1963	1.1964	0.9997	0.1648	0.9947	-	0.53	1.03	1.04
Example 4	1.17	1.17	1.02	0.1912	1.45	0.03	0.1085	1.02	1.49

Table 6.5 Comparison of IAE, ITAE and TV values for nominal process conditions

Examples	**Method**	**Servo response**			**Regulatory response**			$\mathbf{M_s}$
		IAE	**ITAE**	**TV**	**IAE**	**ITAE**	**TV**	
Example 1	Proposed1	694.1	6650	4.128	365.2	11780	1.0046	1.15
	Li et al. (2015)	716	9410	4.334	370	12680	1.323	1.15
Example 2	Proposed2	2.576	3.28	0.355	0.9444	1.667	0.1093	1.51
	Li et al. (2015)	3.502	7.663	0.2008	1.095	3.057	0.0644	1.51
Example 3	Proposed3	0.5756	0.2764	19.794	0.2791	0.4618	0.5014	1.04
	Li et al. (2015)	0.581	0.2771	4.987	0.2801	0.4531	0.4979	1.04
Example 4	Proposed4	0.4761	0.0483	42.56	0.2009	0.2773	0.6106	1.49
	Li et al. (2015)	0.5383	0.1384	25.037	0.2506	0.3776	0.5779	1.49

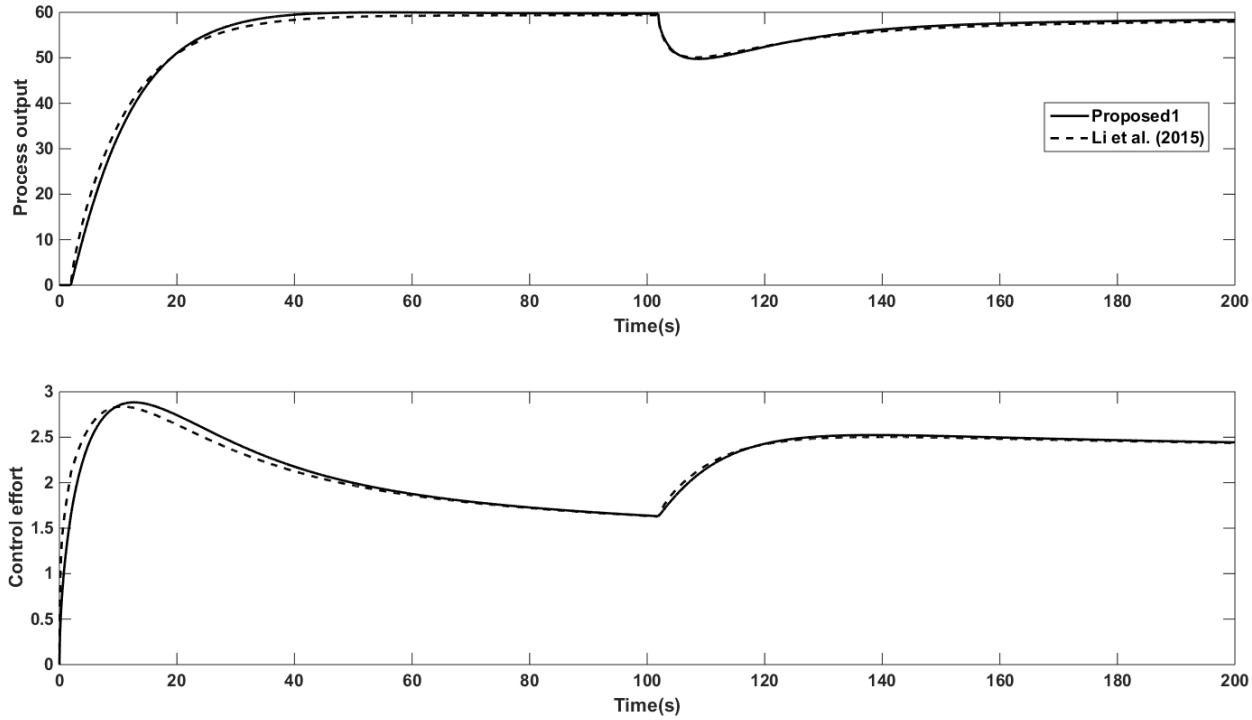

Fig 6.2 Nominal response of Example 1

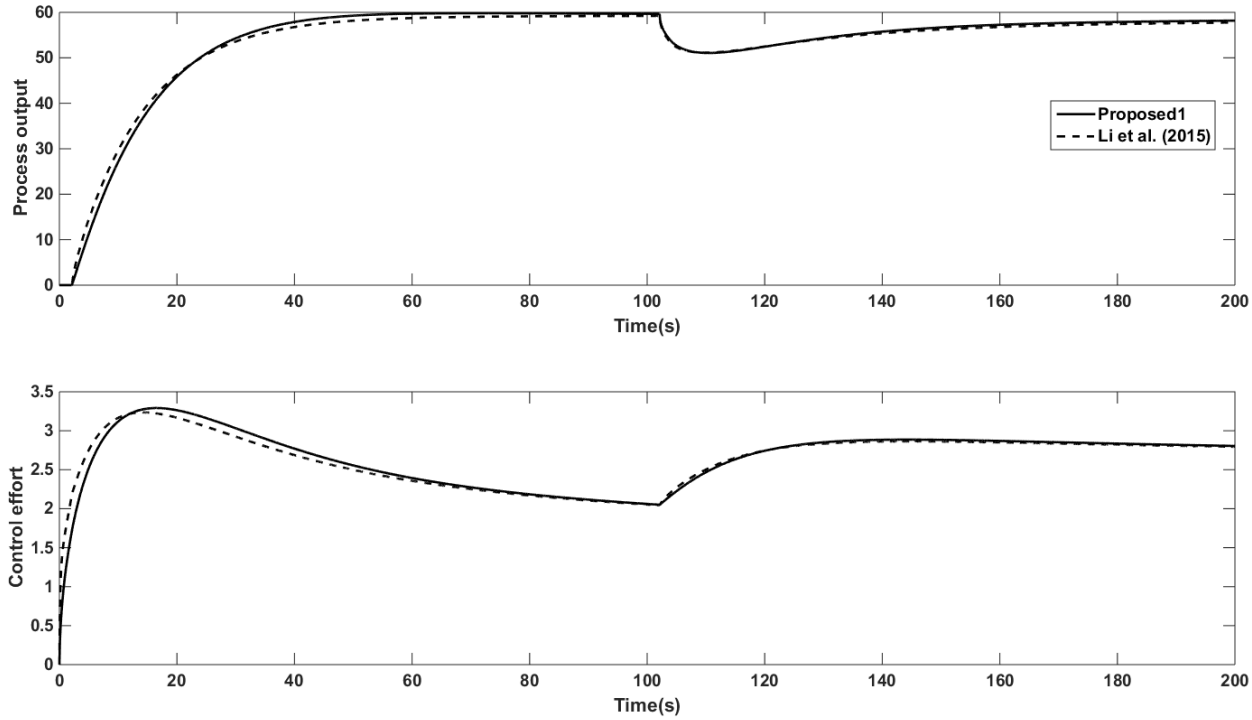

Fig 6.3 Perturbed response of Example 1

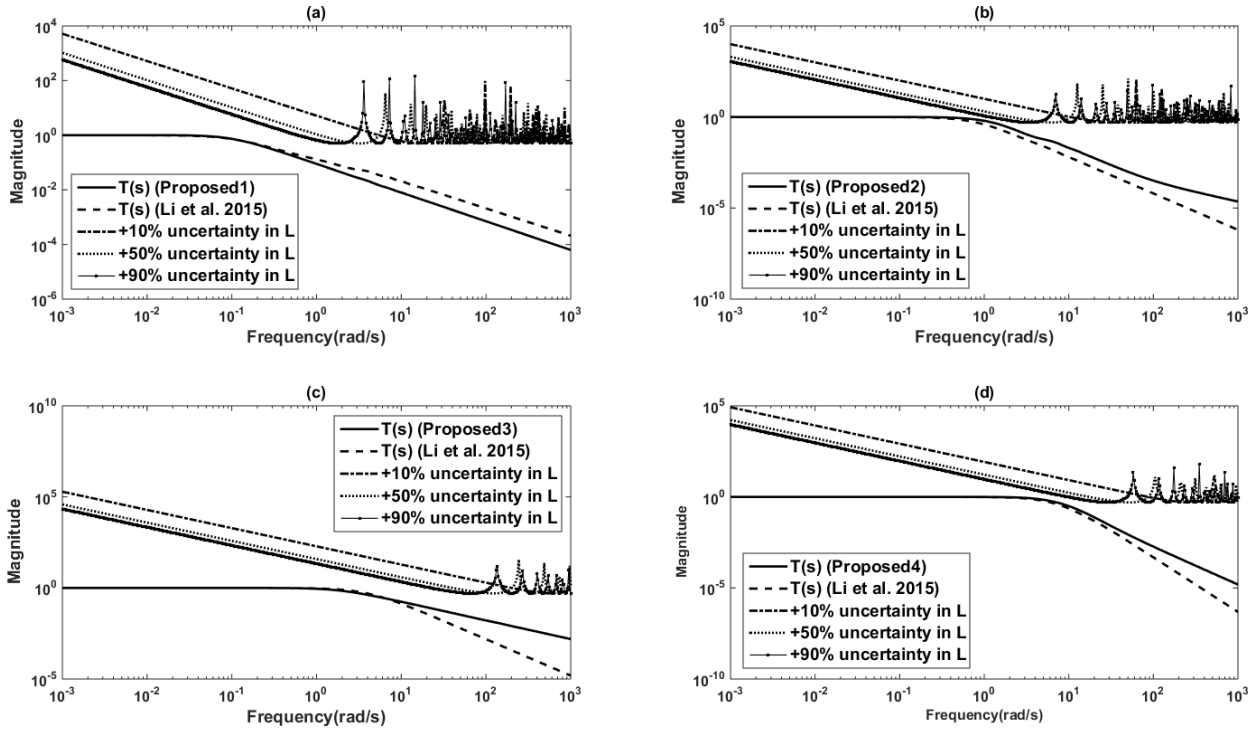

Fig 6.4 Magnitude plot for (a) Example 1 (b) Example 2 (c) Example 3 (d) Example 4

6.1.5.3. Example 2

The example for NIOPTD-I system (Das et al., 2013) with α in the range of 1 to 2 is

$$G_m(s)=\frac{5}{1.5s^{1.5}+1}e^{-s} \tag{6.21}$$

The controller designed according to Li et al. (2015) method is given by

$$C(s)=\left(\frac{0.5s^{1.5}+s^{0.5}}{0.79s^2+2.85s+3.52}\right)\left(0.3+\frac{0.201}{s^{1.5}}\right) \tag{6.22}$$

The frequency used for Oustaloup filter approximation of fractional functions is 0.001-1000rad/s. The Proposed2 method controller settings are listed in Table 6.4. The step response with a disturbance of magnitude -0.05 applied at t=25s is shown in Fig 6.5 and corresponding IAE, ITAE and TV values are given in Table 6.5. The measures for perturbed response and Gaussian noise (variance=0.001) response are listed in Table 6.6 and Table 6.7. It is clear that the Proposed2 method gives improved response for all the input changes and process conditions except for an increase in TV. The Proposed2 and Li et al. (2015) methods obey the stability condition (eq. 6.17) for uncertainty in L which is illustrated with magnitude plot in Fig 6.4.

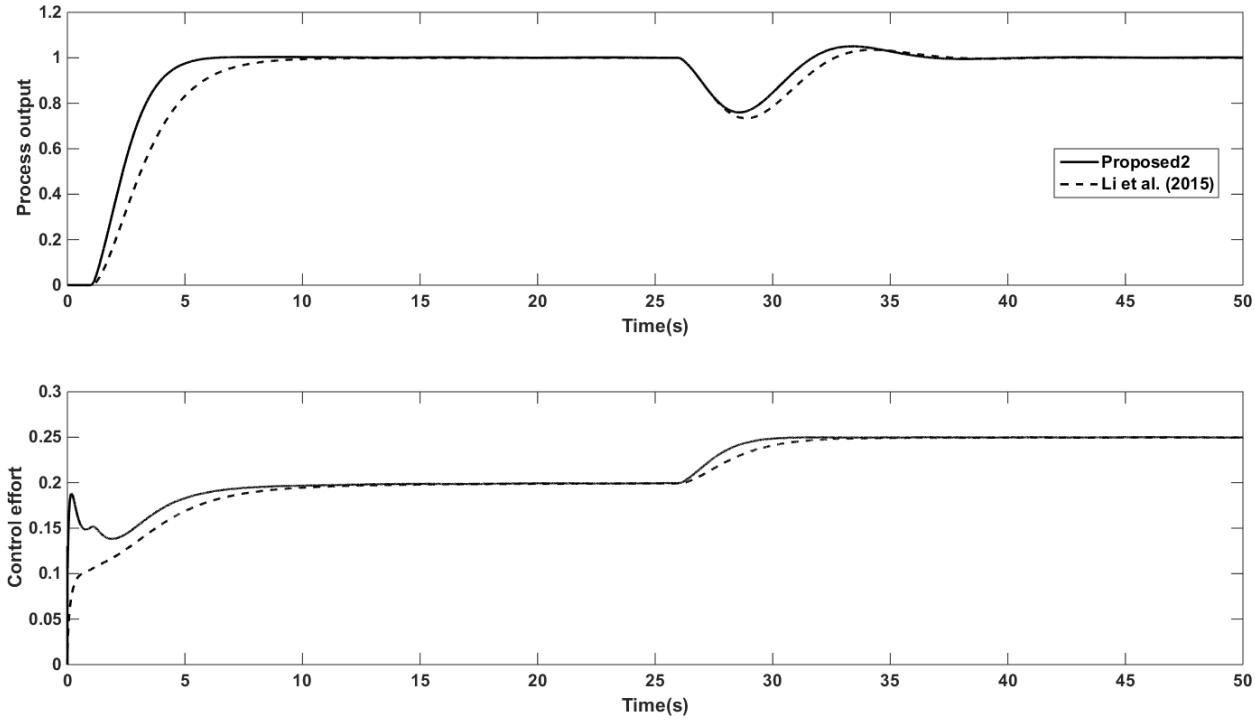

Fig 6.5 Nominal response of Example 2

Table 6.6 Comparison of IAE, ITAE and TV values for perturbations

Examples	Method	Servo response			Regulatory response		
		IAE	ITAE	TV	IAE	ITAE	TV
Example 1	Proposed1	866.1	10480	4.524	361.2	12380	1.0002
	Li et al. (2015)	890.5	13740	4.7928	364.7	13170	1.4437
Example 2	Proposed2	3.184	5.784	0.3817	0.82	2.069	0.1115
	Li et al. (2015)	4.378	12.97	0.2535	0.9372	3.815	0.0596
Example 3	Proposed3	0.718	0.4431	19.5423	0.2776	0.4935	0.4999
	Li et al. (2015)	0.7244	0.4378	4.7374	0.2784	0.4838	0.4968
Example 4	Proposed4	0.5371	0.1067	41.5226	0.201	0.2978	0.5294
	Li et al. (2015)	0.6404	0.2446	24.4893	0.2504	0.4076	0.5098

6.1.5.4. Example 3

The higher order process approximated as NIOPTD-II system (Pan and Das, 2013) is given as follows:

$$G_m(s)=\frac{5.069}{s^{1.9944}+6.0645s^{0.9997}+5.069}e^{-0.0518s} \tag{6.23}$$

The FOPID controller for this system with Li et al. (2015) method is

$$C(s)=\left(\frac{0.0259s+1}{0.0017s^{2.0003}+0.0772s^{1.0003}+0.0582s^{0.0003}}\right)\left(1.1964+\frac{0.9999}{s^{0.9997}}+0.1972s^{0.9957}\right) \quad (6.24)$$

The frequency used for Oustaloup filter approximation is 0.01- 100rad/s. The Proposed3 method controller settings are listed in Table 6.4. The nominal response (for step disturbance of magnitude -0.5 applied at t=5s) is shown in Fig 6.6 and the corresponding measures are listed in Table 6.5. Also, the IAE, ITAE and TV values for system response in presence of perturbations and noise are given in Table 6.6 and Table 6.7. It can be observed that both the methods are performing well while Proposed3 method is showing slight improvement in terms of IAE and ITAE. The robust stability condition is obeyed by both the methods which is illustrated in Fig 6.4.

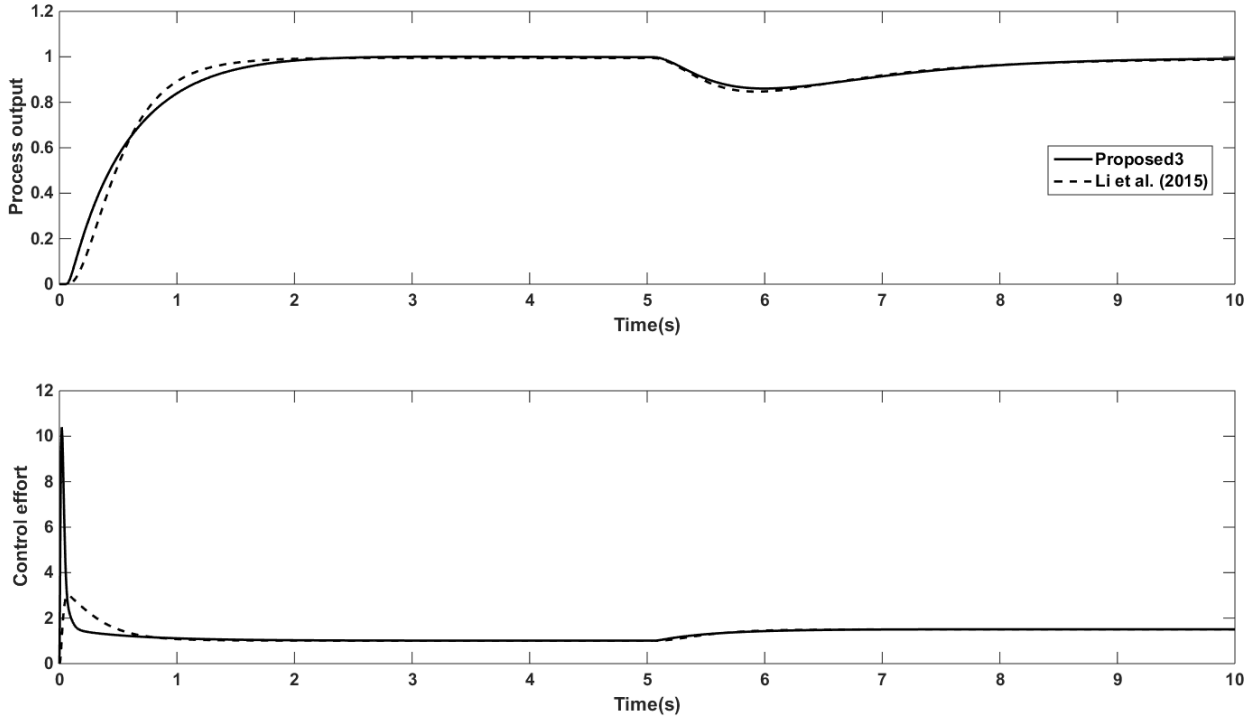

Fig 6.6 Nominal response of Example 3

Table 6.7 Comparison of IAE, ITAE and TV values in presence of output Gaussian noise

Examples	**Method**	**Servo response**			**Regulatory response**		
		IAE	**ITAE**	**TV**	**IAE**	**ITAE**	**TV**
Example 1	Proposed1	244	398.3	5.4628	436.5	12070	5.803
	Li et al. (2015)	245.3	463.3	8.7353	435.6	12990	9.1528
Example 2	Proposed2	3.184	3.091	0.5316	1.436	1.417	0.2929
	Li et al. (2015)	4.019	7.183	0.2699	1.532	2.566	0.1306
Example 3	Proposed3	0.6153	0.615	22.644	0.2767	0.411	3.3611
	Li et al. (2015)	0.615	0.228	5.6143	0.287	0.4039	1.1652
Example 4	Proposed4	0.5332	0.1088	50.158	0.245	0.3379	8.5352
	Li et al. (2015)	0.6164	0.2108	29.530	0.2951	0.4501	5.1956

6.1.5.5. Example 4

This example is taken as an approximation of higher order system (Pan and Das, 2013)

$$G_m(s)=\frac{4.47}{s^{2.47}+5.23s^{1.02}+4.47}e^{-0.12s} \tag{6.25}$$

The values α= 2.47 and β= 1.02 represents case II of NIOPTD-II system. The controller with Li et al. (2015) method is given by eq. (6.26). The Proposed4 controller settings are presented in Table 6.4.

$$C(s)=\left(\frac{0.06s^{1.02}+s^{0.02}}{0.000123s^3+0.005s^2+0.071s+0.5}\right)\left(1.17+\frac{0.9945}{s^{1.02}}+0.2223s^{1.45}\right) \tag{6.26}$$

The frequency used is same as given in Example 3. The step response with a disturbance of magnitude -0.5 applied at t=6s is shown in Fig 6.7. The performance measures are given in Table 6.5-6.7. It is observed that Proposed4 method is superior in performance with low IAE and ITAE but TV is high compared to Li et al. (2015) method. The Proposed4 and Li et al. (2015) methods are robustly stable (Fig 6.5).

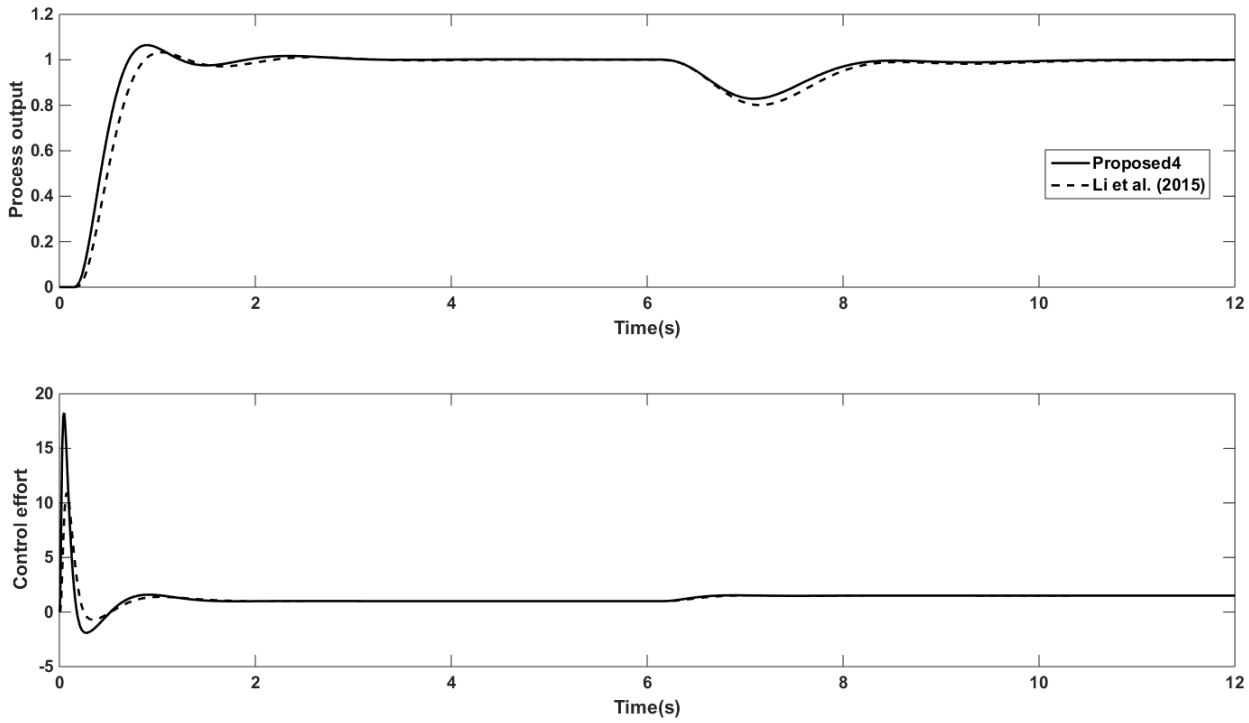

Fig 6.7 Nominal response of Example 4

6.1.5.6. Fragility

The delta 20 fragility index ($RFI_{\Delta 20}$) values are listed in Table 6.8. The observations made from Table 6.8 are: Proposed1 method is nonfragile with respect to Example 1 whereas Li et al. (2015) method is resilient; Proposed2 and Li et al. (2015) methods are fragile in case of Example 2; Proposed3 method is resilient and Li et al. (2015) method is nonfragile for example 3; Proposed4 is fragile and Li et al. (2015) method is nonfragile for Example 4. It is possible to tune nonfragile controllers whereas fragile controllers are difficult to tune. The nonfragile and fragile nature of the controller is caused by variation in any one parameter or more parameters of the controller. Hence, care should be taken while changing those particular parameters so that the closed loop system gives robust response.

Table 6.8 Robustness delta 20 ($RFI_{\Delta 20}$) fragility index for all the examples

Example 1		**Example 2**	
Proposed1	0.1513	Proposed2	3.5165
Li et al. (2015)	0.0035	Li et al. (2015)	0.6874
Example 3		**Example 4**	
Proposed3	0.0027	Proposed4	3.604
Li et al. (2015)	0.1	Li et al. (2015)	0.4697

6.1.6. Conclusions

In this chapter, an improved design of the fractional filter fractional IMC-PID controller is proposed for non-integer order plus time delay systems after identifying the optimum fractional IMC filter based on minimum IAE for a fixed M_s. The proposed method enhances the closed loop performance with additional tuning parameters in the controller design. Improved step response is observed for different input changes on the closed loop system. Improvement is observed with the controller designed using 2/3 order Pade's approximation for time delay. The error values are decreasing with the proposed controller for all the NIOPTD processes but the control effort is increasing with increase in the order of approximation. All the proposed methods give robust and stable performance for parametric uncertainty. The fractional controllers have become fragile for uncertainties in the controller parameters when higher order fractional IMC filter is used during their design. Hence, attention should be needed while changing the fractional orders of the controller and filter.

6.2. Design of fractional filter fractional IMC-PID controller for higher order systems

6.2.1. Introduction

Higher order models describe the process dynamics accurately than lower order models (Isaksson and Graebe, 1999; Malwatkar et al., 2009). However, they complicate the controller design and tuning for quality control. There are several controllers tuning rules for higher order models approximated as FOPTD models. Most of these rules were to tune controller having PID structure which is the widely used till date (Astrom and Hagglund, 1995; Skogestad, 2003). The controller designed for such FOPTD models may not give the satisfactory performance as the dynamics are compromised during the approximation. An alternative to preserve the dynamics while ensuring satisfactory control is to approximate them as NIOPTD models (Pan and Das, 2013). The major advantage of NIOPTD models is that they represent the process behavior compactly than integer order systems (Podlubny, 1999).

Fractional order control for fractional order systems has been in focus since the last two decades (Shah and Agashe, 2016). Several fractional order controller structures have been proposed and the widely accepted one is the FOPID controller (Monje et al., 2008; Luo and Chen 2009, Tavakoli-Kakhki and Haeri, 2011; Padula and Visioli, 2011; Vinopraba et al., 2012; Das et al., 2011; Valerio and da Costa, 2006). The FOPID controller has the ability to enhance the closed loop performance but the tuning is complex as it has more number of tuning parameters than PID controller. Recently, there was a work in the literature where the five FOPID parameters are identified based on the stability regions of closed loop system (Bongulwar and Patre, 2017). Further, the simulation results were shown only for the servo response.

In this chapter, a FFFOPID controller is proposed using IMC. The present work uses a series form of FOPID controller (Hui-fang et al., 2015). The resulting controller has a structure consisting of FOPID term along with fractional filter with only two parameters to be tuned. The tuning parameters are identified such that the IAE and TV are minimum. The selection is proved to be optimum by observing the trends of IAE and TV through an analysis after varying the tuning parameters in the range of +10% and -10%. The simulations have been performed for different inputs and the measures used to assess the system performance are % overshoot (%OS), settling

time (ST), IAE and TVs. Also, the applicability of proposed method for apparent changes in time delay is verified by varying the L/T ratio called as controllability index (Lin et al., 2008). The performance of the proposed method is validated with three different examples.

6.2.2. Design of FFFOPID controller

The structure of the controller used here is

$$C(s)=(\text{fractional filter})K_p\left(\frac{T_i s^{\lambda}+1}{T_i s^{\lambda}}\right)(1+T_d s^{\mu}) \tag{6.27}$$

To design the controller, the higher order system approximated as NIOPTD model is considered and is given by eq. (6.28)

$$\widetilde{G}(s)=\frac{Ke^{-Ls}}{Ts^{\alpha}+1} \tag{6.28}$$

The feedback controller C(s) according IMC design procedure using IMC filter $f(s)=1/(\gamma s^p+1)$ and first Pade's approximation for time delay $e^{-Ls}= (1-0.5Ls)/(1+0.5Ls)$ is

$$C_{proposed}(s)=\left(\frac{1}{0.5\gamma Ls^p+\gamma s^{p-1}+L}\right)\left(\frac{L}{2K}\right)\left(\frac{1+0.5Ls}{0.5Ls}\right)(1+Ts^{\alpha}) \tag{6.29}$$

Comparing equations (6.27) and (6.29), the settings are

$$\left.\begin{aligned} &K_p=\frac{L}{2K};T_i=0.5L;\lambda=1;T_d=T;\mu=\alpha \\ &\text{fractional filter}=\frac{1}{0.5\gamma Ls^p+\gamma s^{p-1}+L} \end{aligned}\right\} \tag{6.30}$$

γ and p are two tuning parameters of the controller.

6.2.2.1. Tuning

The tuning parameters γ and p are chosen in a way that the measures IAE and TV are minimum. The optimum values are identified through the behavior of IAE and TV by varying γ and p in the range of (-10%, +10%). Finally, γ is chosen for the minimum of both IAE and TV and also p.

6.2.3. Robustness analysis

The stability of closed loop system should always be analyzed for process parameter uncertainties because the process model is an approximation of the real plant. The robust stability condition (Morari & Zafiriou 1989) is

$$\|l_m(s)T(s)\|<1; s=j\omega; \forall\omega\in(-\infty,\infty) \quad (6.31)$$

Where $l_m(s)=\frac{G(s)-\tilde{G}(S)}{\tilde{G}(s)}$ is the bound on multiplicative uncertainty and T(s)=C(s)G(s)/1+C(s)G(s) is the complementary sensitivity function. For uncertainty in both L and K, the following condition must be satisfied

$$\|T(j\omega)\|_\infty<\frac{1}{\left(\frac{\Delta K}{K}+1\right)e^{-\Delta L}-1} \quad (6.32)$$

Another constraint to be satisfied for robust control performance is

$$\|T(s)l_m(s)+(1-T(s))w_m(s)\|<1 \quad (6.33)$$

Where 1-T(s) is the sensitivity function and $w_m(s)$ is the uncertainty bound on sensitivity function.

6.2.4. Simulation study

Three higher order systems approximated as NIOPTD models are simulated in MATLAB and the system performance is compared with Bongulwar and Patre (2017) method (hereafter addressed as Patre (2017) method). The effectiveness of the proposed method is verified with the performance measures %OS, ST, IAE and TV which are defined in Table 6.9. Settling time is defined as the time taken for the response to settle within 2% to 5% of its final value.

Table 6.9 Expressions for %OS, IAE and TV

%OS	IAE	TV
$\frac{y_{peak}-y_{ss}}{y_{ss}}\times 100$	$\int_0^\infty \|e(t)\|dt$	$\sum_{i=0}^{\infty}\|u_{i+1}-u_i\|$

The closed loop system's unit step response is observed with step change in disturbance of magnitude 0.5 applied at a later time. Also, the step response is observed for perturbations of +10% in L and K and for measurement noise with a variance of 0.0001. The system robustness for uncertainty is illustrated in the following sections through stability analysis. The frequency used for Oustaloup approximation of fractional order is (0.01,100) rad/s. In addition, the trend of closed loop behavior is interpreted for variation in controllability index i.e., L/T ratio in the range of 0.1 to 2. This analysis demonstrates the difficulty in control for large changes in time delay.

6.2.4.1. Example 1

Consider the higher order system (Shen 2002) and its equivalent NIOPTD (Patre 2017) model

$$G_1(s)=\frac{1}{(s+1)^4}=\frac{0.99149}{2.8015s^{1.0759}+1}e^{-1.6745s} \quad (6.34)$$

The proposed and Patre (2017) controllers are:

$$C_{proposed}(s)=\left(\frac{1}{0.7535s^{1.01}+0.9s^{0.01}+1.6745}\right)(0.99149)\left(\frac{0.8372s+1}{0.8372s}\right)(1+2.8015s^{1.0759}) \quad (6.35)$$

$$C_{old}(s)=1.5129+\frac{0.3432}{s^{1.1}}+0.1733s^{1.05} \quad (6.36)$$

The optimum values of γ and p for the proposed controller are identified as 0.9 and 1.01 (Fig 6.8). The performance measures for set point tracking are given in Table 6.10. The proposed method is superior in performance compared to Patre (2017) method with lower values of %OS, ST, IAE and TV.

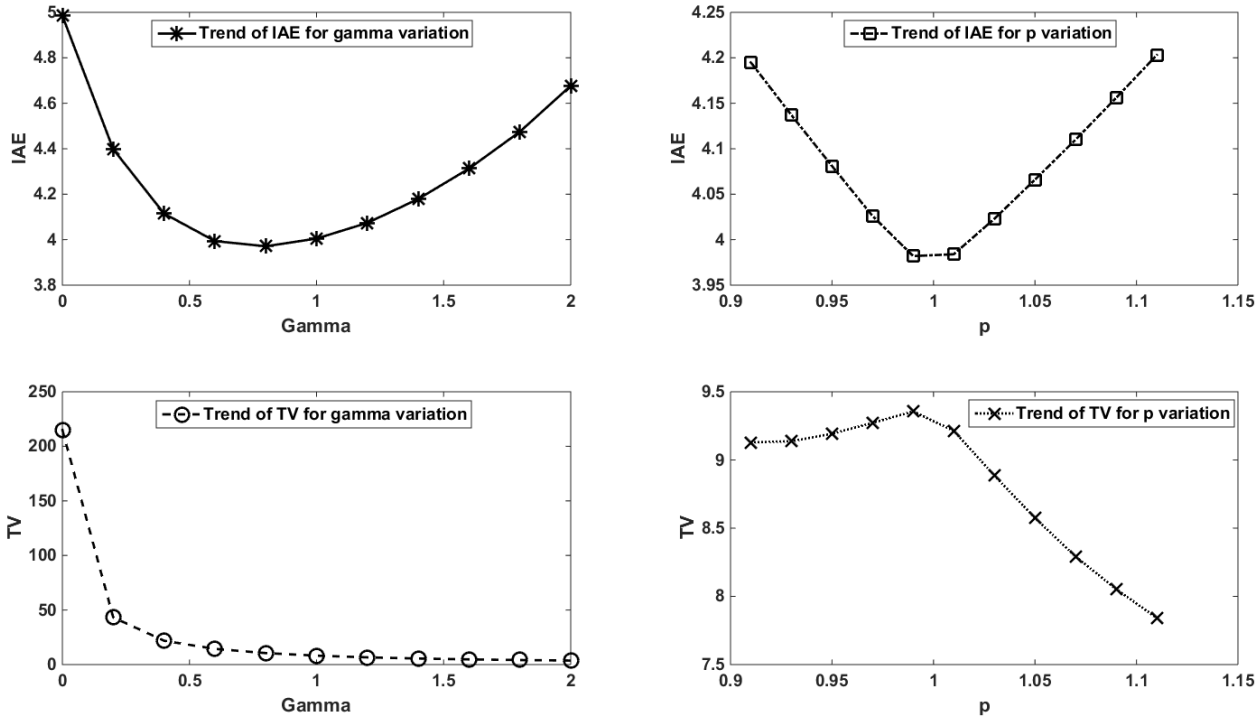

Fig 6.8 Identification of optimum γ and p for example1

Table 6.10 Servo performance comparison for the three different systems

System	Method	%OS	ST	IAE	TV
$G_1(s)$	Proposed	18.2	8.7	2.87	8.45
	Patre (2017)	22.3	15	3.57	18.7
$G_2(s)$	Proposed	2.4	1.54	0.78	3.86
	Patre (2017)	5.02	2.97	0.83	4.75
$G_3(s)$	Proposed	21.2	0.94	0.42	12.74
	Patre (2017)	40.7	1.95	0.53	12.35

The servo response for a disturbance applied at t=30s is illustrated in Fig 6.9. Betterment is observed even with disturbance with lower values of performance measures which is clear from Table 6.11. It is evident from Fig 6.9 that a satisfactory performance is observed in terms of disturbance rejection. Fig 6.10 shows the step response for perturbed model and response for output white noise is illustrated in Fig 6.11. It is observed that there is enhanced performance (Table 6.11) for both the cases with proposed method than the Patre (2017) method. Also, there is significantly less control effort with the proposed method for all the possible input changes.

The magnitude plot is shown in Fig 6.12 for +10% uncertainty in K; +10% and +50% uncertainty in L. Robust stability condition (eq. 6.32) is violated by both the complementary sensitivity functions for +50% uncertainty in L. The proposed method violates the condition a bit earlier than the old method. Fig 6.13 and Fig 6.14 shows the trends of IAE and TV for servo and regulatory response with increasing L/T ratio. It is evident that increasing trends are observed with Patre (2017) method compared to the proposed method. Hence, the proposed method can be considered for enhanced closed loop performance of processes with large changes in time delay.

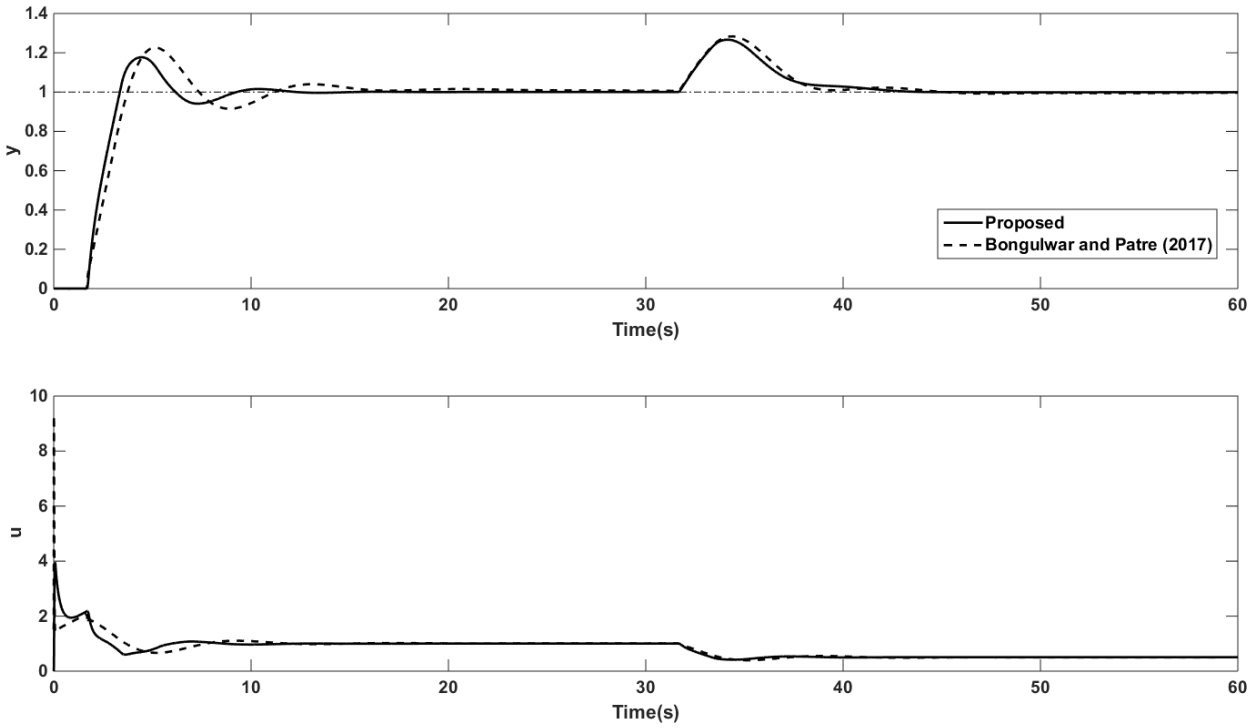

Fig 6.9 Closed loop response of $G_1(s)$ for step input

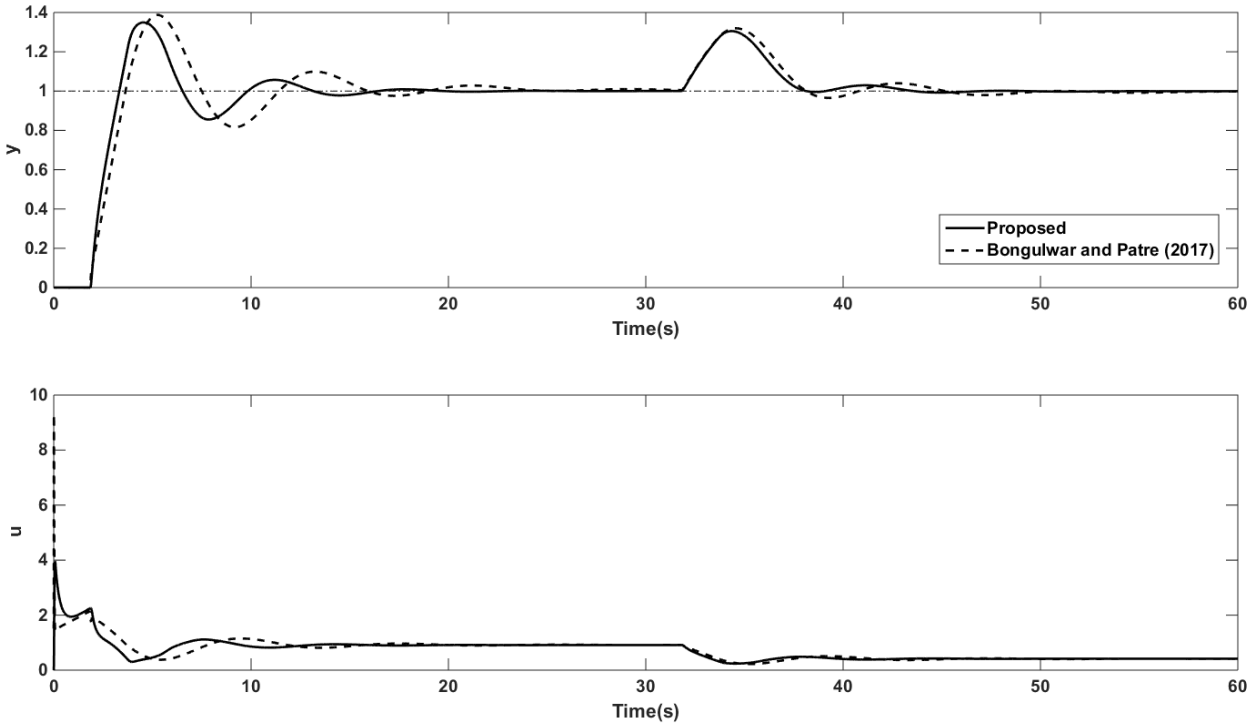

Fig 6.10 Closed loop step response of $G_1(s)$ for perturbations

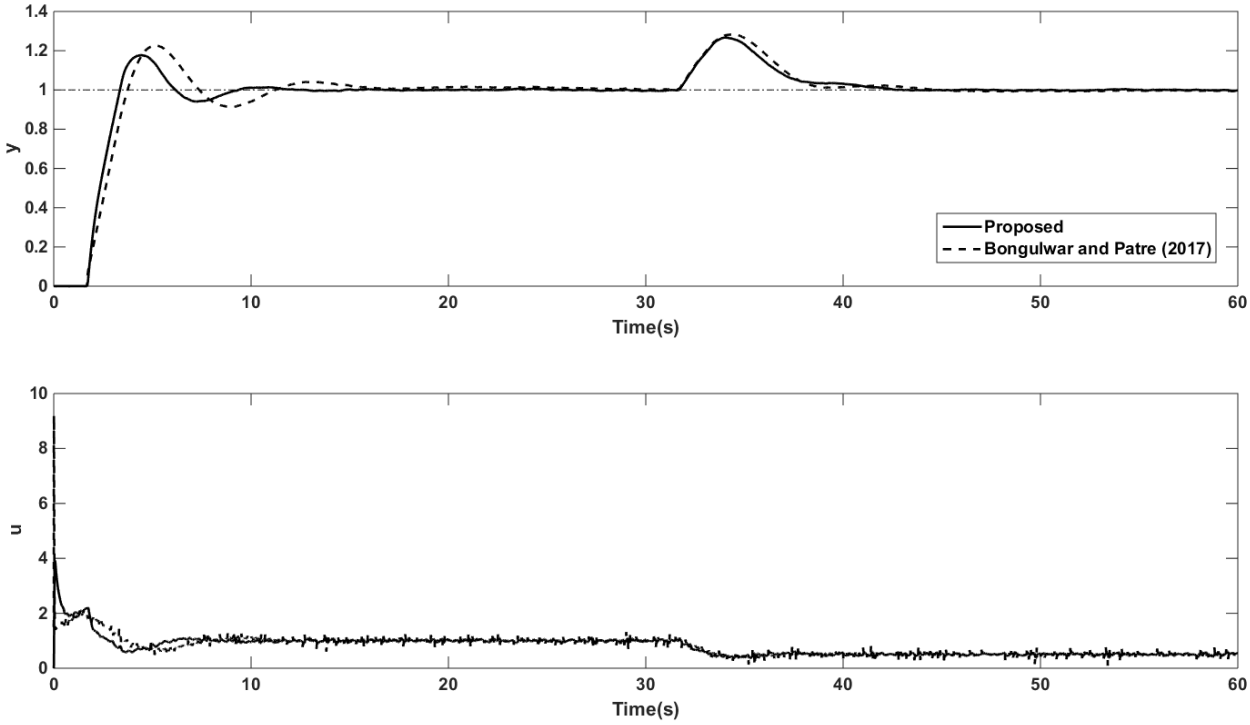

Fig 6.11 Step response in presence of measurement noise

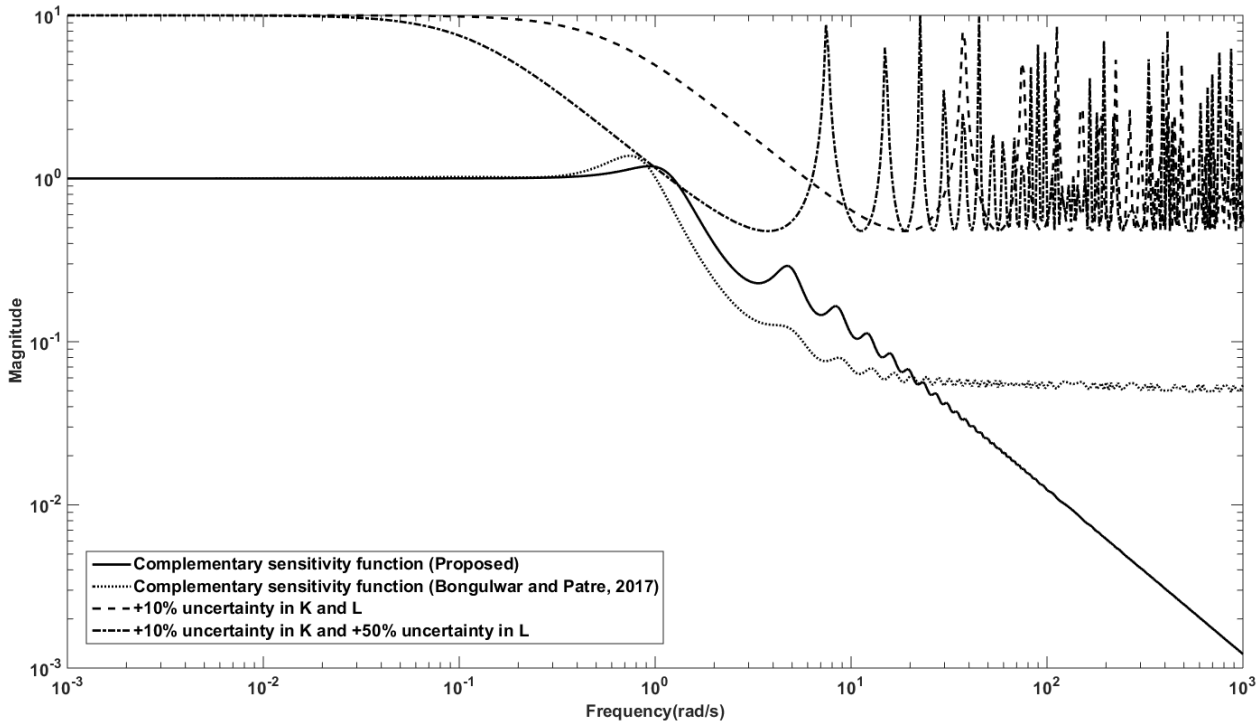

Fig 6.12 Magnitude plot for example 1

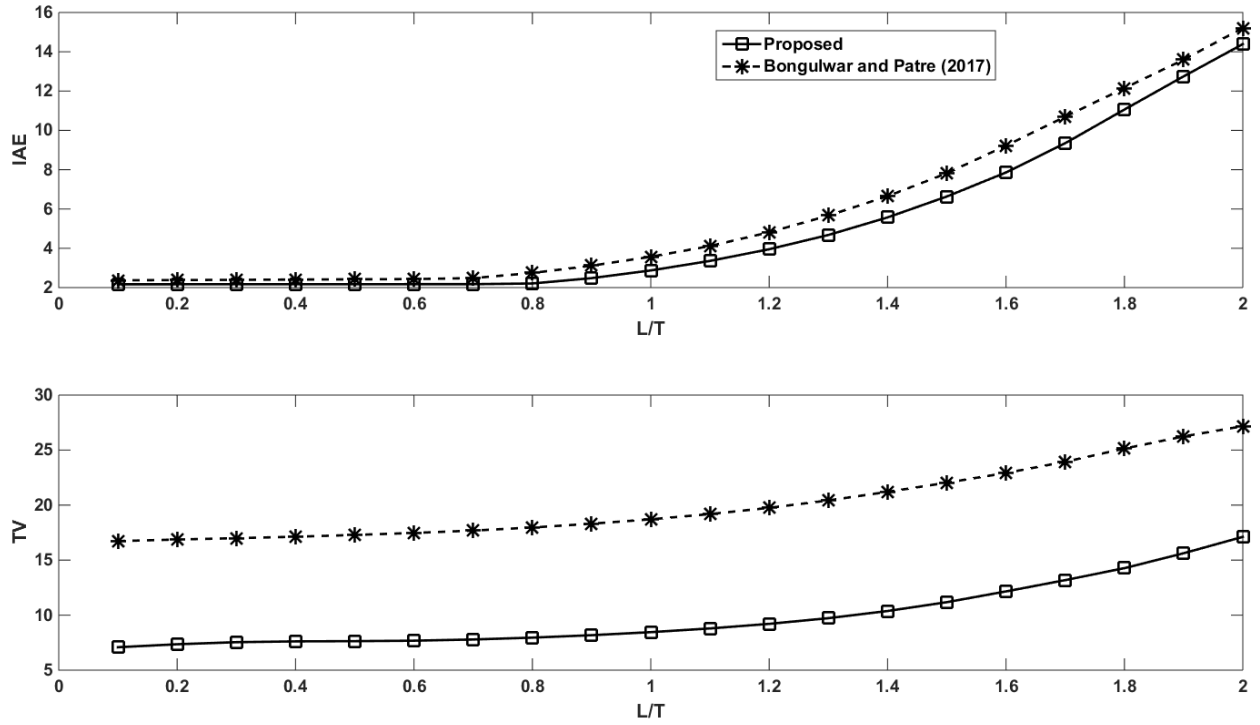

Fig 6.13 L/T ratio versus IAE, TV for step change in set point

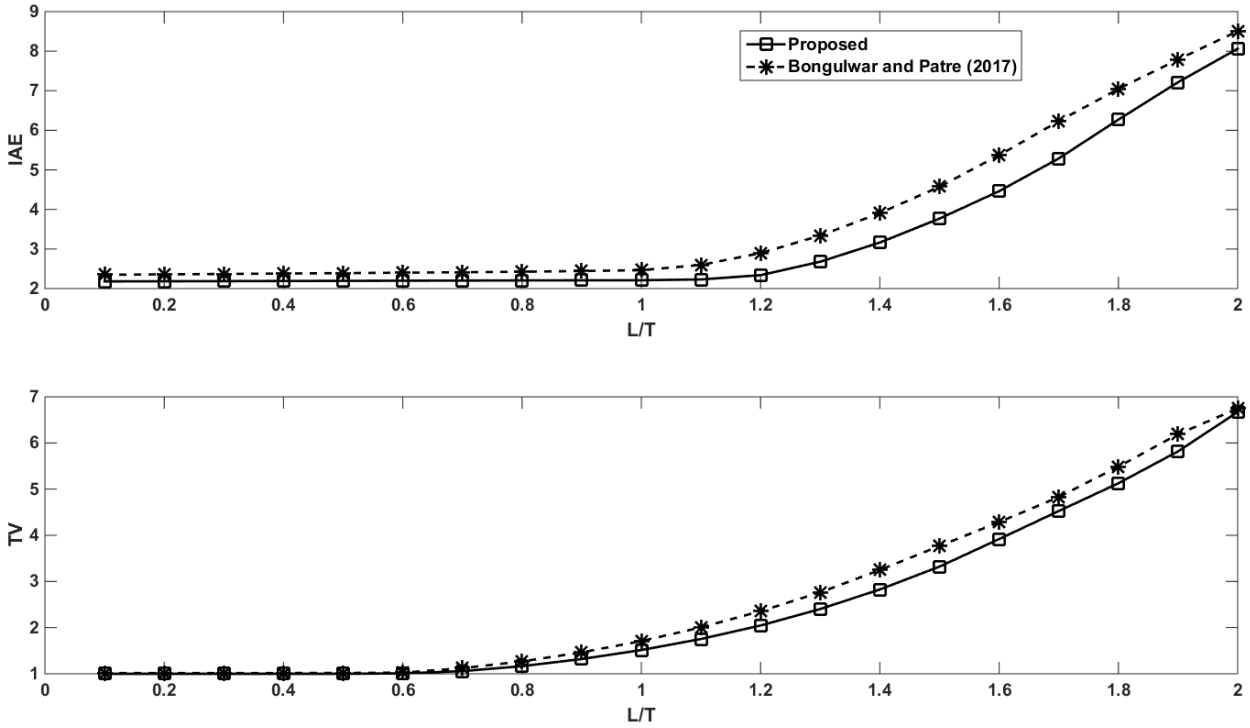

Fig 6.14 L/T ratio versus IAE, TV for step change in disturbance

Table 6.11 Comparison of IAE and TV for the three examples

System	Method	Perfect case		Perturbed case		Noise case	
		IAE	TV	IAE	TV	IAE	TV
$G_1(s)$	Proposed	3.984	9.2133	4.837	10.6533	4.281	38.7359
	Patre (2017)	4.907	19.567	5.988	21.1318	5.02	137.5908
$G_2(s)$	Proposed	1.176	4.393	1.263	4.992	1.207	7.2042
	Patre (2017)	1.243	5.3571	1.353	6.1191	1.248	10.4974
$G_3(s)$	Proposed	0.5663	13.5002	0.6612	16.185	0.6131	20.1658
	Patre (2017)	0.6224	13.506	0.8196	20.2817	0.6767	20.6138

6.2.4.2. Example 2

The second example (Chen et al., 2008; Patre 2017) considered for performance comparison is

$$G_2(s)=\frac{9}{(s+1)(s^2+2s+9)}=\frac{1.0003}{0.8864s^{1.0212}+1}e^{-0.4274s} \tag{6.37}$$

The proposed controller and the controller with Patre (2017) method are:

$$C_{proposed}(s)=\left(\frac{1}{0.07479s^{1.01}+0.35s^{0.01}+0.4274}\right)(0.2136)\left(\frac{0.2137s+1}{0.2137s}\right)(1+0.8864s^{1.0212}) \tag{6.38}$$

$$C_{old}(s)=1.4996+\frac{1.2203}{s^{1.05}}+0.0409s^{1.05} \tag{6.39}$$

The optimum values of γ and p are identified as 0.35 and 1.01. The closed loop system gives good servo response with the proposed method. This is true with the lower values of %OS, ST, IAE and TV given in Table 6.10. The unit step response with disturbance applied at t=6s is shown in Fig 6.15 and the corresponding performance measures are given in Table 6.11. The proposed method is giving better servo response which is evident with lower values of performance measures while the regulatory performance is almost same for both the controllers. The system response for perturbations is presented in Fig 6.16. Fig 6.17 presents the closed loop response for white noise in the output. The proposed method continue to give the superior performance compared to Patre (2017) method which is clear with the lower values of IAE and TV (Table 6.11).

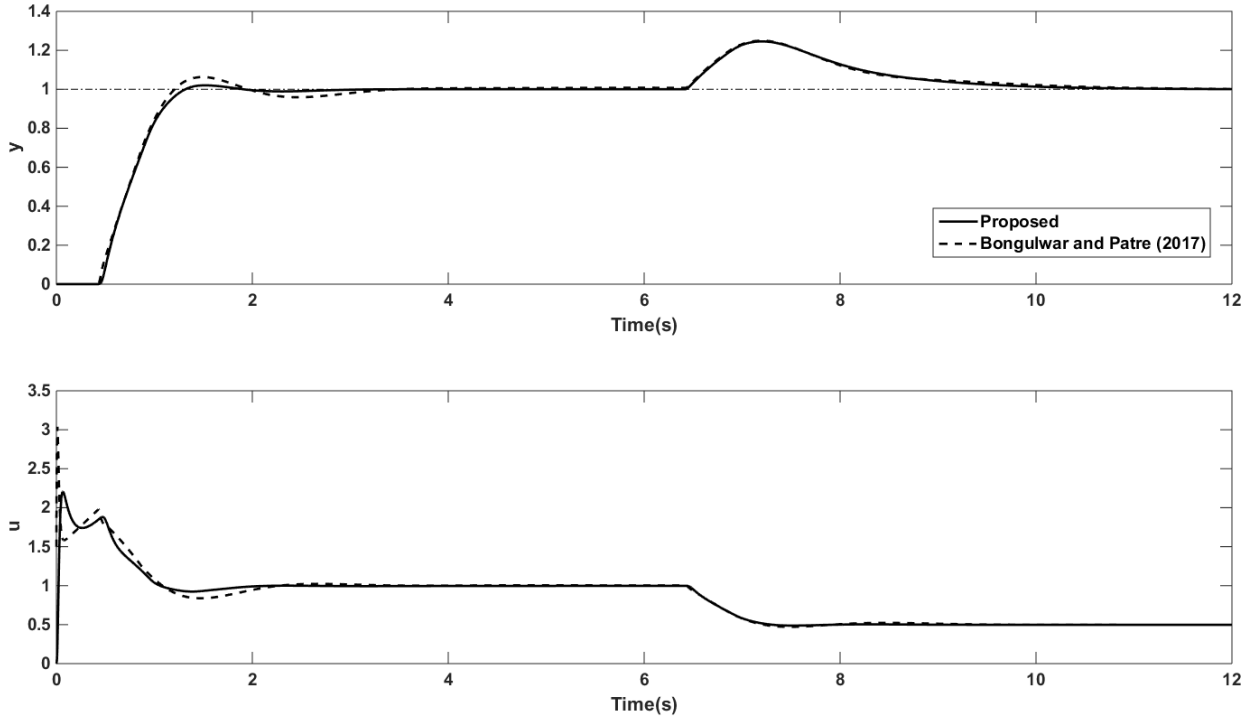

Fig 6.15 Closed loop response of $G_2(s)$ for step input

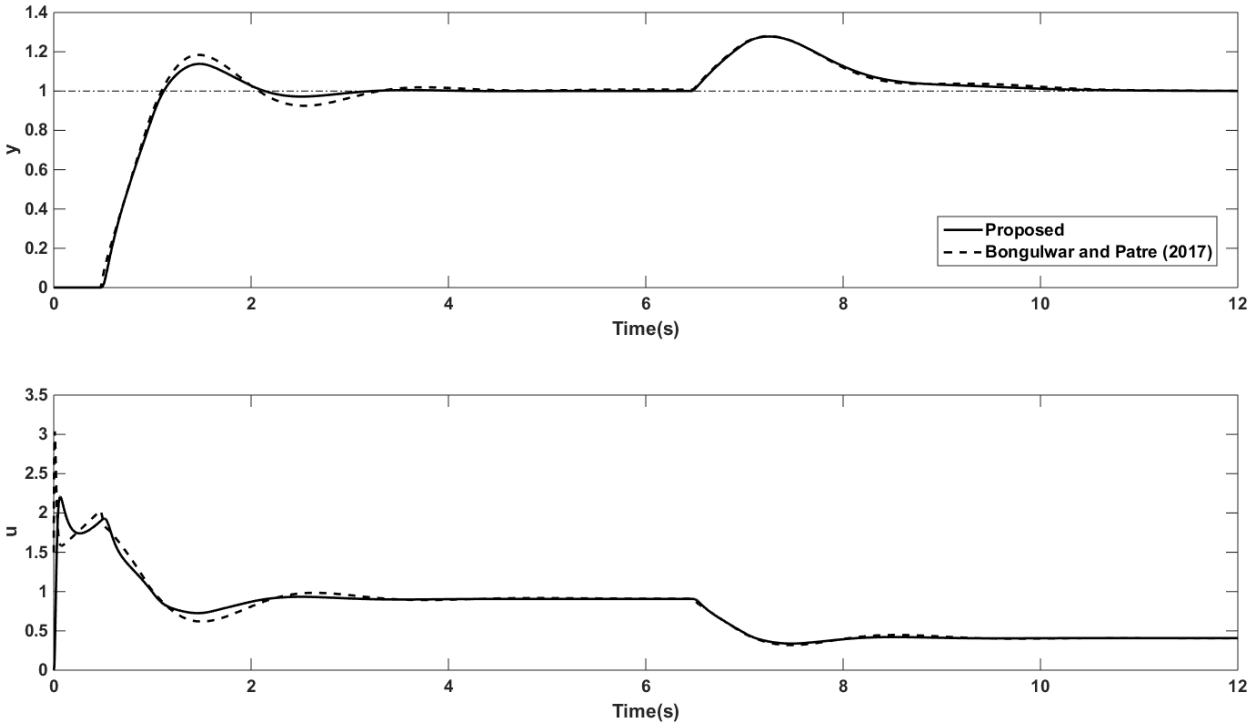

Fig 6.16 Closed loop step response of $G_2(s)$ for perturbations

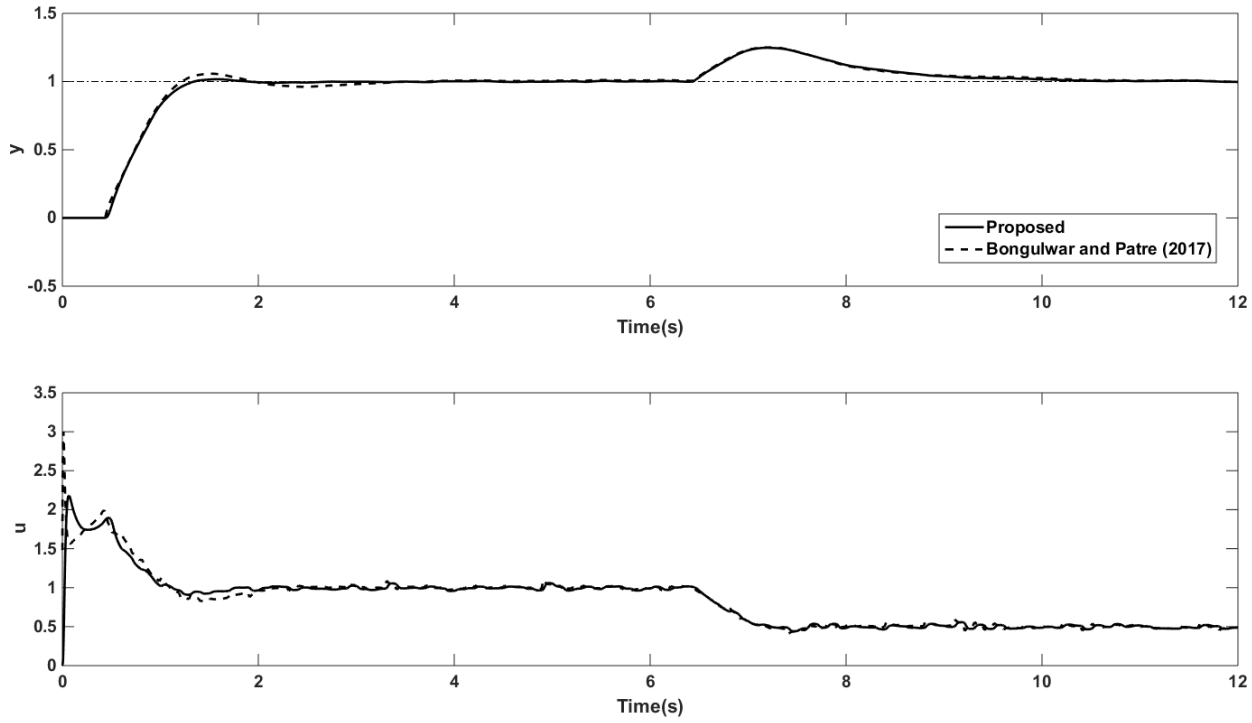

Fig 6.17 Step response in presence of measurement noise

The closed loop robust stability for uncertainties in K and L is illustrated through magnitude plot in Fig 6.18. The closed loop system gives robust performance up to +100% uncertainty in time delay and +10% uncertainty in gain with the proposed controller whereas the stability condition fails for +90% uncertainty in time delay with the Patre (2017) method. Fig 6.19 and Fig 6.20 shows the trends of IAE and TV for servo and regulatory response with increase in L/T ratio. The proposed method is showing less control effort for servo and regulatory response for the entire variation of L/T ratio. The trend followed by IAE for set point tracking is almost same up to L/T ratio of 1 for both the methods, after that it starts increasing with the old method. In case of disturbance rejection the IAE values are lower up to L/T ratio of 1.3 with the old method and then it had increased. Hence, the proposed method is a good choice to have a better control compared to the old method (Patre 2017) for increasing L/T ratio.

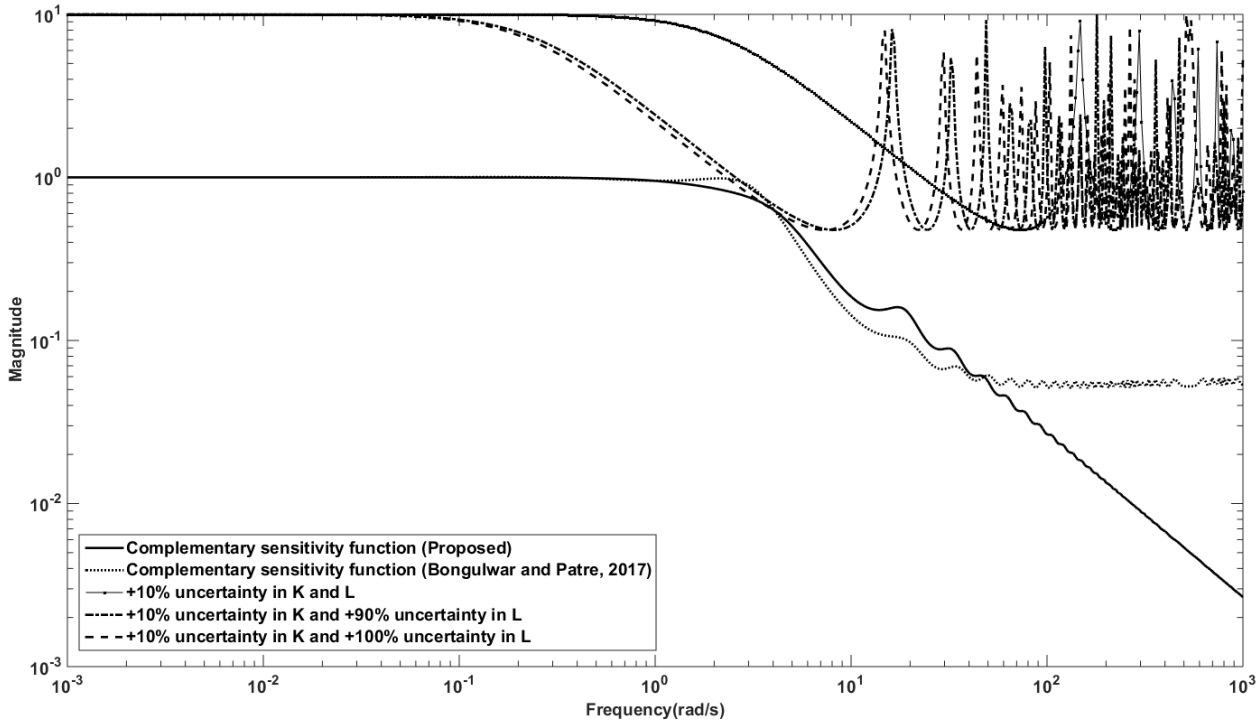

Fig 6.18 Magnitude plot for example 2

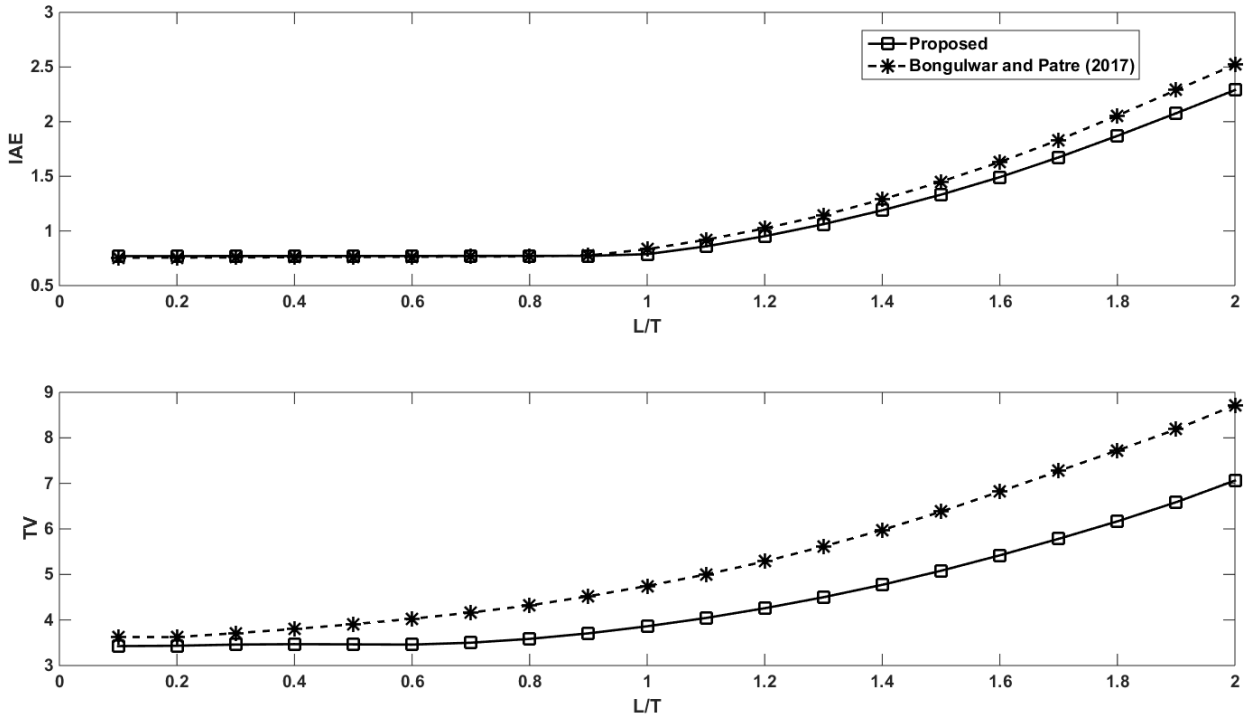

Fig 6.19 L/T ratio versus IAE, TV for step change in set point

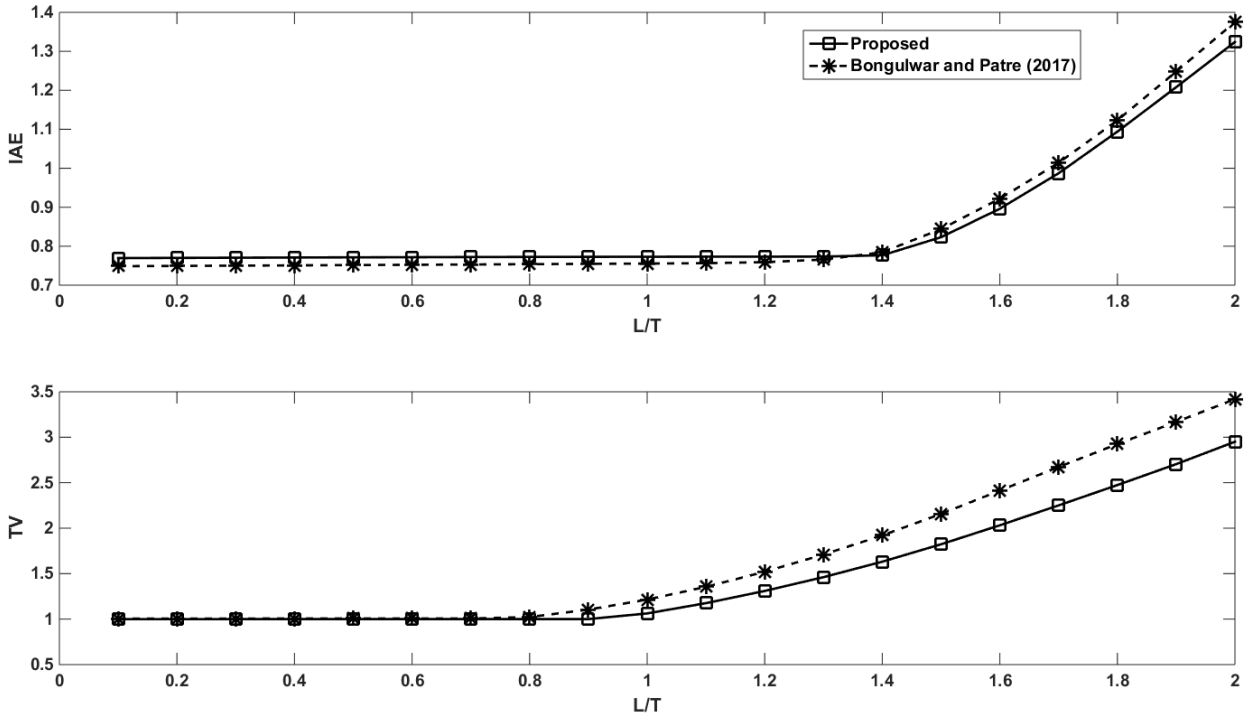

Fig 6.20 L/T ratio versus IAE, TV for step change in disturbance

6.2.4.3. Example 3

The higher order system studied in Panagopoulos et al. (2002) is considered as the third example

$$G_3(s)=\frac{1}{(s+1)(0.2s+1)(0.04s+1)(0.008s+1)}=\frac{0.99932}{1.0842s^{1.0132}+1}e^{-0.1922s} \quad (6.40)$$

The proposed and old (Patre 2017) controllers are given as follows:

$$C_{proposed}(s)=\left(\frac{1}{0.0096s^{1.1}+0.1s^{0.1}+0.1922}\right)(0.0961)\left(\frac{0.0961s+1}{0.0961s}\right)(1+1.0842s^{1.0132}) \quad (6.41)$$

$$C_{old}(s)=5.0034+\frac{6.4}{s^{1.1}}+0.0163s^{1.1} \quad (6.42)$$

The values of γ and p for the proposed method are 0.1 and 1.1. The performance measures shown in Table 6.10 for servo response tells that the %OS, ST and IAE values are lower with the proposed method but the TV value is slightly higher compared to old (Patre 2017) method. Similarly, the step response for a change in disturbance applied at t=5s is shown in Fig 6.21. The closed loop step response for process parameter variations and for output noise is illustrated in Fig 6.22 and Fig 6.23. The corresponding performance measures for all the above cases are presented in Table 6.11. It is evident from all these Figs that the proposed method is giving superior servo performance but a bit slow in rejecting the disturbance compared to the old method.

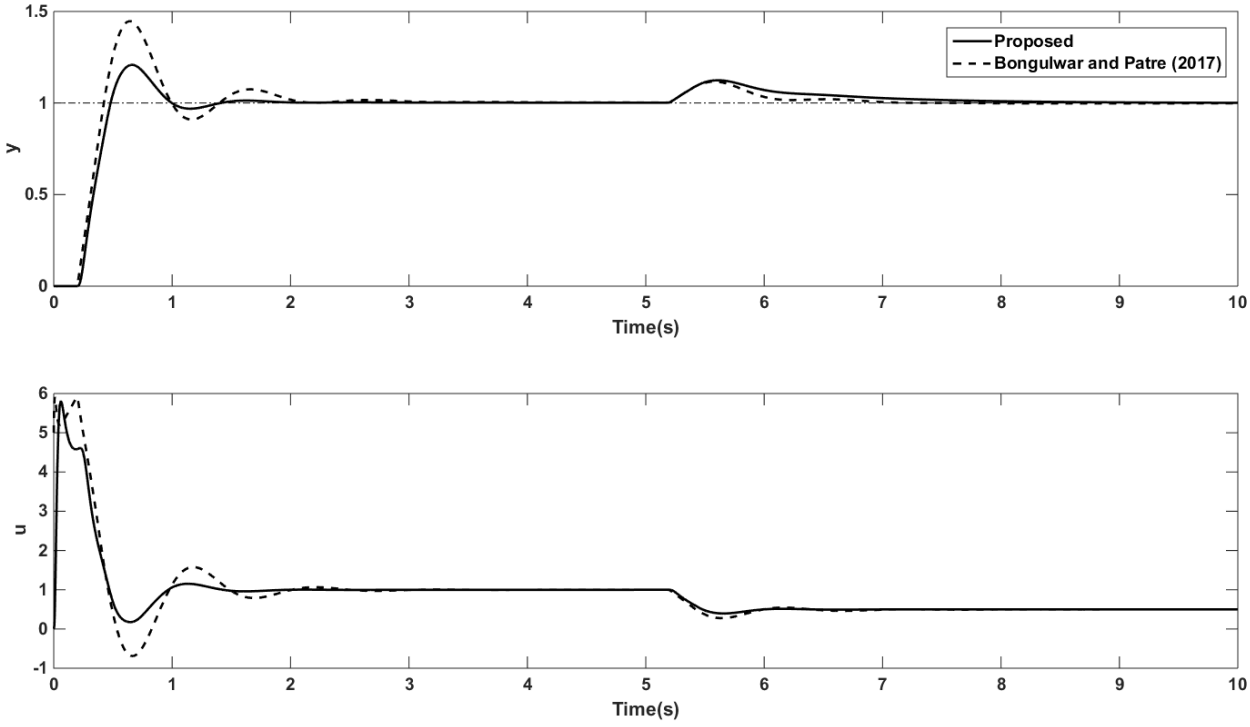

Fig 6.21 Closed loop response of $G_3(s)$ for step input

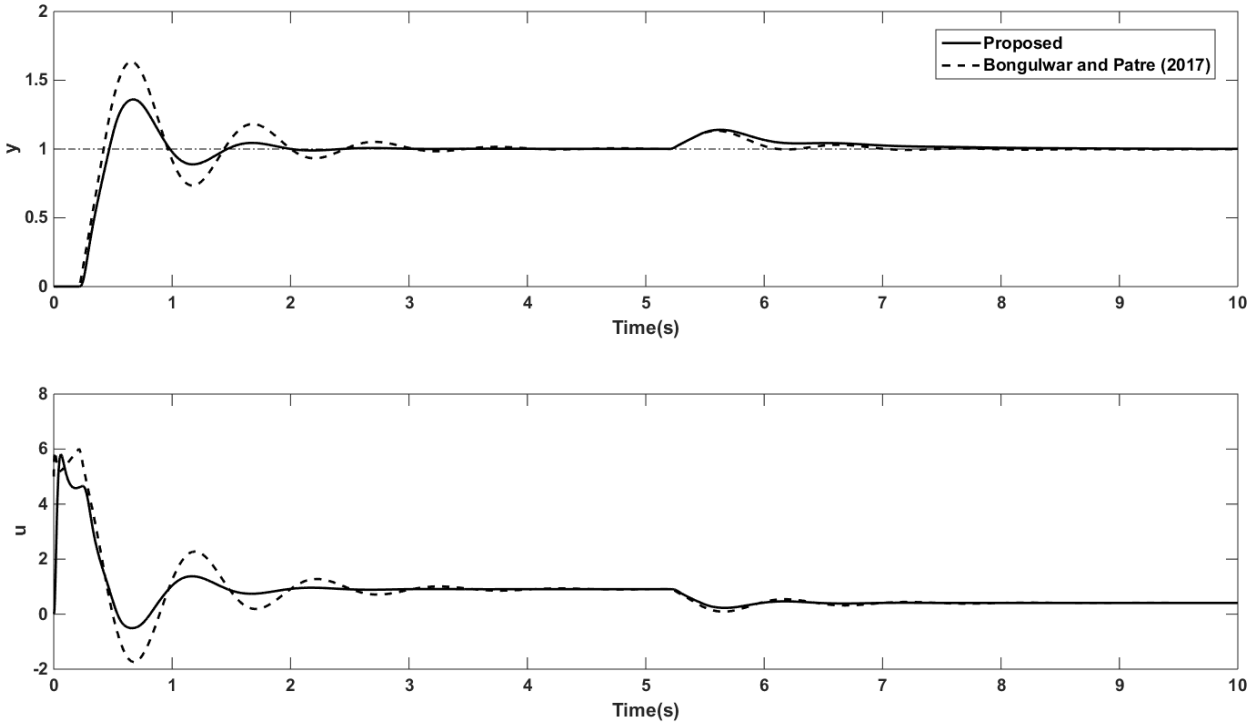

Fig 6.22 Closed loop step response of $G_3(s)$ for perturbations

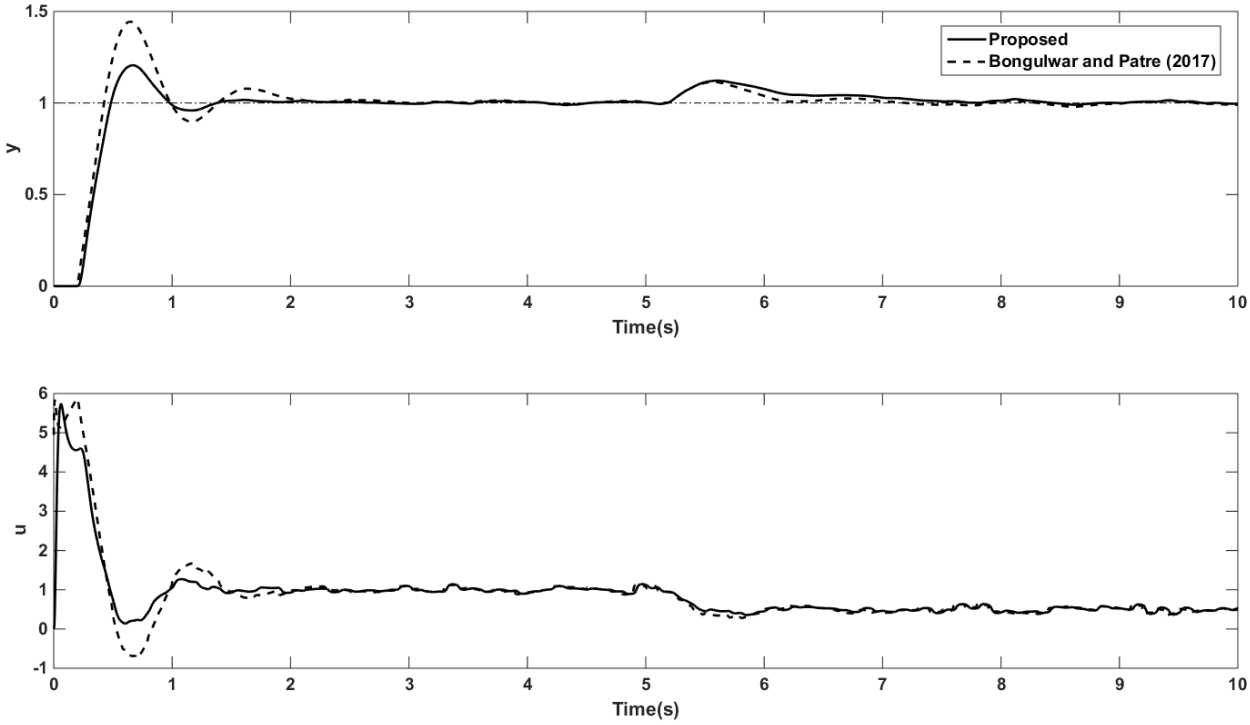

Fig 6.23 Step response in presence of measurement noise

The proposed method gives robust performance up to an uncertainty of +70% in L and +10% in K while the Patre (2017) method fails for less than +50% uncertainty in L (Fig 6.24).

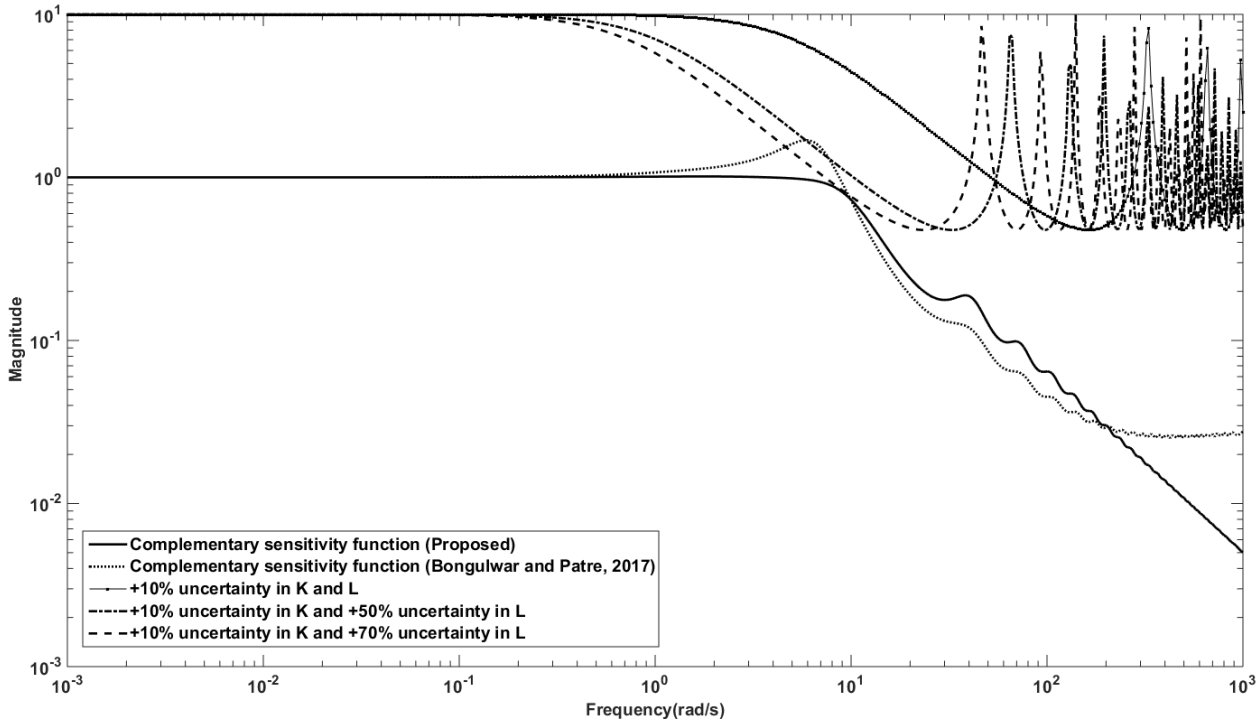

Fig 6.24 Magnitude plot for example 3

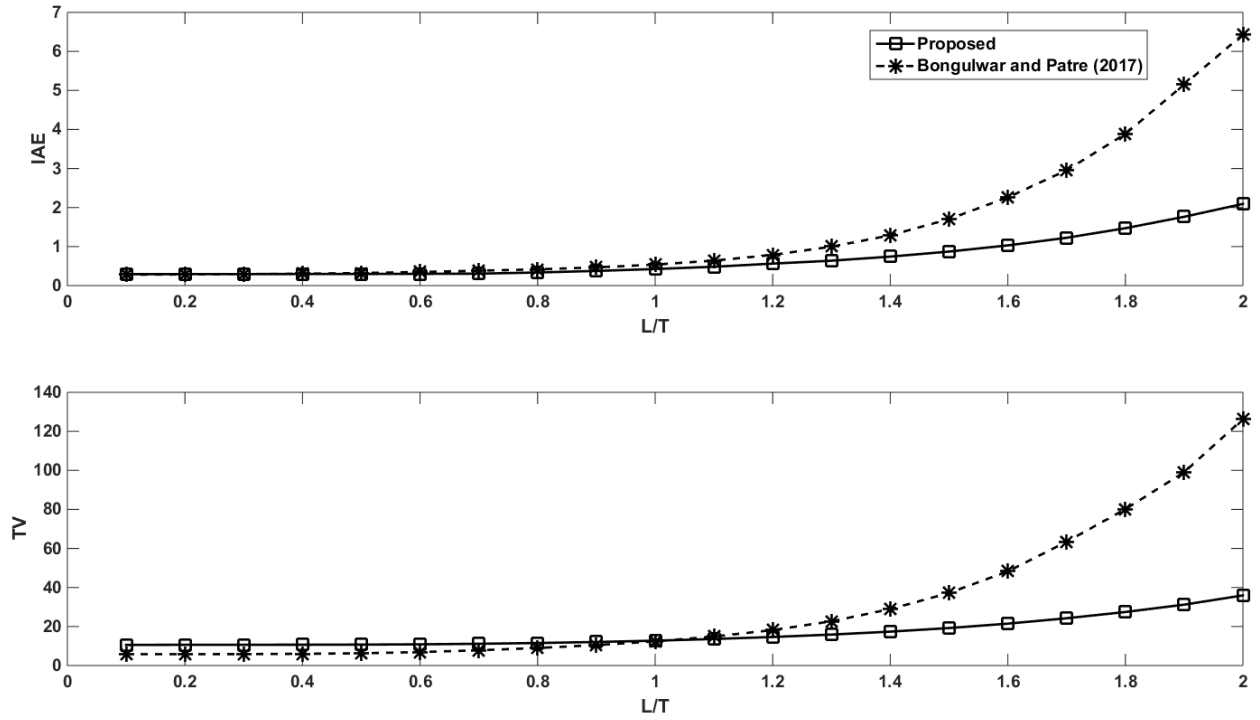

Fig 6.25 L/T ratio versus IAE, TV for step change in set point

Fig 6.25 and Fig 6.26 show the performance for variation of L/T ratio. For servo response, the variation of IAE is low with the proposed method while the control effort is slightly high up to L/T=0.9 and then it increases drastically with the old method. In case of regulatory control, the IAE values are higher with the proposed method and the variation of TV is low. Hence, there is a tradeoff between IAE and TV for increasing L/T and the proposed method is recommended for servo response while it can be used for disturbance rejection at higher values of L/T.

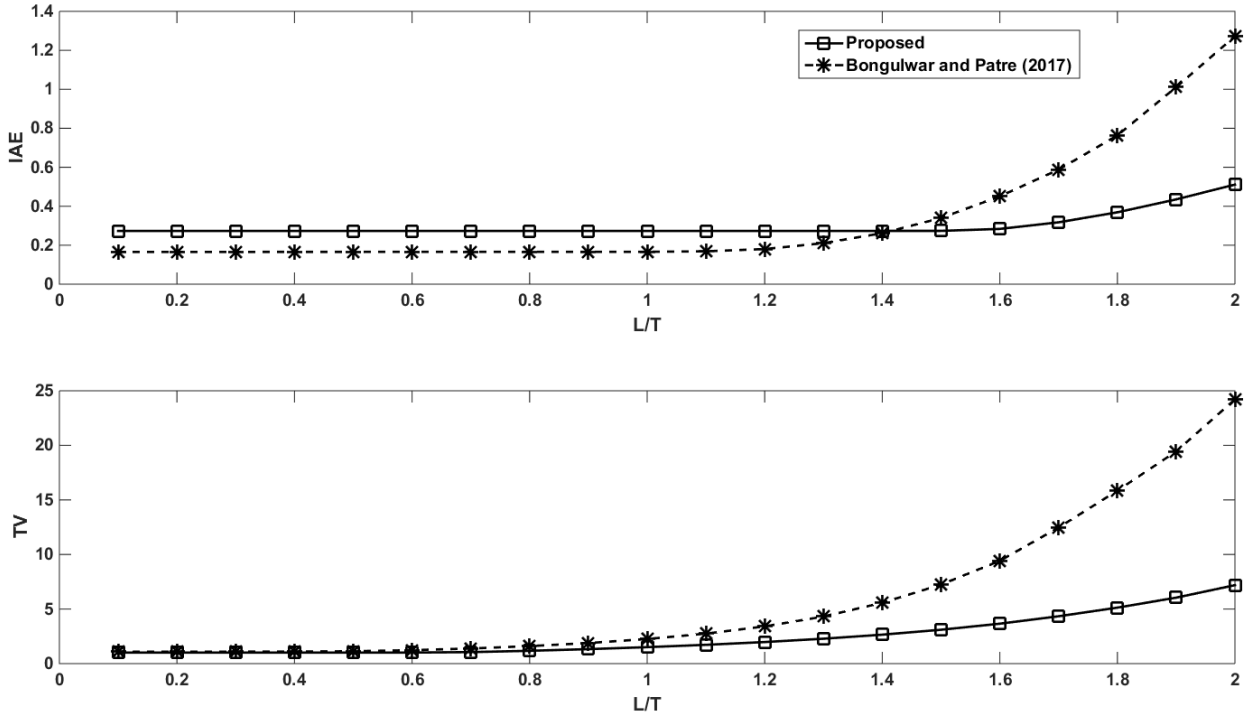

Fig 6.26 L/T ratio versus IAE, TV for step change in disturbance

6.2.5. Conclusions

In this chapter, a FFFOPID controller is proposed for higher order systems approximated as NIOPTD models using IMC method. Analytical method is followed for identifying the tuning parameters by minimizing IAE and TV. Enhanced closed loop performance is observed with the proposed method for changes in set point and disturbance. Especially, the proposed method is effective in terms of less control effort. The closed loop system is robust with proposed method for high uncertainty in process parameters. Also, the proposed method assures better control for large changes in time delay which is proved through the variation of L/T ratio.

6.3. Fragility of FFFOPID Controller for higher order processes approximated as NIOPTD systems

6.3.1. Introduction

The controller for a feedback system should be designed to provide desired closed loop performance to input changes and robust performance to perturbations in the process parameters. However, another prominent topic to be considered is the controller fragility to variations in the controller parameters. It has been found in literature (Keel and Bhattacharyya, 1997) that the fragility analysis carried out for controllers designed using H_2, H_∞ and l_2 norms provide optimal and robust performance but highly fragile controller for minor changes in the controller parameters. The fragile nature of the controller would make the system unstable. There are several works on the design of nonfragile controllers (Ho M-T, 2000) and an index to estimate the fragility (Alfaro, 2007) of the controllers.

The main reason to estimate the fragility of the controller is its fine tuning for changes in the controller parameters. This fragility is further addressed in the context of not only the robustness but also the closed loop performance to produce robust and optimal closed loop system (Alfaro et al., 2009; Alfaro and Vilanova, 2012; Padula and Visioli, 2016).

FOPID controller design has been in focus from the past few years due to its flexibility in tuning with additional tuning parameters (Podlubny, 1999; Valerio and Sada Costa, 2006; Monje et al., 2008; Padula and Visioli, 2011). Further, such controllers were designed for integer and noninteger order time delay systems (Bettayeb and Mansouri, 2014; Hui-fang et al., 2015). The current work aims at the fragility analysis of FFFOPID controller in series form designed for higher order systems approximated as NIOPTD systems (section 6.2). The reason for using NIOPTD systems (Pan and Das, 2013) is that they represent the system dynamics in a better way than the integer order systems (Valerio and Sada Costa, 2006). The main reason for investigating the fragility of FFFOPID controller is to understand which parameter change is making the system fragile. Hence, the fragility analysis is carried out for changes in the individual parameter of the controller apart from all parameter changes at a time.

6.3.2. Controller fragility analysis

This section briefly describes the fragility indices proposed based on the works in the literature (Alfaro, 2007; Alfaro et al., 2009; Alfaro and Vilanova, 2012). The expressions for FFFOPID controller structure, NIOPTD system and the proposed FFFOPID controller are given in equations 6.27- 6.29.

The performance measure used to assess the unit step response of closed loop system is the integral absolute error (IAE) defined in eq. (6.43).

$$J_E = \int_0^{\infty} |e(t)| dt \tag{6.43}$$

The robustness measure of the closed loop system is the maximum sensitivity, M_s (eq. (6.44))

$$M_s = \max_{0<\omega<\infty} \left| \frac{1}{1+C(j\omega)G(j\omega)} \right| \tag{6.44}$$

6.3.2.1. Fragility indices

The controller fragility is investigated for both robustness and closed loop performance using robustness fragility indices (RFI) and performance fragility indices (PFI) (Alfaro and Vilanova, 2012). The delta epsilon robustness fragility index ($RFI_{\Delta\varepsilon}$) for a controller parameter vector [K_p, T_i, T_d, μ, γ, p] is defined as

$$RFI_{\Delta\varepsilon} = \frac{M_{s\Delta\varepsilon}}{M_s} - 1 \tag{6.45}$$

$M_{s\Delta\varepsilon}$ in eq. (6.45) is the extreme maximum sensitivity for same variation (ε = 0.05 (5%), 0.1 (10%), 0.15 (15%), 0.2 (20%), 0.25 (25%)) in all parameters of the controller from nominal values and M_s is the nominal maximum sensitivity. Similarly, the parametric delta epsilon robustness fragility index ($RFI_{\delta\varepsilon}$) for variation in any of the controller parameters can be calculated using eq. (6.46).

$$RFI_{\delta\varepsilon p} = \frac{M_{s\delta\varepsilon p}}{M_s} - 1 \tag{6.46}$$

The delta 20 robustness fragility index ($RFI_{\Delta 20}$) for 20% variation in the controller parameters is

$$RFI_{\Delta 20} = \frac{M_{s\Delta 20}}{M_s} - 1 \tag{6.47}$$

Any controller is said to be robustness fragile if $RFI_{\Delta 20} > 0.5$; robustness nonfragile if $RFI_{\Delta 20} \leq 0.5$ and robustness resilient if $RFI_{\Delta 20} \leq 0.1$.

The performance fragility indices for variation in all controller parameters ($PFI_{\Delta\varepsilon}$); for variation in one parameter at a time ($PFI_{\delta\varepsilon}$) and for 20% variation in the controller parameters ($PFI_{\Delta 20}$) are defined in equations (6.48) to (6.50).

$$PFI_{\Delta\varepsilon}=\frac{J_{E\Delta\varepsilon}}{J_E}-1 \tag{6.48}$$

$$PFI_{\delta\varepsilon p}=\frac{J_{E\Delta\varepsilon p}}{J_E}-1 \tag{6.49}$$

$$PFI_{\Delta 20}=\frac{J_{E\Delta\varepsilon 20}}{J_E}-1 \tag{6.50}$$

Any controller is said to be performance fragile if $PFI_{\Delta 20}>0.5$; performance nonfragile if $PFI_{\Delta 20}\leq 0.5$ and performance resilient if $PFI_{\Delta 20}\leq 0.1$.

In addition, the controller fragility balance is investigated with average parametric fragility index which is defined for both robustness and performance in eq. (6.51) and eq. (6.52)

$$RFI_{\delta\varepsilon a}=\frac{1}{6}\sum_{i=1}^{6} RFI_{\delta\varepsilon p} \tag{6.51}$$

$$PFI_{\delta\varepsilon a}=\frac{1}{6}\sum_{i=1}^{6} PFI_{\delta\varepsilon p} \tag{6.52}$$

The controller fragility balance around a selected band helps to estimate which parameter of the controller is causing unbalance in the fragility of controller.

6.3.3. Fragility plots and discussion

This section presents the fragility plots for two examples (eq. (6.53), eq. (6.54)). The nominal controller parameters, performance measure and maximum sensitivity for the two examples (section 6.2) are listed in Table 6.12.

$$G_1(s)=\frac{9}{(s+1)(s^2+2s+9)}=\frac{1.0003}{0.8864s^{1.0212}+1}e^{-0.4274s} \tag{6.53}$$

$$G_2(s)=\frac{1}{(s+1)(0.2s+1)(0.04s+1)(0.008s+1)}=\frac{0.99932}{1.0842s^{1.0132}+1}e^{-0.1922s} \tag{6.54}$$

Table 6.12 Controller settings and nominal performance measures for the two examples

Example	$\mathbf{K_p}$	$\mathbf{T_i}$	$\mathbf{T_d}$	**μ**	**γ**	**p**	$\mathbf{J_E}$	$\mathbf{M_s}$
$G_1(s)$	0.214	0.214	0.886	1.021	0.35	1.01	1.176	1.625
$G_2(s)$	0.096	0.096	1.084	1.013	0.1	1.1	0.566	1.81

6.3.3.1. Robustness fragility plots

The robustness fragility plot for variation in all of the controller parameters of the two examples is shown in Fig 6.27. It can be observed that the FFFOPID controller designed for $G_1(s)$ is nonfragile whereas the controller designed for $G_2(s)$ is fragile. The parameter causing the fragility is found out from the parametric robustness fragility plots shown Fig 6.28 and Fig 6.29. It is evident from Fig 6.28 that the controller for $G_1(s)$ is resilient: for variations in T_i, μ, γ, p and nonfragile: for variations in K_p, T_d. The controller for $G_2(s)$ is resilient for variation in T_i, γ, p and nonfragile for changes in K_p, T_d and μ which is evident from Fig 6.29. The variation of controller parameter μ is responsible for fragile nature of the controller of $G_2(s)$ which can be observed for the delta 20 fragility indices shown in Table 6.13. This parameter (μ) change causes instability in the closed loop system. In case of $G_1(s)$, controller fine tuning is required as it loses 17% (Table 6.13) of the robustness. The controller for $G_2(s)$ is difficult to tune as it lose more than 50% (Table 6.13) of its robustness.

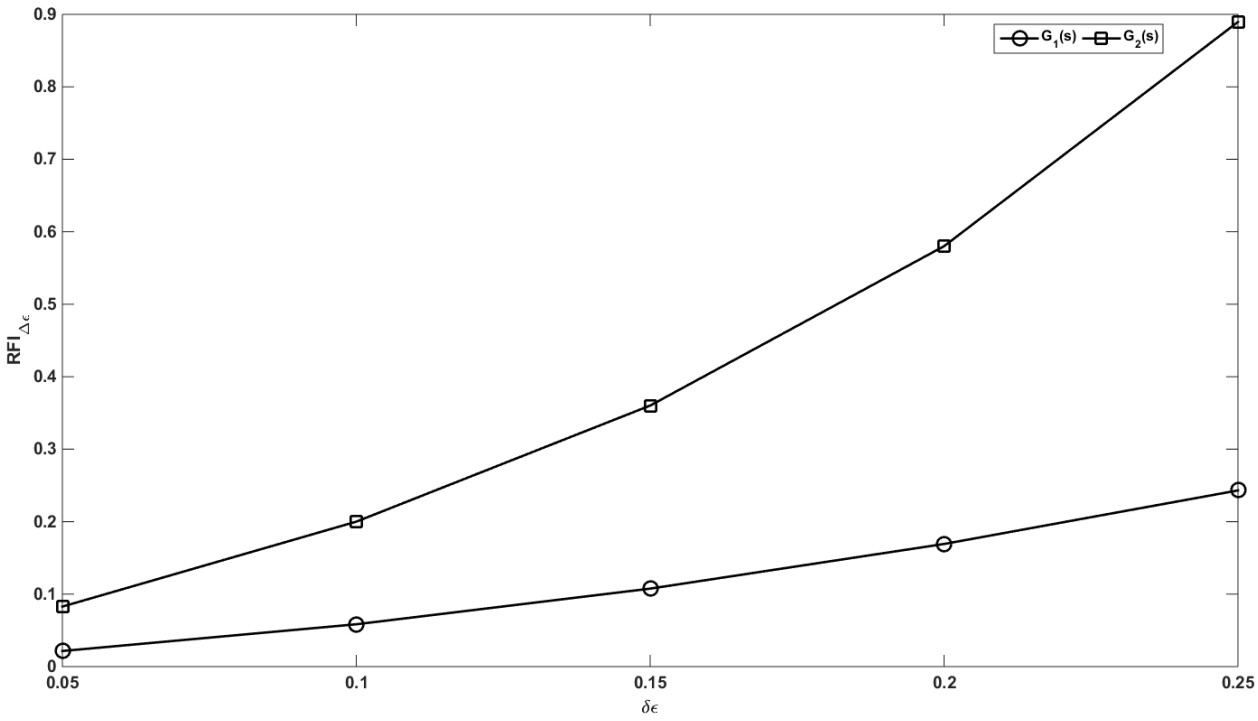

Fig 6.27 Robustness fragility plot for the two examples

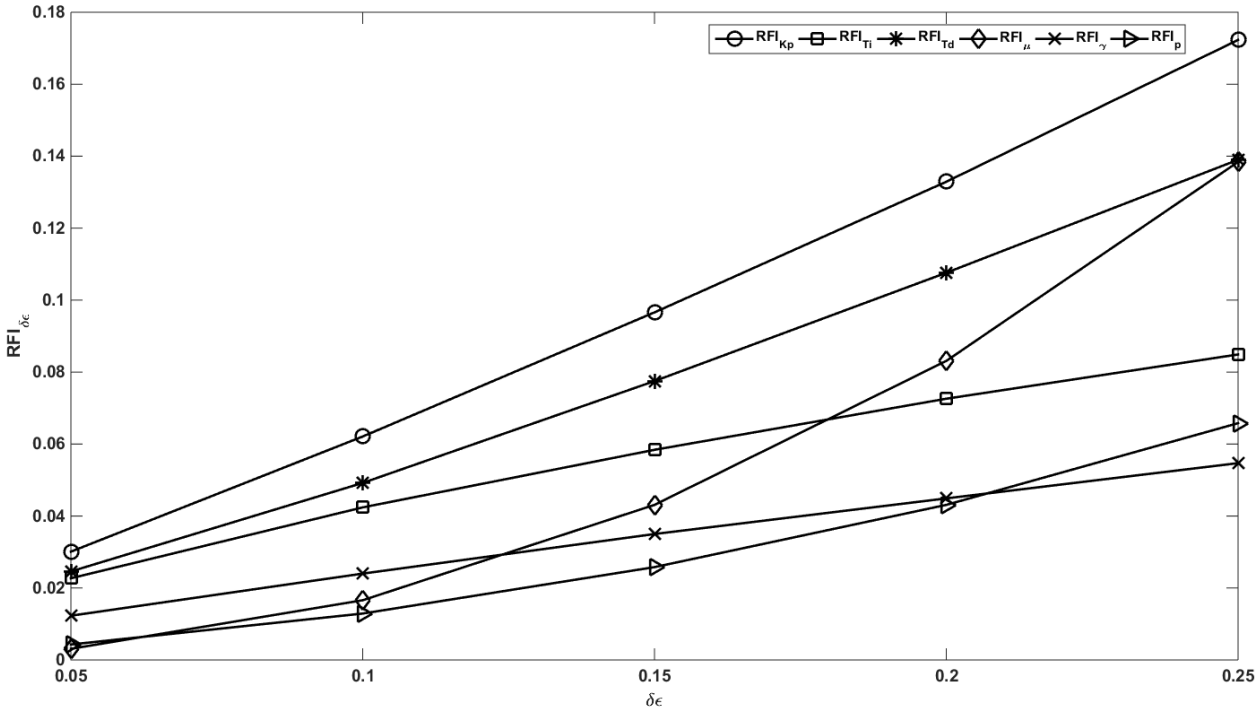

Fig 6.28 Robustness parametric fragility plot for $G_1(s)$

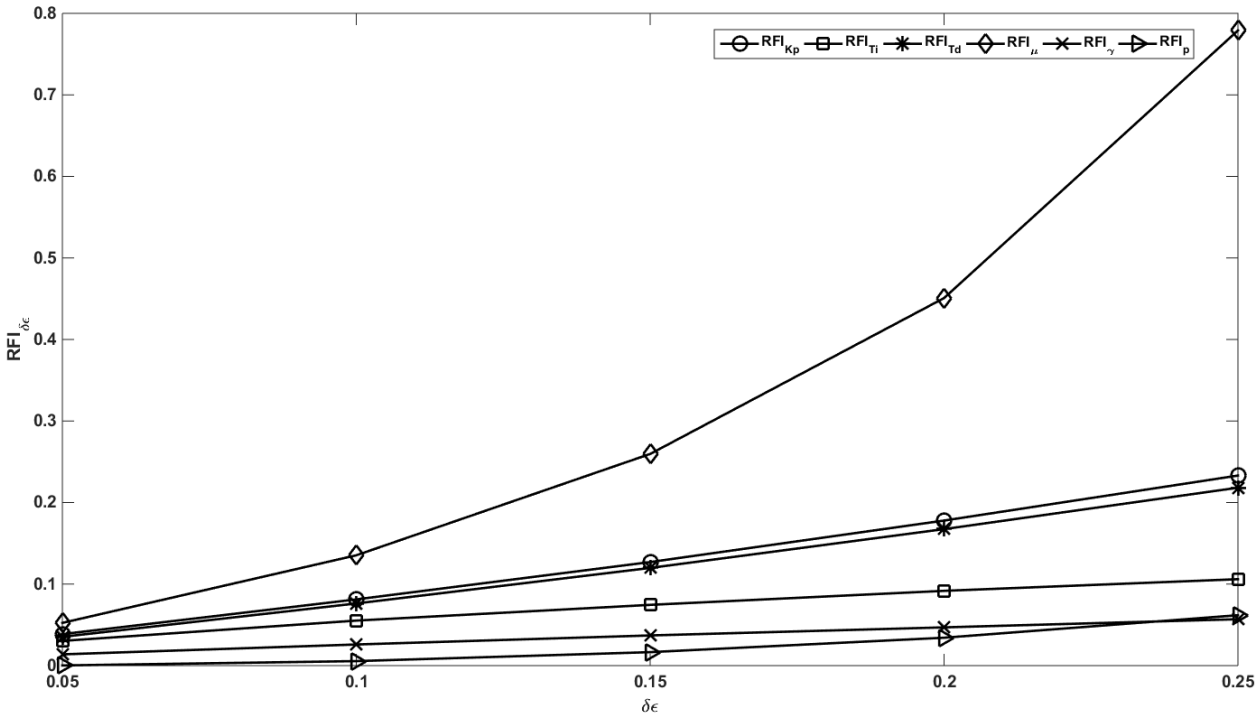

Fig 6.29 Robustness parametric fragility plot for $G_2(s)$

Table 6.13 Delta 20 fragility indices ($FI_{\Delta 20}$) for the two examples

Robustness fragility indices (RFI)			**Performance fragility indices (PFI)**		
$RFI_{\Delta 20}$	**$G_1(s)$**	**$G_2(s)$**	**$PFI_{\Delta 20}$**	**$G_1(s)$**	**$G_2(s)$**
$RFI_{\delta 20Kp}$	0.1329	0.1779	$PFI_{\delta 20Kp}$	0.0476	0.0591
$RFI_{\delta 20Ti}$	0.0726	0.0917	$PFI_{\delta 20Ti}$	0.1819	0.0164
$RFI_{\delta 20Td}$	0.1076	0.1674	$PFI_{\delta 20Td}$	0.0161	0.0688
$RFI_{\delta 20\mu}$	0.0831	0.4508	$PFI_{\delta 20\mu}$	0.1734	0.1629
$RFI_{\delta 20\gamma}$	0.0449	0.0469	$PFI_{\delta 20\gamma}$	0.0756	0.0233
$RFI_{\delta 20p}$	0.0431	0.0342	$PFI_{\delta 20p}$	0.1573	0.1919
$RFI_{\Delta 20}$	0.1692	0.5801	$PFI_{\Delta 20}$	0.2006	0.3542

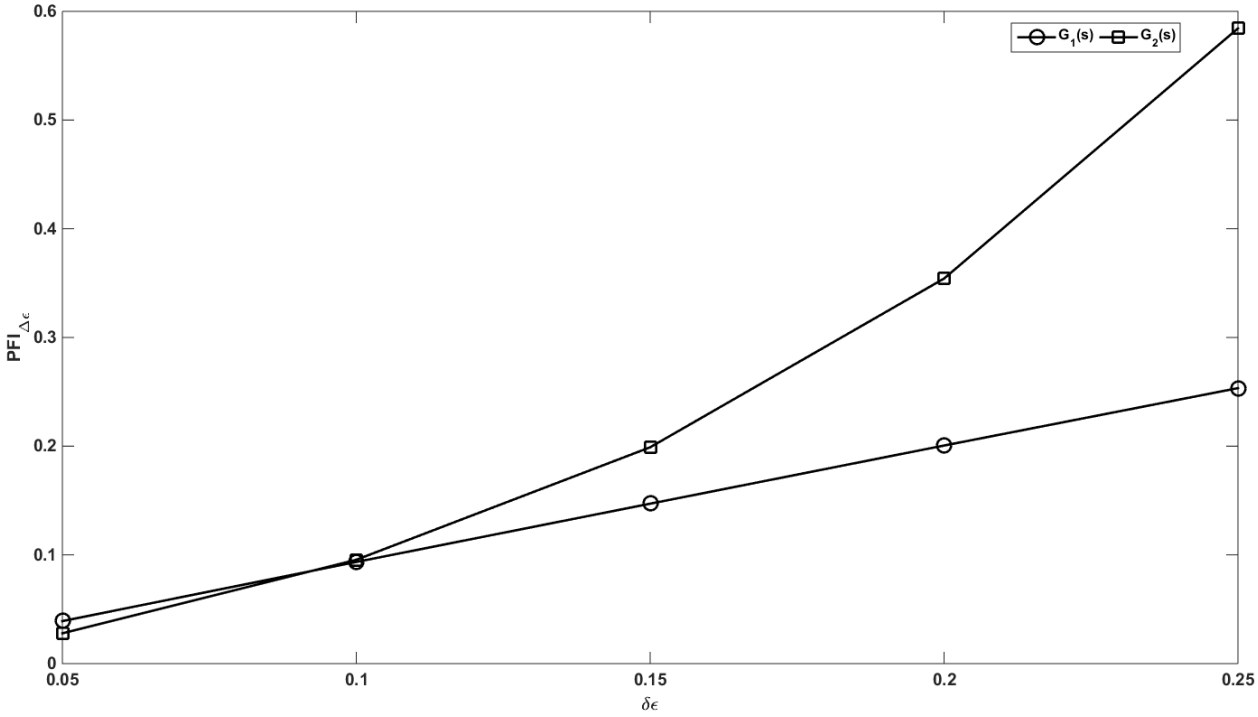

Fig 6.30 Performance fragility plot for the two examples

6.3.3.2. Performance fragility plots

The performance fragility plot shown in Fig 6.30 and performance fragility indices listed in Table 6.13 tells the controller for both the examples are performance nonfragile for variation in all parameters of the controller. The variations in K_p, T_d and γ results in a resilient controller for $G_1(s)$ and makes it nonfragile for variations T_d, μ and p which is evident from parametric performance fragility plot shown in Fig 6.31. In case of $G_2(s)$, the FFFOPID controller is resilient for variations in K_p, T_i, T_d, γ and nonfragile for variations in μ and p which is clear from Fig 6.32. Hence, fine

tuning is required as the controllers of both the systems lose more than 10% and less than 35% (Table 6.13) of its nominal performance.

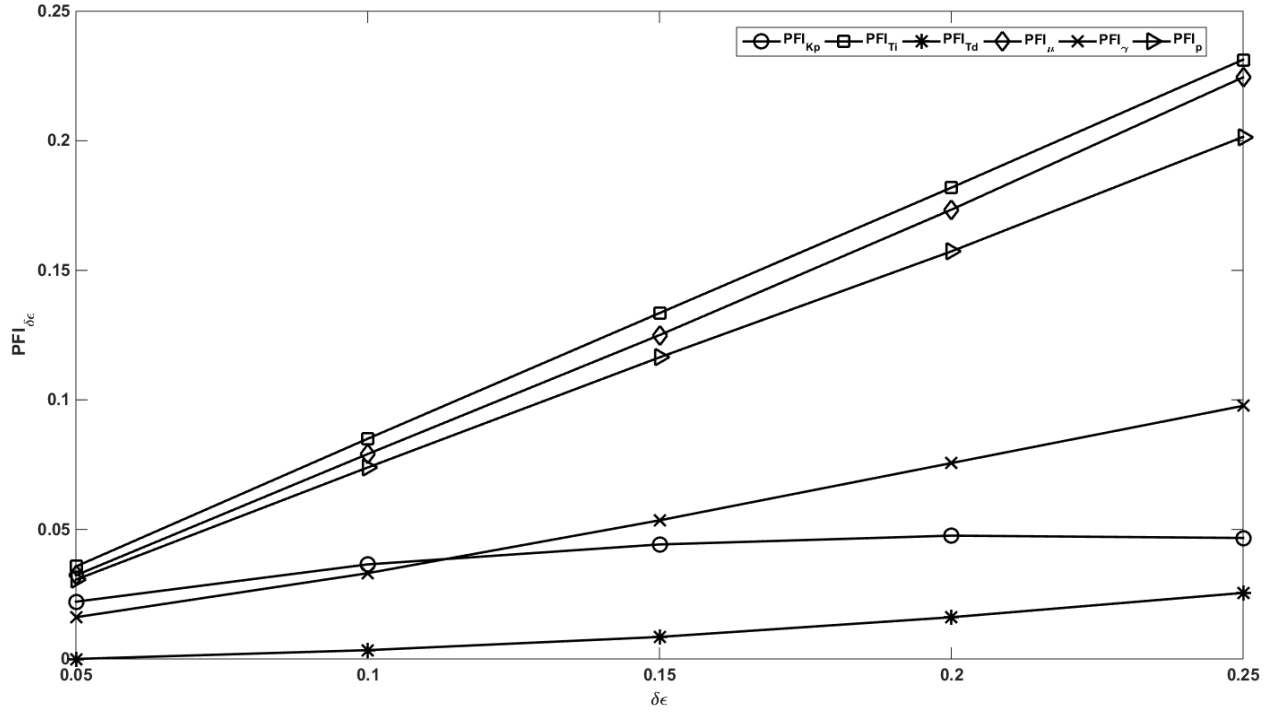

Fig 6.31 Performance parametric fragility plot for $G_1(s)$

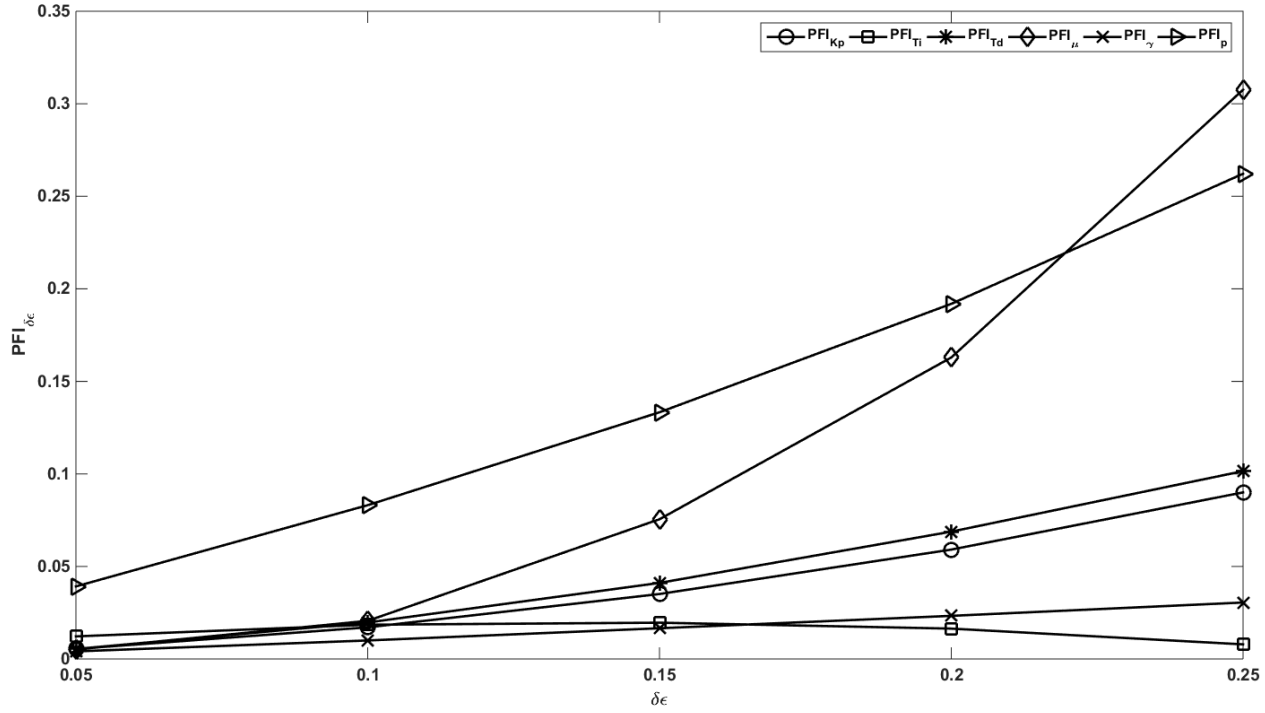

Fig 6.32 Performance parametric fragility plot for $G_2(s)$

6.3.3.3. Controller fragility balance

A fragility balanced controller can be identified with parametric delta epsilon fragility plots using average fragility indices and a band of fragility indices around the average value. The robustness and performance fragility balance plots for the two examples are shown in Fig 6.33 and Fig 6.34. The following observations are made from the fragility balance plots:

1) The FFFOPID controller for $G_1(s)$ is fragility unbalanced with respect to robustness and performance.

2) The robustness fragility unbalance is caused by the variation of proportional gain (K_p) and derivative time (T_d).

3) The performance fragility unbalance is caused by the variation of T_i, μ and p.

4) The controller for $G_2(s)$ is robustness fragility balanced controller with respect to the variation of K_p, T_i, T_d, γ and μ. The unbalance in the fragility is caused by the variation of fractional order (μ) of the derivative term.

5) Similarly, the unbalance in the performance fragility of the controller for $G_2(s)$ is due to the change in the parameters μ and p.

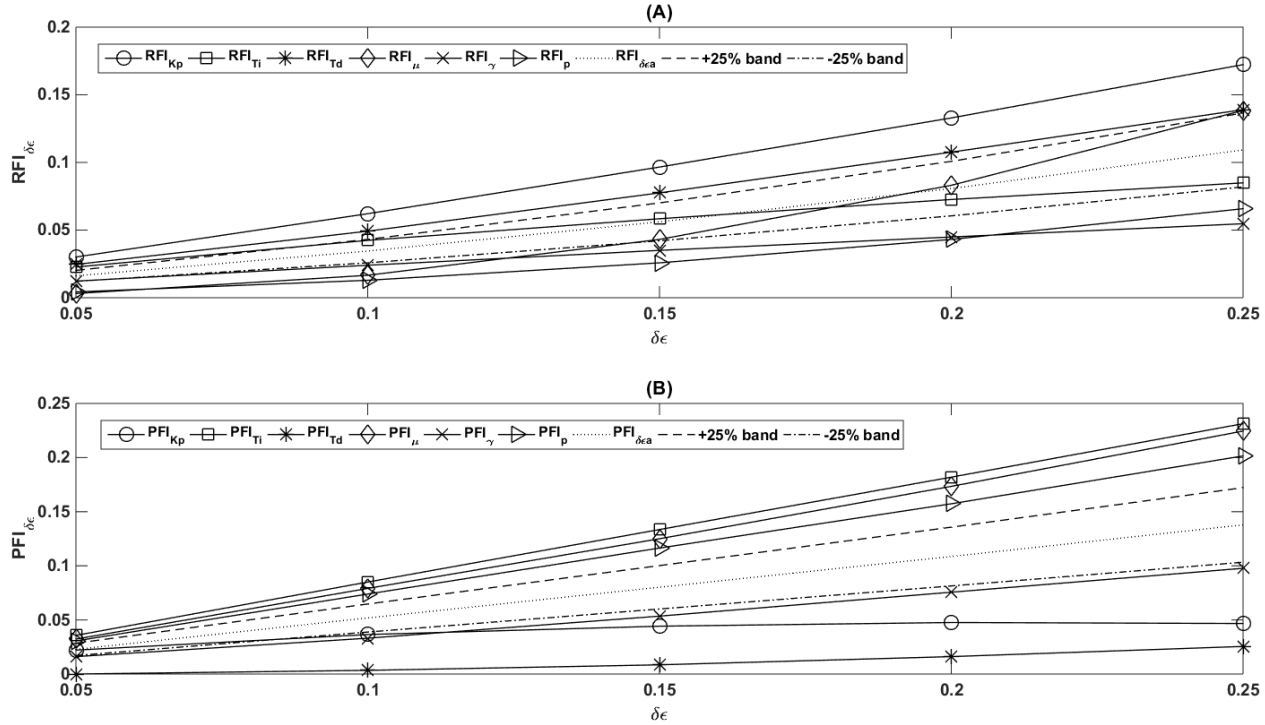

Fig 6.33 Fragility balance plot for $G_1(s)$ (A) robustness fragility (B) performance fragility

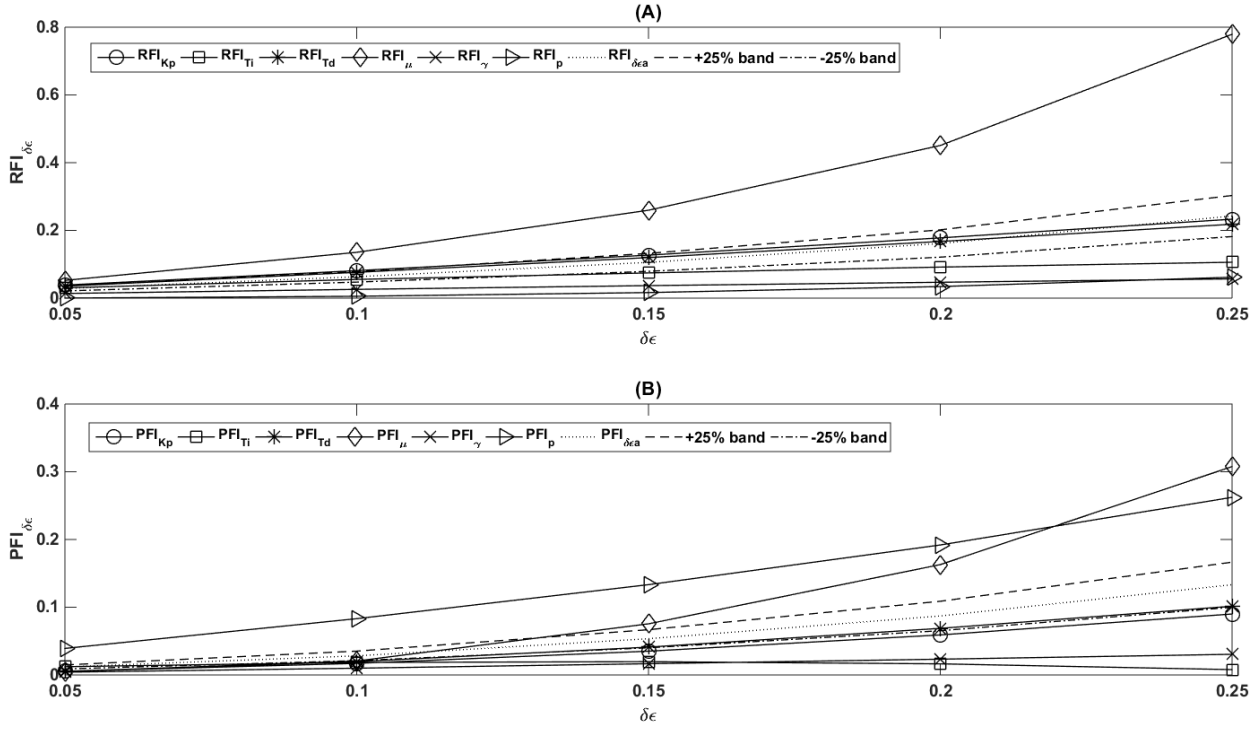

Fig 6.34 Fragility balance plot for $G_2(s)$ (A) robustness fragility (B) performance fragility

6.3.4. Conclusions

The fragility analysis of FFFOPID controller for higher order systems approximated as NIOPTD systems is presented for performance and robustness. The fragility plots indicate the influence of specific controller parameter on the performance and stability. The FFFOPID controller used for the current analysis is nonfragile in terms of both performance and robustness as the controllers won't lose more than 50% of their performance and robustness up to a variation of 20% in the controller parameters. This nonfragile nature of the controllers allow for the fine tuning of the controller. Care should be taken while changing the fractional order of the derivative term as it mostly affects the fragility of controller. This analysis helps to design a resilient (preferred) or nonfragile fractional controller to ensure the stability of closed loop system. A key point to note here is that the fragility of the controller can also be affected by the process model. Hence, care must be taken to design a nonfragile controller considering the effect of model parameter changes apart from controller parameter variation which can be taken up as a future work.

Chapter 7

Design of fractional filter IMC - PID control strategy for performance enhancement of cascade control systems

7. Design of fractional filter IMC - PID control strategy for performance enhancement of cascade control systems*

Cascade control is widely used in chemical industries for disturbance attenuation as an alternative to single feedback loop. This article presents an IMC based series cascade control system for different time delay process models. The novelty of the work lies in the use of fractional order IMC filter of first order and higher order for designing controller in the outer loop. The controller designed for inner loop assumes the standard PID controller structure and the outer loop controller takes fractional filter IMC-PID controller structure. The proposed method gives improved performance for set point tracking and disturbance rejection. Further, the proposed method gives robust performance for noise in the measured signal. Also, the robustness analysis is performed to check the insensitivity of the closed loop system for process parameter variations. The fragility of the controller is investigated for perturbations in the controller parameters.

7.1. Introduction

Cascade control is an advanced control structure widely used in chemical process industry with flow, pressure, level and temperature control loops to attenuate the external disturbances for improved and rapid performance of the single feedback loop (Seborg et al., 2004; Krishnaswamy et al., 1990; Raja and Ali, 2017). This structure also handles nonlinearities in the process elements and ensures accurate control performance in presence of large time delays. The cascade control structure consists of inner (secondary) loop and outer (primary) loop. The enhanced performance of cascade system depends on the effective tuning of these loops (Huang et al., 1998; Leva and Marinelli, 2009) and PID controllers are mostly used for the purpose due to their adopted structure and range of tuning methods available (Song et al., 2003; Brambilla and Semino, 1992; Veronesi, and Visioli, 2011; Vivek and Chidambaram, 2013). However, the tuning is quite complex because the changes encountered by the inner loop must be considered for tuning the primary loop.

A series cascade control structure (Raja and Ali, 2017) is widely used in the industries which comes with minimum number of controllers and hence less parameters to be tuned.

* This work has been submitted to the journal International Journal of Systems Science (under review)

Initially, sequential tuning was used for tuning the cascade control loop where in the secondary loop is tuned first followed by primary loop. Another familiar tuning method used with cascade systems is IMC (Leva and Donida, 2009) which offers flexibility in tuning. In the present article, a fractional filter IMC-PID tuning method is proposed for cascade control systems by considering the tuning flexibility of IMC method (Lee et al., 1998). Firstly, the inner loop controller is designed and then the outer loop controller is designed by considering the desired response of inner loop (Azar and Serrano, 2014).

Fractional order control has been in focus for controlling different time delay systems using fractional order differentiation and fractional order integration. The analytical controller design using fractional IMC filter produce a fractional filter PID controller in spite of conventional three term PID controller (Padula and Visioli, 2014). The additional tuning parameters of the fractional filter allows for precise control. Vu and Le developed FOPI controller tuning rules for cascade control systems (Vu and Le Hieu Giang, 2016). Hence, in the present paper a fractional order IMC filter has been used for designing the outer loop controller. The controllers are tuned using the generalized systematic design procedure minimizing IAE and TV. The simulations have been done for different process models in the inner loop and outer loop. FOPTD models and IPTD models are used in the outer loop whereas SOPTD and FOPTD models are used in the inner loop. The simulations are carried out for external perturbations, process parameter variations and for noise in the measured signal. Further, robustness analysis is carried out for robust stability of the closed loop system for uncertainties in the process parameters.

7.2. IMC based design of series cascade control system

The IMC based series cascade control structure is shown in Fig 7.1. $C_1(s)$ is the controller and $G_1(s)$ is the process model for inner loop while $C_2(s)$ and $G_2(s)$ are the outer loop controller and outer loop process model respectively. d_1 and d_2 are the disturbance inputs for the inner and outer loops. The controllers for both the loops using IMC method are derived in the following sections.

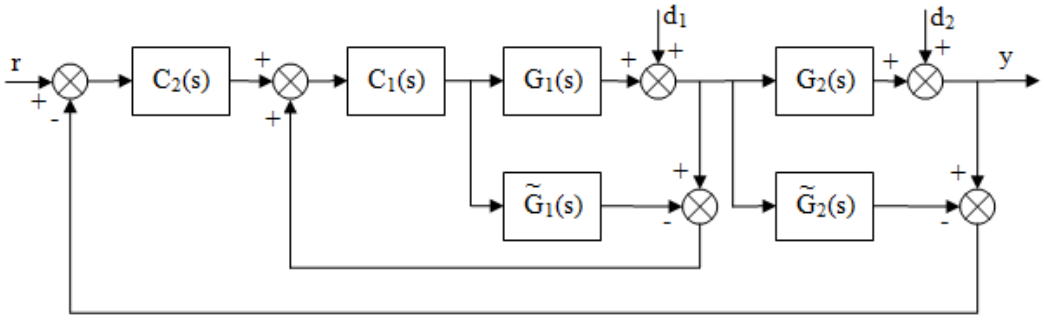

Fig 7.1 IMC based series cascade control structure

7.2.1. Inner loop controller design

The IMC controller for the inner loop is given by

$$C_{IMC1}(s)=\frac{f_1(s)}{\tilde{G}_1^-(s)} \tag{7.1}$$

Where $\tilde{G}_1^-(s)$ is the invertible part of $G_1(s)$ and $f_1(s)$ is the inner loop IMC filter

The inner loop feedback controller is

$$C_1(s)=\frac{C_{IMC1}(s)}{1-C_{IMC1}(s)G_1(s)} \tag{7.2}$$

7.2.2. Outer loop controller design

The design procedure is similar to the one used for inner loop. The outer loop process model considering the inner loop is

$$\tilde{G}_{p2}(s)=\frac{\tilde{G}_1^+(s)}{f_1(s)}\tilde{G}_2(s) \tag{7.3}$$

The IMC controller for the outer loop is given by

$$C_{IMC2}(s)=\frac{f_2(s)}{\tilde{G}_{p2}^-(s)} \tag{7.4}$$

Where $\tilde{G}_{p2}^-(s)$ is the invertible part of $G_{p2}(s)$ and $f_2(s)$ is the outer loop IMC filter

The outer loop controller $C_2(s)$ is

$$C_2(s)=\frac{C_{IMC2}(s)}{1-C_{IMC2}(s)G_{p2}(s)} \tag{7.5}$$

7.3. Cascade loop controller design with different process models

The controller structure for inner and outer loops used in the current work takes the following form:

$$C_1(s)=(\text{filter term})K_p\left[1+\frac{1}{T_i s}+T_d s\right] \quad (7.6)$$

$$C_2(s)=(\text{fractional filter})K_p\left[1+\frac{1}{T_i s}+T_d s\right] \quad (7.7)$$

K_p, T_i and T_d are proportional gain, integral time and derivative time

7.3.1. Design of controllers for cascade loop: SOPTD system in the inner loop and FOPTD system in the outer loop

7.3.1.1. Inner loop controller design with SOPTD model

Consider a SOPTD model

$$G_1(s)=\frac{K_1 e^{-L_1 s}}{(T_1 s+1)(T_2 s+1)};\ K_1\text{-gain};L_1\text{-time delay};T_1 \text{and } T_2 \text{ are time constants} \quad (7.8)$$

Inner loop IMC filter

$$f_1(s)=\frac{1}{\gamma_1 s+1};\ \gamma_1\text{-filter time constant} \quad (7.9)$$

Using Taylor series approximation and IMC method, the expression for $C_1(s)$ is

$$C_1(s)=\left[\frac{T_1+T_2}{K_1(\gamma_1+L_1)}\right]\left[1+\frac{1}{(T_1+T_2)s}+\left(\frac{T_1 T_2}{T_1+T_2}\right)s\right] \quad (7.10)$$

7.3.1.2. Outer loop controller design with FOPTD model

Consider the FOPTD model

$$G_2(s)=\frac{K_2 e^{-L_2 s}}{T_3 s+1};\ K_2\text{-gain};L_2\text{-time delay};T_3\text{- time constant} \quad (7.11)$$

Now, by considering the effect of inner loop, the outer loop process becomes

$$G_{p_2}(s)=\frac{K_2 e^{-(L_1+L_2)s}}{(T_3 s+1)(\gamma_1 s+1)};\ L_1+L_2=L \quad (7.12)$$

The outer loop higher order IMC filter [16] is

$$f_2(s)=\frac{\beta s+1}{(\gamma_2 s^p+1)^2} \quad (7.13)$$

Where γ_2 is the time constant; p is the fractional order and β is the additional degree of freedom of $f_2(s)$

The outer loop controller $C_2(s)$ using Taylor series approximation for time delay is

$$C_2(s)=\frac{\beta s+1}{[\gamma_2^2 s^{2p-1}+\beta L s+2\gamma_2 s^{p-1}+(L-\beta]}\left(\frac{T_3+\gamma_1}{K_2}\right)\left[1+\frac{1}{(T_3+\gamma_1)s}+\left(\frac{T_3\gamma_1}{T_3+\gamma_1}\right)s\right] \quad (7.14)$$

The outer loop controller $C_2(s)$ using IMC filter $1/(\gamma_2 s^p+1)$ and Taylor series approximation for time delay is

$$C_2(s)=\left(\frac{1}{\gamma_2 s^{p-1}+L}\right)\left(\frac{T_3+\gamma_1}{K_2}\right)\left[1+\frac{1}{(T_3+\gamma_1)s}+\left(\frac{T_3\gamma_1}{T_3+\gamma_1}\right)s\right] \quad (7.15)$$

7.3.2. Design of controllers for cascade loop: FOPTD system in the inner loop; FOPTD and IPTD systems in the outer loop

7.3.2.1. Inner loop controller design with FOPTD model

Consider an FOPTD model

$$G_1(s)=\frac{K_1 e^{-L_1 s}}{T_1 s+1} \quad (7.16)$$

Using IMC filter in eq. (7.9) and first Pade's procedure, the expression for $C_1(s)$ is

$$C_1(s)=\left[\frac{1}{(0.5\gamma_1 L_1)s+(\gamma_1+L_1)}\right]\left(\frac{T_1+0.5L_1}{K_1}\right)\left[1+\frac{1}{(T_1+0.5L_1)s}+\left(\frac{0.5T_1L_1}{T_1+0.5L_1}\right)s\right] \quad (7.17)$$

7.3.2.2. Outer loop controller design with FOPTD model

Consider the FOPTD model

$$G_2(s)=\frac{K_2 e^{-L_2 s}}{T_2 s+1};\ K_2\text{-gain; } L_2\text{-time delay; } T_2\text{ - time constant} \quad (7.18)$$

Now, by considering the effect of inner loop, the outer loop process becomes

$$G_{p_2}(s)=\frac{K_2 e^{-(L_1+L_2)s}}{(T_2 s+1)(\gamma_1 s+1)} \quad (7.19)$$

The outer loop controller $C_2(s)$ using higher order fractional IMC filter in eq. (7.13) and 2/3 Pade's approximation for time delay is

$$C_2(s)=\frac{\beta L^3 s^4+(L^3+9\beta L^2)s^3+(9L^2+36\beta L)s^2+(36L+60\beta)s+60}{\left[\begin{array}{c}\gamma_2^2 L^3 s^{2p+2}+9\gamma_2^2 L^2 s^{2p+1}+2\gamma_2 L^3 s^{p+2}+36\gamma_2^2 L s^{2p}+18\gamma_2 L^2 s^{p+1}+(L^3-3\beta L^2)s^2+60\gamma_2^2 s^{2p-1}+\\ 72\gamma_2 L s^p+(6L^2+24\beta L)s+120\gamma_2 s^{p-1}+(60L-60\beta)\end{array}\right]}\left(\frac{T_2+\gamma_1}{K_2}\right)\left[1+\frac{1}{(T_2+\gamma_1)s}+\left(\frac{T_2\gamma_1}{T_2+\gamma_1}\right)s\right] \quad (7.20)$$

The outer loop controller $C_2(s)$ using IMC filter $1/(\gamma_2 s^p+1)$ and 2/3 Pade's approximation for time delay is

$$C_2(s)=\left(\frac{L^3 s^3+9L^2 s^2+36Ls+60}{\gamma_2 L^3 s^{p+2}+9\gamma_2 L^2 s^{p+1}+L^3 s^2+36\gamma_2 L s^p+6L^2 s+60\gamma_2 s^{p-1}+60L}\right)\left(\frac{T_2+\gamma_1}{K_2}\right)\left[1+\frac{1}{(T_2+\gamma_1)s}+\left(\frac{T_2\gamma_1}{T_2+\gamma_1}\right)s\right] \quad (7.21)$$

7.3.2.3. Outer loop controller design with IPTD model

Consider an integrating process model

$$G_2(s)=\frac{K_2 e^{-L_2 s}}{s} \quad (7.22)$$

Now, by considering the effect of inner loop, the outer loop process becomes

$$G_{p_2}(s)=\frac{K_2 e^{-(L_1+L_2)s}}{s(\gamma_1 s+1)} \quad (7.23)$$

The outer loop higher order IMC filter is

$$f_2(s)=\frac{\beta s+1}{(\gamma_2 s^p+1)^3} \quad (7.24)$$

The outer loop controller $C_2(s)$ using 2/3 Pade's approximation for time delay is

$$C_2(s)=\frac{\beta L^3 s^4+(9\beta L^2+L^3)s^3+(36\beta L+9L^2)s^2+(36L+60\beta)s+60}{\left[\begin{array}{c}\gamma_2^3 L^3 s^{3p+2}+9\gamma_2^2 L^3 s^{3p+1}+3\gamma_2^2 L^3 s^{2p+2}+36\gamma_2^3 L s^{3p}+27\gamma_2^2 L^2 s^{2p+1}+3\gamma_2 L^3 s^{p+2}+60\gamma_2^3 s^{3p-1}+108\gamma_2^2 L s^{2p} \\ +27\gamma_2 L^2 s^{p+1}+(L^3-3\beta L^2)s^2+180\gamma_2^2 s^{2p-1}+108\gamma_2 L s^p+(24\beta L+6L^2)s+180\gamma_2 s^{p-1}+(60L-60\beta)\end{array}\right]}\left(\frac{1}{K_2}\right)\left[1+\gamma_1 s\right] \quad (7.25)$$

The outer loop controller $C_2(s)$ using IMC filter $1/(\gamma_2 s^p+1)$ and 2/3 Pade's approximation for time delay is

$$C_2(s)=\frac{L^3 s^3+9L^2 s^2+36Ls+60}{\gamma_2 L^3 s^{p+2}+9\gamma_2 L^2 s^{p+1}+L^3 s^2+36\gamma_2 L s^p+6L^2 s+60\gamma_2 s^{p-1}+60L}\left(\frac{1}{K_2}\right)\left[1+\gamma_1 s\right] \quad (7.26)$$

The higher order fractional IMC filter structures are identified according to the systematic design procedure given in Figure 7.2.

7.4. Robustness and fragility analysis

7.4.1. Robustness analysis

The Robustness analysis is important to assess the stability of closed loop control system. This is due to the fact that the model behavior used for controller design is different from the real time system. Hence, the closed loop system must be insensitive for variations in the process parameters. This insensitive capacity of the closed loop system for parameter variations can be expressed through robustness analysis.

The robust stability condition according to the small gain theorem (Zhou and Doyle, 1998) is

$$\|\delta(j\omega)T(j\omega)\|<1 \forall \omega \in (-\infty,\infty) \quad (7.27)$$

Where $T(j\omega)$ is the complementary sensitivity function and $\delta(j\omega)$ is the bound on process multiplicative uncertainty.

The controller must be tuned according to eq. (7.28) for uncertainty in L

$$\|T(j\omega)\|_\infty<\frac{1}{|e^{-\Delta L}-1|} \quad (7.28)$$

The following constraint should also be satisfied for robust closed loop performance

$$\|\delta(j\omega)T(j\omega)+w(j\omega)S(j\omega)\|<1 \quad (7.29)$$

Where $S(j\omega) = 1 - T(j\omega)$ is the sensitivity function and $w(j\omega)$ is the bound on $S(j\omega)$.

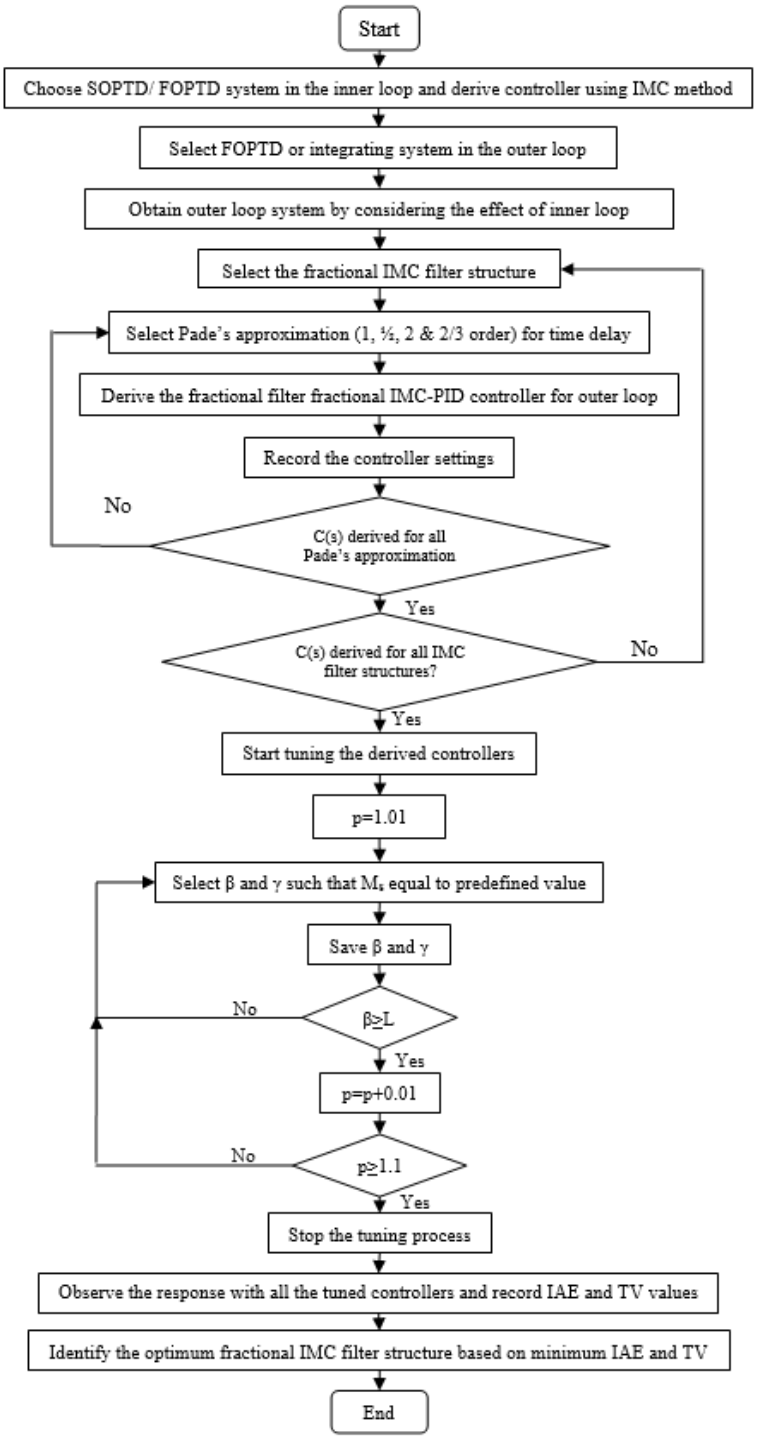

Figure 7.2 Systematic design procedure for identification of optimum fractional IMC filter structure

7.4.2. Fragility analysis

The Fragility analysis tells us the robust closed loop performance for perturbations in the controller parameters. The controller fragility (Alfaro and Vilanova, 2012) is based on the following criteria:

$$\begin{aligned} &\text{resilient} \quad \text{if, } RFI_{\Delta 20} \leq 0.1 \\ &\text{nonfragile} \quad \text{if, } RFI_{\Delta 20} \leq 0.5 \\ &\text{fragile} \quad \text{if, } RFI_{\Delta 20} > 0.5 \end{aligned} \tag{7.30}$$

$$RFI_{\Delta 20} = \frac{M_{s\Delta 20}}{M_s} - 1 \tag{7.31}$$

Where $M_{s\Delta 20}$ is the M_s for 20% perturbation in all parameters of the controller and M_s in the nominal maximum sensitivity.

7.5. Results and discussion

Three examples have been considered for simulation to show the effectiveness of the proposed method. The closed loop performance is assessed with the help of performance metrics: IAE, TV and M_s. The values of IAE and TV should be small, but an increase in IAE leads to a decrease in TV and vice versa (Shamsuzzoha and Skogestad, 2010). It means, there always exists a trade-off between IAE and TV. All the proposed methods are further termed as Proposed1, Proposed2, Proposed3 and Proposed4 which are listed in Table 7.1.

Table 7.1 Proposed methods for the three examples

Method	**IMC filters and Pade's procedure used in both the loops**
Proposed1	$f_1(s)=\frac{1}{\gamma_1+1}$+Taylor (inner loop) and $f_2(s)=\frac{\beta s+1}{(\gamma_2 s^p+1)^2}$ + Taylor (outer loop)
Proposed2	$f_1(s)=\frac{1}{\gamma_1+1}$+ Taylor (inner loop) and $f_2(s)=\frac{1}{\gamma_2 s^p+1}$ + Taylor (outer loop)
Proposed3	$f_1(s)=\frac{1}{\gamma_1+1}$+1st Pade (inner loop) and $f_2(s)=\frac{\beta s+1}{(\gamma_2 s^p+1)^2}$ + 2/3 Pade (outer loop)
Proposed4	$f_1(s)=\frac{1}{\gamma_1+1}$+1st Pade (inner loop) and $f_2(s)=\frac{1}{\gamma_2 s^p+1}$ + 2/3 Pade (outer loop)
Proposed5	$f_1(s)=\frac{1}{\gamma_1+1}$+1st Pade (inner loop) and $f_2(s)=\frac{\beta s+1}{(\gamma_2 s^p+1)^3}$ + 2/3 Pade (outer loop)
Proposed6	$f_1(s)=\frac{1}{\gamma_1+1}$+1st Pade (inner loop) and $f_2(s)=\frac{1}{\gamma_2 s^p+1}$ + 2/3 Pade (outer loop)

$$IAE=\int_0^\infty |e(t)|dt \tag{7.32}$$

$$TV=\sum_{i=0}^{\infty} |u_{i+1}-u_i| \tag{7.33}$$

$$M_s=\max_{0<\omega<\infty} \left|\frac{1}{1+C(j\omega)G(j\omega)}\right| \tag{7.34}$$

7.5.1. Example 1

The inner loop and outer loop models (Azar and Serrano, 2014) considered for the study are:

$$G_1(s)=\frac{100e^{-0.0005s}}{(s+1)(0.0015s+1)} \quad (7.35)$$

$$G_2(s)=\frac{20e^{-0.375s}}{0.495s+1} \quad (7.36)$$

The Proposed controller settings for both the loops of Example 1 are listed in Table 7.2. The closed loop step response of the cascade system with d_1 of magnitude 1 applied at t=10s and d_2 of magnitude 1 applied at t=20s is shown in Figure 7.3. The corresponding IAE and TV are given in Table 7.3. These values are low with the Proposed1 and Proposed2 methods for both the loops compared to Azar and Serrano (2014) method. The response of cascade loop for perturbations of +10% in K and L is shown in Figure 7.4 and the associated IAE and TV are given in Table 7.4. The performance measures for an output white noise of zero mean and a variance of 0.1 introduced in the outer loop is given in Table 7.4. It is evident that the Proposed1 and Proposed2 methods are giving better performance with low IAE and TV compared to Azar and Serrano (2014) method. The magnitude plot illustrating the robust stability of overall cascade loop is shown in Figure 7.5. It is observed that both the proposed methods are robustly stable with the Proposed1 method being more robust compared to Proposed2 method whereas Azar and Serrano (2014) method violates the robust stability condition for an uncertainty of +80% in L.

Table 7.2 Controller settings for Example 1

	Method	**K_p**	**T_i**	**T_d**	**β**	**γ_1**	**γ_2**	**P**	**M_s**
Inner loop	Proposed1/Proposed2	11.3163	1.0015	0.00149	-	0.000385	-	-	1.7
	Azar (2014)	0.2173	1	0.0015	-	0.0455	-	-	1.7
Outer loop	Proposed1	0.0247	0.495385	0.000379	0.00021	-	0.225	1.02	1.63
	Proposed2	0.0247	0.495385	0.000379	-	-	0.342	1.02	1.63
	Azar (2014)	0.00146	0.0455	0.495	-	-	0.1842		1.63

Table 7.3 Performance measures for nominal response of Example 1

Method	**Inner loop**		**Outer loop**		
	IAE	**M_s**	**IAE**	**TV**	**M_s**
Proposed1	0.0069	1.7	1.982	0.1506	1.63
Proposed2	0.0069	1.7	1.708	0.1613	1.63
Azar and Serrano (2014)	0.0661	1.7	2.836	0.9966	1.63

Table 7.4 Performance measures for perturbations and measurement noise of Example 1

	Perturbed response			**Noise response**		
Method	**Inner loop**	**Outer loop**		**Inner loop**	**Outer loop**	
	IAE	**IAE**	**TV**	**IAE**	**IAE**	**TV**
Proposed1	0.0117	2.137	0.1717	0.0089	9.412	2.3066
Proposed2	0.0119	1.86	0.1868	0.0115	9.372	4.3776
Azar and Serrano (2014)	0.0642	3.36	1.0986	0.3384	9.942	51.9231

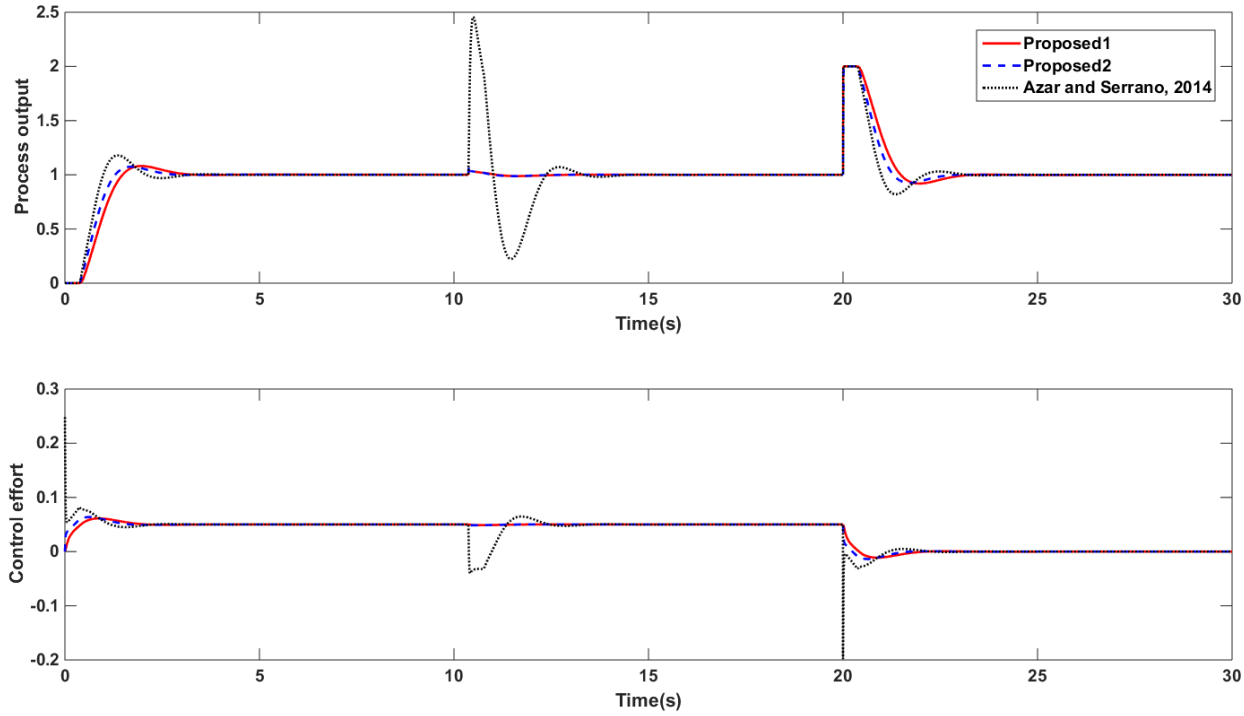

Figure 7.3 Nominal response for Example 1

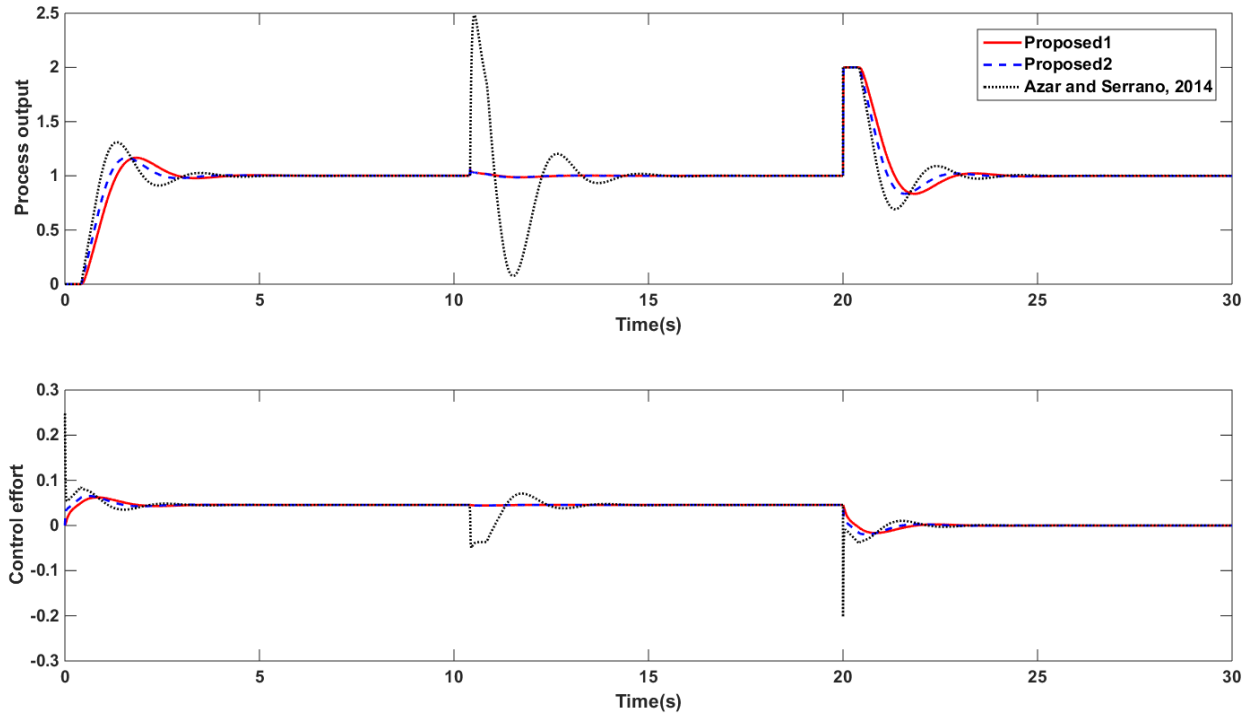

Figure 7.4 Perturbed response for Example 1

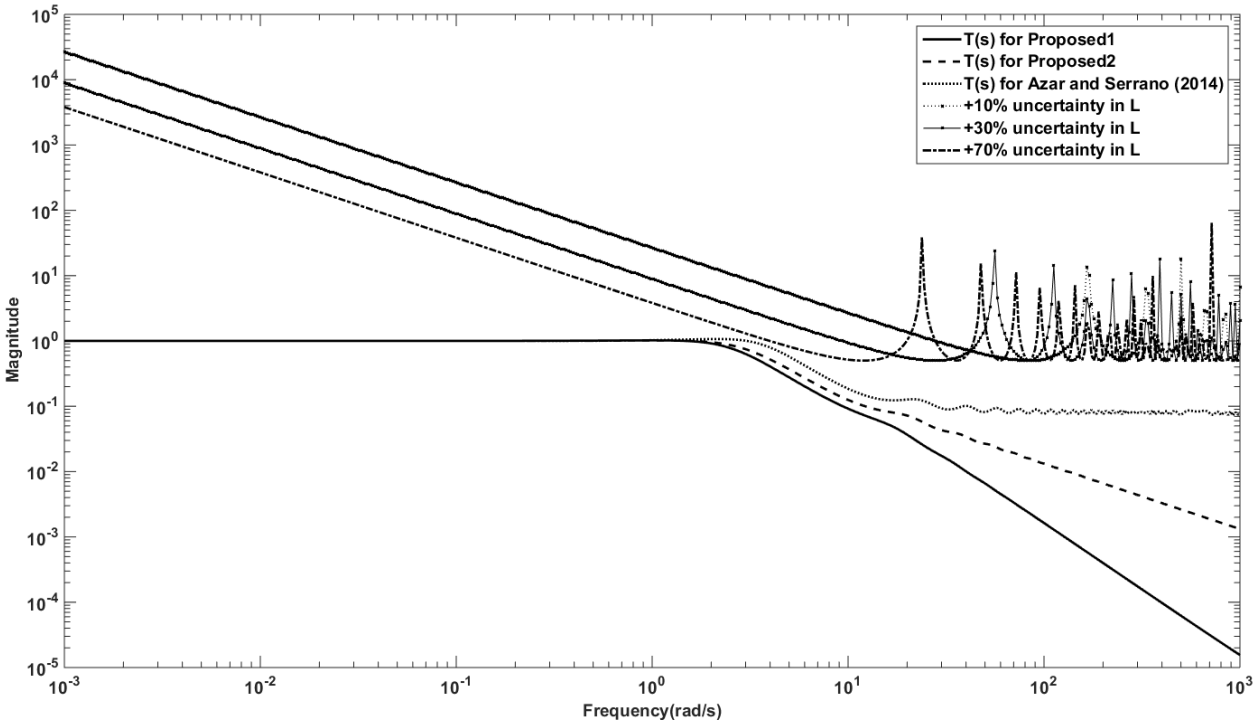

Figure 7.5 Robustness analysis of overall cascade loop for Example 1

7.5.2. Example 2

The inner loop and outer loop process models (Alfaro et al., 2008) considered for the study are:

$$G_1(s)=\frac{e^{-0.3s}}{s+1} \tag{7.37}$$

$$G_2(s)=\frac{e^{-1.5s}}{5s+1} \tag{7.38}$$

The Proposed controller settings for the inner loop and outer loop of Example 2 are listed in Table 7.5. The step response of cascade loop with d_1 of magnitude 1 applied at t=50s and d_2 of magnitude 0.1 applied at t=100s is shown in Figure 7.6. The corresponding performance metrics are given in Table 7.6. The value of IAE for the inner loop is small with the Proposed1 method whereas IAE for the outer loop is almost same with Proposed3 and Proposed4 methods. The TV representing control effort is small with Propsed3 method and very high with Proposed4 method. The cascade system response for perturbations of +10% in K and L is shown in Figure 7.7 and the associated IAE and TV are given in Table 7.7. The performance measures for white noise in the output introduced in the outer loop are listed in Table 7.7. It can be observed that the IAE of inner loop is small with Proposed1 method for both responses and the IAE of outer loop with Proposed3

method is slightly higher compared to Proposed4 method. But, the TV is small with Proposed3 method for both the responses and too high for Proposed4 method.

Table 7.5 Controller settings for Example 2

	Method	K_p	T_i	T_d	β	γ_1	γ_2	P	M_s
Inner loop	Proposed3/ Proposed4	1.15	1.15	0.1304	-	0.338	-	-	1.5
Outer loop	Proposed3	5.338	5.338	0.3165	0.2	-	0.68	1.02	1.7
	Proposed4	5.338	5.338	0.3165	-	-	0.9	1.02	1.7

Table 7.6 Performance measures for nominal response of Example 2

Method	Inner loop		Outer loop		
	IAE	M_s	IAE	TV	M_s
Proposed3	5.843	1.5	5.364	55.651	1.7
Proposed4	9.162	1.5	5.034	152.783	1.7

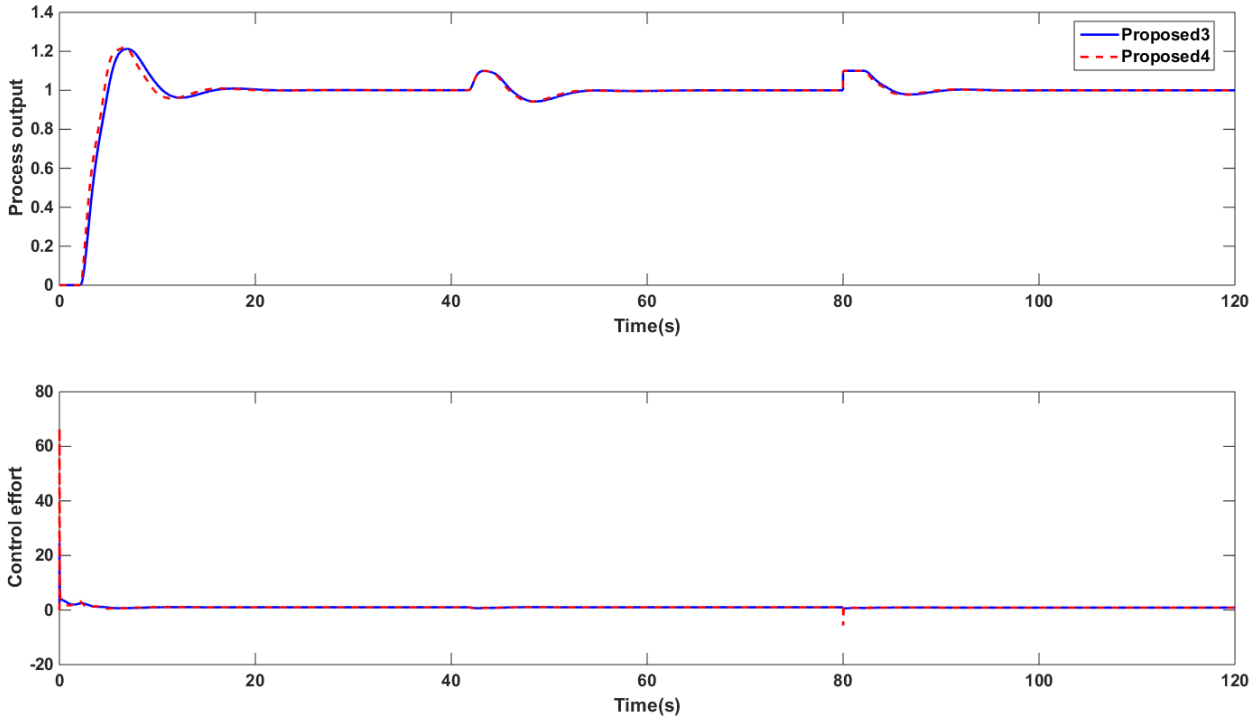

Figure 7.6 Nominal response for Example 2

Table 7.7 Performance measures for perturbations and measurement noise of Example 2

Method	Perturbed response			Noise response		
	Inner loop	Outer loop		Inner loop	Outer loop	
	IAE	IAE	TV	IAE	IAE	TV
Proposed3	7.04	6.299	57.638	392.4	34.62	20597
Proposed4	12.2	5.991	157.528	950.9	34.44	59109

The overall cascade loop is robust up to an uncertainty of +60% in L which is illustrated in Figure 7.8. It is observed that Proposed3 method is more robust compared to Proposed4 method.

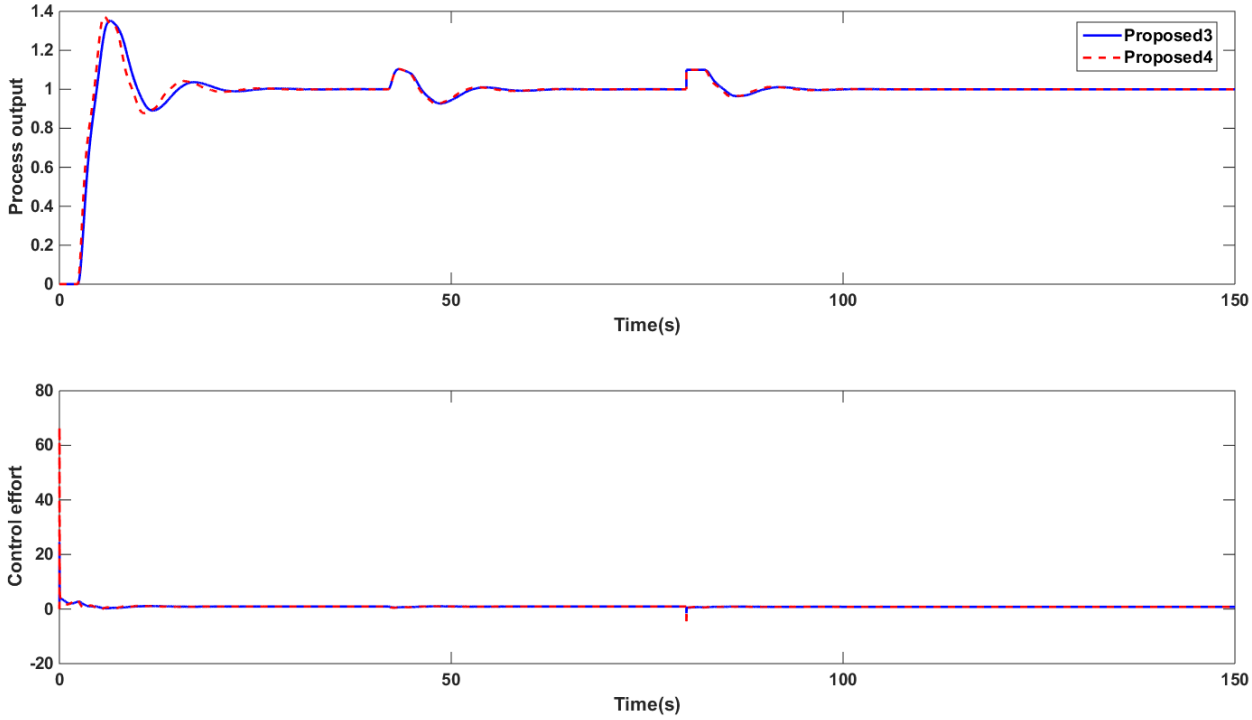

Figure 7.7 Perturbed response for Example 2

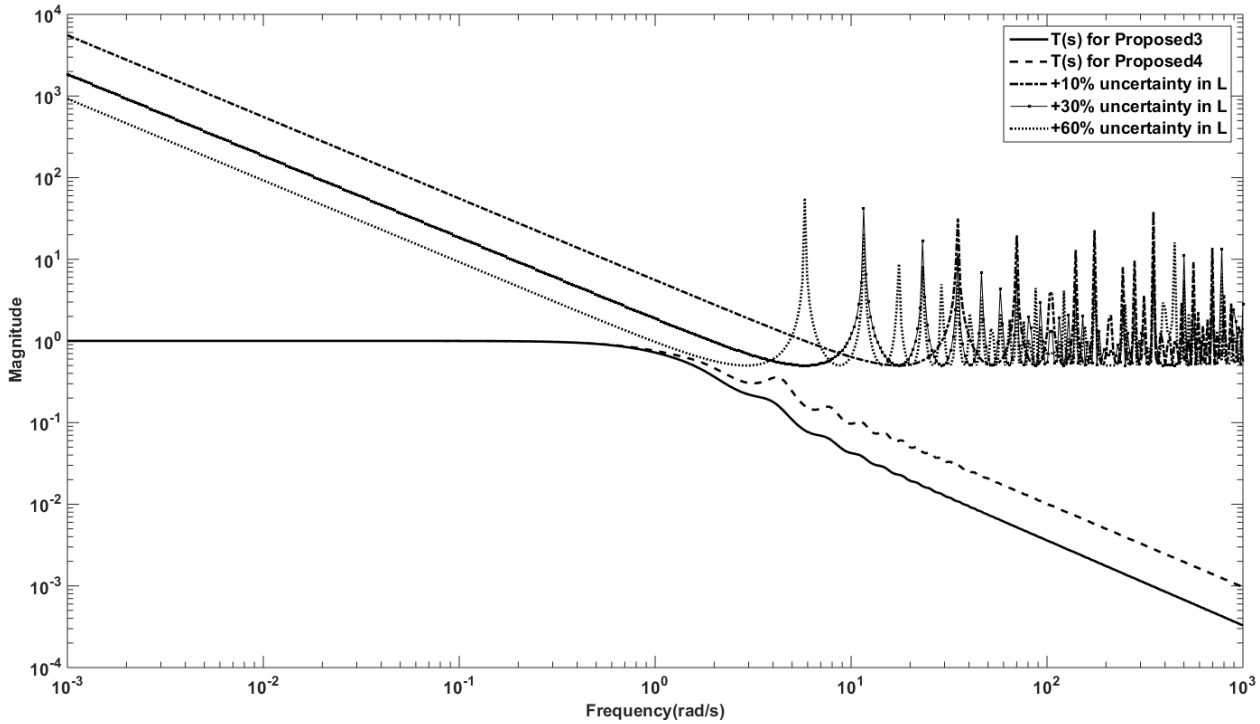

Figure 7.8 Robustness analysis of overall cascade loop for Example 2

7.5.3. Example 3

The process models (Padhan and Majhi, 2013) used here are an integrating process in the outer loop and FOPTD system in the inner loop.

$$G_1(s)=\frac{4e^{-s}}{s+1} \tag{7.39}$$

$$G_2(s)=\frac{2e^{-2s}}{s} \tag{7.40}$$

The proposed controller settings for inner loop and outer loop are given in Table 7.8. The step response of cascade loop with step disturbances d_1 of magnitude 0.05 and d_2 of magnitude 0.1 applied at t=100s and t=200s is shown in Figure 7.9. Figure 7.10 shows the response for perturbations of +10% in K and L. The performance measures for both the cases are listed in Table 7.9 and Table 7.10. It can be observed from nominal response and perturbed response that the IAE is low for inner loop with the Proposed5 method. The IAE for outer loop with the Proposed5 method is a bit high compared to Proposed6 method whereas TV is close to zero with Proposed5 method and too high with Proposed6 method with respect to nominal response. In case of perturbed response, the IAE is slightly low with Proposed5 method compared to Proposed6 method and the TV is very high with Proposed6 method. The performance measures for output white noise are listed in Table 7.10. The change of error and TV is same as observed for nominal response. The robust stability of cascade loop is illustrated in Figure 7.11. The Proposed5 method can give robust and stable performance up to an uncertainty of +100% in L whereas the Proposed6 method violates the robust stability condition after +90% uncertainty in L.

Table 7.8 Controller settings for Example 3

	Method	$\mathbf{K_p}$	$\mathbf{T_i}$	$\mathbf{T_d}$	$\boldsymbol{\beta}$	$\boldsymbol{\gamma_1}$	$\boldsymbol{\gamma_2}$	**P**	$\mathbf{M_s}$
Inner loop	Proposed5/ Proposed6	0.375	1.5	0.333	-	1.525	-	-	1.4
Outer loop	Proposed5	0.5	-	1.525	1	-	1.65	1.02	1.6
	Proposed6	0.5	-	1.525	-	-	2.11	1.02	1.6

Table 7.9 Performance measures for nominal response of Example 3

Method	**Inner loop**		**Outer loop**		
	IAE	$\mathbf{M_s}$	**IAE**	**TV**	$\mathbf{M_s}$
Proposed5	0.973	1.4	17.07	0.5406	1.6
Proposed6	1.645	1.4	16.75	278.098	1.6

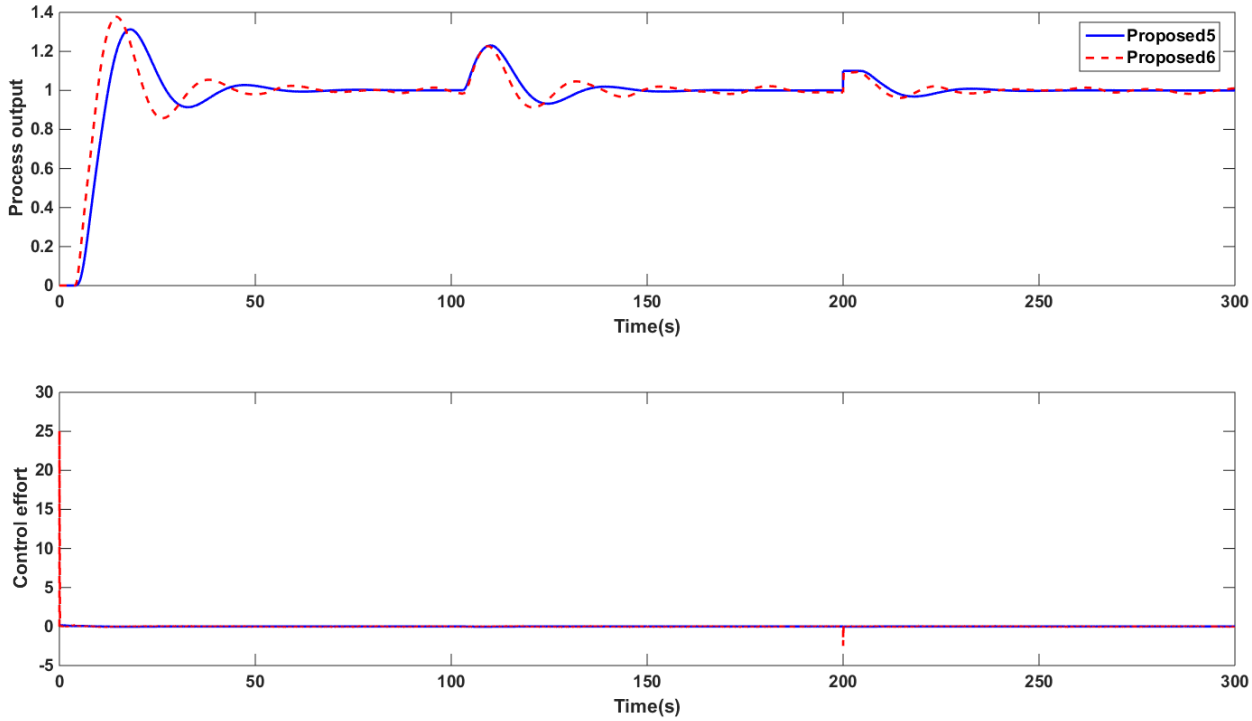

Figure 7.9 Nominal response for Example 3

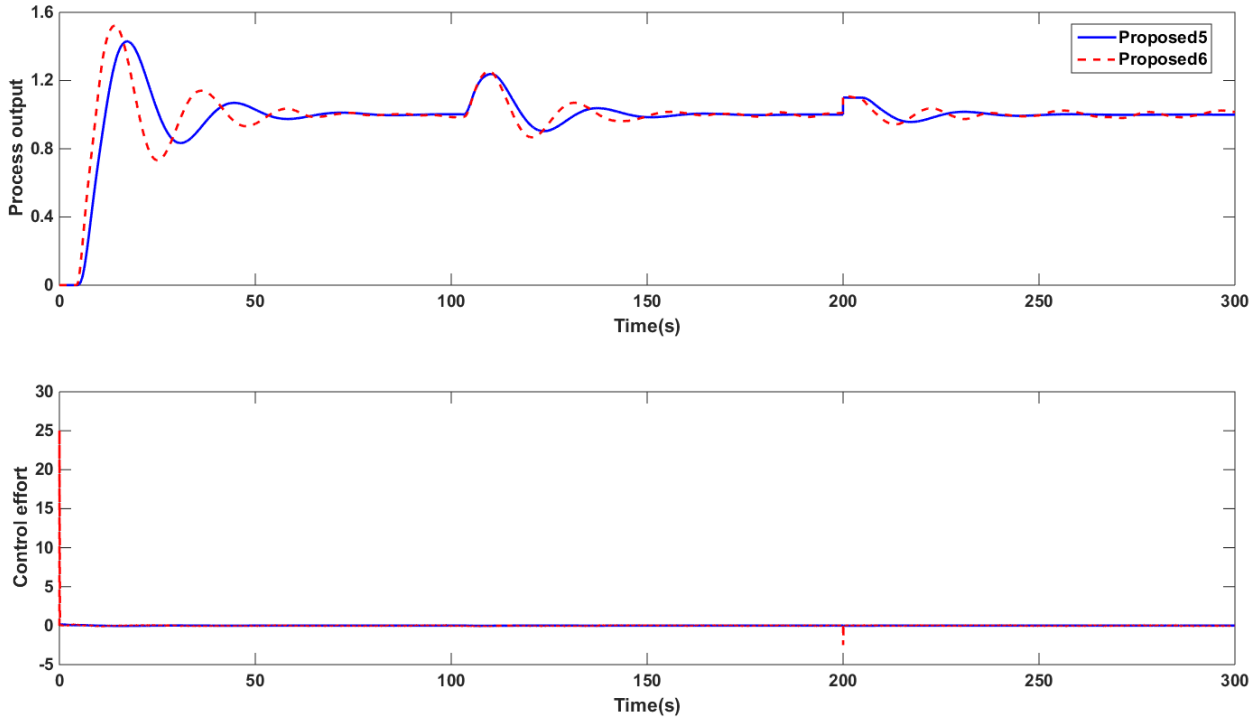

Figure 7.10 Perturbed response for Example 3

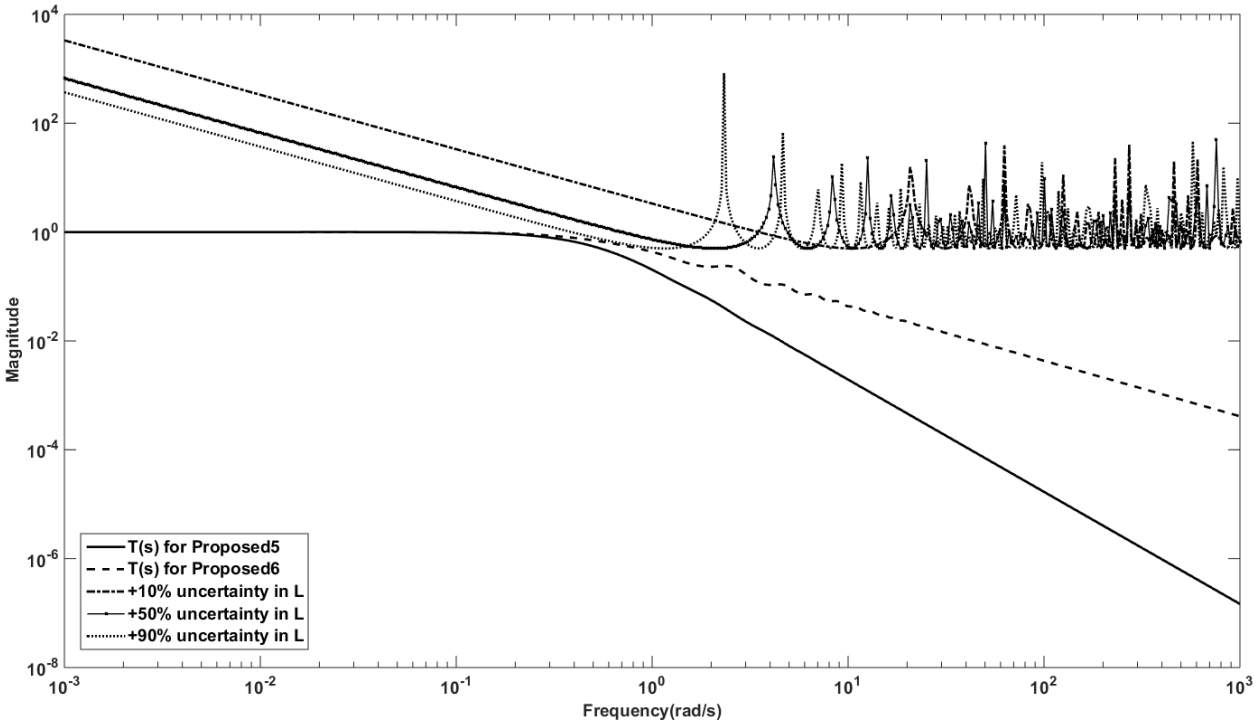

Figure 7.11 Robustness analysis of overall cascade loop for Example 3

Table 7.10 Performance measures for perturbations and measurement noise of Example 3

	Perturbed response			**Noise response**		
Method	**Inner loop**	**Outer loop**		**Inner loop**	**Outer loop**	
	IAE	**IAE**	**TV**	**IAE**	**IAE**	**TV**
Proposed5	1.09	19.64	0.608	11.53	85.02	165.514
Proposed6	1.756	20.5	282.678	393.4	84.16	30946

7.5.4. Controller fragility

The robustness delta epsilon fragility plot for all the examples is shown in Figure 7.12. The delta 20 fragility index values are listed in Table 7.11. It is observed that all the proposed controllers are nonfragile except for Proposed5 method which is fragile. Hence, it is possible to retune the proposed controllers for variation in the controller parameters.

Table 7.11 Robustness delta 20 ($RFI_{\Delta 20}$) fragility index for the three examples

Examples	**Method**	**$RFI_{\Delta 20}$**
Example1	Proposed1	0.1472
	Proposed2	0.0184
	Azar and Serrano (2014)	0.0969
Example2	Proposed3	0.447
	Proposed4	0.2705
Example3	Proposed5	0.6812
	Proposed6	0.275

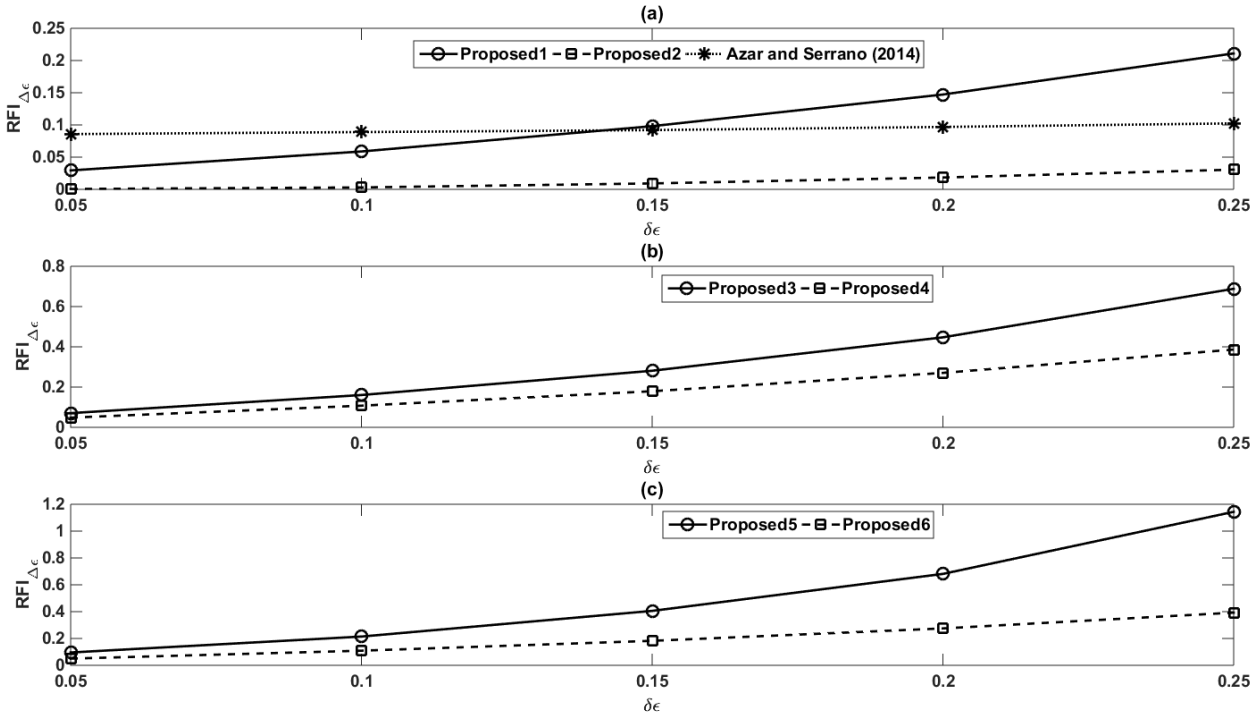

Fig 7.12 Fragility index variation for all the examples of cascade loop

7.6. Conclusions

An IMC based series cascade control system is designed for different process models in inner and outer loops. Inner loop controller is designed using integer order IMC filter. The outer loop controller is designed using fractional order IMC filter of first order and higher order for different time delay process models. Improved performance is observed with outer loop controller designed using higher order fractional IMC filter especially in terms of control effort. The performance with conventional fractional IMC filter is also good in terms of IAE but the control effort is very high. Also, the similar enhanced performance is observed for perturbations in process parameters and with measurement noise. The robust stability analysis is carried out with multiplicative uncertainties in the process parameters and it was found that the controller designed with higher order fractional IMC filter is more robust compared to the controller designed using conventional fractional IMC filter. The outer loop controllers are nonfragile except for Proposed3 method which is fragile.

Chapter 8

Conclusions and Future work

8. Conclusions and Future work

General Conclusions

Apart from the specific conclusions made at the end of each chapter of this dissertation, the general conclusions of this thesis are drawn as following:

A systematic design procedure is developed to design the novel fractional controller based on IMC for different classes of integer (second order, integrating) and non-integer order systems with time delay. A fractional filter IMC-PID controller is designed using conventional fractional IMC filter plus first order pade's approximation for time delay. The design method is improved by considering higher order fractional IMC filter structures and higher order pade's approximation for time delay. The improvement is carried out through a systematic design procedure for the robustness (M_s) specification based on minimum IAE. An optimum higher order fractional IMC filter structure is identified for each and every time delay system using the systematic procedure. To quantify the superiority of the proposed controllers, four performance metrics, ISE, IAE, ITAE and TV have been used.

The closed loop performance with the proposed controller is illustrated for various numerical examples representing the integer and non-integer order systems. It is observed that there is a significant improvement in the performance of closed-loop system. The improvement is evident in terms of low values of errors. The errors are decreasing with increase in the order of Pade's approximation for time delay but the control effort is slightly increasing. Robustness analysis is performed for variations in the process parameters and robustness analysis is carried out using sensitivity functions. The performance is also observed for noise in the measurement. It is found that the proposed fractional filter controllers for different time delay systems are giving robust performance for parametric uncertainties and improved performance is seen even with output noise.

Fragility analysis is carried out for uncertainties in the controller parameters to know the deterioration of closed loop performance and robustness. It is observed that the proposed controllers for integer order time delay systems are either resilient or nonfragile assuring robust performance for +20% uncertainty in the controller parameters. In case of the proposed controllers

designed for NIOPTD systems both nonfragile and fragile nature is observed. Hence, care should be taken while designing the fractional filter FOPID controller for NIOPTD systems.

The proposed method is extended to design a series cascade control system for different process models using first order and higher order fractional IMC filter structures. Improved performance is observed with outer loop controller designed using higher order fractional IMC filter especially in terms of TV.

Perspective of Future work

The present work can be extended for further investigation in the following areas:

1. Experimental evaluation of the proposed design method
   The proposed method can be validated through experiments via chemical processes i.e., CSTR and p^H neutralization processes etc.

2. Optimization based design of optimal fractional filter PID controller.
   It would be of interest to consider a multi objective dynamic optimization approach, where both robustness and noise sensitivity can be used as constraints to enhance the performance.

3. Performance evaluation of proposed method on unstable systems
   The present work considered stable single input single output systems for controller design. The proposed method can be extended to unstable integer and fractional order systems; multiple input multiple output systems consisting of integer and fractional order models.

4. Performance evaluation for advanced control strategies (Feed forward control) using the proposed analytical design approach.

References

Alagoz, B.B., Tan, N., Deniz, F.N., Keles, C., 2015. Implicit disturbance rejection performance analysis of closed loop control systems according to communication channel limitations. IET Control Theory and Applications, 9, 2522–2531.

Alfaro, V.M., 2007. PID controllers' fragility. ISA Transactions, 46, 555-559.

Alfaro, V.M., Vilanova, R. and Arrieta, O., 2008, December. Two-degree-of-freedom PI/PID tuning approach for smooth control on cascade control systems. In Decision and Control, 2008. CDC 2008. 47th IEEE Conference on (pp. 5680-5685). IEEE.

Alfaro V.M., Vilanova R, Arrieta O. Fragility analysis of PID controllers. In: Proceedings IEEE international conference on control applications, St. Petersburg, Russia; 2009. p. 725–30.

Alfaro V.M., Vilanova, R. Fragility evaluation of PI and PID controllers tuning rules. In: Vilanova R, Visioli A, editors. PID control in the third millennium - lessons learned and new approaches. London, UK: Springer; 2012. p. 349–380.

Astrom, K.J., Hagglund, T., 1995. PID controllers: theory, design, and tuning. ISA Research Triangle Park, NC.

Atherton, D. P., Tan, N., Yüce, A., 2014. Methods for computing the time response of fractional-order systems. IET Control Theory & Applications, 9(6), 817-830.

Azar, A.T., Serrano, F.E., 2014. Robust IMCPID tuning for cascade control systems with gain and phase margin specifications. Neural Computing and Applications, 25, 983-995.

Barbosa, R.S., Machado, J.T., Galhano, A.M., 2007. Performance of fractional PID algorithms controlling nonlinear systems with saturation and backlash phenomena. Journal of Vibration and Control, 13, 1407–1418.

Bettayeb, M., Mansouri, R., 2014. Fractional IMC-PID-filter controllers design for non-integer order systems. Journal of Process Control, 24, 261-271.

Bongulwar, M.R., Patre, B.M., 2017. Stability regions of closed loop system with one non-integer plus time delay plant by fractional order PID controller. International Journal of Dynamics and Control, 5, 159-167.

Brambilla, A., Semino, D., 1992. Nonlinear filter in cascade control schemes. Industrial & Engineering Chemistry Research, 31(12), 2694-2699.

Chen, Y., Bhaskaran, T., Xue, D., 2008. Practical Tuning Rule Development for Fractional Order Proportional and Integral controllers. Journal of Computational and Nonlinear Dynamics, 3, 0214031-8.

Chen, Y., Petras, I., Xue, D., 2009. Fractional order control - A tutorial. 2009 American Control Conference, St. Louis, MO, 1397-1411.

Chen, D., Seborg, D.E., 2002. PI/PID Controller Design Based on Direct Synthesis and Disturbance Rejection. Industrial & Engineering Chemistry Research, 41, 4807–4822.

Das, S., 2011. Functional fractional calculus. Springer Science & Business Media.

Das, S., Pan, I., Das, S., 2013. Performance comparison of optimal fractional order hybrid fuzzy PID controllers for handling oscillatory fractional order processes with dead time. ISA transactions, 52(4), 550-566.

Das, S., Saha, S., Das, S., Gupta, A., 2011. On the selection of tuning methodology of FOPID controllers for the control of higher order processes. ISA Transactions, 50, 376-388.

Dey, C., Mudi, R.K., 2009. An improved auto-tuning scheme for PID controllers. ISA Transactions, 48, 396–409.

Feliu-Batlle, V., Rivas-Perez, R., Castillo-Garcia, F., 2009. Fractional order controller robust to time delay variations for water distribution in an irrigation main canal pool. Computers and Electronics in Agriculture, 69, 185–197.

Fruehauf, P.S., Chien, I.L., Lauritsen, M.D., 1994. Simplified IMC-PID tuning rules. ISA Transactions, 33, 43-59.

García, P., Albertos, P., 2013. Robust tuning of a generalized predictor-based controller for integrating and unstable systems with long time-delay. Journal of Process Control, 23(8), 1205-1216.

Ho M-T. Non-fragile PID controller design. In: Proceedings of IEEE international conference on decision and control, Sydney, Australia; 2000. p. 4903–8.

Horn, I.G., Arulandu, J.R., Gombas, C.J., VanAntwerp, J.G., Braatz, R.D., 1996. Improved filter design in internal model control. Industrial & Engineering Chemistry Research, 35, 3437-3441.

Huang, C.E., Li, D.H., Su, Y., 2011. Simulation and robustness studies on an inverted pendulum. proceedings of the 30th Chinese Control conference, Yantai, 615-619.

Huang, H.P., Chien, I.L., Lee, Y.C., Wang, G.B., 1998. A simple method for tuning cascade control systems. Chemical Engineering Communications, 165(1), 89-121.

Hui-fang, W., Qiu-sheng, H., Zhi-cheng, Z., Jing-gang, Z., 2015. A design method of fractional order $PI^{\lambda}D^{\mu}$ controller for higher order systems. In 34th Chinese Control Conference (CCC), Hangzhou, China, pp. 272-277.IEEE.

Isaksson, A., Graebe, S., 1999. Analytical PID parameter expressions for higher order systems. Automatica, 35, 1121-1130.

Jeng, J.-C., Tseng, W.-L., Chiu, M.-S., 2014. A one step tuning method for PID controllers with robustness specification using plant step-response data. Chemical Engineering Research and Design, 92, 545–558.

Keel, L.H., Bhattacharyya, S.P., 1997. Robust, fragile, or optimal?. IEEE Transactions on Automatic Control, 42(8), 1098–1105.

Khalil, H. K., 1996. Nonlinear Systems. Prentice Hall, New Jersey.

Krishnaswamy, P.R., Rangaiah, G.P., Jha, R.K., Deshpande, P.B., 1990. When to use cascade control. Industrial & Engineering Chemistry Research, 29(10), 2163-2166.

Kumar, D.S., Sree, R.P., 2016. Tuning of IMC based PID controllers for integrating systems with time delay. ISA Transactions, 63, 242-255.

Kuo, B. C., 1991. Automatic control systems. Prentice-Hall.

Kwakernaak, H., Sivan, R., 1972. Linear Optimal Control Systems. Wiley, Newyork.

Lee, J., Cho, W., Edgar, T.F., 2013. Simple analytic PID controller tuning rules revisited. Industrial & Engineering Chemistry Research, 53, 5038–5047.

Lee, Y., Lee, J., Park, S., 2000. PID controller tuning for integrating and unstable processes with time delay. Chemical Engineering Science, 55(17), 3481-3493.

Lee, Y., Park, S., Lee, M., 1998. PID controller tuning to obtain desired closed loop responses for cascade control systems. Industrial & Engineering Chemistry Research, 37, 1859-1865.

Lee, Y., Park, S., Lee, M., Brosilow, C., 1998. PID controller tuning for desired closed-loop responses for SI/SO systems. AIChE Journal, 44, 106–115.

Leva, A., Donida, F., 2009. Autotuning in cascaded systems based on a single relay experiment. Journal of Process Control. 19(5), 896-905.

Leva, A., Marinelli, A., 2009. Comparative Analysis of Some Approaches to the Autotuning of Cascade Controls. Industrial & Engineering Chemistry Research, 48(12), 5708-5718.

Li, D., Liu, L., Jin, Q., Hirasawa, K., 2015. Maximum sensitivity based fractional IMC–PID controller design for non-integer order system with time delay. Journal of Process Control, 31, 17-29.

Lin, M.G., Lakshminarayanan, S., Rangaiah, G. P., 2008. A comparative study of recent/popular PID tuning rules for stable, first-order plus dead time, single–input single-output processes. Industrial & Engineering Chemistry Research, 47, 344-368.

Lundberg, K.H., Barton, T.W., 2010. History of inverted pendulum systems. IFAC Proceedings Volumes, 42, 131-135.

Luo, Y., Chen, Y., 2009. Fractional order [proportional derivative] controller for a class of fractional order systems. Automatica, 45, 2446-2450.

Maamar, B., Rachid, M., 2014. IMC-PID-fractional-order-filter controllers design for integer order systems. ISA Transactions, 53(5), 1620-1628.

Maciejowski, J. M., 1989. Multivariable feedback design, Electronic Systems Engineering Series, Addison-Wesley, Wokingham, England.

Madhuranthakam, C., Elkamel, A., Budman, H., 2008. Optimal tuning of PID controllers for FOPTD, SOPTD and SOPTD with lead processes. Chemical Engineering and Processing: Process Intensification, 47, 251–264.

Deepyaman, M., Ayan, A., Mithun, C., Amit, K. and Ramdoss, J., 2008. Tuning PID and $PI^{\lambda}D^{\delta}$ controllers using the integral time absolute error criterion. In 4th International Conference on Information and Automation for Sustainability (ICIAFS), Colombo, Sri Lanka, 457-462.

Malwatkar, M., Sonawane, S., Waghmare, L., 2009. Tuning PID controllers for higher-order oscillatory systems with improved performance. ISA Transactions, 48, 347-353.

Miller, K.S., Ross, B., 1993. An introduction to the fractional calculus and fractional differential equations. A Wiley-Inderscience Publication.

Monje, C.A., Vinagre, B.M., Feliu, V., Chen, Y., 2008. Tuning and auto-tuning of fractional order controllers for industry applications. Control Engineering Practice, 16, 798-812.

Morari, M., Zafiriou, E., 1989. Robust process control, Prentice hall, Englewood Cliffs, NJ.

Padhan, D.G., Majhi, S., 2013. Enhanced cascade control for a class of integrating processes with time delay. ISA Transactions, 52(1), 45-55.

Padula F., Visioli A., 2011. Tuning rules for optimal PID and fractional order PID controllers. Journal of Process Control, 21, 69-81.

Padula, F., Visioli, A., 2014. Advances in robust fractional control. Springer, London, UK.

Padula, F., Visioli, A., 2015. Advances in Robust Fractional Control. Department of Mechanical and Industrial Engineering, University of Brescia, Italy, 2015.

Padula, F., Visioli, A., 2016. On the fragility of fractional-order PID controllers for FOPDT processes. ISA Transactions, 60, 228-243.

Panagopoulos, H., Astrom, K.J., Hagglund, T., 2002. Design of PID controllers based on constrained optimization. IEEE Proceedings of Control Theory and Applications, 149, 32-40.

Pan I., Das S., 2013. Model Reduction of Higher Order Systems in Fractional Order Template. In: Intelligent Fraction al Order Systems and Control. Springer, Berlin Heidelberg, 241-256.

Panda, R.C., Yu, C.-C., Huang, H.-P., 2004. PID tuning rules for SOPDT systems: Review and some new results. ISA Transactions, 43, 283–295.

Panda, R.C., 2009. Synthesis of PID controller for unstable and integrating processes. Chemical Engineering Science, 64(12), 2807-2816.

Podlubny, I., 1994. Fractional-order systems and fractional-order controllers. Inst Exp Phys Slovak Acad Sci, Kosice.

Podlubny, I., 1999. Fractional-order systems and $PI^{\lambda}D^{\mu}$ controllers. IEEE Transactions on Automatic Control, 44, 208–214.

Raja, G.L., Ali, A., 2017. Series cascade control: An outline survey. 2017 Indian Control Conference (ICC), Guwahati, 409-414.

Rao, A.S., Rao, V., Chidambaram, M., 2009. Direct synthesis-based controller design for integrating processes with time delay. Journal of Franklin Institute, 346, 38–56.

Rao, C.N., Rao, A.S., Sree, R.P., 2011. Design of PID controllers for pure integrator systems with time delay. International Journal of Applied Science and Engineering, 9(4), 241-260.

Rao, C.N., Sree, R.P, 2010. IMC Based Controller Design for Integrating Systems with Time Delay. Indian Chemical Engineer, 52(3), 194-218.

Rice, B., Cooper, D., Design and tuning of PID controllers for integrating (non-self regulating) processes. TECHNICAL PAPERS-ISA, 422, 437-448.

Seborg, D. E., Edgar, T. F., Mellichamp, D. A., 2004. Process Dynamics and Control, Second Edition, John Wiley and Sons, New York.

Shah, P., Agashe, S., 2016. Review of fractional PID controller. Mechatronics, 38, 29-41.

Shamsuzzoha, M., Lee, M., 2007. IMC- PID controller design for improved disturbance rejection of time-delayed processes. Industrial & Engineering Chemistry Research, 46, 2077–2091.

Shamsuzzoha, M., Lee, M., 2008. Design of advanced PID controller for enhanced disturbance rejection of second order processes with time delay. AIChE Journal, 54, 1526–1536.

Shamsuzzoha, M., 2013. Closed-loop PI/PID controller tuning for stable and integrating process with time delay. Industrial & Engineering Chemistry Research, 52, 12973-12992.

Shamsuzzoha, M., 2015. A unified approach for proportional-integral-derivative controller design for time delay processes. Korean Journal of Chemical Engineering, 32, 583-596.

Shamsuzzoha, M., Skogestad, S., 2010. The setpoint overshoot method: A simple and fast closed-loop approach for PID tuning. Journal of Process Control, 20(10), 1220-1234.

Shen, J.C., 2002. New tuning method for PID controller. ISA Transactions, 41, 473-484.

Silva, G.J., Datta, A., Bhattacharyya, S.P., 2007. PID controllers for time-delay systems. Springer Science & Business Media.

Skogestad, S., 2003. Simple analytic rules for model reduction and PID controller tuning. Journal of Process Control, 13, 291–309.

Song, S., Cai, W., Wang, Y.G., 2003. Auto-tuning of cascade control systems. ISA Transactions, 42(1), 63-72.

Srivastava, S., Misra, A., Thakur, S., Pandit, V., 2016. An optimal PID controller via LQR for standard second order plus time delay systems. ISA Transactions, 60, 244–253.

Srivastava, S., Pandit, V.S., 2016. A PI/PID controller for time delay systems with desired closed loop time response and guaranteed gain and phase margins. Journal of Process Control, 37, 70-77.

Tavakoli-Kakhki, M., Haeri, M., 2011. Fractional order model reduction approach based on retention of the domi nant dynamics: Application in IMC based tuning of FOPI and FOPID controllers. ISA Transactions, 50, 432-442.

Thyagarajan, T., Yu, C.C., 2003. Improved autotuning using the shape factor from relay feedback. Industrial & Engineering Chemistry Research, 42, 4425-4440.

Vajta, M. (2000, September). Some remarks on Padé-approximations. In Proceedings of the 3rd TEMPUS-INTCOM Symposium (Vol. 2).

Valerio, D., da Costa, J.S., 2006. Tuning of fractional PID controllers with Ziegler Nichols-type rules. Signal Processing, 86, 2771-2784.

Veronesi, M., Visioli, A., 2011. Simultaneous closed-loop automatic tuning method for cascade controllers. IET Control Theory and Applications, 5(2), 263-270.

Vilanova, R., Visioli, A., 2012. PID control in the third millennium, Springer, London.

Vinopraba, T., Sivakumaran, N., Narayanan, S., Radhakrishnan, T.K., 2012. Design of internal model control based fractional order PID controller. Journal of Control Theory and Applications, 10, 297-302.

Vivek, S., Chidambaram, M., 2013. A simple method of tuning cascade controllers. Journal of Indian Institute of Science, 84(6), 233-242.

Vu, T.N.L., Le Hieu Giang, L.L., 2016. Fractional-Order PI Controller Tuning Rules for Cascade Control System. World Academy of Science, Engineering and Technology, International Journal of Electrical, Computer, Energetic, Electronic and Communication Engineering. 10(7), 882-886.

Vu, T.N.L., Linh, L., Chuong, V.L., 2017, July. Advanced IMC-PID controller design for the disturbance rejection of first order plus time delay processes. In System Science and Engineering (ICSSE), 2017 International Conference on (pp. 279-283). IEEE.

Wang, J.J., 2011. Simulation studies of inverted pendulum based on PID controllers. Simulation Modeling Practice and Theory, 19, 440-449.

Wang, C., Yin, G., Liu, C., Fu, W., 2016. Design and simulation of inverted pendulum system based on the fractional PID controller. 2016 IEEE 11th Conference on Industrial Electronics and Applications (ICIEA), Hefei, 1760-1764.

Wang, Q., Lu, C., Pan, W., 2016. IMC PID controller tuning for stable and unstable processes with time delay. Chemical Engineering Research and Design, 105, 120–129.

Weigand, W.A., Kegerreis, J. E., 1972. Comparison of controller-setting techniques as applied to second-order dead time processes. Industrial & Engineering Chemistry Process Design and Development, 11(1), 86-90.

Yang, J.H., Shim, S.Y., Seo, J.H., Lee, Y.S., 2009. Swing up control for an inverted pendulum with restricted cart rail length. International journal of Control, Automation and Systems, 7, 674-680.

Yeroglu, C., Tan, N., 2011. Note on fractional-order proportional–integral–differential controller design. IET Control Theory and Applications, 5, 1978-1989.

Zhou, K., Doyle., J.C. 1998. Essentials of robust control. Prentice hall, NJ.

Appendix A

Program for obtaining the closed loop response of Example 1 (Chapter 3.1)

```
%-------------------------------------------------Closed loop response-------------------------------------------
clc
sim 'secondorderexample';
load proposed
subplot(2,1,1)
plot(a(1,:),a(2,:),'r')
hold on
sim 'secondorderexample';
load wang
subplot(2,1,1)
plot(b(1,:),b(2,:),'b')
hold on
sim 'secondorderexample';
load setpoint
subplot(2,1,1)
plot(c(1,:),c(2,:),'k')
hold off
xlabel('Time(s)')
ylabel('Process output')
%-----------------------------------------------------Control effort-----------------------------------------------
sim 'secondorderexample';
load proposedtv
subplot(2,1,2)
plot(A(1,:),A(2,:),'r')
hold on
sim 'secondorderexample';
load wangtv
subplot(2,1,2)
plot(B(1,:),B(2,:),'b')
hold off
xlabel('Time(s)')
ylabel('Control effort')
%-------------------------------------------------------------TV-------------------------------------------------
sim 'secondorderexample';
load proposed1
TV=sum(abs(diff(proposed1)))
sim 'secondorderexample';
load proposed
TV=sum(abs(diff(proposed)))
```

Program for obtaining the magnitude plot (robust stability)

```
%-------------------------------------------------Proposed-------------------------------------------------------
clear all
clc
ww=logspace(-3,3,500);
for i=1:500
   w=ww(i);
```

```
    xx = j*w;
    Gp(i) = 1*exp(-2*xx)/(0.7*xx^2+1.7*xx+1);
    Gc(i) = (1.7+(1/xx)+0.6998*xx)*((xx+1)/(2*xx^1.02+2*xx^0.02+2));
    T(i) = abs((Gc(i)*Gp(i))/(1+Gc(i)*Gp(i)));
end
loglog(ww,T,'r')
hold on;
%-------------------------------------------------time delay variation-----------------------------------------------
ww=logspace(-3,3,500);
for i=1:500
    w=ww(i);
    xx = j*w;
    G(i)=1/(exp(0.2*xx)-1)
    T(i) = abs(G(i));
end
loglog(ww,T,'g')
ylabel('Magnitude', 'FontSize',12);
xlabel('Frequency(rad/s)', 'FontSize',12);
hold off;
```

Simulink diagram for Example 1

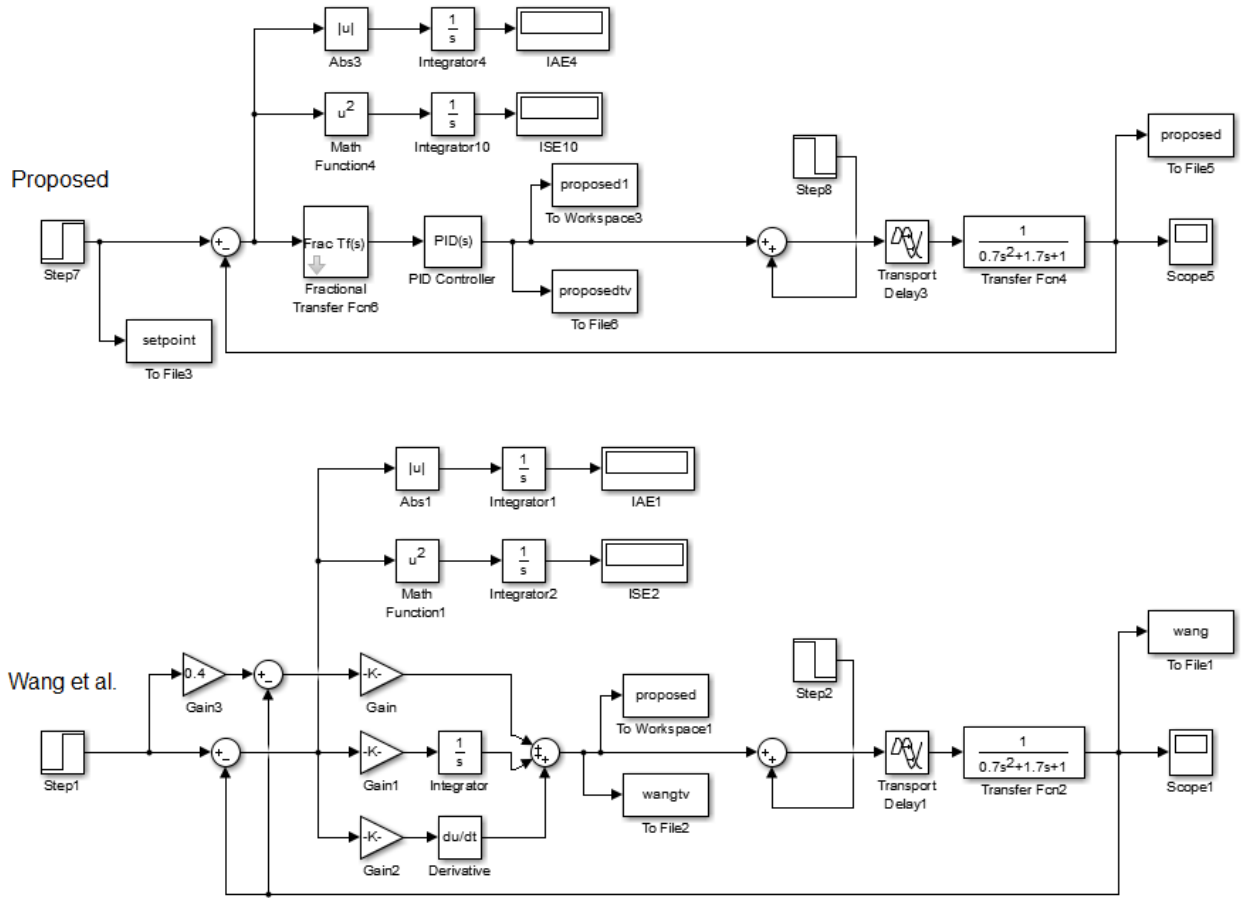

Program for obtaining the closed loop response (Chapter 3.2)

```
%-----------------------------------------------Closed loop response-----------------------------------------------
clc
sim 'invertedpendulum';
load wang
subplot(2,1,1)
plot(a(1,:),a(2,:),'k--')
hold on
sim 'invertedpendulum';
load wang1
subplot(2,1,1)
plot(b(1,:),b(2,:),'b-.')
hold on
sim 'invertedpendulum';
load wang2
subplot(2,1,1)
plot(c(1,:),c(2,:),'m:')
hold on
sim 'invertedpendulum';
load proposed
subplot(2,1,1)
plot(d(1,:),d(2,:),'r')
hold on
sim 'invertedpendulum';
load setpoint
subplot(2,1,1)
plot(e(1,:),e(2,:),'k')
hold off
xlabel('Time(s)')
ylabel('Process output')
%-----------------------------------------------------control effort-----------------------------------------------
sim 'invertedpendulum';
load wangtv
subplot(2,1,2)
plot(A(1,:),A(2,:),'k--')
hold on
sim 'invertedpendulum';
load wang1tv
subplot(2,1,2)
plot(B(1,:),B(2,:),'b-.')
hold on
sim 'invertedpendulum';
load wang2tv
subplot(2,1,2)
plot(C(1,:),C(2,:),'m:')
hold on
sim 'invertedpendulum';
load proposedtv
subplot(2,1,2)
plot(D(1,:),D(2,:),'r')
```

hold off
xlabel('Time(s)')
ylabel('Control effort')

Simulink diagram

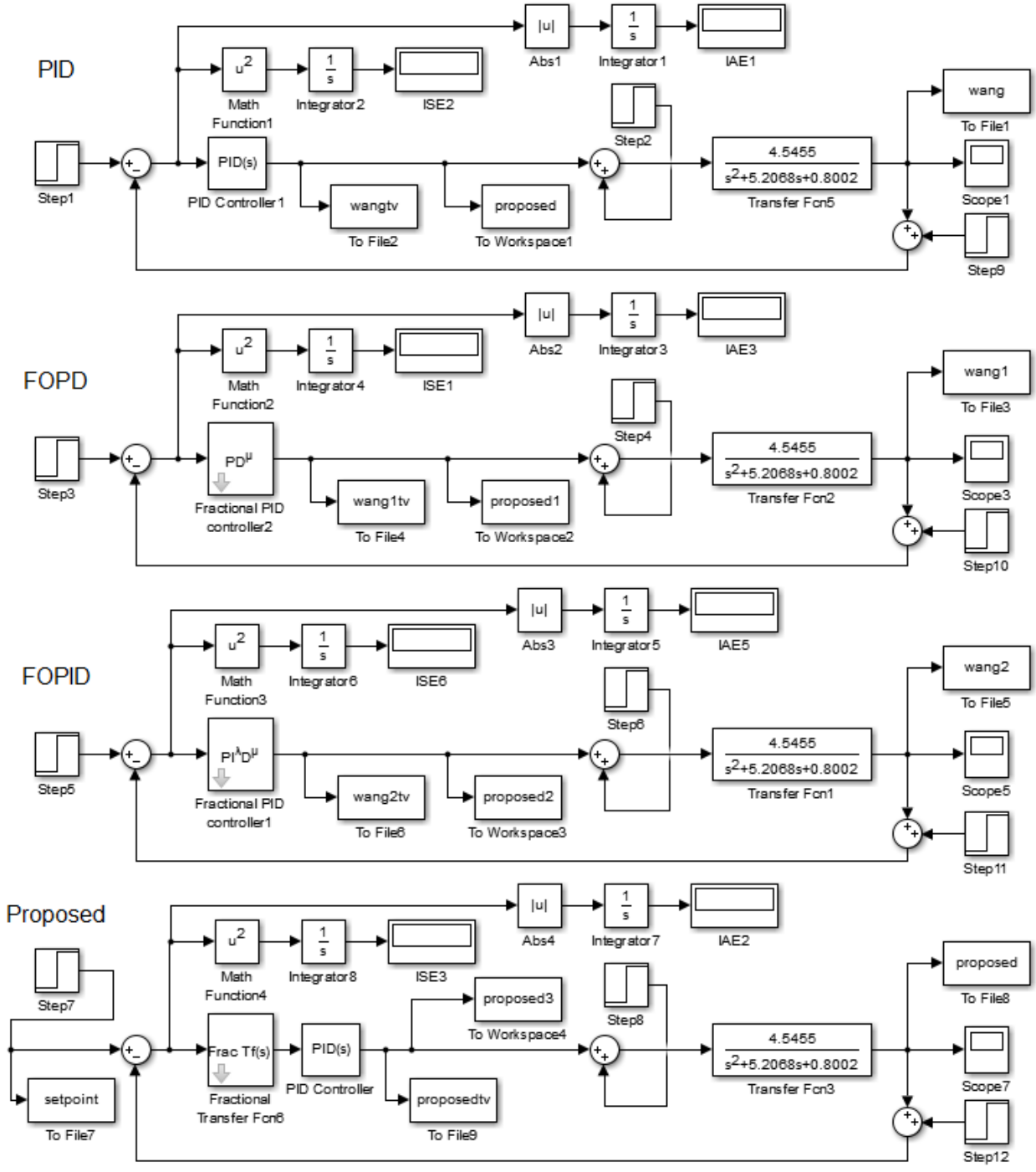

Appendix B

Program for obtaining the closed loop response Example 1

```
%-------------------------------------------------Closed loop response-------------------------------------------------
sim 'SOPTDexample1finalrevision';
load proposed
subplot(2,1,1)
plot(a(1,:),a(2,:),'r-.','LineWidth',1)
hold on
sim 'SOPTDexample1finalrevision';
load proposed1
subplot(2,1,1)
plot(b(1,:),b(2,:),'r--','LineWidth',1)
hold on
sim 'SOPTDexample1finalrevision';
load proposed2
subplot(2,1,1)
plot(c(1,:),c(2,:),'b','LineWidth',1)
hold on
sim 'SOPTDexample1finalrevision';
load proposed3
subplot(2,1,1)
plot(f(1,:),f(2,:),'b--','LineWidth',1)
hold on
sim 'SOPTDexample1finalrevision';
load proposedconventional
subplot(2,1,1)
plot(e(1,:),e(2,:),'g','LineWidth',1)
hold on
sim 'SOPTDexample1finalrevision';
load wang
subplot(2,1,1)
plot(d(1,:),d(2,:),'k','LineWidth',1)
hold on
sim 'SOPTDexample1finalrevision';
load setpoint
subplot(2,1,1)
plot(g(1,:),g(2,:),'k--','LineWidth',0.5)
hold off
xlabel('Time(s)')
ylabel('Process output')
%-----------------------------------------------------Control effort-----------------------------------------------
sim 'SOPTDexample1finalrevision';
load proposedtv
subplot(2,1,2)
plot(A(1,:),A(2,:),'r-.','LineWidth',1)
hold on
sim 'SOPTDexample1finalrevision';
load proposedtv1
subplot(2,1,2)
```

```
plot(B(1,:),B(2,:),'r--','LineWidth',1)
hold on
sim 'SOPTDexample1finalrevision';
load proposedtv2
subplot(2,1,2)
plot(C(1,:),C(2,:),'b','LineWidth',1)
hold on
sim 'SOPTDexample1finalrevision';
load wangtv
subplot(2,1,2)
plot(D(1,:),D(2,:),'k','LineWidth',1)
hold on
sim 'SOPTDexample1finalrevision';
load proposedtvconventional
subplot(2,1,2)
plot(E(1,:),E(2,:),'g','LineWidth',1)
hold on
sim 'SOPTDexample1finalrevision';
load proposedtv3
subplot(2,1,2)
plot(F(1,:),F(2,:),'m','LineWidth',1)
hold off
xlabel('Time(s)')
ylabel('Control effort')
%------------------------------------------------------------TV-----------------------------------------------------
sim 'SOPTDexample1finalrevision';
load proposed4
TV=sum(abs(diff(proposed4)))
sim 'SOPTDexample1finalrevision';
load proposed3
TV=sum(abs(diff(proposed3)))
sim 'SOPTDexample1finalrevision';
load proposed1
TV=sum(abs(diff(proposed1)))
sim 'SOPTDexample1finalrevision';
load proposed
TV=sum(abs(diff(proposed)))
sim 'SOPTDexample1finalrevision';
load proposed2
TV=sum(abs(diff(proposed2)))
sim 'SOPTDexample1finalrevision';
load proposed5
TV=sum(abs(diff(proposed5)))
```

Program for obtaining the magnitude plot (robust stability)

```
%-----------------------------------------------------Proposed1-----------------------------------------------------
clear all
clc
ww=logspace(-3,3,500);
for i=1:500
   w=ww(i);
```

```
   xx = j*w;
   Gp(i) = 1*exp(-2*xx)/(0.7*xx^2+1.7*xx+1);
   Gc(i) = (1.7+(1/xx)+0.7*xx)*((0.3658*xx^2+1.3658*xx+1)/ (1.3572*xx^2.04
         +1.3572*xx^1.04+2.33*xx^1.02+0.3658*xx+2.33*xx^0.02+1.6342));
   T(i) = abs((Gc(i)*Gp(i))/(1+Gc(i)*Gp(i)));
end
subplot(2,1,1)
loglog(ww,T,'r-.')
hold on;
%-----------------------------------------------------Proposed2-----------------------------------------------------
ww=logspace(-3,3,500);
for i=1:500
   w=ww(i);
   xx = j*w;
   Gp(i) = 1*exp(-2*xx)/(0.7*xx^2+1.7*xx+1);
   Gc(i) = (1.7+(1/xx)+0.6998*xx)*((0.1601*xx^3+0.8135*xx^2+1.4802*xx+1)/
         (0.3072*xx^3.04 +0.9216*xx^2.04+0.64*xx^2.02-0.1601*xx^2 +0.9216*xx^1.04
         +1.92*xx^1.02+0.4802*xx+1.92*xx^0.02+1.5198));
   T(i) = abs((Gc(i)*Gp(i))/(1+Gc(i)*Gp(i)));
end
subplot(2,1,1)
loglog(ww,T,'r--')
hold on;
%-----------------------------------------------------Proposed3-----------------------------------------------------
ww=logspace(-3,3,500);
for i=1:500
   w=ww(i);
   xx = j*w;
   Gp(i) = 1*exp(-2*xx)/(0.7*xx^2+1.7*xx+1);
   Gc(i) = (1.7+(1/xx)+0.7*xx)*((3.884*xx^4+25.478*xx^3+70.956*xx^2+101.13*xx+60)/
         (7.22*xx^4.04+32.49*xx^3.04+15.2*xx^3.02+64.98*xx^2.04+68.4*xx^2.02
         +2.174*xx^2+54.15*xx^1.04+136.8*xx^1.02+47.304*xx+114*xx^0.02+90.87));
   T(i) = abs((Gc(i)*Gp(i))/(1+Gc(i)*Gp(i)));
end
subplot(2,1,1)
loglog(ww,T,'b')
hold on;
%-----------------------------------------------------Proposed4-----------------------------------------------------
ww=logspace(-3,3,500);
for i=1:500
   w=ww(i);
   xx = j*w;
   Gp(i) = 1*exp(-2*xx)/(0.7*xx^2+1.7*xx+1);
   Gc(i) = (1.7+(1/xx)+0.7*xx)*((1.7696*xx^3+7.5392*xx^2+10.6544*xx+6)/
         (4.2436*xx^3.04+8.4872*xx^2.04+8.24*xx^2.02+6.3654*xx^1.04+16.48*xx^1.02
         +5.7696*xx+12.36*xx^0.02+9.3456));
   T(i) = abs((Gc(i)*Gp(i))/(1+Gc(i)*Gp(i)));
end
subplot(2,1,1)
loglog(ww,T,'b--')
hold on;
```

```
%-----------------------------------------------------Proposed-----------------------------------------------
ww=logspace(-3,3,500);
for i=1:500
   w=ww(i);
   xx = j*w;
   Gp(i) = 1*exp(-2*xx)/(0.7*xx^2+1.7*xx+1);
   Gc(i) = (1.7+(1/xx)+0.7*xx)*((xx+1)/(1.635*xx^1.02+1.635*xx^0.02+2));
   T(i) = abs((Gc(i)*Gp(i))/(1+Gc(i)*Gp(i)));
end
subplot(2,1,1)
loglog(ww,T,'g')
hold on;
%-------------------------------------------------time delay variation-----------------------------------------
ww=logspace(-3,3,500);
for i=1:500
   w=ww(i);
   xx = j*w;
   G(i)=1/(exp(0.2*xx)-1)
   T(i) = abs(G(i));
end
subplot(2,1,1)
loglog(ww,T,'k')
ylabel('Magnitude', 'FontSize', 12);
xlabel('Frequency(rad/s)', 'FontSize', 12);
hold on;
legend('complementary sensitivity function (proposed1)','complementary sensitivity function (proposed2)',
'complementary sensitivity function (proposed3)','complementary sensitivity function (proposed4)',
'complementary sensitivity function (proposed)','+10% uncertainty in time delay')

%-------------------------------------------------Gamma variation----------------------------------------------
%-----------------------------------------------------Proposed1----------------------------------------------
clear all
clc
ww=logspace(-3,3,500);
for i=1:500
   w=ww(i);
   xx = j*w;
   Gp(i) = 1*exp(-2*xx)/(0.7*xx^2+1.7*xx+1);
   Gc(i) = (1.7+(1/xx)+0.7*xx)*((0.3658*xx^2+1.3658*xx+1)/(1.6422*xx^2.04
         +1.6422*xx^1.04+2.563*xx^1.02+0.366*xx+2.563*xx^0.02+1.6342));
   T(i) = abs((Gc(i)*Gp(i))/(1+Gc(i)*Gp(i)));
end
subplot(2,1,2)
loglog(ww,T,'r-.')
hold on;
%-----------------------------------------------------Proposed2----------------------------------------------
ww=logspace(-3,3,500);
for i=1:500
   w=ww(i);
   xx = j*w;
   Gp(i) = 1*exp(-2*xx)/(0.7*xx^2+1.7*xx+1);
```

```
   Gc(i) = (1.7+(1/xx)+0.6998*xx)*((0.1601*xx^3+0.8135*xx^2+1.4802*xx+1)/
         (0.3717*xx^3.04+1.1151*xx^2.04+0.704*xx^2.02-0.1601*xx^2+1.1151*xx^1.04
         +2.112*xx^1.02+0.4802*xx+2.112*xx^0.02+1.5198));
   T(i) = abs((Gc(i)*Gp(i))/(1+Gc(i)*Gp(i)));
end
subplot(2,1,2)
loglog(ww,T,'r--')
hold on;
%----------------------------------------------------Proposed3----------------------------------------------------
ww=logspace(-3,3,500);
for i=1:500
   w=ww(i);
   xx = j*w;
   Gp(i) = 1*exp(-2*xx)/(0.7*xx^2+1.7*xx+1);
   Gc(i) = (1.7+(1/xx)+0.7*xx)*((3.884*xx^4+25.478*xx^3+70.956*xx^2+101.13*xx+60)/
         (8.7362*xx^4.04+39.3129*xx^3.04+16.72*xx^3.02+78.6258*xx^2.04+75.24*xx^2.02
         +2.174*xx^2+65.5215*xx^1.04+150.48*xx^1.02+47.304*xx+125.4*xx^0.02+90.87));
   T(i) = abs((Gc(i)*Gp(i))/(1+Gc(i)*Gp(i)));
end
subplot(2,1,2)
loglog(ww,T,'b')
hold on;
%----------------------------------------------------Proposed4----------------------------------------------------
ww=logspace(-3,3,500);
for i=1:500
   w=ww(i);
   xx = j*w;
   Gp(i) = 1*exp(-2*xx)/(0.7*xx^2+1.7*xx+1);
   Gc(i) = (1.7+(1/xx)+0.7*xx)*((1.7696*xx^3+7.5392*xx^2+10.6544*xx+6)/
         (5.1347*xx^3.04+10.2695*xx^2.04+9.064*xx^2.02+7.7021*xx^1.04+18.128*xx^1.02
         +5.7696*xx+13.596*xx^0.02+9.3456));
   T(i) = abs((Gc(i)*Gp(i))/(1+Gc(i)*Gp(i)));
end
subplot(2,1,2)
loglog(ww,T,'b--')
hold on;
%----------------------------------------------------Proposed----------------------------------------------------
ww=logspace(-3,3,500);
for i=1:500
   w=ww(i);
   xx = j*w;
   Gp(i) = 1*exp(-2*xx)/(0.7*xx^2+1.7*xx+1);
   Gc(i) = (1.7+(1/xx)+0.7*xx)*((xx+1)/(2.2*xx^1.02+2.2*xx^0.02+2));
   T(i) = abs((Gc(i)*Gp(i))/(1+Gc(i)*Gp(i)));
end
subplot(2,1,2)
loglog(ww,T,'g')
hold on;
%-------------------------------------------------time delay variation-------------------------------------------------
ww=logspace(-3,3,500);
for i=1:500
```

```
    w=ww(i);
    xx = j*w;
    G(i)=1/(exp(0.2*xx)-1)
    T(i) = abs(G(i));
end
subplot(2,1,2)
loglog(ww,T,'k')
ylabel('Magnitude', 'FontSize', 12);
xlabel('Frequency(rad/s)', 'FontSize', 12);
hold off;
legend('complementary sensitivity function with +10% variation in \gamma (proposed1)', 'complementary sensitivity function with +10% variation in \gamma (proposed2)', 'complementary sensitivity function with +10% variation in \gamma (proposed3)', 'complementary sensitivity function with +10% variation in \gamma (proposed4)', 'complementary sensitivity function with +10% variation in \gamma (proposed)', '+10% uncertainty in time delay')
```

Simulink diagram for Example 1

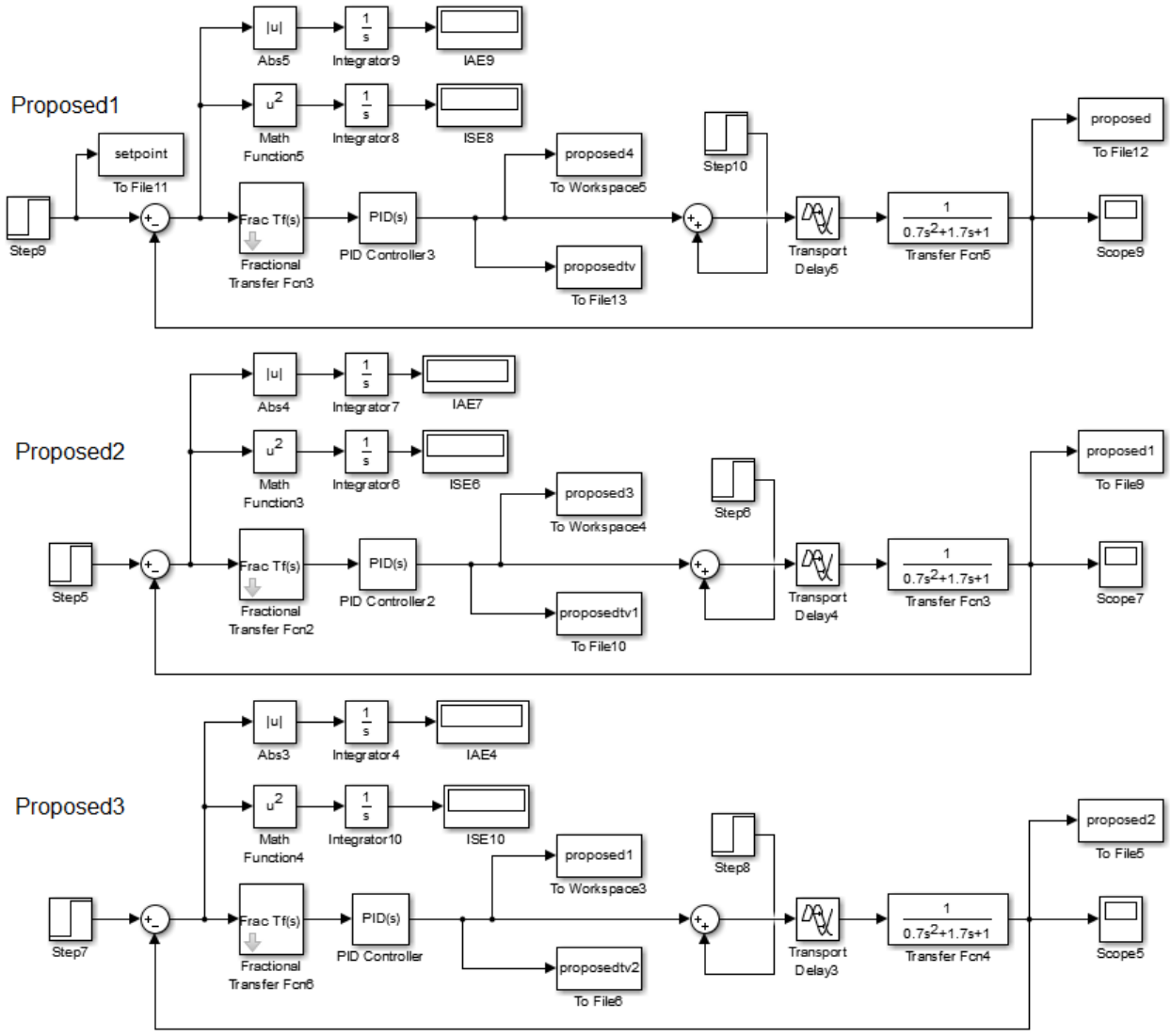

(Simulink diagram contd..)

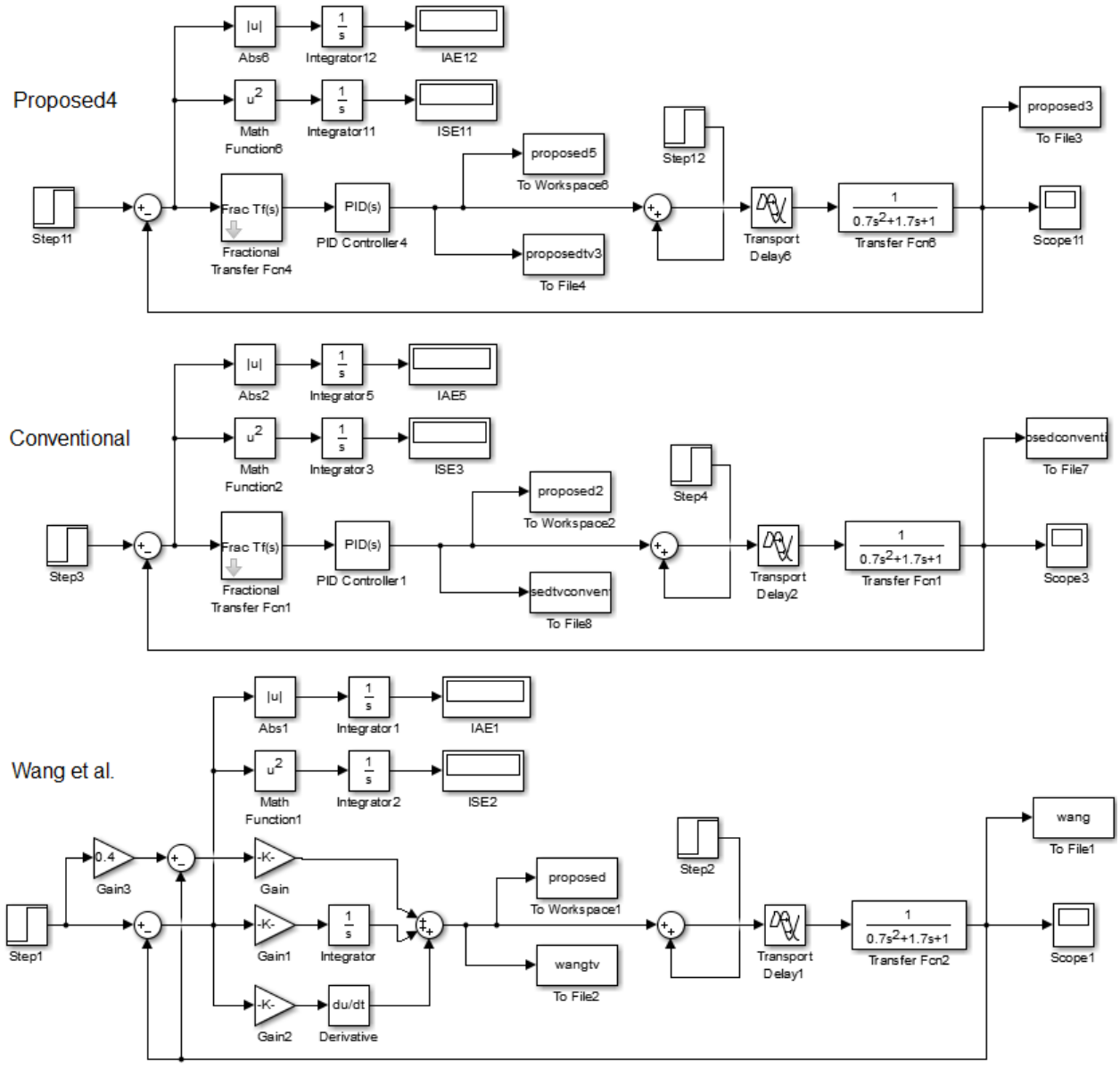

Appendix C

Program for obtaining the closed loop response of Example 1

```
%-------------------------------------------------Nominal response-------------------------------------------------
clc
sim 'PUREFINAL';
load proposed
subplot(2,1,1)
plot(a(1,:),a(2,:),'r','LineWidth',1)
hold on
sim 'PUREFINAL';
load proposed1
subplot(2,1,1)
plot(b(1,:),b(2,:),'b','LineWidth',1)
hold on
sim 'PUREFINAL';
load padma
subplot(2,1,1)
plot(c(1,:),c(2,:),'k','LineWidth',1)
hold on
sim 'PUREFINAL';
load input
subplot(2,1,1)
plot(d(1,:),d(2,:),'k--')
hold on
xlabel('Time(s)')
ylabel('Process output')
legend('Proposed','Proposed1','Kumar and sree(2016)')
%-----------------------------------------------------control effort-----------------------------------------------
sim 'PUREFINAL';
load proposedtv
subplot(2,1,2)
plot(A(1,:),A(2,:),'r','LineWidth',1)
hold on
sim 'PUREFINAL';
load proposedtv1
subplot(2,1,2)
plot(B(1,:),B(2,:),'b','LineWidth',1)
hold on
sim 'PUREFINAL';
load padmatv
subplot(2,1,2)
plot(C(1,:),C(2,:),'k','LineWidth',1)
hold on
xlabel('Time(s)')
ylabel('Control effort')
%-------------------------------------------------------------TV-------------------------------------------------
sim 'PUREFINAL';
load proposed1
TV=sum(abs(diff(proposed1)))
```

```
sim 'PUREFINAL';
load proposed2
TV=sum(abs(diff(proposed2)))
sim 'PUREFINAL';
load proposed
TV=sum(abs(diff(proposed)))
```

Simulink diagram for Example 1

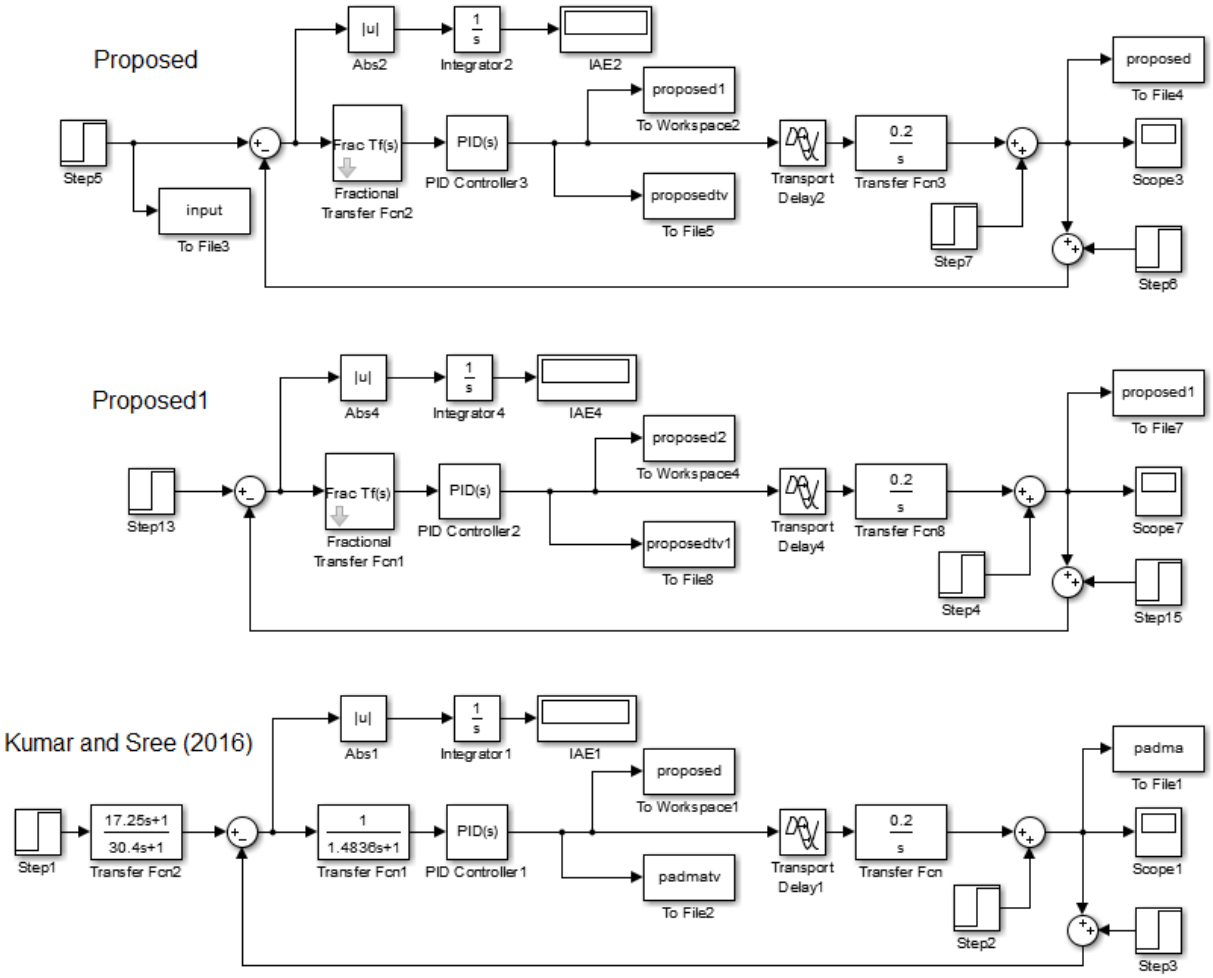

Appendix D

Program for obtaining the closed loop response of Example 1 (Chapter 6.1)

```
%-----------------------------------------------Closed loop response-----------------------------------------------
clc
sim 'NIOPTDIexample1FINAL';
load proposed
subplot(2,1,1)
plot(b(1,:),b(2,:),'b','LineWidth',2)
hold on
sim 'NIOPTDIexample1FINAL';
load old
subplot(2,1,1)
plot(a(1,:),a(2,:),'r--','LineWidth',2)
hold on
xlabel('Time(s)')
ylabel('Process output')
legend('Proposed1','Li et al.')
%-----------------------------------------------------control effort-----------------------------------------------------
sim 'NIOPTDIexample1FINAL';
load proposedtv
subplot(2,1,2)
plot(B(1,:),B(2,:),'b','LineWidth',2)
hold on
sim 'NIOPTDIexample1FINAL';
load oldtv
subplot(2,1,2)
plot(A(1,:),A(2,:),'r--','LineWidth',2)
hold off
xlabel('Time(s)')
ylabel('Control effort')
%-------------------------------------------------------------TV-------------------------------------------------------
sim 'NIOPTDIexample1FINAL';
load proposed
TV=sum(abs(diff(proposed)))
sim 'NIOPTDIexample1FINAL';
load old
TV=sum(abs(diff(old)))
```

Simulink diagram for Example 1

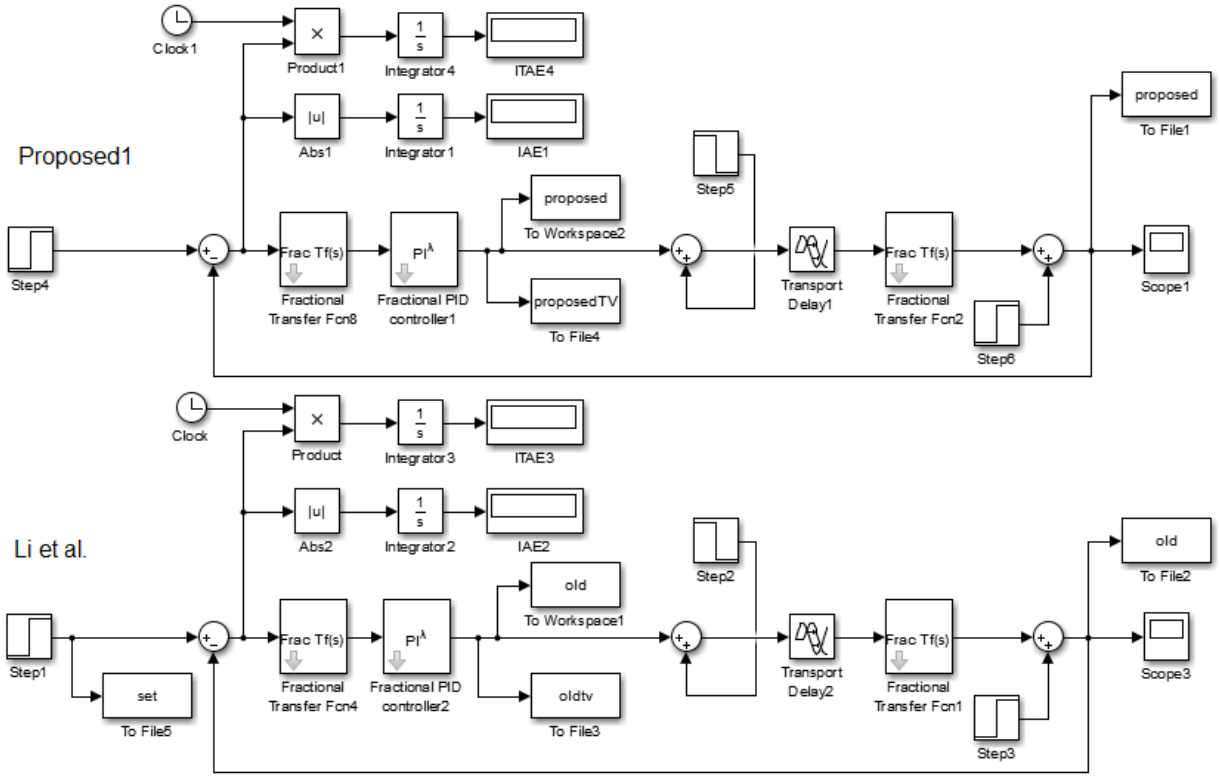

Program for obtaining the closed loop response of Example 1 (Chapter 6.2)

```
%----------------------------------------------closed loop response----------------------------------------------
clc
sim 'new2';
load new
subplot(2,1,1)
plot(a(1,:),a(2,:),'k')
hold on
sim 'new2';
load old
subplot(2,1,1)
plot(b(1,:),b(2,:),'k--')
hold on
sim 'new2';
load set
subplot(2,1,1)
plot(c(1,:),c(2,:),'k-.')
hold on
xlabel('Time(s)')
ylabel('y')
legend('Proposed method','Bongulwar & Patre (2017) method')
%-----------------------------------------------------control effort-----------------------------------------------
sim 'new2';
```

```
load proposed
subplot(2,1,2)
plot(A(1,:),A(2,:),'k')
hold on
sim 'new2';
load old1
subplot(2,1,2)
plot(B(1,:),B(2,:),'k--')
hold on
xlabel('Time(s)')
ylabel('u')
%----------------------------------------------------------TV-----------------------------------------------------
sim 'new2';
load proposed
TV=sum(abs(diff(proposed)))
sim 'new2';
load proposed1
TV=sum(abs(diff(proposed1)))
```

Simulink diagram

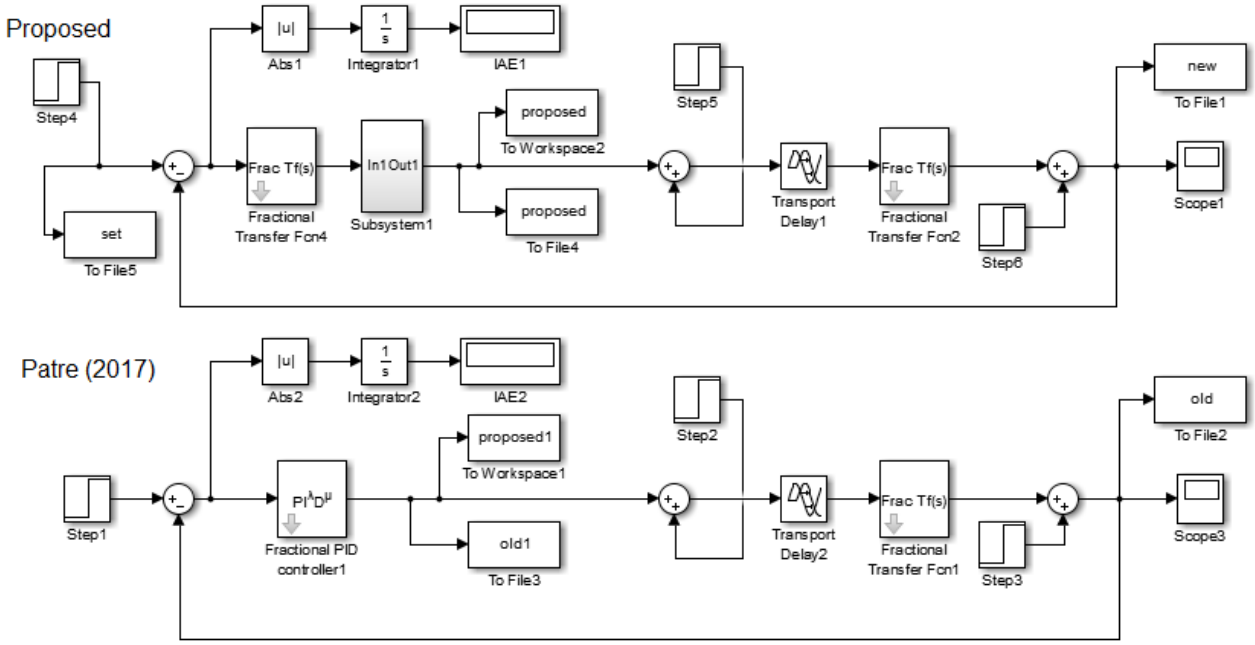

Appendix E

Program for obtaining the closed loop response of Example 1

```
%-------------------------------------------------Closed loop response-------------------------------------------------
sim 'CASCADEsoptdINNERfoptdOUTERFINAL';
load proposed
subplot(2,1,1)
plot(a(1,:),a(2,:),'r','LineWidth',2)
hold on
sim 'CASCADEsoptdINNERfoptdOUTERFINAL';
load old
subplot(2,1,1)
plot(b(1,:),b(2,:),'b--','LineWidth',2)
hold on
sim 'CASCADEsoptdINNERfoptdOUTERFINAL';
load ahmad
subplot(2,1,1)
plot(c(1,:),c(2,:),'k:','LineWidth',2)
hold off
xlabel('Time(s)')
ylabel('Process output')
legend('Proposed1','Proposed2','Azar and Serrano, 2014')
%-----------------------------------------------------control effort-----------------------------------------------------
sim 'CASCADEsoptdINNERfoptdOUTERFINAL';
load proposedtv
subplot(2,1,2)
plot(A(1,:),A(2,:),'r','LineWidth',2)
hold on
sim 'CASCADEsoptdINNERfoptdOUTERFINAL';
load oldtv
subplot(2,1,2)
plot(B(1,:),B(2,:),'b--','LineWidth',2)
hold on
sim 'CASCADEsoptdINNERfoptdOUTERFINAL';
load ahmadtv
subplot(2,1,2)
plot(C(1,:),C(2,:),'k:','LineWidth',2)
hold off
xlabel('Time(s)')
ylabel('Control effort')
%-------------------------------------------------------------TV-------------------------------------------------------
sim 'CASCADEsoptdINNERfoptdOUTERFINAL';
load proposed2
TV=sum(abs(diff(proposed2)))
sim 'CASCADEsoptdINNERfoptdOUTERFINAL';
load proposed3
TV=sum(abs(diff(proposed3)))
sim 'CASCADEsoptdINNERfoptdOUTERFINAL';
load proposed
TV=sum(abs(diff(proposed)))
```

Simulink diagram for Example 1

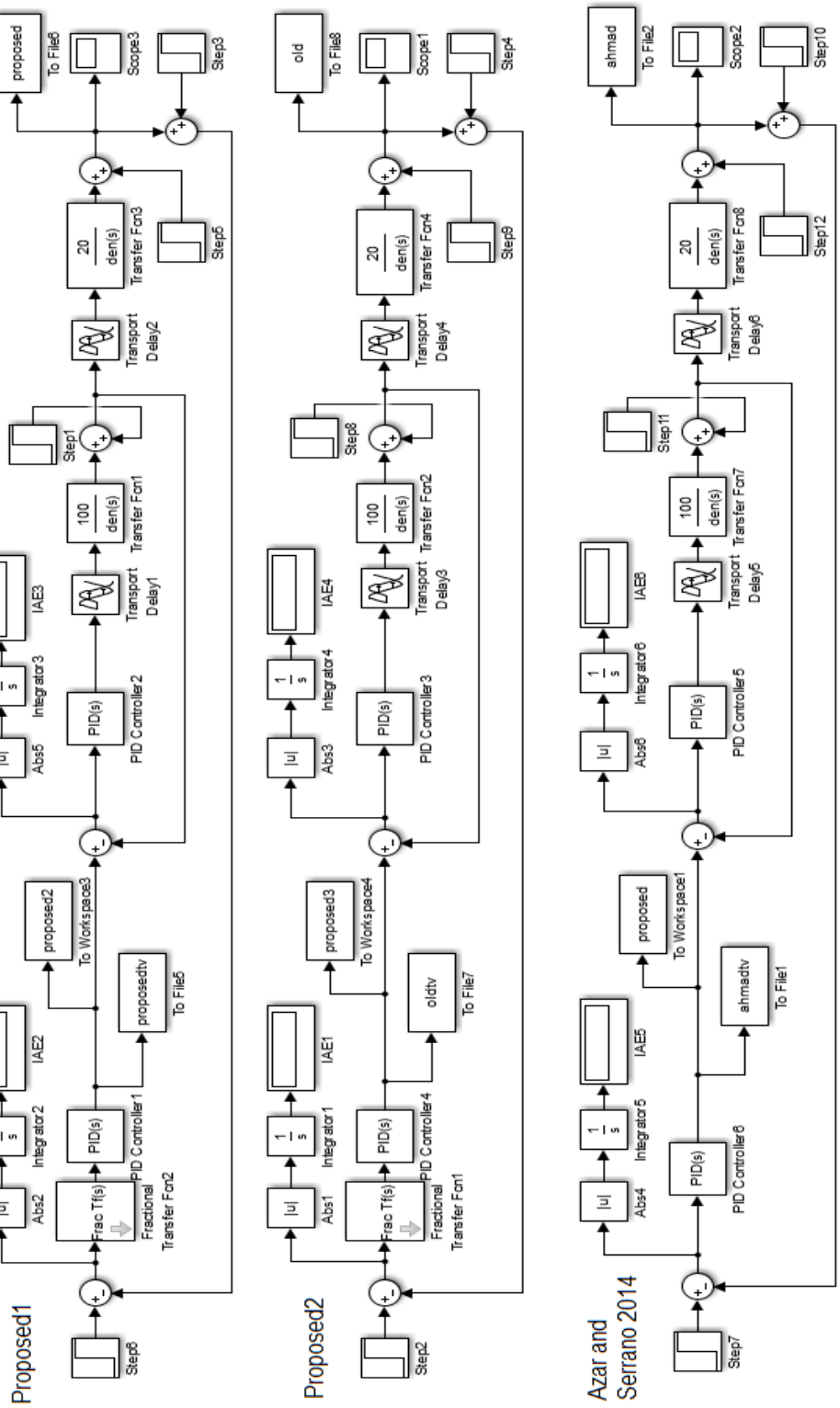

List of Publications

Journal articles

1. R. Ranganayakulu, A. Seshagiri Rao and G. Uday Bhaskar Babu. "Analytical design of fractional IMC filter – PID control strategy for performance enhancement of cascade control systems". International Journal of Systems Science (Taylor & Francis): 2019 (under review).
2. R. Ranganayakulu, A. Seshagiri Rao and G. Uday Bhaskar Babu. "An Improved Fractional Filter Fractional IMC-PID Controller design for enhanced performance of Non-Integer Order Plus Time Delay Processes". European Journal of Electrical Engineering: 21(2), 139-147, 2019. https://doi.org/10.18280/ejee.210203
3. R. Ranganayakulu, A. Seshagiri Rao and G. Uday Bhaskar Babu. "Improved Fractional Filter IMC-PID Controller Design for enhanced performance of Integrating Plus Time Delay processes". Indian Chemical Engineer (Taylor & Francis): 1-18, 2019. (Available online). https://doi.org/10.1080/00194506.2019.1656553.
4. R. Ranganayakulu, G. Uday Bhaskar Babu and A. Seshagiri Rao. "Analytical design of Enhanced Fractional filter PID controller for improved disturbance rejection of second order plus time delay processes". Chemical product and Process Modeling (De Gruyter): 14(1), 2018. https://doi.org/10.1515/cppm-2018-0012
5. R. Ranganayakulu, G. Uday Bhaskar Babu and A. Seshagiri Rao. "Fractional Filter IMC-PID controller design for second order plus time delay processes". Cogent Engineering (Taylor & Francis): 4(1), 1366888, 2017. https://doi.org/10.1080/23311916.2017.1366888
6. R. Ranganayakulu, G. Uday Bhaskar Babu, A. Seshagiri Rao and Dipesh Shikchand Patle. "A comparative study of fractional order PI/PID tuning rules for stable first order plus time delay processes". Resource-Efficient Technologies (Elsevier): 2, S136-S152. 2016. http://dx.doi.org/10.1016/j.reffit.2016.11.009

Book chapters

1. R. Ranganayakulu, G. Uday Bhaskar Babu and A. Seshagiri Rao, "Design of Fractional Filter Fractional Order Proportional Integral Derivative (FFFOPID) controller for higher order systems." Emerging Trends in Engineering, Science and Technology for Society, Energy and Environment. CRC Press, 2018. 535-546.

International conference proceedings

1. R. Ranganayakulu, G. Uday Bhaskar Babu and A. Seshagiri Rao, "On the fragility of fractional filter fractional order PID controller for higher order processes approximated as non-integer order plus time delay systems", *2nd International Conference on New Frontiers in Chemical, Energy and Environmental Engineering (INCEEE 2019)*, Warangal, 15 - 16 February 2019.
2. R. Ranganayakulu, G. Uday Bhaskar Babu and A. Seshagiri Rao, "Design of Fractional Filter Fractional Order PID controller for higher order systems', *5th biennial International Conference on Emerging Trends in Engineering, Science and Technology (ICETEST 2018)*, Government Engineering College, Thrissur, 18-20 January 2018.
3. R. Ranganayakulu, G. U. B. Babu and A. Seshagiri Rao, "Fractional filter IMC-PID controller design for an unstable inverted pendulum system", *IEEE International Conference on Smart Technologies and Management for computing, communication, controls, energy and materials (ICSTM 2017)*, Chennai, 2-4 August 2017, pp. 411-416. DOI: 10.1109/ICSTM.2017.8089195
4. R. Ranganayakulu, G. Uday Bhaskar Babu and A. Seshagiri Rao, "Simple $PI^{\lambda}D^{\mu}$ controller tuning rules for improved closed loop performance of First Order Plus Time Delay processes", *Second International Conference on Intelligent and Efficient Electrical Systems (ICIEES'17)*, PSG college of technology, Coimbatore, 20-21 January 2017. (awarded as the best paper)
5. R. Ranganayakulu**,** G. U. B. Babu, A. S. Rao, and D. S. Patle. "A Comparative Study of Recent Fractional Order PI^{λ}/$PI^{\lambda}D^{\mu}$ Tuning Rules for Stable First Order Plus Time Delay Processes." *International conference on Separation Technologies in Chemical, Biochemical, Petroleum and Environmental Engineering (TECHNOSCAPE16)*, VIT University, Vellore, 20 - 21 October 2016.
6. R. Ranganayakulu and G. U. B. Babu, "Control performance enhancement using fractional $PI^{\lambda}D^{\mu}$ controller for first order time delay systems," *2016 IEEE 1st International Conference on Power Electronics, Intelligent Control and Energy Systems (ICPEICES)*, Delhi Technological University, New Delhi, 4 – 6 July 2016. DOI: 10.1109/ICPEICES.2016.7853386

Curriculum vitae

Rayalla Ranganayakulu

Email: rayalla.ranga@gmail.com

ACADEMIC PROFILE

Ph.D.: Pursuing (Since December 2014) from Department of Chemical Engineering, National Institute of Technology, Warangal, Telangana, India

M.E.: Instrumentation & Control Engineering from Birla Institute of Technology, Mesra, Ranchi, Jharkhand, India, 2009.

B.Tech.: Electronics & Instrumentation Engineering from Lakireddy Bali Reddy College of Engineering, Mylavaram, Andhra Pradesh, India, 2007.

PROFESSIONAL EXPERIENCE (4.6 years)

1. Assistant professor at Lakireddy Bali Reddy College of Engineering (2011-2014)
2. Assistant professor at Sir C R Reddy College of Engineering (2010-2011)
3. Assistant professor at SAMS College of Engineering and Technology (2009-2010)